UNIVERSITY OF LONDON THESIS

Degree PhD Year 2006 Name of Author DUNLEVY
Louisa Patricia Elizabeth

The role of the folate and methylation cycles in neural tube closure

Louisa Patricia Elizabeth Dunlevy

❖

A thesis submitted for the degree of Doctor of Philosophy

University of London

June 2006

❖

Neural Development Unit

The Institute of Child Health

30 Guilford Street

London WC1N 1EH

❖

ProQuest LLC
789 East Eisenhower Parkway
P.O. Box 1346
Ann Arbor, MI 48106-1346

Declaration

I, Louisa Patricia Elizabeth Dunlevy, confirm that the work presented in this thesis is my own. Where information has been derived from other sources, I confirm that this has been indicated in the thesis.

Signed :

Abstract

Neural tube defects (NTD) are congenital malformations caused by abnormalities in the developmental process of neurulation. Folate metabolism appears to be a determinant of risk of NTD since periconceptional supplementation with folic acid has been shown to reduce the frequency of NTD in humans while sub-optimal folate levels are a risk factor. The mechanisms underlying prevention of NTD by folic acid or susceptibility owing to reduced levels are not known. The aims of this thesis were to understand the role of the folate and, the closely linked, methylation cycle in the cause and prevention of NTD.

The effect of methylation cycle intermediates, homocysteine and methionine, on cranial neural tube closure were investigated in cultured mouse embryos. Homocysteine exposure was embryotoxic but did not increase the incidence of NTD, which suggests that increased levels of homocysteine are not a direct cause of cranial NTD. Embryos cultured with high levels of methionine or methylation cycle inhibitors specifically developed cranial NTD in the absence of other developmental defects. These results suggest that the integrity of the methylation cycle is essential for cranial neural tube closure to occur.

Mouse embryos that are homozygous for the *Splotch*^{2H} mutation exhibit NTD that are preventable by folic acid. In *Splotch* mice, increased apoptosis has been suggested to be responsible for the production of NTD in homozygous embryos. However, in this study immunohistochemical measurement of apoptosis and proliferation in the

neuroepithelium in the cranial region of neurulation-stage embryos suggest that the *Splotch*^{2H} mutation does not result in increased apoptosis.

Finally, in order to test whether there is an underlying defect in folate metabolism in human NTD fetuses, a series of human embryonic cell lines were analysed. The deoxyuridine monophosphate (dUMP) suppression test was modified for use with mammalian fibroblast cell lines and the efficiency and sensitivity of the modified test were analysed by the use of inhibitors of one-carbon metabolism. The test was then applied to human NTD and control cell lines and the results indicate that a subset of the NTD cases have a diminished response, suggestive of an abnormality of folate metabolism.

Table of contents

DECLARATION **2**

ABSTRACT **3**

TABLE OF CONTENTS **5**

LIST OF FIGURES **13**

LIST OF TABLES **17**

ACKNOWLEDGEMENTS **20**

DEDICATION **22**

CHAPTER 1; INTRODUCTION **23**

1.1 Neurulation **24**

1.1.1 Primary neurulation 25

1.2 Mechanisms of primary neurulation **28**

1.2.1 Cranial neurulation 28

1.2.2 Spinal neurulation 31

1.3 Neural Tube Defects **33**

1.4 Causes of NTD in humans **33**

1.4.1 Genetic predisposition 36

1.4.2 Environmental influences 38

1.5 The mouse as an experimental model for NTD 42

1.5.1 The full spectrum of NTD is represented in mouse 42

1.5.2 Genetic and environmental influences affect the incidence of NTD in mouse models 43

1.6 Genetic and Cellular mechanisms in normal neurulation 44

1.6.1 Different mechanisms are involved in neural tube closure along the cranial-caudal axis of the embryo 44

1.6.2 Factors involved in cranial neurulation – evidence from mouse models 45

1.6.2.1 Cranial mesenchyme 45

1.6.2.2 Actin cytoskeleton 51

1.6.2.3 Apoptosis 52

1.6.3 Factors involved in spinal neurulation – evidence from mouse models 52

1.6.3.1 Planar cell polarity pathway 52

1.6.3.2 Axial curvature 53

1.7 Folate prevents NTD in humans 54

1.8 One carbon metabolism 56

1.8.1 Folate metabolism 56

1.8.2 The methylation cycle 60

1.9 Folate-related risk factors for the development of NTD in humans 64

1.10 Prevention of NTD in mouse models 69

1.10.1 *Splotch* mice 72

1.10.2 Possible mechanisms of folate prevention of NTD 74

1.10.2.1 Correction of maternal folate deficiency 74

1.10.2.2 Overcoming abnormalities in folate metabolism 75

1.10.2.3 Overcoming abnormalities in the methylation cycle 75

1.11 Investigating folate metabolism in the closure of the mammalian neural tube 77

CHAPTER 2; MATERIALS AND METHODS 78

2.1 Mouse strains and generation of experimental litters 79

2.2 Dissection of embryos 79

2.3 Whole embryo culture 80

2.3.1 Preparation of rat serum 80

2.3.2 Whole embryo culture 83

2.3.3 Solutions for whole embryo culture 84

2.3.4 Measurements after whole embryo culture 84

2.4 Processing of embryos 87

2.5 Genotyping of mutant embryos by polymerase chain reaction (PCR) 87

2.5.1 Extraction of DNA from yolk sac samples 87

2.5.2 PCR protocol 88

2.5.3 Agarose gel electrophoresis 89

2.6 Histological analysis 90

2.6.1 Embedding and sectioning 90

2.6.2 Preparation of TESPA-coated slides 91

2.6.3 Haematoxylin and Eosin (H&E) staining 92

2.7 Immunohistochemistry with anti-phosphorylated histone H3 and anti-activated caspase 3 antibodies 93

2.7.1 Sample preparation 93

2.7.2 Immunohistochemistry 93

2.8 Whole Mount TUNEL 96

2.8.1 Sample preparation 96

2.8.2 Terminal transferase reaction 97

2.8.3 Detection 97

2.9 Probe generation for whole mount *in situ* hybridisation 98

2.9.1 Transformation 98

2.9.2 Isolation of plasmid DNA 99

2.9.3 Linearisation of plasmid DNA 101

2.9.4 Phenol-chloroform DNA extraction 102

2.9.5 Synthesis of digoxygenin (DIG)-labelled probes 102

2.10 Whole Mount *in situ* hybridisation 103

2.10.1 Embryo pre-treatment 103

2.10.2 Hybridisation and post-hybridisation washes 104

2.10.3 Preparation of preabsorbed antibody solution 104

2.10.4 Post-antibody washes and development 105

2.11 Cell culture of human embryonic fibroblasts 106

2.11.1 Basic cell culture procedures 106

2.11.2 Sample collection and processing 106

2.11.3 Maintenance of cells in culture 107

2.11.4 Solutions for the deoxyuridine (dU) suppression test 108

2.11.5 dU suppression test 109

2.11.6 Determination of protein content 109

2.11.7 Measurement of [^{3}H]-thymidine incorporation 110

CHAPTER 3; INVESTIGATING THE EFFECT OF HOMOCYSTEINE ON CRANIAL NEURAL TUBE CLOSURE 111

3.1 Introduction 112

3.2 Results 115

3.2.1 Dose-dependent embryotoxicity of homocysteine thiolactone in CD1 mice 115

3.2.2 Developmental defects in homocysteine thiolactone-treated embryos 116

3.2.3 The effect of homocysteine thiolactone treatment on somitogenesis in CD1 embryos 121

3.3 Discussion 125

CHAPTER 4; THE EFFECT OF DISRUPTING THE METHYLATION CYCLE ON CRANIAL NEURAL TUBE CLOSURE 135

4.1 Introduction 136

4.2 Results 140

4.2.1 Methionine, ethionine and cycloleucine specifically cause cranial NTD in CD1 mouse embryos 140

4.2.1.1 Methionine specifically causes cranial NTD in CD1 mouse embryos.. 140

4.2.1.2 Ethionine specifically causes NTD in CD1 mouse embryos 144

4.2.1.3 Cycloleucine causes isolated NTD in CD1 mouse embryos 148

4.2.2 The morphological appearance of exencephaly differs between methionine, ethionine and cycloleucine-induced defects 150

4.2.3 Different morphology through the cranial regions of treated embryos..... 153

4.2.3.1 Reduced cranial mesenchyme density in methionine-treated embryos. 154

4.2.3.2 The cranial neuroepithelium is less thick in ethionine-treated embryos *157*

4.2.3.3 Increased cranial mesenchyme density in cycloleucine-treated embryos *157*

4.2.4 Quantitative analysis of neuroepithelial thickness and cranial mesenchyme density in methionine, ethionine, cycloleucine and PBS-treated embryos 158

4.2.4.1 Method for quantitative analysis of neuroepithelial thickness *158*

4.2.4.2 Neuroepithelial thickness in treated embryos compared to control embryos *161*

4.2.4.3 Quantitative analysis of mesenchymal cell density in transverse sections through the cranial region of cultured embryos *166*

4.2.4.4 Cranial mesenchyme density in treated and control embryos *167*

4.2.5 Whole mount TUNEL analysis of methionine and ethionine-treated embryos 171

4.2.6 Quantitative analysis of proliferation and cell death in methionine and ethionine-treated embryos 174

4.2.6.1 Method for quantitative immunohistochemical analysis of proliferation and apoptosis in methionine, ethionine and cycloleucine-treated and control embryos *175*

4.2.6.2 Analysis of proliferation in the cranial mesenchyme of methionine, ethionine and cycloleucine-treated embryos *182*

4.2.6.3 Apoptosis levels in the cranial mesenchyme of methionine, ethionine and cycloleucine-treated embryos compared to control embryos *185*

4.2.7 Can co-treatment with folic acid prevent methionine or ethionine-induced NTD? 188

4.3 Discussion 192

CHAPTER 5; INVESTIGATION OF THE CAUSES OF CRANIAL NTD IN *SPLOTCH^{2H}* MICE 203

5.1 Introduction 204

5.2 Results 205

5.2.1 Whole mount TUNEL in *Splotch*^{2H} embryos during neural tube closure..... 205

5.2.2 Method for quantitative analysis of proliferation and apoptosis levels in *Splotch*^{2H} embryos during cranial neural tube closure 210

5.2.3 Proliferation and apoptosis levels in the cranial neuroepithelium of E9 *Splotch*^{2H} embryos 214

5.2.4 Proliferation and apoptosis levels in the cranial neuroepithelium of E9.5 *Splotch*^{2H} embryos 219

5.2.5 Method for quantitative analysis of apoptosis in the *Pax3* expression domain of the cranial neuroepithelium in E9 *Splotch*^{2H} embryos 223

5.2.6 Apoptosis in the *Pax3* expression domain in the cranial neuroepithelium of E9 *Splotch*^{2H} embryos 227

5.3 Discussion 228

CHAPTER 6; DETECTION OF FOLATE CYCLE ABNORMALITIES IN CELL CULTURE BY THE DEOXYURIDINE MONOPHOSPHATE SUPPRESSION TEST 236

6.1 Introduction 237

6.2 Results 243

6.2.1 Dose-dependant suppression of [^{3}H]-thymidine DNA incorporation by dUMP 243

6.2.2 Detection of impaired folate metabolism by the dUMP suppression test in mouse fibroblasts 246

6.2.2.1 Inhibition of [^{3}H]-thymidine incorporation into DNA by 5-fluorouracil 246

6.2.2.2 Inhibition of [^{3}H]-thymidine incorporation into DNA by aminopterin. 250

6.2.2.3 Lack of inhibition of [^{3}H]-thymidine incorporation into DNA by cycloleucine 253

6.2.3 dUMP suppression test of human embryonic fibroblasts derived from fetuses with NTD 256

6.2.3.1 Summary of human samples 256

6.2.3.2 Results of the dUMP suppression test on human embryonic fibroblast cells 259

6.3 Discussion 267

CHAPTER 7; GENERAL DISCUSSION 272

7.1 General discussion 273

REFERENCES 281

APPENDIX - PUBLICATIONS 322

List of Figures

Figure 1.1 The three sites of initiation of neural tube closure in mouse 26

Figure 1.2 The two phases of cranial neurulation in mammals 29

Figure 1.3 Morphological modes of neural closure in the PNP 32

Figure 1.4 Neural tube defects in humans and mice 34

Figure 1.5 A representation of the molecular structure of folic acid 56

Figure 1.6 The folate cycle 58

Figure 1.7 The methylation cycle 61

Figure 2.1. Dissection steps for whole embryo culture 81

Figure 2.2. Embryo morphology and measurements before and after whole embryo culture 85

Figure 2.3 Visualisation of Sp^{2H} PCR products after agarose gel electrophoresis 90

Figure 3.1. Developmental abnormalities induced by homocysteine thiolactone treatment 119

Figure 3.2 Expression of *Dll1* and *Dll3* in homocysteine thiolactone-treated embryos 123

Figure 4.1 Simplified diagram of the methylation cycle 138

Figure 4.2 Methionine specifically causes cranial NTD in CD1 embryos 143

Figure 4.3 Ethionine specifically causes cranial NTD in CD1 embryos. 147

Figure 4.4 Regions of open neural tube in methionine, ethionine and cycloleucine-treated embryos. 150

Figure 4.5 Positions of open neural folds in the cranial region of embryos treated with methionine, ethionine or cycloleucine 151

Figure 4.6 Transverse sections stained with haematoxylin and eosin, through the cranial region of exencephalic methionine, ethionine and cycloleucine-treated embryos and control PBS-treated embryos 155

Figure 4.7 Quantitative analysis of transverse sections, stained with haematoxylin and eosin, through the cranial region of methionine, ethionine, cycloleucine and PBS-treated embryos 159

Figure 4.8 Measurement of the width of the neuroepithelium in embryos after 24 hours culture in the presence of PBS, 5 mM methionine, 5 mM ethionine or 15 mM cycloleucine. 164

Figure 4.9 Mesenchyme density in the cranial region of embryos after 24 hours in culture in the presence of PBS, 5 mM methionine, 5 mM ethionine or 15 mM cycloleucine. 169

Figure 4.10 Whole mount TUNEL on methionine, ethionine and PBS-treated CD-1 embryos. 172

Figure 4.11 Sections used to calculate labelling indices for apoptosis and proliferation in the cranial mesenchyme of embryos after 16 hours culture in the presence of methionine, ethionine, cycloleucine or PBS. 176

Figure 4.12 Cranial mesenchyme proliferation in embryos at the stage of cranial neural tube closure after culture with PBS, 5 mM methionine, 5 mM ethionine or 15 mM cycloleucine 184

Figure 4.13 Cranial mesenchyme apoptosis levels in embryos at the time of cranial neural tube closure after culture with PBS, 5 mM methionine, 5 mM ethionine or 15 mM cycloleucine 187

Figure 5.1 Whole mount TUNEL on E8.5 *Splotch*^{2H} embryos 206

Figure 5.2 Whole mount TUNEL on E9.5 *Splotch*^{2H} embryos 208

Figure 5.3 Whole mount TUNEL on E10.5 *Splotch*^{2H} embryos 211

Figure 5.4 Analysis of apoptosis and proliferation in the cranial neuroepithelium of *Splotch*^{2H} embryos. 213

Figure 5.5 Apoptosis in the neuroepithelium of E9 *Splotch*^{2H} embryos. 216

Figure 5.6 Proliferation in the neuroepithelium of E9 *Splotch*^{2H} embryos. 218

Figure 5.7 Apoptosis in the neuroepithelium of E9.5 *Splotch*^{2H} embryos. 221

Figure 5.8 Proliferation in the neuroepithelium of E9.5 *Splotch*^{2H} embryos. 223

Figure 5.9 *Pax3* expression boundaries in the neural tube of E9 mouse embryos 226

Figure 6.1 The deoxyuridine suppression test 239

Figure 6.2 A simplified diagram of the folate and methylation cycles 241

Figure 6.3 The dose-dependent suppression of [^{3}H]-thymidine incorporation into DNA by deoxyuridine monophosphate in mouse fibroblast cells 244

Figure 6.4 Dose-dependent suppression of [^{3}H]-thymidine incorporation into DNA by deoxyuridine monophosphate in human fibroblast cells 245

Figure 6.5 Inhibition of the dUMP mediated suppression of [^{3}H]-thymidine incorporation into DNA by 5-fluorouracil in mouse fibroblast cells. 248

Figure 6.6 Inhibition of the dUMP mediated suppression of [^{3}H]-thymidine incorporation into DNA by 5-fluorouracil in human fibroblast cells. 248

Figure 6.7 Inhibition of the dUMP mediated suppression of [^{3}H]-thymidine incorporation into DNA by aminopterin in mouse fibroblast cells. 251

Figure 6.8 Inhibition of the dUMP mediated suppression of [^{3}H]-thymidine incorporation into DNA by aminopterin in human fibroblast cells. 251

Figure 6.9 Lack of inhibition of the dUMP mediated suppression of [^{3}H]-thymidine incorporation into DNA by cycloleucine in mouse fibroblast cells. 254

Figure 6.10 Lack of inhibition of the dUMP mediated suppression of [^{3}H]-thymidine incorporation into DNA by cycloleucine in human fibroblast cells. 254

Figure 6.11 Human embryonic fibroblast cell lines 258

Figure 6.12 dUMP suppression test results for human embryonic fibroblast cell lines 262

Figure 6.13 Distribution of the suppression of [^{3}H]-thymidine incorporation into DNA by dUMP in human embryonic fibroblast cells 264

List of Tables

Table 1.1 Mouse genetic models of NTD with suggested underlying mechanisms 50

Table 1.2 Mouse models in which NTD are preventable by folate-related treatments... 71

Table 1.3 *Splotch* allele phenotypes and mutations in *Pax3* 73

Table 2.1 Gas mixtures required for whole embryo culture of embryos at different developmental ages. 83

Table 2.2 The primer sequences and product sizes for genotyping Sp^{2H} mice. 88

Table 2.3 Antisense RNA probes used for whole mount *in situ* hybridisation..... 101

Table 3.1 Growth and development of CD1 mouse embryos cultured in the presence of homocysteine thiolactone 116

Table 3.2 Incidence of developmental defects in mouse embryos exposed to homocysteine thiolactone 117

Table 4.1 Growth and development of mouse embryos cultured in the presence of methionine 141

Table 4.2 Growth and development of mouse embryos cultured in the presence of ethionine. 145

Table 4.3 Growth and development of mouse embryos cultured in the presence of cycloleucine 149

Table 4.4 Comparison of the apical-basal thickness of the hindbrain and forebrain neuroepithelium in cultured embryos. 162

Table 4.5 Neuroepithelial thickness measurements in cranial sections after whole embryo culture with PBS, 5 mM methionine, 5 mM ethionine or 15 mM cycloleucine. 163

Table 4.6 Cranial mesenchyme density measurements in sections after whole embryo culture with PBS, 5 mM methionine, 5 mM ethionine or 15 mM cycloleucine... 168

Table 4.7 Initial counting strategy for anti-phosphorylated histone H3 labelled cells in the cranial mesenchyme in sections through PBS-treated embryos. 178

Table 4.8 Initial counting strategy for anti-activated caspase 3 labelled cells in the cranial mesenchyme in sections through PBS-treated embryos. 180

Table 4.9 Cranial mesenchyme proliferation in embryos after culture with PBS, 5 mM methionine, 5 mM ethionine or 15 mM cycloleucine 183

Table 4.10 Cranial mesenchyme apoptosis in embryos after culture with PBS, 5 mM methionine, 5 mM ethionine or 15 mM cycloleucine 186

Table 4.11 Growth and development of mouse embryos cultured in the presence of methionine with or without folic acid 190

Table 4.12 Growth and development of mouse embryos cultured in the presence of ethionine with or without folic acid 191

Table 4.13 Quantification of SAM and SAH in cultured embryos 198

Table 5.1 Anti-activated caspase 3 antibody labelling in the neuroepithelium of E9 *Splotch*^{2H} embryos 215

Table 5.2 Anti-phosphorylated histone H3 antibody labelling in the neuroepithelium of E9 *Splotch*^{2H} embryos 217

Table 5.3 Anti-activated caspase 3 antibody labelling in the neuroepithelium of E9.5 *Splotch*^{2H} embryos 220

Table 5.4 Anti-phosphorylated histone H3 antibody labelling in the neuroepithelium of E9.5 *Splotch*^{2H} embryos 222

Table 5.5 *Pax3* expression in coronal sections through the cranial region of E9 embryos 225

Table 5.6 Apoptosis in the neuroepithelium of E9 *Splotch*^{2H} embryos with regard to *Pax3* expression 228

Table 6.1 Summary of human samples collected for dUMP suppression test investigation. 257

Table 6.2 Summary of human samples used in the dUMP suppression test investigation. 261

Table 6.3 dUMP suppression test scores for human embryonic fibroblast samples..... 265

Table 6.4 Source of established cell lines 269

Table 7.1 The genotype of the successful dUST cell lines for several known polymorphisms in folate-related genes 279

Acknowledgements

I would like to take this opportunity to officially thank those without whom it would not have been possible to complete this thesis. I am sincerely grateful to Dr. Nicholas Greene. I would like to thank him for the opportunity to carry out this study, his encouragement and for all the support he has shown me. Nick has always been a very approachable supervisor and has provided sound advice and guidance throughout this project. Thank you.

I would like to thank Professor Andrew Copp my secondary supervisor. Alan Burns, Andy Stoker, JP Martinez-Barbera and Jane Sowden have not been official supervisors, but their input and advice has been really appreciated.

I should like to thank Lynn Chitty, Tatiana Tstojilkovic and Rosemary Scott for their involvement in collecting diagnostic samples and the staff of the NE London Regional Cytogenetics Laboratory, Great Ormond Street Hospital for establishing cell lines from the diagnostic samples. I should also like to thank Katie Burren and Kit Doudney for sharing their results with me and allowing me to discuss them in this thesis.

There are many other people that have helped and advised me in all aspects of this research project. All the members of NDU and DBU over the years have had an influence whether through comments in lab meetings or general chats in the lab. In particular, I should like to mention Pachy Ybot-Gonzalez, Dianne Gerrelli, Caroline Paternotte, Dawn Savery and members of the 'Greene team' past and present; Patricia

Cogram, Dina Lad and Katie Burren. An extra special mention goes to Diane Austin and Brenda Gulliver, many thanks for all your help.

Life as a PhD student at ICH has been great. I shall look back on these years with great fondness. It has been a wonderful environment for learning, and the diverse array of characters on the seventh floor over the years has been extraordinary, leading to many new experiences and friends! I should like to give a special mention to the 'friends of the Percy'; Carles Gaston, Ailish Murray, Gemma Brindley, Paul O'Neill, Vicky Reed, Gustavo Sajnani, Jean-Marie Delalande, Alan Burns, Sarah Reid (Greenwood), Clare Faux and Adam Wallace.

On a more personal note, the encouragement and emotional (and financial) support from my parents John and Alana, and my sisters has been invaluable. Their help and input through these years have enabled me to achieve all that I have wanted. My love and thanks to them. Thanks to my long suffering flat-mate Helen Moore, her support and belief were continuous and the hours spent listening to my grumbling were above and beyond a flat-mates duty!

My final mention goes to Patrick who was my saving grace, my sanity. Thank you.

Dedication

To my family,

Mum,

Dad,

Leeann,

Joanna,

Alana-Naomh,

Katie-George

and

Rebecca.

xxx

CHAPTER 1; INTRODUCTION

1.1 NEURULATION

In vertebrates, formation of the primordium of the central nervous system, the neural tube, occurs by a process referred to as neurulation. This process begins with the induction of a subset of ectodermal cells along the dorsal midline of the embryo, which subsequently segregate and thicken to form the neural plate. The neural plate then undergoes a number of morphological changes that result in the formation of the neural tube. Impairment of this process results in a group of anomalies termed neural tube defects (NTD).

The molecular mechanisms underlying neurulation are not yet completely understood, however, the morphological process has been described in detail in both chick and mouse (Schoenwolf and Smith, 1990;Shum and Copp, 1996;Morriss-Kay *et al.*, 1994). There are two phases of neurulation in the developing vertebrate embryo, termed primary and secondary neurulation. Primary neurulation results in the formation of the neural tube in the cranial and upper spinal regions of the embryo. The lateral edges of the neural plate elevate to form neural folds. This elevation continues until the apical tips of the neural folds are apposed when they then fuse along the dorsal midline to form a tube. Secondary neurulation occurs later in development after primary neurulation is complete; condensation of mesenchymal cells in the tailbud of the embryo is followed by cavitation that results in the creation of the neural tube at the low sacral and coccygeal levels (Schoenwolf, 1984). Although the mechanisms of neural tube formation differ between the two phases, the transition between primary and secondary neurulation results in a continuous tube along the body axis of the embryo. All cranial NTD and open spina bifida arise from defects during primary neurulation in both mouse

and humans (Copp and Brook, 1989;Müller and O'Rahilly, 1987). Therefore, this study concentrates on the period of development in which primary neurulation occurs.

1.1.1 Primary neurulation

In mouse embryos, primary neurulation is a discontinuous process with closure of the neural tube starting at a number of *de novo* initiation sites along the neural tube (Sakai, 1989). The first initiation site, termed closure 1, is at the level of the second and third somites of embryos with 4-6 somites. Closure then continues in a `zippering' action in both cranial and caudal directions. After closure 1, two further sites of initiation, termed closure 2 and closure 3, occur when embryos typically have 11 and 12 somites respectively. Fusion from the site of closure 2 at the forebrain/midbrain boundary, continues in both caudal and rostral directions. Closure 3 is situated at the extreme rostral end of the neural tube and further closure occurs in a caudal direction. (Figure 1.1).

The areas of neural folds that remain open after fusion at the initiation sites are termed neuropores. These neuropores gradually shorten and close as neurulation proceeds, resulting in an intact closed tube. The anterior neuropore (ANP), formed in the forebrain region between closures 2 and 3, closes at around the 15/16-somite stage of development. Closure of the hindbrain neuropore (HNP), formed between closures 1 and 2, is completed at the 16/17-somite stage of development. The final neuropore located at the posterior end of the embryo, referred to as the posterior neuropore (PNP), closes when the embryo has approximately 29 somites (Copp *et al.*, 1990) (Figure 1.1). The exact timing and duration of these events can vary between mouse strains

(MacDonald et al., 1989;Golden and Chernoff, 1993), and the timing given here is therefore for an 'average' mouse strain (Copp *et al.*, 1990).

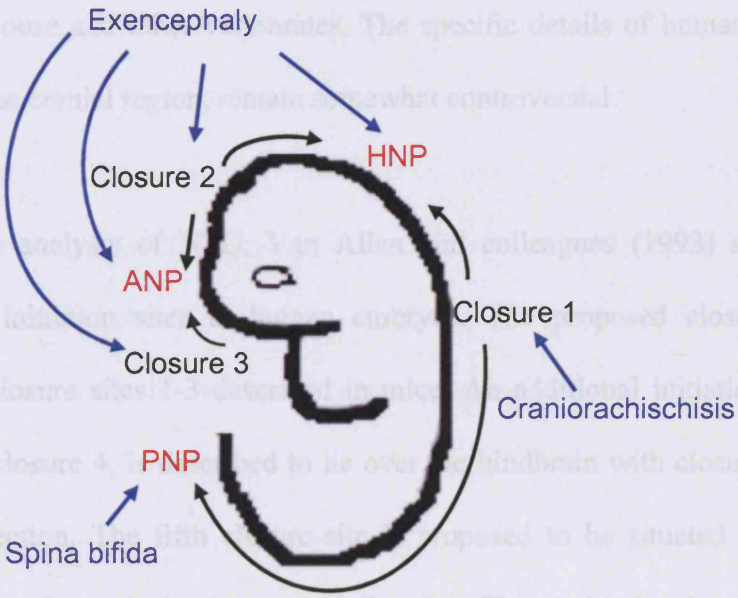

Figure 1.1 The three sites of initiation of neural tube closure in mouse

Diagram to illustrate the three sites of initiation of neural tube closure (black text), the direction closure proceeds in (black arrows) and the three neuropores formed during primary neurulation (red text). The main subtypes of NTD, which result from a failure of closure initiation or failure to complete closure of a neuropore, are shown in blue (Copp and Bernfield, 1994). Abbreviations: ANP, anterior neuropore; HNP, hindbrain neuropore; PNP, posterior neuropore.

Neurulation has been described as a multi-step process, with initiation of closure occurring at a number of *de novo* sites in many other vertebrates including rabbit (Peeters *et al.*, 1998b), chick (Van Straaten *et al.*, 1996) and pig (Van Straaten *et al.*, 2000). Analysis of human NTD has suggested that neural tube closure in humans

involves *de novo* initiation at multiple sites in a similar manner to that seen in mouse neurulation (Van Allen *et al.*, 1993; Martinez-Frias *et al.*, 1996). Most studies to date have investigated the positions of NTD in regard to the multi-site closure theories described for mouse and other vertebrates. The specific details of human neurulation, particularly in the cranial region, remain somewhat controversial.

Thus, based on analysis of NTD, Van Allen and colleagues (1993) suggested the presence of 5 initiation sites in human embryos. The proposed closure sites 1-3 correspond to closure sites 1-3 described in mice. An additional initiation site in the cranial region, closure 4, is described to lie over the hindbrain with closure continuing in a rostral direction. The fifth closure site is proposed to be situated at the caudal extremity of the embryo closing in a rostral direction. This multi-site closure theory was supported by Martinez-Frias and colleagues (1996) after the investigation of 744 live-born infants with NTD. A further study of cranial NTD (Golden and Chernoff, 1995) supported Van Allen's model of multi-site closure. However, analysis of 'normal' neurulation in early human embryos (Carnegie stages 10-12) provided evidence to support a 3 site closure model (Nakatsu *et al.*, 2000). In this model the sites of closure initiation correspond to the three closure sites described in mouse neurulation except closure 2 is in a more caudal position at the midbrain-hindbrain border. The authors also related this model to the various types of NTD exhibited in human embryos. A more recent study, again using 'normal' human embryos at the time of neural tube closure has suggested a 2 site closure model, corresponding to mouse closure sites 1 and 3 (O'Rahilly and Müller, 2002). The authors also describe the presence of accessory loci of fusion, that is small, variable points of fusion observed in a small number of embryos

usually in the hindbrain region. These could represent the closure 2 site classified by the Nakatsu study, however, whether these fusion points are consistent in occurrence or position remains contentious and they were not classified as initiation sites by O'Rahilly and Muller.

Although there are discrepancies in the exact position and number of fusion sites during neural tube closure in human embryos, there is a large body of evidence to support a model of multi-site closure of the human neural tube. Perhaps definite patterns will become apparent as more early embryo samples are examined.

1.2 MECHANISMS OF PRIMARY NEURULATION

Different mechanisms are involved in the closure of the neural folds along the cranio-caudal axis of the mouse embryo and, in particular, there are differences between cranial and spinal neural tube closure.

1.2.1 Cranial neurulation

The presumptive brain region of the neural plate is wider than the presumptive spinal region in vertebrate embryos, and this is more pronounced in mammalian embryos. Different mechanisms may be needed in the presumptive brain region to allow closure to occur from a wider starting position and to overcome cranial flexure, ventral bending of the cranial region that occurs throughout cranial neurulation in mammals (Kaufman, 1979;Morriss-Kay *et al.*, 1994). Neurulation in the cranial region of mammals has been described as a two-stage process. The first stage appears to be unique to the cranial

region of mammalian embryos, whereas the second stage is similar to the neurulation process in more caudal regions of the neural tube (Morriss and Solursh, 1978b;Copp *et al.*, 2003b). The first stage involves the formation of bihemispherical neural folds. During cranial neurulation the neural folds enlarge and initially bend outwards with the cranial flexure (Kaufman, 1979) resulting in a biconvex morphology. During the first stage of cranial neurulation the neural folds 'flip around' from the biconvex morphology to become biconcave (Figure 1.2).

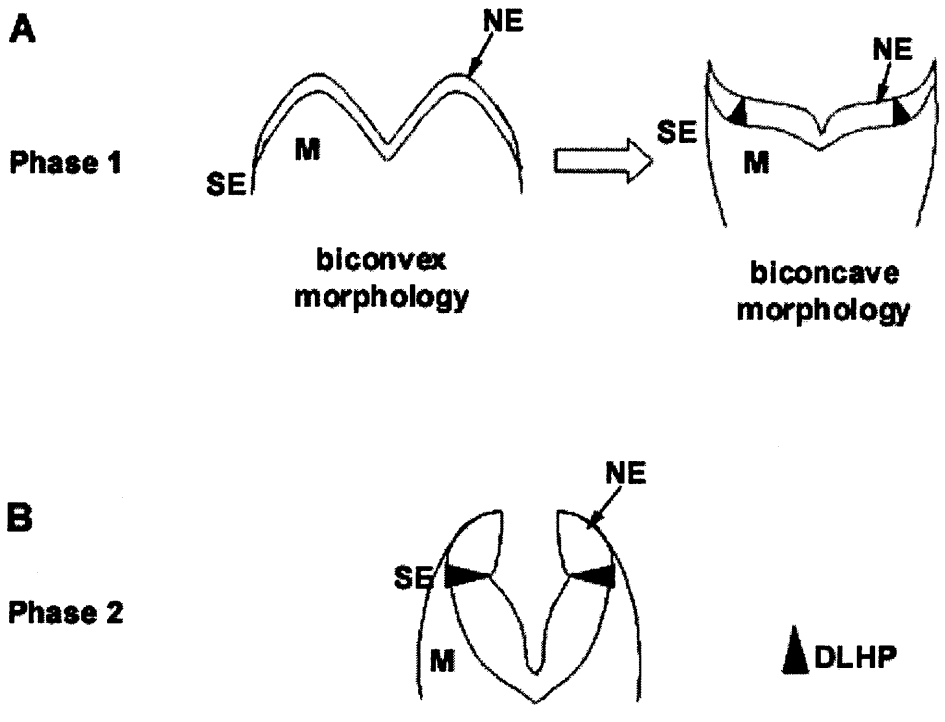

Figure 1.2 The two phases of cranial neurulation in mammals

The first phase of cranial neurulation in mammalian development (**A**) is unique and involves the formation of bihemispherical neural folds, first showing a biconvex morphology followed by a biconcave morphology. The second phase (**B**) is similar to the neurulation process seen in the spinal region. Abbreviations: DLHP, dorsolateral hinge points; M, mesenchyme; NE, neural epithelium; SE, surface ectoderm.

The forebrain neuroepithelium expands greatly during cranial neurulation through internal cell division and cell migration from the presumptive midbrain and hindbrain regions (Tuckett and Morriss-Kay, 1985). The midbrain and hindbrain neural epithelium cell number stays constant throughout neurulation. Although cell division occurs, the mitotic spindles are oriented parallel to the anterior-posterior axis of the embryo resulting in longitudinal growth (Morriss-Kay, 1981;Tuckett *et al.*, 1985). Changes in cell arrangement in both the neural epithelium and the underlying mesenchyme occur while the neural folds are in the initial biconvex morphology, these changes lead to the flipping of the neural folds to the biconcave morphology. The organisation of the neuroepithelium changes from columnar to a pseudostratified appearance, which subsequently thickens (Morris-Wiman and Brinkley, 1990). The mesenchyme undergoes a large expansion that includes both an increase in cell number and intercellular space (Morriss *et al.*, 1978b). Changes in cell orientation in the cranial mesenchyme also occur, from a random distribution to an arrangement where the cells lie parallel to the neuroepithelial basal lamina (Morris-Wiman *et al.*, 1990). In addition, a hyaluronate-rich extracellular matrix accumulates around the mesenchymal cells during this stage of cranial neurulation (Morriss and Solursh, 1978a). The second stage of cranial neurulation involves the medial convergence, apposition and fusion of the tips of the neural folds to form a closed neural tube. During the 'flipping' process, bending regions of lateral neuroepithelium, dorsolateral hinge points, are formed which then, as the folds elevate, allow the lateral edges of the neural folds to move medially and subsequently allow apposition and fusion to occur (Morris-Wiman *et al.*, 1990) (Figure 1.2).

During cranial neurulation, as neural tube closure continues from closure initiation site 1 into the hindbrain region, the apposition and fusion of the neural folds at the forebrain-midbrain boundary (closure 2) and fusion of the folds at the rostral extremity (closure 3) also occur (Section 1.1.1). The exact position of closure 2 varies in different mouse strains (Juriloff *et al.*, 1991) and this can affect the susceptibility of the strain to developing exencephaly. A more rostral position of closure 2 confers greater susceptibility to the development of cranial NTD (Fleming and Copp, 2000). It has been suggested that closure 2 is not present at all in one mouse strain (SELH/Bc), leaving the embryos highly susceptible to developing exencephaly with a spontaneous cranial NTD incidence of 10-20% (Gunn *et al.*, 1995).

1.2.2 Spinal neurulation

Closure of the neural tube in the spinal region occurs in a similar manner to the second phase of cranial neurulation, that is the neural folds elevate, appose and fuse along the midline. However, the neuroepithelial morphology in spinal neural tube closure differs along the longitudinal axis of the mouse embryo (Shum *et al.*, 1996) suggesting different mechanisms of closure are involved as translocation of the posterior neuropore (PNP) proceeds in a cranio-caudal direction. There are three modes of closure that differ in the number and location of specific bending sites seen in the neuroepithelium, and vary with the position of the PNP along the axis of the embryo.

In mode 1 the neuroepithelium bends only in the region above the notochord, forming a median hinge point. Mode 1 neurulation can be seen at the PNP of embryos at the 8-15 somite stages and results in a slit-like lumen of the neural tube. Mode 2 occurs at the 16-

23 somite stages of development and, in addition to a median hinge point, the neuroepithelium also bends at paired lateral sites, referred to as dorso-lateral hinge points, resulting in a diamond shaped lumen. From the 24 somite stage onwards, mode 3 closure is observed at the PNP. In mode 3, specific bending of the neuroepithelium only occurs at the dorso-lateral hinge points resulting in a round lumen (Figure 1.3) (Shum *et al.*, 1996).

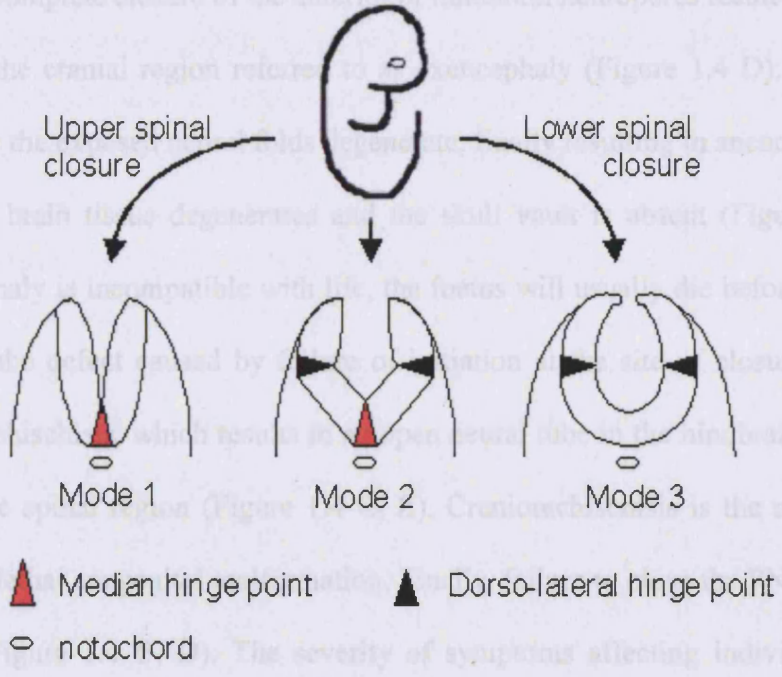

Figure 1.3 Morphological modes of neural closure in the PNP

Diagram to illustrate the three modes of closure of the neural tube at the PNP, at different axis levels in primary neurulation of mouse. (Adapted from (Ybot-Gonzalez *et al.*, 2002)).

1.3 NEURAL TUBE DEFECTS

NTD are among the most common congenital malformations in humans with an incidence of approximately 0.5-3 in every 1000 births although there is considerable variation in incidence world-wide (Copp *et al.*, 1994). The term NTD covers a range of anomalies that can result from a failure of one or a number of initial closure events or a failure to complete closure of a neuropore. There are three main subcategories of NTD which occur at different axial levels of the embryo. Failure of initiation at closures 2 or 3 and incomplete closure of the anterior or hindbrain neuropores result in an open neural tube in the cranial region referred to as exencephaly (Figure 1.4 D). As development proceeds the exposed neural folds degenerate, finally resulting in anencephaly where the exposed brain tissue degenerates and the skull vault is absent (Figure 1.4 A). Since anencephaly is incompatible with life, the foetus will usually die before or at birth. The neural tube defect caused by failure of initiation at the site of closure 1 is known as craniorachischisis, which results in an open neural tube in the hindbrain and throughout the entire spinal region (Figure 1.4 C, E). Craniorachischisis is the most severe NTD and is a lethal congenital malformation. Finally, failure to close the PNP results in spina bifida (Figure 1.4 B, D). The severity of symptoms affecting individuals with spina bifida is dependent on the type and position of the lesion but generally affect the musculoskeletal, gastrointestinal and urinary systems (Harding and Copp, 2002).

1.4 CAUSES OF NTD IN HUMANS

The cause of most NTD in humans is believed to be multifactorial involving both environmental and genetic influences. Changes in the prevalence of NTD in different

Figure 1.4 Neural tube defects in humans and mice

Human newborns illustrate the appearance of anencephaly (**A** dorsal view figure adapted from Volpe (1995)), spina bifida (**B** dorsal view courtesy of Prof. A.J.Copp) and craniorachischisis (**C** lateral view courtesy of Prof A.J.Copp). In craniorachischisis, the region of open neural tube extends from the forebrain to the lower spine (**C** black arrows). Mouse foetuses at E15.5 also illustrate the various types of NTD. A *curly tail* mutant with open regions of neural tube in the cranial region, exencephaly (**D,** flanked by white arrows) and caudal region, spina bifida (**D,** flanked by white arrowheads). Craniorachischisis is shown in a *Celsr1* mutant (**E**), where the neural tube is open from the midbrain to the lower spinal region (**E**, white arrows). Asterisks in **D** and **E** highlight curly tails in both mutants. **D** and **E** are adapted from Copp *et al.* (2003b).

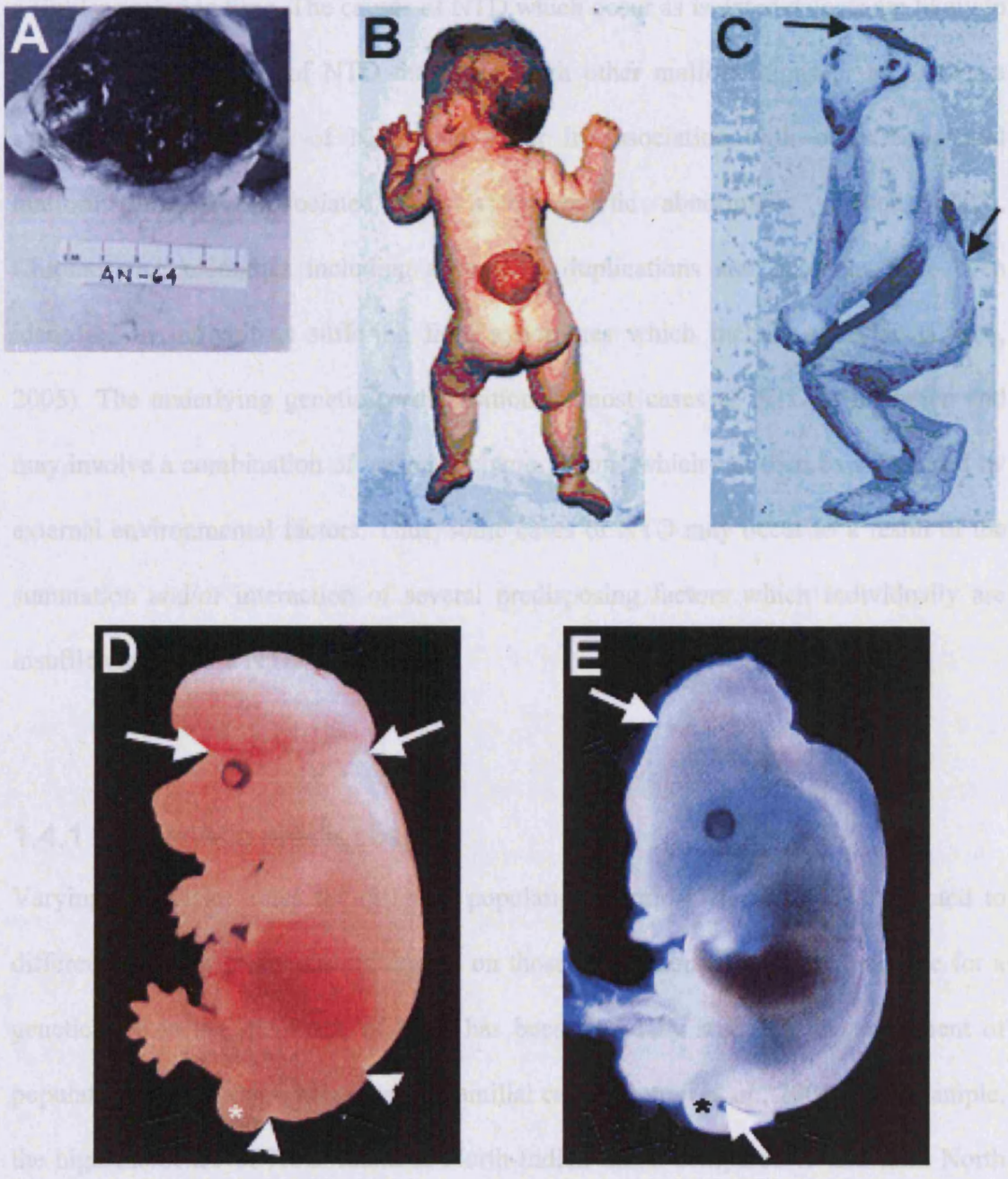
A
AN-64
B
C
D
E

populations indicate that there is heterogeneity in the aetiology of NTD. For example, the incidence ranges from 1.0 in 1000 births, in Paris (EUROCAT Working Group, 1991), to 10.6 in 1000, in Shanxi Province in the north of China (Xiao *et al.*, 1990) over a similar period in time. The causes of NTD which occur as isolated defects are likely to differ from the causes of NTD that occur with other malformations or as part of a syndrome. Up to 24% of NTD that occur in association with other congenital malformations are associated with a cytogenetic abnormality (Lynch, 2005). Chromosome anomalies including aneuplody, duplications and deletions have been identified in individuals suffering from syndromes which include an NTD (Lynch, 2005). The underlying genetic predisposition in most cases of NTD is unknown and may involve a combination of various polymorphisms which can then be influenced by external environmental factors. Thus, some cases of NTD may occur as a result of the summation and/or interaction of several predisposing factors which individually are insufficient to cause NTD.

1.4.1 Genetic predisposition

Varying prevalence rates for different populations world-wide could be attributed to differences in environmental influences on those populations. However, evidence for a genetic role in the incidence of NTD has been found by studying the movement of populations and through investigating familial cases (Detrait *et al.*, 2005). For example, the high incidence of NTD found in North-Indian Sikhs compared to non-Sikh North Indians (Verma, 1978) is believed to be due to genetic factors, as this elevated prevalence continues in Sikh communities that have migrated to a different area of the world (British Columbia, Canada) (Hall *et al.*, 1988;Baird, 1983). In addition, a study of

the prevalence of NTD in a number of ethnic groups in Boston, Massachusetts showed higher prevalence rates in those with Irish ancestry than the Jewish population reflecting the higher prevalence rates in Ireland compared to Israel (Naggan and MacMahon, 1967).

Investigations into familial cases have shown that there is an increased risk of an NTD affected pregnancy following a previous affected pregnancy, referred to as the recurrence risk. The recurrence risk for siblings varies between different populations and is related to the occurrence risk (Carter and Evans, 1973;Carter *et al.*, 1968). Populations with a relatively high occurrence risk, Britain and Ireland, have a sibling recurrence risk of up to 5% (Elwood and Elwood, 1980) whereas populations with a low occurrence risk, white infants in North America, have a lower recurrence risk of 1.7% (Holmes *et al.*, 1976). In addition, a study in a low incidence population in New York State (data collected between 1950-1974) showed that the recurrence risk is higher in concordant twins (6.8%) than full siblings (1.8%) which have a higher risk than half-siblings (0.8%), that share one parent, suggesting that NTD follow a polygenic mode of inheritance (Janerich and Piper, 1978). Moreover, the occurrence of NTD among first-, second-, and third-degree relatives of probands in the USA were 3.2%, 0.5%, and 0.17% respectively (Toriello and Higgins, 1983), all of which were elevated compared to the general population occurrence rate of 0.12%, again suggesting genetic influences are involved in the aetiology of NTD.

Further evidence for a genetic influence on the aetiology of NTD is the higher prevalence rate in females compared to males. This observation has been made in many

different populations (Xiao *et al.*, 1990;Naggan *et al.*, 1967;Sever, 1982;Carter *et al.*, 1968;Carter *et al.*, 1973;Snyder *et al.*, 1991). When NTD were categorised according to the axial level of the lesion there was a preponderance among females at all levels except in low spinal regions where there was a male excess (Seller, 1987). The reasons behind an increased predisposition for females to develop NTD more often than males are not known. One theory suggested a difference in growth rates between the sexes in which neurulation occurred over a longer time period in females, rendering them more susceptible to neurulation problems (Seller, 1987). However, a subsequent study in mice showed that although males are more advanced than their female littermates, the duration of neurulation was similar in both sexes (Brook *et al.*, 1994).

1.4.2 Environmental influences

In addition to genetic susceptibility a number of environmental factors are believed to affect the prevalence rates of NTD. These include seasonal trends, variations in geographic area, social class, maternal age and reproductive history, maternal illness, exposure to toxins and maternal nutrition. Obviously, several of these factors are inter-related and it should also be noted that there are likely to be differences in accuracy of diagnosis and reporting between studies.

The different prevalence rates throughout the world could be due to differences in local environmental influences. One trend that may be due to the effect of environmental factors on the aetiology of NTD is the declining prevalence rate of NTD detected over the last century in Britain and the USA. In Britain, the prevalence fluctuated from 2 per 1,000 births in 1936-7 to a peak of 2.8 per 1,000 in 1940. This was followed by a drop

to 1.54 per 1,000 births in 1948 and then another peak in 1956 of 2.8 per 1,000 births. (Leck, 1966). Records for the prevalence of NTD in America also show fluctuations with a peak in NTD incidence in 1932 of 5 per 1,000 births rising from a steady rate of 2 per 1,000 between 1890-1920 (MacMahon and Yen, 1971). The prevalence of NTD has continued to decline in both these populations (Janerich, 1973;Stone, 1987;Snyder *et al.*, 1991), and a number of possible explanations have been suggested. The screening and termination of NTD affected pregnancies has often been believed to account for declining rates of NTD births. However, the decline in NTD prevalence in North America began before screening was available (Yen *et al.*, 1992). In addition, a decline of 52% in the rate of perinatal mortality from anencephaly was recorded in the Republic of Ireland between 1974-82 even though screening and termination of affected foetuses was not available (Kirke and Elwood, 1984). Moreover, a decline in total prevalence rate (including terminations, still-births and live-births) was detected in the UK between 1984-96, indicating a decrease in NTD prevalence that is unrelated to prenatal diagnosis and termination (Rankin *et al.*, 2000). The exact reason for the decline in NTD prevalence has not been established but may be due to changes in maternal nutrition or other environmental factors.

The socio-economic status of the proband's family, usually determined by father's occupation, has been associated with NTD. For example, an increased NTD prevalence was associated with lower socio-economic status in Boston, USA, in a number of different ethnic groups (Naggan *et al.*, 1967). Seasonal variation in the prevalence of NTD has also been reported in some studies. Within each country in the UK, seasonal peaks for the development of anencephaly were observed in May-June and spina bifida

in July over a number of years (Maclean and MacLeod, 1984). Another study described a higher prevalence of NTD for conceptions in February to April in Greater London (Carter *et al.*, 1973), although, seasonal variation in NTD prevalence has not been detected in all studies (Sever, 1982).

In some ethnic groups, the prevalence of NTD in the descendants of migrants changes to the prevalence of the adoptive countries rather than their ancestral home which suggests environmental factors in either country may have an effect on the NTD prevalence rate. For example, the prevalence among Bostonians of Irish ancestry is lower than that of Irish-born mothers in Boston (Naggan *et al.*, 1967).

Reproductive history and birth order have also been suggested to play a role in the prevalence rate of NTD. In a number of studies carried out in Britain, a 'U'-shaped risk pattern of maternal age was found, with a higher risk factor in the youngest and oldest mothers (Carter *et al.*, 1968;Carter *et al.*, 1973). A U-shaped curve was also described for birth order risk in many different ethnic groups in Boston, USA (Naggan *et al.*, 1967). In particular, there appears to be an elevated risk of NTD in the first pregnancy (Carter *et al.*, 1968;Carter *et al.*, 1973;Janerich *et al.*, 1978).

Maternal illness during the period of neurulation has been associated with an increased risk of the embryo developing an NTD. Embryos of diabetic mothers are up to 21 times more likely to develop an NTD than control embryos (Zacharias *et al.*, 1984). Several factors may contribute to the occurrence of diabetes-associated NTD, including elevated levels of glucose and free radicals (Loeken, 2005). In addition, a retrospective study

discovered a two- to four-fold increase in risk for NTD-affected offspring in mothers who had a fever or febrile illness within the first trimester of pregnancy, suggesting that hyperthermia can increase the risk of NTD (Suarez *et al.*, 2004). Maternal exposure to toxins has also been suggested to induce NTD. Consumption of blighted potatoes or fumonisin-contaminated maize have both been associated with temporal periods and geographical areas of high NTD prevalence (Renwick, 1972;Marasas *et al.*, 2004).

A number of the environmental factors that are believed to play a role in the aetiology of NTD in humans could be related to maternal nutrition. The peaks of prevalence in the US (1930s) and Britain (early 1940s, mid 1950s) could be due to poor maternal nutrition during the Great Depression (US) (MacMahon *et al.*, 1971) or as children during the World Wars (Britain) (Stone, 1987). Improvements in maternal nutrition during the last five decades may account for the continued decline in NTD prevalence observed in both US and British populations (Yen *et al.*, 1992). Variation in maternal intake of nutrients could also relate to seasonal variations and the impact of socio-economic status on the risk of NTD. Smithells et al. (1977) found lower intakes of all nutrients in mothers of lower social classes. Particular nutrients that have been studied with regard to the aetiology of NTD include folic acid and vitamin B_{12} (Section 1.9).

In considering a multifactorial aetiology for NTD, in which both genetic and environmental factors play a role, the initial prevalence rate of each population may need to be taken into account. For example, it has been hypothesised that in low prevalence populations environmental influences are less important than in high prevalence areas (Janerich *et al.*, 1978). For example, in an area of low prevalence of

NTD there were no detectable associations between NTD-affected births and seasonal or annual variation, maternal age or parity and fathers occupation (socio-economic status) (Sever, 1982). In this population, differences in sex ratios, a high concordant rate in twins and differences between racial groups were detected, illustrating clearly that genetic influences are involved in the aetiology of NTD. In areas of high prevalence the influence of genetic factors are not as apparent, possibly due to the effect of environmental factors on the incidence of NTD (Carter *et al.*, 1968). In addition, greater fluctuations in the prevalence rate from year to year have been detected in high prevalence populations compared to low prevalence populations over the same time period (EUROCAT Working Group, 1991) possibly indicating the greater influence of environmental factors.

1.5 THE MOUSE AS AN EXPERIMENTAL MODEL FOR NTD

A large number of genetic mutant mouse strains exhibit NTD. These include models that arose spontaneously and models that were generated experimentally (Copp *et al.*, 2003b).

1.5.1 The full spectrum of NTD is represented in mouse

Mouse models are available that exhibit the different subsets of NTD resulting from failure of different neurulation events. The majority of NTD mouse models exhibit exencephaly either alone, as observed in *Cited-2* null mutants (Martinez-Barbera *et al.*, 2002) or together with caudal NTD as seen in *splotch* (*Sp*) mice (Auerbach, 1954). The *looptail* (*Lp*) mouse has a mutation in the *Vangl2* gene that results in the most severe

type of neural tube defect, craniorachischisis (Murdoch *et al.*, 2001;Kibar *et al.*, 2001) arising from the failure of initiation at the site of closure 1. Spina bifida can be exhibited either alone, as observed in *Vacuolated lens* (*vl*) mice (Wilson and Wyatt, 1988) or with exencephaly (as in *splotch* (*Sp*) mice).

1.5.2 Genetic and environmental influences affect the incidence of NTD in mouse models

Causes of NTD in humans are thought to be multifactorial. This is reflected in mouse models such as *curly tail* (*ct*) (Seller and Adinolfi, 1981), in which the incidence of NTD is affected by genetic and environmental factors. In this strain the penetrance of spinal NTD varies considerably depending on the genetic background (Gruneberg, 1954;Neumann *et al.*, 1994) and is influenced by exogenous agents such as retinoic acid (Chen *et al.*, 1994) or inositol (Greene and Copp, 1997;Cogram *et al.*, 2004).

In addition to genetic mouse models, a number of teratogen-induced NTD mouse models may also be useful to study the process of neurulation or the development of NTD. Post-conceptional exposure to valproic acid (VPA), an anti-convulsant agent, induces NTD in mouse embryos (Kao *et al.*, 1981), mirroring the effect of VPA administration on human embryos (Robert and Guidbaud, 1982). NTD can also be induced in mice by environmental influences such as brief maternal hyperthermia (Shiota, 1988). Moreover, genetic background can affect responses to environmental factors as may be the case in human NTD. For example, the ability of maternal hyperthermia to induce cranial NTD varies in different strains of mice. In one study, identical treatment of different mouse strains resulted in exencephaly incidences ranging

from 44% (SWV) to 0% (DBA/2J) (Finnell *et al.*, 1986). Reciprocal crosses between sensitive and insensitive strains showed that it was the embryo genotype, not the maternal genotype, that influenced the susceptibility to heat-induced NTD. Differences in the rate of teratogen-induced cranial NTD between mouse strains may be related to strain differences in the position of closure 2 (Section 1.2.1) (Fleming *et al.*, 2000).

With a plethora of mutant mouse models available, the mouse is an excellent system to investigate the molecular mechanisms of mammalian neural tube closure and defects. Another advantage of mice as an experimental model is the ability to manipulate environmental factors that may affect neural tube closure, especially through the technique of whole embryo culture. This technique permits investigations into the direct effect of environmental/nutritional factors on neural tube closure in the embryo, without the added complexity of maternal metabolism.

1.6 GENETIC AND CELLULAR MECHANISMS IN NORMAL NEURULATION

Studies in mouse models have highlighted some genetic pathways and mechanisms required for neurulation to occur (Table 1.1).

1.6.1 Different mechanisms are involved in neural tube closure along the cranial-caudal axis of the embryo

Genetic analysis of NTD in mice provides evidence to support the theory that different mechanisms of neural tube closure are involved at different axial levels of the embryo,

both in terms of the molecular requirements and the morphological events. Different mutations give rise to cranial and/or caudal NTD (Section 1.5.1) suggesting that specific gene products are required for neural tube closure at different levels along the body axis. In addition, disruption of neurulation by teratogens may also show different effects on cranial versus spinal neural tube closure (Section 3.1). This is perhaps not surprising, as *de novo* initiation most likely involves different processes to continuation or completion of closure at the neuropores. Moreover, the embryo continues to develop while neurulation progresses, such that the extrinsic factors affecting the neural tube may differ throughout neurulation.

1.6.2 Factors involved in cranial neurulation – evidence from mouse models

1.6.2.1 Cranial mesenchyme

The first phase of cranial neurulation in mammalian embryos involves the expansion of the mesenchyme underlying the neural folds. This expansion is believed to have a mechanical role in supporting the neural folds in preparation for apposition and fusion and is driven by an increase in both mesenchymal cell number and extracellular matrix volume (Morriss *et al.*, 1978b). Exposure of neurulation stage rat embryos to excess Vitamin-A results in reduced numbers of mesenchyme cells and 'floppy' neural folds that fail to appose and fuse resulting in exencephaly (Morriss and Steele, 1974). Exencephaly also occurs in association with a reduction of the number of mesenchymal cells in genetic mouse models (Table 1.1) such as *Twist* and *Cart1* deficient mice (Chen and Behringer, 1995;Zhao *et al.*, 1996). In addition to the number of mesenchymal cells

Mutant name	Type of NTD	Gene mutated	Mutation	Protein function	Possible mechanism	References
					Dysregulated apoptosis	
AP2α	Ex	AP2α	Null	Transcription factor	Increased apoptosis in cranial mesenchyme, and HB and MB NE	(Schorle *et al.*, 1996)
Apaf1 and fog	Ex and/or SB	*Apaf1*	Apaf1 –null fog – aberrant mRNA processing, greatly reduced mRNA, protein and activity	Apoptosis activating factor	Reduced apoptosis and increased cell proliferation	(Harris *et al.*, 1997;Yoshida *et al.*, 1998;Honarpour *et al.*, 2001)
Apolipoprotein B	Ex	*Apob*	Truncated protein – 50% reduction in circulating cholesterol	Plasma lipoprotein	Increased apoptosis in HB NE	(Homanics *et al.*, 1995)
Bcl10	Ex	*Bcl10*	Null	Regulator of NF-κB activation	Increased apoptosis in HB NE	(Ruland *et al.*, 2001)
Bmp5/Bmp7	Ex	*Bmp5,* *Bmp7*	Null Null	Signalling proteins	Reduced apoptosis	(Solloway and Robertson, 1999)
Brca1	Ex and SB	*Brca1*	Null	Transcription factor	Increased apoptosis in HB NE and increased proliferation in luminal NE	(Gowen *et al.*, 1996)
Caspase 9	Ex	*Casp9*	Null	Cysteine-containing, aspartate-specific protease	Reduced apoptosis	(Kuida *et al.*, 1998)

Cited2	Ex	*Cited2*	Null	Transcriptional coactivator	Increased apoptosis in MB region	(Bamforth *et al.*, 2001;Martinez-Barbera *et al.*, 2002)
IKK1/IKK2	Ex	*Chuk*, *Ikbkb*	Null Null	Kinases activating NF-κB transcription factors	Increased apoptosis	(Li *et al.*, 2000)
Jnk1/Jnk2	Ex	*Mapk8*, *Mapk9*	Null Null	c-Jun-N-terminal kinases	Increased apoptosis in HB NE and reduced apoptosis in FB NE	(Kuan *et al.*, 1999)
Mdm4	Ex	*Mdm4*	Null	p53-dependant cell cycle regulation	Increased apoptosis	(Migliorini *et al.*, 2002)
MEKK4	Ex and/or SB/CT	*MEKK4*	Null	Mitogen-activated protein kinase kinase kinase	Increased apoptosis in NE	(Chi *et al.*, 2005)
Ski	Ex	*ski*	Null	Transcription factor	Increased apoptosis in cranial NE and cranial mesenchyme	(Berk *et al.*, 1997)
Telomerase RNA	Ex and SB	*Terc*	Null	Component of the telomerase reverse transcriptase complex	Increased apoptosis	(Herrera *et al.*, 1999)
Treacle	Ex	*Tcof1*	Heterozygous; loss of a single allele	Nucleolar phosphoprotein	Excessive apoptosis in the neural tube and cranial region	(Dixon *et al.*, 2000)
Tubby-like protein 3	Ex and SB	*Tulp3*	Unknown; C-terminal deletion	Unknown	Increased apoptosis in ventral region of HB NE and caudal neural tube	(Ikeda *et al.*, 2001)

					Aberrant proliferation	
Curly tail	Ex and SB	*Grhl-3?*	Unknown; 30% reduction of *Grhl-3* expression in *ct/ct*	Transcription factor	Defective ventral cell proliferation	(Van Straaten and Copp, 2001;Ting *et al.*, 2003)
n-cofilin	CRN	*n-cof*	Null	F-actin depolymerising factor	Reduced cell proliferation in NE	(Gurniak et al., 2005)
					Disrupted cytoskeleton	
Abl/Arg	Ex	*Abl1, Abl2*	Null Null	Non-receptor tyrosine kinases	Disrupted apical neuroepithelial actin distribution	(Koleske *et al.*, 1998)
MARCKS	Ex	*Macs*	Null	cytoskeleton-related protein	Disrupted cytoskeletal function	(Stumpo *et al.*, 1995)
MARCKS-related protein	Ex with/ without SB	*Mlp*	Null	cytoskeleton-related protein	Disrupted cytoskeletal function	(Wu *et al.*, 1996)
Mena/profilin1	Ex	*Enah, Pfn1*	Null for Mena, heterozygous for profilin 1	Regulation of actin polymerisation	Disrupted cytoskeletal function	(Lanier *et al.*, 1999)
RhoGAP P190	Ex	*Grlf1*	Truncated protein; loss-of-function	Glucocorticoid-receptor DNA-binding factor	Disrupted neuroepithelial actin distribution	(Brouns *et al.*, 2000)
Shroom	Ex and SB	*shrm*	Null	F-actin binding cytoskeletal protein	Disturbed F-actin localisation	(Hildebrand and Soriano, 1999)

Vinculin	Ex	*Vcl*	Null	Cytoskeletal protein	Disrupted cytoskeletal function; cell migration and adherence	(Xu *et al.*, 1998)
					Abnormal cranial mesenchyme	
Cartl	Ex	*Cartl*	Null	Transcription factor	Reduced cranial mesenchyme	(Zhao *et al.*, 1996)
Twist	Ex	*Twist*	Null	Transcription factor	Reduced cranial mesenchyme	(Chen *et al.*, 1995)
					Defective planar cell polarity pathway	
Circle tail	CRN	*Scrb1*	Frameshift mutation; unknown result	Cytoplasmic protein with a role in apico-basal polarity	Defective planar cell polarity	(Murdoch *et al.*, 2003)
Crash	CRN	*Celsr1*	Point mutation; disrupted function	Transmembrane non-classical cadherin	Defective planar cell polarity	(Curtin *et al.*, 2003)
Dishevelled 1 and 2	CRN	*Dvl1* *Dvl2*	Null Null	Cytoplasmic proteins	Defective planar cell polarity	(Hamblet *et al.*, 2002)
Loop-tail	CRN	*Vangl2*	Null	Transmembrane protein	Defective planar cell polarity	(Murdoch *et al.*, 2001)
					Other suggested mechanisms	
Eph-A7	Ex	*Epha7*	Null	Receptor tyrosine kinase	Defective neural fold fusion	(Holmberg *et al.*, 2000)
Ephrin-A5	Ex	*Efna5*	Null	Receptor tyrosine kinase	Defective neural fold fusion	(Holmberg *et al.*, 2000)

Folate-binding protein 1	Ex	*Folbp1*	Null	folate transport	Reduced folate availability	(Piedrahita *et al.*, 1999)
Hairy	Ex	*Hes1*	Null	Transcription factor	Premature neuronal differentiation in FB	(Ishibashi *et al.*, 1995)
Numb	Ex	*Numb*	Null	Membrane-bound protein involved in asymmetric cell division	Premature neuronal differentiation in FB	(Zhong *et al.*, 2000)

Table 1.1 Mouse genetic models of NTD with suggested underlying mechanisms

Abbreviations: CRN, craniorachischisis; CT, curly tail; Ex, exencephaly; FB, forebrain; HB, hindbrain; MB, midbrain; NE, neuroepithelium; SB, spina bifida.

present in the cranial region, the integrity of extracellular matrix surrounding the cranial mesenchyme may also play an important role in cranial neurulation (Morriss-Kay and Crutch, 1982).

1.6.2.2 Actin cytoskeleton

Cranial neurulation requires a functional actin cytoskeleton. Targeting of genes that encode proteins involved in cytoskeletal function results in cranial NTD. For example, knockout mouse models of shroom (an actin-binding protein) and vinculin (a cytoskeletal protein) result in a 100% incidence of exencephaly in homozygous embryos (Hildebrand *et al.*, 1999;Xu *et al.*, 1998). Similarly, deficiency of MARCKS (an actin binding protein) also results in cranial neural tube defects in a significant number of homozygous embryos (25%) (Stumpo *et al.*, 1995). The actin cytoskeleton appears to be particularly involved in the closure of the cranial neural folds as the majority of neural tube defects exhibited by these mouse models affect the cranial region (Table 1.1). In addition, disruption of the actin cytoskeleton by cytochalasin D treatment also resulted in isolated cranial neural tube defects with caudal closure unaffected (Ybot-Gonzalez and Copp, 1999). The exact role of the actin cytoskeleton in neurulation is unclear. However, evidence from mouse and other animal studies, points to possible roles in medial convergence of the neural folds through the formation of DLHP (Morriss-Kay and Tuckett, 1985;Schoenwolf *et al.*, 1988) and in providing stability for the lateral neural folds (Morriss-Kay *et al.*, 1985;Ybot-Gonzalez *et al.*, 1999).

1.6.2.3 Apoptosis

Correct regulation of apoptosis in the neuroepithelium and the underlying cranial mesenchyme appears to be necessary for cranial neurulation to occur normally. Both increases and decreases in the rate of apoptosis have been associated with the development of exencephaly (Table 1.1). Mouse mutant models that develop cranial neural tube defects in association with increased levels of apoptosis include the *Mdm4* knockout (Migliorini *et al.*, 2002) and mice lacking the *ski* oncogene (Berk *et al.*, 1997). In addition, some mouse models exhibit exencephaly in association with reduced levels of apoptosis including the *Bmp5/Bmp7* double knockout (Solloway *et al.*, 1999) and mice deficient for *caspase 9* (Kuida *et al.*, 1998). Moreover, the importance of regulation of apoptosis in cranial neurulation is evident from exposure of neurulation stage embryos to various teratogens. For example, lithium-induced cell death in the neuroepithelium of mouse embryos has been suggested to lead to the subsequent cranial neural tube defects (Giles and Bannigan, 1997), although the possibility that apoptosis is secondary to another effect of lithium cannot be excluded.

1.6.3 Factors involved in spinal neurulation – evidence from mouse models

1.6.3.1 Planar cell polarity pathway

In mice, the development of craniorachischisis has been linked to a non-canonical Wnt signalling pathway called the planar cell polarity pathway. Disruption of genes involved in this pathway lead to the development of craniorachischisis in mice (Table 1.1) (Murdoch *et al.*, 2001;Kibar *et al.*, 2001;Curtin *et al.*, 2003). The phenotypes are

believed to be caused by the inhibition of convergent extension, a morphogenetic process of cell movement in which a field of cells lengthens along one axis and narrows in a perpendicular axis (Wallingford *et al.*, 2002). Suppression of convergent extension leads to an abnormally wide floorplate, and excessively wide spacing of the neural folds, which cannot converge in the midline resulting in failure of neural tube closure at initiation site closure 1 (Ueno and Greene, 2003;Copp *et al.*, 2003a).

1.6.3.2 Axial curvature

Axial curvature has been suggested to have an important influence on spinal neural tube closure. The rate of neural tube closure has been shown to correlate with the degree of axial curvature in a number of vertebrates (Peeters *et al.*, 1998a). In the mouse, axial curvature decreases at the PNP region as neurulation proceeds along the cranio-caudal axis, correlating with an increase in the rate of PNP closure throughout neurulation (Peeters *et al.*, 1998a). In addition, studies in the *curly tail* mouse indicate that an increase in axial curvature caused by reduced proliferation in the ventral hindgut, slows down PNP closure. The consequent delay or failure of closure of the PNP, results in a curly tail phenotype or spina bifida, respectively (Copp *et al.*, 1988a). Correction of the increased ventral curvature mechanically or by hyperthermia-induced growth retardation has been shown to reduce the incidence of caudal NTD in *curly tail* mice (Copp *et al.*, 1988b;Brook *et al.*, 1991). These studies show that both correct axial curvature and co-ordinated proliferation are required for PNP closure.

1.7 FOLATE PREVENTS NTD IN HUMANS

Periconceptional vitamin supplementation was initially implicated as a potential approach for the prevention of NTD following the observation that supplementation reduced the risk of recurrence of an NTD-affected pregnancy in humans (Smithells *et al.*, 1981). Further evidence has indicated that supplementation with folic acid alone reduces the risk of an NTD-affected pregnancy. A randomised double-blind clinical trial conducted at 33 centres across 7 countries showed that NTD recurrence was reduced by up to 70 % following periconceptional supplementation with 4 mg/day folic acid (Wald *et al.*, 1991). This result has been confirmed by a number of smaller studies using supplements of folic acid alone or in combination with other vitamins (Mulinare *et al.*, 1988;Milunsky *et al.*, 1989). In addition, maternal supplementation with multi-vitamins containing folic acid reduced the incidence of a first occurrence of NTD (Czeizel and Dudás, 1992). A more recent study has investigated the prevention of NTD in high and low risk areas in China by periconceptional supplementation with 400 μg/day folic acid. Both populations showed a significant reduction in the rate of NTD after folic acid supplementation. Moreover, in a subgroup of women with high compliance (those who took the supplementation more than 80 % of the time) similar rates of NTD were observed in both supplemented populations, with a reduced risk for an NTD-affected pregnancy of 85 % in the high prevalence area (Berry *et al.*, 1999).

As a result of these studies, women of childbearing age are advised to take 400 μg/day folic acid prior to, and for three months following conception, to reduce the risk of an NTD-affected pregnancy. On 1st January 1998, the addition of folic acid to enriched cereal grain products became mandatory in the USA. The addition of 140 μg folic acid

per 100 g cereal grain product was introduced with the aim of increasing the daily intake of folic acid of women of childbearing age (Mills and Signore, 2004). Subsequently, a number of other countries (including Canada (150 μg per 100 g of flour) (Mills *et al.*, 2004) and Chile (220 μg per 100g of flour) (Hertrampf *et al.*, 2003)) have established fortification programmes. The current levels of fortification are relatively conservative, and it is estimated that the resultant additional folic acid intake in the USA and Canada is 100 μg/day (Liu *et al.*, 2004). Preliminary studies indicate that this level of fortification has reduced the prevalence of NTD to various degrees, by 31 % in the USA (Williams *et al.*, 2002) to 78 % in a high risk area of Newfoundland, Canada (Liu *et al.*, 2004). Continued surveillance is required to clearly distinguish the effects of folic acid fortification from the declining trend in NTD prevalence observed in these populations over the last few decades (Section 1.4.2) (Williams *et al.*, 2002). Nevertheless, the current level of fortification has succeeded in increasing folate status, as indicated by increased serum folate, red blood cell folate levels and reduced homocysteine levels, in the overall US population (Rader, 2002) and in women of childbearing age (19-44 years) and seniors (65 years or over) in Canada (Liu *et al.*, 2004). In response to the limited reductions in NTD risk in some populations, there have been suggestions that the level of fortification is not currently high enough, and increased levels would prevent further cases of NTD (Wald *et al.*, 2001). However, there are concerns over the effects of long term exposure to high levels of folic acid on specific subgroups in the population (Campbell, 1996;Reynolds, 2002;Rader and Yetley, 2002;Kim, 2004). The possibility of detrimental effects on non-targeted members of the population has led to several countries rejecting the implementation of

fortification strategies in favour of public education campaigns to increase folic acid supplementation among women of childbearing age (Bailey *et al.*, 2003).

1.8 ONE CARBON METABOLISM

1.8.1 Folate metabolism

Folate metabolism is essential for a number of important cellular processes, including the synthesis of purines, thymidylate and methionine. Eukaryotes are unable to synthesise folate and, therefore, rely on dietary sources to provide sufficient amounts. In

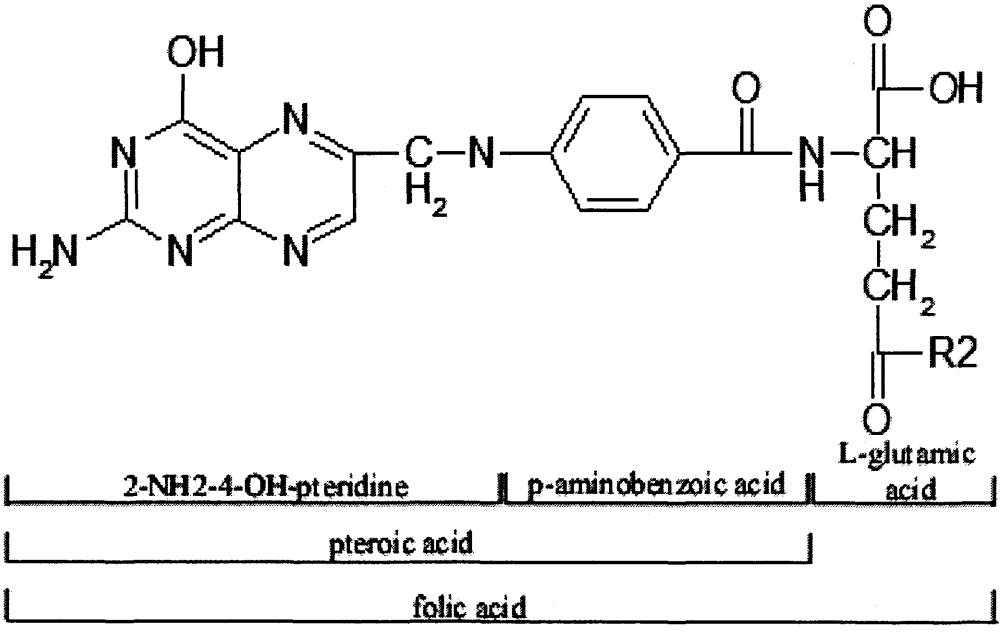

Figure 1.5 A representation of the molecular structure of folic acid

The molecular structure of folic acid and its components. R2 denotes the site of γ-carboxyl peptide bond links to glutamic acid moieties in polyglutamate folates (Adapted from (Van der Put *et al.*, 2001)).

the circulation, folate is present in monoglutamated form and following cellular uptake polyglutamated by the action of folylpolyglutamate synthase (Lucock, 2000). The polyglutamate moieties ensure folate is retained in the cell, maintaining cellular folate pools, and increase the affinity of folate for folate-dependant enzymes.

The circulating form of folate, 5-methyltetrahydrofolate (5-methyl THF), is a co-substrate for the remethylation of homocysteine to methionine which is mediated by methionine synthase (MS). This reaction, which is vitamin B_{12}-dependent, connects the folate and methylation cycles (Figure 1.6). The folate-derived product of the MS-mediated reaction, tetrahydrofolate (THF), can be converted to 5,10-methylenetetrahydrofolate (5,10-methylene THF) by a reversible reaction catalysed by serine hydroxymethyltransferase (SH); this reaction also mediates the interconversion of serine and glycine (Figure 1.6). 5,10-methylene THF is the substrate for three different reactions, all of which are involved in important pathways in the cell:

(i). Reduction of 5,10-methylene THF by methylenetetrahdrofolate reductase (MTHFR) replenishes 5-methyl THF levels (Figure 1.6). This is the only reaction capable of producing 5-methyl THF and polymorphisms in MHTFR have been associated with increased NTD risk (Section 1.9).

(ii). The conversion of 5,10-methylene THF back to THF via the trifunctional enzyme, methylenetetrahydrofolate dehydrogenase /methenyltetrahydrofolate cyclohydrolase /formyltetrahydrofolate synthetase (MTHFD1), results in the intermediates, 5,10-methenyl tetrahydrofolate (5,10-methenyl THF) and 10-formyltetrahydrofolate (10-formyl THF). 10-formyl THF donates a one-carbon unit in synthesis of the purine ring (Figure 1.6).

Figure 1.6 The folate cycle

A simplified diagram of the folate cycle. Folate and methylation cycle intermediates are in black text and the enzymes involved in the cycle are shown in blue. Biosynthetic pathways are boxed.

Abbreviations: DHF, dihydrofolate; DHFR, dihydrofolate reductase (EC 1.5.1.3); dUMP, deoxyuridine monophosphate; dTMP, deoxythymidine monophosphate; MS, methionine synthase (EC 2.1.1.13); MTHFD1, methylenetetrahydrofolate dehydrogenase (EC 1.5.1.5) /methenyltetrahydrofolate cyclohydrolase (EC 3.5.4.9) /formyltetrahydrofolate synthetase (EC 6.3.4.3); MTHFR, methylenetetrahydrofolate reductase (EC 1.5.1.20); SH, serine hydroxymethyltransferase (EC 2.1.2.1); TS, thymidylate synthase (EC 2.1.1.45).

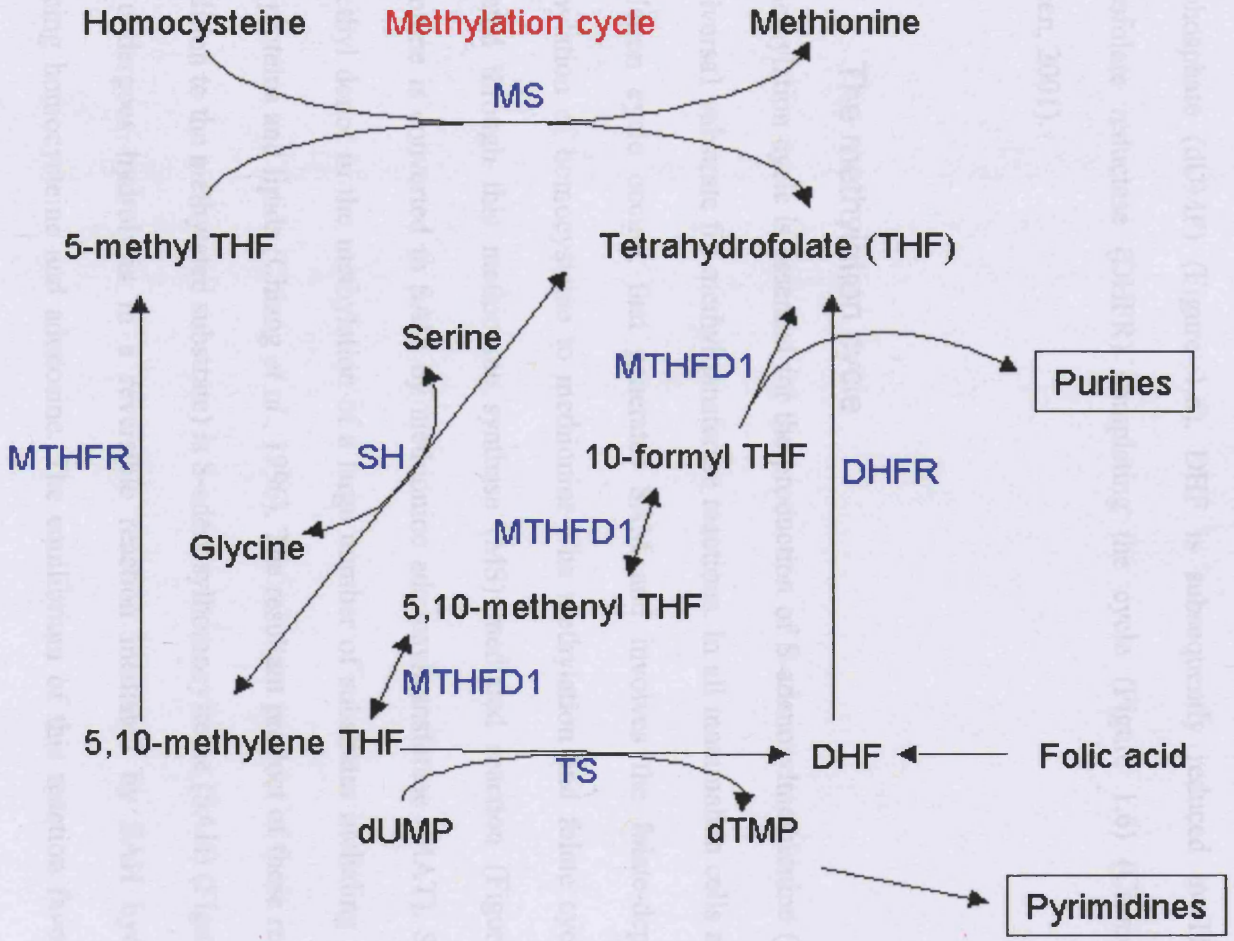
Homocysteine
Methylation cycle
Methionine
MS
5-methyl THF
Tetrahydrofolate (THF)
Serine
MTHFD1
Purines
MTHFR
SH
10-formyl THF
DHFR
Glycine
MTHFD1
5,10-methenyl THF
MTHFD1
5,10-methylene THF
DHF
Folic acid
TS
dUMP
dTMP
Pyrimidines

(iii). In the *de novo* pathway of pyrimidine biosynthesis, the thymidylate synthase (TS) mediated reaction converts 5,10-methylene THF to dihydrofolate (DHF) during the production of deoxythymidine monophosphate (dTMP) from deoxyuridine monophosphate (dUMP) (Figure 1.6). DHF is subsequently reduced to THF by dihydrofolate reductase (DHFR) completing the cycle (Figure 1.6) (Carmel and Jacobsen, 2001).

1.8.2 The methylation cycle

The methylation cycle is essential for the production of S-adenosylmethionine (SAM), the universal substrate for methyltransferase reactions. In all mammalian cells a 'core' methylation cycle occurs, that generates SAM and involves the folate-dependant remethylation of homocysteine to methionine The methylation and folate cycles are connected through this methionine synthase (MS) mediated reaction (Figure 1.7). Methionine is converted to SAM by methionine adenosyltransferase (MAT). SAM is the methyl donor in the methylation of a large number of substrates including nucleic acids, proteins and lipids (Chiang *et al.*, 1996). The resultant product of these reactions (in addition to the methylated substrate) is S-adenosylhomocysteine (SAH) (Figure 1.7). SAH undergoes hydrolysis in a reversible reaction mediated by SAH hydrolase, producing homocysteine and adenosine. The equilibrium of this reaction favours the synthesis of SAH, such that rapid removal of the products is required to maintain flux through the methylation cycle (Finkelstein, 1998).

SAH and SAM levels have a regulatory role in both methylation and folate cycles. When cellular levels of SAH are elevated, SAH acts as a product inhibitor of

Figure 1.7 The methylation cycle

A simplified diagram of the methylation cycle. Methylation and folate cycle intermediates are in black text and the enzymes involved in the cycle are shown in blue. Additional pathways are boxed and cell specific reactions are indicated by dotted lines.
Abbreviations: BHMT, betaine-homocysteine methyltransferase (EC 2.1.1.5); MAT, methionine adenosyltransferase (EC 2.5.1.6); MS, methionine synthase (EC 2.1.1.13); SAH, S-adenosylhomocysteine; SAH hydrolase, S-adenosylhomocysteine hydrolase (EC 3.3.1.1); SAM, S-adenosylmethionine; SAMDC, S-adenosylmethionine decarboxylase (EC 4.1.1.50); THF, tetrahydrofolate.

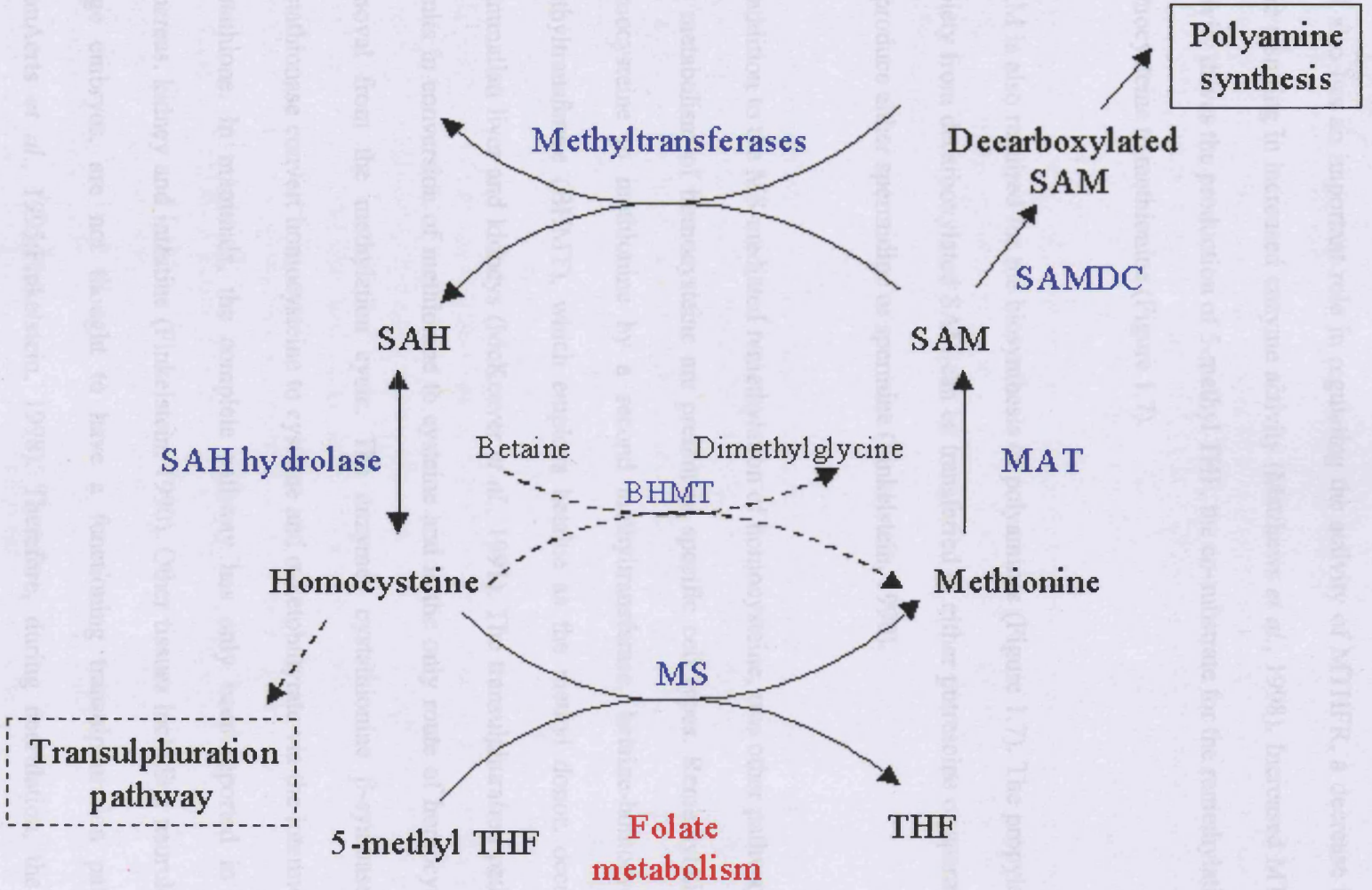
Polyamine synthesis
Methyltransferases
Decarboxylated SAM
SAMDC
SAH
SAM
SAH hydrolase
Betaine
Dimethylglycine
BHMT
MAT
Homocysteine
Methionine
MS
Transulphuration pathway
5-methyl THF
Folate metabolism
THF

methyltransferase reactions (Carmel *et al.*, 2001). The ratio of SAM:SAH levels in the cell also has an important role in regulating the activity of MTHFR, a decrease in the ratio resulting in increased enzyme activity (Matthews *et al.*, 1998). Increased MTHFR activity drives the production of 5-methyl THF, the co-substrate for the remethylation of homocysteine to methionine (Figure 1.7).

SAM is also required for the biosynthesis of polyamines (Figure 1.7). The propylamine moiety from decarboxylated SAM can be transferred to either putrescine or spermidine to produce either spermidine or spermine (Finkelstein, 1990).

In addition to the MS-mediated remethylation of homocysteine, two other pathways for the metabolism of homocysteine are present in specific cell types. Remethylation of homocysteine to methionine by a second methyltransferase, betaine-homocysteine methyltransferase (BHMT), which employs betaine as the methyl donor, occurs in mammalian liver and kidneys (McKeever *et al.*, 1991). The transulphuration pathway, results in conversion of methionine to cysteine and is the only route of homocysteine removal from the methylation cycle. The enzymes cystathionine β-synthase and cystathionase convert homocysteine to cysteine and α-ketobutyrate via the intermediate cystathione. In mammals, the complete pathway has only been reported in liver, pancreas, kidney and intestine (Finkelstein, 1990). Other tissues including neurulation-stage embryos, are not thought to have a functioning transulphuration pathway (VanAerts *et al.*, 1995;Finkelstein, 1998). Therefore, during neurulation, the only functional pathway for the removal of homocysteine in the embryo is likely to be the folate-dependant MS mediated reaction.

1.9 FOLATE-RELATED RISK FACTORS FOR THE DEVELOPMENT OF NTD IN HUMANS

A number of environmental and genetic factors have been associated with the aetiology of NTD-affected pregnancies (Section 1.4). Due to the complex aetiology of NTD, the identification of individual factors that are directly involved in determining the susceptibility to NTD (risk factors) is difficult. Some risk factors have been identified through studying associations between NTD-affected pregnancies and maternal nutritional status.

Sub-optimal maternal folate levels have been associated with increased risk of an NTD-pregnancy in a number of studies (Smithells *et al.*, 1976;Kirke *et al.*, 1993). It is interesting to note that red cell folate levels detected in these studies were within the 'normal' range and therefore the mothers were not classified as folate deficient. Vitamin B_{12} insufficiency has also been suggested as a risk factor for NTD-affected pregnancies. Reduced levels of vitamin B_{12} have been detected in amniotic fluid and maternal plasma samples of NTD-affected pregnancies compared to control samples (Kirke *et al.*, 1993;Steen *et al.*, 1998;Ray and Blom, 2003;Felix *et al.*, 2004). Several studies have also shown that women carrying embryos with NTD (Mills *et al.*, 1995) and women who have had children affected with NTD (Steegers-Theunissen *et al.*, 1994) have significantly elevated levels of plasma homocysteine. In addition, elevated levels of total homocysteine have also been detected in spina bifida patients and their parents (Van der Put *et al.*, 1997a) suggesting elevated homocysteine levels may be a risk factor for NTD.

Not all populations exhibit these risk factors, for example, several studies have not identified NTD associations with maternal folate status (Economides *et al.*, 1992;Mills *et al.*, 1992;Van der Put *et al.*, 1997a), folate levels in amniotic fluid (Economides *et al.*, 1992;Steen *et al.*, 1998) or maternal vitamin B_{12} status (Economides *et al.*, 1992;Mills *et al.*, 1992). As discussed previously, different populations are likely to be affected by genetic and environmental factors in different ways with respect to NTD (Section 1.4). For example, areas with a high prevalence of NTD tend to have greater response to folate supplementation than areas of low prevalence (Section 1.7). This correlation may also be evident in the association of NTD risk in certain populations with folate-related nutritional status (Mills *et al.*, 1992).

In many studies, investigation of potential genetic risk factors has been based on the known prevention of NTD by folic acid supplementation. The possibility that supplementation may be overcoming a defect in folate metabolism has led to the analysis of many folate-related genes. In addition, the association of elevated homocysteine, reduced vitamin B_{12} and sub-optimal folate levels with risk for NTD, led to the analysis of enzymes directly involved in maintaining cellular levels of these nutrients.

The first folate-related genetic risk factor to be identified was a polymorphism in the MTHFR gene (Whitehead *et al.*, 1995;Van der Put *et al.*, 1995). A point mutation, 677C>T, causing an alanine-valine amino acid substitution produces a thermolabile variant of the enzyme that has reduced activity (Frosst *et al.*, 1995). Homozygous individuals for the 677T allele have significantly elevated plasma homocysteine levels

(Frosst *et al.*, 1995;Van der Put *et al.*, 1996;Friso *et al.*, 2002) and hypomethylated DNA when they also have low serum folate values (Friso *et al.*, 2002;Castro *et al.*, 2004). A number of studies have shown that the frequency of the 677T allele is increased in NTD-affected patients (Shields *et al.*, 1999;Whitehead *et al.*, 1995;Van der Put *et al.*, 1995;Wenstrom *et al.*, 2000;De Marco *et al.*, 2002;Rampersaud *et al.*, 2003). However, other studies carried out in different population groups have not identified an increased risk of NTD in association with the MTHFR 677T allele (Papapetrou *et al.*, 1996;Koch *et al.*, 1998;Perez *et al.*, 2003;Felix *et al.*, 2004). In addition, elevated homocysteine levels have been observed in patients with NTD, independent of their MTHFR 677 genotype (Wenstrom *et al.*, 2000;Perez *et al.*, 2003), suggesting that other risk factors which affect folate metabolism may be involved in the aetiology of some NTD.

A second single nucleotide polymorphism (SNP) (1298A>C) has been identified in the MTHFR gene which causes a glutamate–alanine substitution resulting in decreased MTHFR activity. This mutation does not result in a thermolabile enzyme and the reduction in activity is not as pronounced as for the 677C>T mutation. In addition, homozygotes for the 1298CC allele do not show elevated homocysteine levels or reduced plasma folate levels (Van der Put *et al.*, 1998). At present there are no studies supporting an independent role for the presence of the 1298C allele in the aetiology of NTD (Parle-McDermott *et al.*, 2003;Felix *et al.*, 2004). However, it has been suggested to have an exacerbating effect on the risk of NTD in patients when present in combined heterozygosity with the MTHFR 667T allele (Van der Put *et al.*, 1998).

The methionine synthase mediated reaction, in which homocysteine is remethylated to methionine, has also been investigated in respect to NTD risk. Analysis of polymorphisms in the methionine synthase gene (MTR; 2756A>G) and methionine synthase reductase gene (MTRR; 66A>G) have been carried out in many populations. The MTR 2756A>G polymorphism results in an aspartic acid to glycine amino acid change in the activation domain of the enzyme (Leclerc *et al.*, 1996). Methionine synthase reductase reactivates methionine synthase (MS) that has lost activity due to the oxidation of its co-factor cob(I)alamin to cob(II)alamin, and therefore, is required to maintain MS activity. The MTRR 66A>G polymorphism is thought to affect the binding affinity for MS and reduce the reductive activities of the enzyme(Olteanu *et al.*, 2004). Both variants, MTR 2756A>G and MTRR 66A>G, have been identified as individual maternal (Doolin *et al.*, 2002) and infant (Zhu *et al.*, 2003) risk factors for spina bifida. The presence of G alleles at both loci has been suggested to result in a greater risk for NTD than either alone (Zhu *et al.*, 2003). However, other studies have not identified associations of variants in either gene with NTD risk (Morrison *et al.*, 1997;Van der Put *et al.*, 1997b;Christensen *et al.*, 1999;De Marco *et al.*, 2002;O'Leary *et al.*, 2005).

A number of other potential genetic risk factors have been identified in folate-related genes in some populations. These include maternal homozygosity for the R653Q polymorphism in the MTHFD1 gene (Brody *et al.*, 2002), maternal homozygosity for a DHFR allele with a 19bp deletion in intron 1 (Johnson *et al.*, 2004) or maternal homozygosity for the 776C>G polymorphism in the gene encoding the vitamin B_{12} binding protein, transcobalamin II (TCII) (Pietrzyk and Bik-Multanowski, 2003).

Polymorphisms in the promoter enhancer region and 3'UTR of the TS gene have been associated with elevated risk of spina bifida in non-Hispanic whites (Volcik *et al.*, 2003). A significant association has also been detected between NTD risk and the presence of a polymorphism in the reduced folate carrier gene (RFC1), 80A>G (Pei *et al.*, 2005). Microconversion events in the FRα gene have also been suggested to act as genetic risk factors for NTD (De Marco *et al.*, 2000). Thus, a range of studies have implicated polymorphisms in several folate-related proteins in mildly elevated risks of NTD.

However, several studies have failed to detect associations between polymorphisms in these genes and NTD (Barber *et al.*, 1998;Wilding *et al.*, 2004;Swanson *et al.*, 2005). In addition, studies in other folate-related genes; cSHMT/mSHMT (Heil *et al.*, 2001), BHMT/BHMT2 (Zhu *et al.*, 2005), FRβ (O'Leary *et al.*, 2003) and CBS (Afman *et al.*, 2003b), have so far failed to identify any genetic variants that are significantly associated with NTD.

Currently the known genetic risk factors are not sufficient to explain the susceptibility to NTD for all cases. For example, in populations with a positive association between MTHFR genotype and NTD occurrence, the frequency of the 677T allele cannot account for all the folate-preventable NTD (Shields *et al.*, 1999). As discussed previously (Section 1.4), susceptibility to NTD probably follows a polygenic mode of inheritance in addition to being influenced by environmental factors. A number of studies have analysed the impact of combinations of potential risk factors on the aetiology of NTD. Combined genetic and/or environmental risk factors could result in a

greater risk for NTD than either factor alone. For example, homozygosity for MTHFR 677T allele and low RBC folate in cases and mothers were independent risk factors that showed possible synergistic effects, resulting in increased NTD risk in a Canadian study (Christensen *et al.*, 1999). In another study, a MTRR 66GG maternal genotype increased NTD risk when vitamin B_{12} was low (valued within the lowest quartile of the control range) or in the presence of a MTHFR 677TT genotype (Wilson *et al.*, 1999). These studies indicate that gene-nutrient and gene-gene interactions may be involved in determining the susceptibility to NTD. In support of these findings, another study observed an increase in NTD risk in individuals carrying both the MTRR 66G and MTHFR 677T variants (Relton *et al.*, 2004). Further studies have indicated that the possession of more than one polymorphism at folate-related loci can elevate risk of NTD (Van der Put *et al.*, 1998;Gueant-Rodriguez *et al.*, 2003;Zhu *et al.*, 2003). In order to understand the complex aetiology and potential contributions of possible risk factors to the susceptibility for NTD, more sophisticated studies are required that account for summation and interaction of multiple risk factors. Such studies could possibly elucidate some of the biological mechanisms underlying NTD.

1.10 PREVENTION OF NTD IN MOUSE MODELS

In humans, clinical trials have demonstrated that folic acid supplementation can prevent the recurrence of up to 70 % of NTD (Wald *et al.*, 1991). Therefore, 30 % of pregnancies developed NTD despite folate supplementation, suggesting that some NTD are resistant to folic acid administration. This observation is mirrored among the mouse models. Several models respond to folic acid or folate-related metabolites (Table 1.2),

showing a decrease in the incidence of NTD, while others do not (Copp and Greene, 2000).

One example of an apparently folate-insensitive NTD mouse model is *curly tail* (*ct*) in which supplementation with folic acid, folinic acid or methionine do not affect the frequency of NTD among homozygous *ct/ct* embryos (Seller, 1994;Van Straaten *et al.*, 1995). However, maternal administration of myo-inositol significantly reduces the incidence of spinal NTD in homozygous *ct/ct* embryos. The preventative effect of myo-inositol of NTD in these mice is mediated by the activation of protein kinase C (PKC) (Greene *et al.*, 1997;Cogram *et al.*, 2004). This mechanism of NTD prevention is thought to be unrelated to folate metabolism, suggesting that alternative preventative approaches to folate supplementation need to be investigated. However, a better understanding of the mechanism underlying folate-responsive NTD may enable improvement of current prevention strategies.

A number of mouse NTD models have been tested for sensitivity to folic acid and/or folate-related metabolites. Identification of strains that are responsive to supplementation with folic acid (Carter *et al.*, 1999;Martinez-Barbera *et al.*, 2002) or folate-related metabolites, such as methionine (Essien, 1992;Greene and Copp, 2005) (Table 1.2) confirm the ability of folic acid treatment to prevent some NTD. In addition, some teratogen-induced NTD can also be prevented by folate treatment (Shin and Shiota, 1999;Trotz *et al.*, 1987;Sadler *et al.*, 2002) (Table 1.2).

Mouse Model	Type of NTD	Preventative treatment	Reference
Genetic models			
Axial defects (Axd)	SB	Methionine Maternal i.p. administration On E8 and E9	(Essien, 1992)
Cartilage homeoprotein 1 (Cartl)	Ex	Folic acid Maternal i.p. administration Throughout pregnancy	(Zhao *et al.*, 1996)
Cited2	Ex	Folic acid Maternal i.p. administration Throughout pregnancy	(Martinez-Barbera *et al.*, 2002)
Crooked tail (Cd)	Ex	Folic acid Dietary maternal administration Prior to conception and throughout pregnancy	(Carter *et al.*, 1999)
Folate binding protein 1 (Folbp1)	Ex	Folinic acid Maternal intubation Prior to conception and throughout pregnancy	(Piedrahita *et al.*, 1999)
Splotch (Sp^{2H})	Ex and/or SB	Folic acid and thymidine Maternal i.p. administration On E8.5 and E9.5 Whole embryo culture E8.5 to E10.5	(Fleming and Copp, 1998)
Teratogen models			
Fumonisins	Ex	Folinic acid Whole embryo culture E9 to E10	(Sadler *et al.*, 2002)
Hyperthermia	Ex	Folic acid Maternal intubation E0.5 to E9.5	(Shin *et al.*, 1999)
Valproic acid	SB and Ex	Folinic acid Maternal i.p administration On E8 only or thrice daily from E5 to E10	(Trotz *et al.*, 1987;Padmanabhan and Shafiullah, 2003)

Table 1.2 Mouse models in which NTD are preventable by folate-related treatments

Abbreviations: Ex, exencephaly; i.p. intraperitoneal injection; SB, spina bifida.

These folate-responsive mouse models may be useful tools in the investigation of the mechanisms of prevention of NTD by folic acid, and one such model, *splotch*, is used in this project.

1.10.1 *Splotch* mice

There are six variants of the *splotch* allele that all encode mutant forms of the *Pax3* gene (Table 1.3). Pax3 is a transcription factor that contains paired-box and homeobox DNA binding motifs. It is expressed in the dorsal neural tube, dermomyotome and neural crest cells of neurulation stage embryos (Goulding *et al.*, 1991). The *splotch* phenotype includes NTD (comprising exencephaly and/or spina bifida), limb muscle defects and defects in neural crest cell derivatives. The severity of the abnormalities seen in *splotch* homozygotes differ between the allelic variants (Table 1.3). However, all heterozygotes are characterised by a white patch on the abdomen due to impaired migration of melanocytes, which are derived from the neural crest (Auerbach, 1954). The *splotch* allele utilised in this study is Sp^{2H}. This mutation was induced by X-ray irradiation, resulting in a 32bp deletion in the paired box region of the *Pax3* gene that causes premature termination of the protein, which is predicted to result in a functionally null allele (Epstein *et al.*, 1991). In Sp^{2H} mice, treatment with folic acid or thymidine reduces the incidence of cranial and caudal NTD, both in whole embryo culture and through maternal intraperitoneal injections (Fleming *et al.*, 1998).

Abnormal folate metabolism in Sp^{2H}/Sp^{2H} embryos was detected using the deoxyuridine monophosphate (dUMP) suppression test in whole embryo culture. The ability of exogenous dUMP to suppress the incorporation of exogenous [^{3}H] thymidine into DNA

Splotch allele	Mutation in *Pax3*	Effect on Pax3 protein	Mode of mutation	Homozygous phenotype	References
Splotch (Sp)	Mutation in splice acceptor site in intron 3	Four aberrantly spliced transcripts – none expected to result in functional Pax3 proteins	Spontaneous	Exencephaly and/or spina bifida, Defects in neural crest derivatives*. Lethal between E13-16	(Russell, 1947;Auerbach, 1954;Epstein *et al.*, 1993)
Splotch-delayed (Sp^{d})	Point mutation	Non-conservative amino acid substitution within the paired box	Spontaneous	Spina bifida, Reduced size and number of spinal ganglia Perinatally lethal	(Dickie, 1964;Moase and Trasler, 1989;Vogan *et al.*, 1993)
Splotch-retarded (Sp^{r})	Large chromosomal deletion including entire *Pax3* gene	Null mutation	X-ray induced	Preimplantation lethal	(Beechey and Searle, 1986)
$Splotch^{1H}$ (Sp^{1H})	Unknown	Unknown	X-ray induced	Exencephaly and/or spina bifida, Defects in neural crest derivatives* Lethal between E13-16	(Beechey *et al.*, 1986)
$Splotch^{2H}$ (Sp^{2H})	32bp deletion	Truncated protein	X-ray induced	Exencephaly and/or spina bifida, Defects in neural crest derivatives* Lethal between E13 and birth	(Beechey *et al.*, 1986;Epstein *et al.*, 1991)
$Splotch^{4H}$ (Sp^{4H})	Entire *Pax3* gene deleted	Null mutation	X-ray induced	Lethal before E7	(Goulding *et al.*, 1993;Fleming *et al.*, 1996)

Table 1.3 *Splotch* allele phenotypes and mutations in *Pax3*

* includes absent or abnormal spinal ganglia, enteric ganglia, limb muscles and melanocytes, and cardiac defects (Auerbach, 1954;Moase *et al.*, 1989;Franz, 1989;Machado *et al.*, 2001).

relies on the integrity of the folate cycle. An intermediate of the folate cycle, 5,10-methylene tetrahydrofolate, is the co-substrate, with dUMP, for thymidylate synthase in the *de novo* pathway of pyrimidine synthesis. In homozygous Sp^{2H} embryos, the extent of suppression of [^{3}H]-thymidine incorporation by exogenous dUMP is significantly reduced compared to heterozygotes and wild type littermates (Fleming *et al.*, 1998). This could indicate a restricted supply of 5,10-methylene tetrahydrofolate resulting from impairment in the folate cycle. These results indicate that the prevention of NTD in Sp^{2H} embryos by folic acid supplementation may be mediated through the correction of an abnormality in folate metabolism. Another possible explanation is that Sp^{2H}/Sp^{2H} embryos have an increased requirement for dTMP. The exact abnormality affecting folate metabolism in Sp^{2H} homozygotes has yet to be discovered.

1.10.2 Possible mechanisms of folate prevention of NTD

As stated earlier, the mechanism of folate prevention of NTD is not known. Folate treatment does not appear to prevent a specific subtype of NTD suggesting that folic acid protection may act through a general effect on neurulation (Seller, 1995).

1.10.2.1 Correction of maternal folate deficiency

A number of potential mechanisms have been suggested, including the possibility that folate supplementation simply corrects a maternal deficiency. This is unlikely as maternal folate levels during NTD-affected pregnancies are normal or only mildly deficient (Scott *et al.*, 1994). In addition, dietary folate deficiency in mice results in

reduced litter sizes and embryonic growth retardation but does not induce NTD (Heid *et al.*, 1992;Burgoon *et al.*, 2002).

1.10.2.2 Overcoming abnormalities in folate metabolism

Folate supplementation could act to overcome a metabolic block within the folate cycle. Inborn errors in folate metabolism or transport could leave embryos requiring an increased supply of folic acid and render them susceptible to NTD. Murine studies involving the disruption of a number of enzymes in the folate cycle by chemical inhibitors and the production of null mutants of folate-related genes have allowed investigation of the role of specific enzymes in the development of NTD (Juriloff and Harris, 2000). A number of the enzymes involved in folate metabolism are essential for the viability of embryos, but to date no single genetic mutation of a folate-related gene in mice has been identified that mirrors NTD in humans. Alternatively, folate protection against NTD could be achieved through stimulation of proliferation, with folic acid driving the production of purines and pyrimidines for DNA synthesis (Section 1.8.1). Cells are dividing rapidly during the process of neurulation resulting in a high demand for nucleotides, a possible limiting factor for embryos susceptible to NTD.

1.10.2.3 Overcoming abnormalities in the methylation cycle

Another possible mechanism for the folate prevention of NTD may be through overcoming defects within the methylation cycle. It has been hypothesised that defects in the methylation cycle may be involved in the production of NTD, either through changes in cellular methylation or through causing an increase in the concentration of

homocysteine. Folic acid supplementation could increase the supply of 5-methyl THF, thereby facilitating the remethylation of homocysteine to methionine (Section 1.8). This could increase the flux through the methylation cycle, ensuring the production of SAM and reducing cellular homocysteine levels.

Conversion of methionine to SAM provides the universal substrate for methyltransferase reactions. Methylation of DNA, proteins and phospholipids, all utilise SAM as the methyl donor (Chiang *et al.*, 1996). Changes in cellular methylation processes could affect protein function and gene expression (Carmel *et al.*, 2001), which could potentially result in the production of NTD in the developing embryo.

As discussed earlier, elevated levels of homocysteine have been identified as a risk factor for NTD in some human populations (Section 1.9). However, it is unclear whether increased homocysteine levels are directly involved in the production of NTD. Moreover, the effect of elevated levels of homocysteine on neural tube closure in various animal models has given conflicting results, ranging from NTD-induction and non-specific embryotoxicity, to no detrimental effects on embryo development (VanAerts *et al.*, 1994;Rosenquist *et al.*, 1996;Hansen *et al.*, 2001). Therefore the role of elevated homocysteine in the induction of NTD is still unclear.

1.11 INVESTIGATING FOLATE METABOLISM IN THE CLOSURE OF THE MAMMALIAN NEURAL TUBE

The aim of this study is to investigate the role of folate and methylation cycle intermediates in neural tube closure. The project can be separated into three areas of investigation:

(i) Examination of the effect of methylation cycle intermediates on neural tube closure in non-mutant mice (Chapter 3 and 4).

(ii) Investigation into the mechanisms of NTD production in a folate-responsive mouse model (Chapter 5).

(iii) The analysis of folate metabolism in fibroblastic cell lines derived from human NTD-affected fetuses (Chapter 6).

CHAPTER 2; MATERIALS AND METHODS

2.1 MOUSE STRAINS AND GENERATION OF EXPERIMENTAL LITTERS

In the experiments reported in this thesis two different mouse strains have been studied; one non-mutant strain, CD1, and one mutant strain, *splotch* (Sp^{2H}). The CD1 mice (purchased from Charles River) were used as non-mutant controls in all the experiments. The Sp^{2H} mice were maintained as a randomly bred colony. Heterozygous animals were selected by the presence of a white belly spot and mated to produce experimental litters.

Mice were maintained under light/dark conditions with a 24 hour cycle consisting of 12 light hours from 7 am to 7 pm and then 12 dark hours. Adult mice were paired overnight and females were checked for copulation plugs the following morning. The day of finding a copulation plug was designated embryonic day 0.5 (E0.5) at midday. Pregnant females were killed by cervical dislocation on the desired day of gestation. The uterus was removed and placed in Dulbecco's modified Eagles medium (DMEM, Gibco) containing 10% fetal calf serum (FCS, Sigma) for further dissection.

2.2 DISSECTION OF EMBRYOS

Dissection was carried out in DMEM with 10% FCS under a stereo-microscope (Zeiss, Stemi SV6) using fine forceps (Weiss, No. 5). The individual decidual swellings (Figure 2.1A,B) containing the embryos were removed from the uterus and transferred to a fresh petri dish (Greiner) containing DMEM with 10% FCS (Figure 2.1C). The decidual layer was then removed to reveal the trophoblast (Figure 2.1D) when the conceptus was again

transferred to a petri dish containing fresh DMEM/10% FCS (Figure 2.1E). The decidual layer was removed from each conceptus in turn before further dissection took place. Immediately beneath the trophoblast layer is a very thin 'elastic' layer called Reichert's membrane which was then carefully removed along with the trophoblast layer (Figure 2.1F). The embryo, with yolk sac and ectoplacental cone intact, was then ready for whole embryo culture (Figure 2.2A).

Embryos not used for whole embryo culture needed further dissection. The yolk sac, ectoplacental cone and amnion were removed. Where necessary the yolk sac was rinsed in 1X phosphate-buffered saline (PBS, Sigma) and stored at –20 °C for genotyping. Care was taken to ensure that no maternal tissue was transferred with the yolk sac as contamination could lead to incorrect genotyping.

2.3 WHOLE EMBRYO CULTURE

2.3.1 Preparation of rat serum

Following the method described by Cockroft (1990), blood was collected from the dorsal aorta of diethyl ether anaesthetised male Wistar rats. The rats were culled by cutting the diaphragm after exsanguination. The blood was immediately centrifuged at 4,000 rpm for 5 minutes to pellet the red blood cells. The serum was expelled from the fibrin clot by gently squeezing the clot with a pair of forceps. Centrifugation was repeated and the serum supernatant was transferred to a clean tube; at this point the serum from several rats was pooled together. Centrifugation was again used to pellet any remaining red blood cells and the supernatant was pipetted into a

Figure 2.1. Dissection steps for whole embryo culture

The decidual swellings (white arrows in A) were dissected from the uterus (B) and transferred to fresh medium (C). The decidua (De) was opened revealing the trophoblast (* in D) which was dissected free from decidual tissue and transferred to fresh medium (E) The trophoblast layer and underlying Reichert's membrane were then removed (white arrowhead in F) to reveal the embryo within the yolk sac (white arrow in F). Scale bars represent 1 mm.

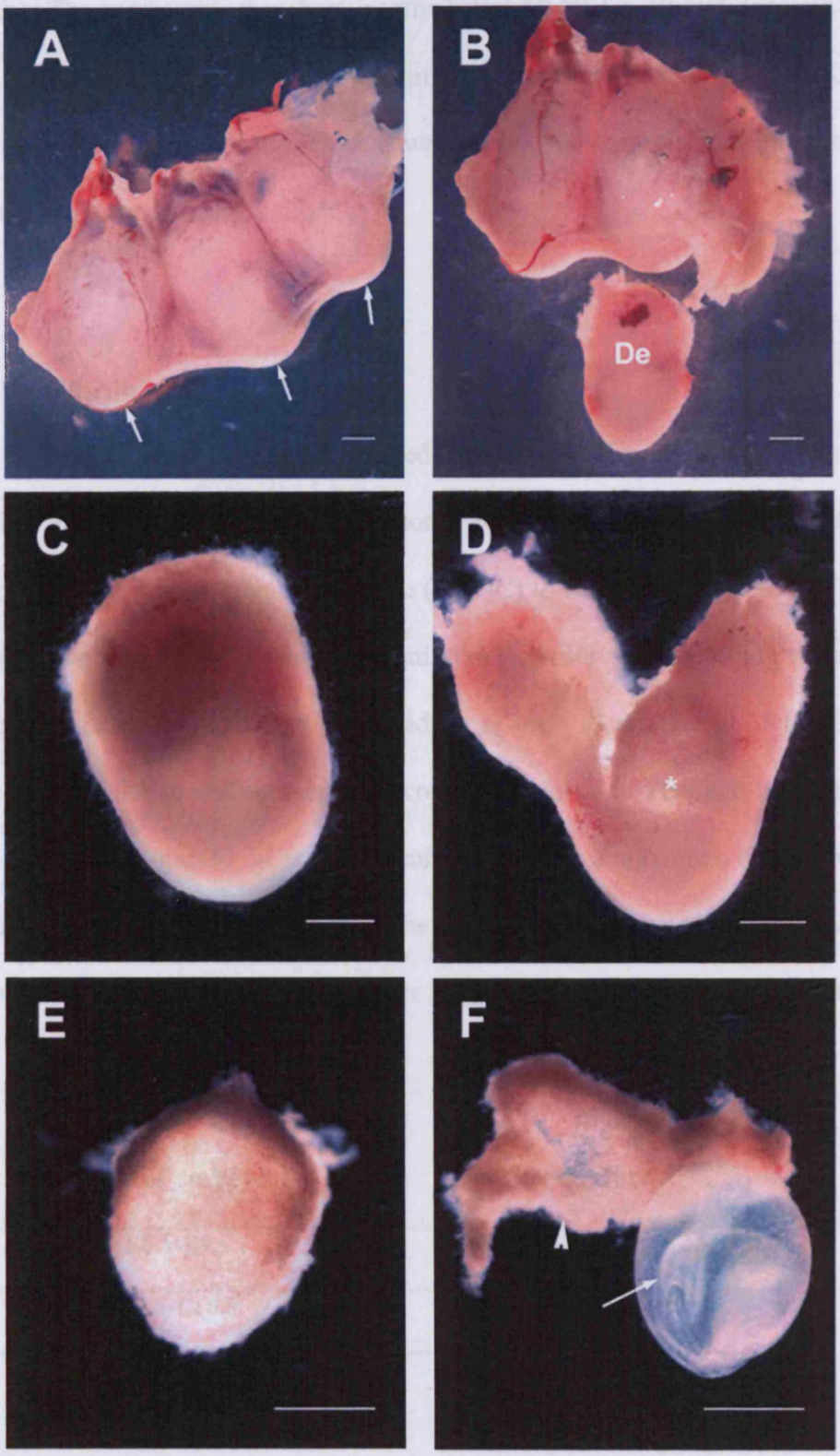
A
B
De
C
D
*
E
F

fresh tube. The serum was then heat-inactivated at 56 °C for 30 minutes with the lids loosely secured to the tubes to allow maximum evaporation of dissolved ether. Once the serum had cooled to room temperature it was pooled and then pipetted into 5 ml, 3 ml and 2 ml aliquots and stored at -20 °C.

2.3.2 Whole embryo culture

Before use, rat serum was thawed, filtered through a 0.45 μm filter (Millipore) and warmed to 38 °C in a rolling tube incubator. Vacuum grease (Glisseal, Borer Chemie) was applied to the rim of each culture tube (NUNC) to form a gas-tight seal. The tubes were gassed with an O_2, CO_2, and N_2 gas mixture (Cryoservice) according to the age of the embryos (Table 2.1) and then incubated for at least 15 minutes at 38 °C. Embryos with an intact yolk sac and ectoplacental cone were rinsed in PBS and transferred into the pre-warmed, pre-gassed rat serum (1 embryo/ml) with a maximum of 3 embryos per tube. The culture tubes were placed in the rolling tube incubator at 38 °C. After 30 minutes, treatment or control solutions were added to the serum and the tubes were

Age of embryo	Gas mixture
E8.5-E9.5	5% O_2, 5% CO_2, 90% N_2
E9.5-E10.5	20% O_2, 5% CO_2, 75% N_2
E10.5 onwards	40% O_2, 5% CO_2, 55% N_2

Table 2.1 Gas mixtures required for whole embryo culture of embryos at different developmental ages.

returned to the rolling incubator for the duration of the culture period. The tubes were re-gassed every time they were opened and at least every 16 hours during the culture period with the appropriate gas mixture (Table 2.1) for the age of the embryo at that time.

2.3.3 Solutions for whole embryo culture

All reagents used in whole embryo culture were of cell culture grade and were obtained from Sigma Chemicals unless otherwise stated. The reagent stock solutions were made up in distilled water or PBS and added as 1-4% (v/v) additions to the culture medium (10-40 µl/ml). The equivalent volume of vehicle alone was added to control groups.

2.3.4 Measurements after whole embryo culture

Embryos were assessed for developmental progress and viability at the end of the culture period. The yolk sac circulation (Figure 2.2B) was described on a scale of 0 to 3 with 0 indicating no circulation and 3 being full and complete circulation throughout the whole yolk sac. The yolk sac, ectoplacental cone and amnion were then dissected away from the embryo (Figure 2.2D) and where necessary yolk sacs were kept for genotyping. Progression of cranial neural tube closure and axial rotation were recorded, the number of somites were counted and the crown-rump length (Figure 2.2D) was measured with an eyepiece graticule for each embryo. Any morphological abnormalities were also recorded. The embryos were washed in PBS and fixed overnight in 4% paraformaldehyde (PFA) in diethyl pyrocarbonate treated PBS (DEPC-PBS) or immediately frozen on dry ice.

Figure 2.2. Embryo morphology and measurements before and after whole embryo culture

An E8.5 embryo ready for whole embryo culture (**A**), with yolk sac (YS) and ectoplacental cone (EC) intact. After embryo culture (**B** shows an embryo after 24 hours in culture from E8.5 to E9.5) the YS circulation (white arrows in **B**) was scored as an indication of the health of the embryos during the culture period. Embryos dissected clear of the YS, EC and amnion (AM) at E8.5 (**C**) and E9.5 (**D**). The crown-rump length was measured for E9.5 embryos (between dotted lines in **D**) as an indication of growth and the number of somites was counted as an indicator of developmental progression. Scale bar(s) in **C** represents 200 μm, **A** and **D** represent 500 μm, and **B** represents 1 mm. Abbreviations; AM, amnion; EC, ectoplacental cone; FB, forebrain; HB, hindbrain; H, heart; HF, head folds; MB, midbrain; OC, optic cup; OV, otic vesicle; PNP, posterior neuropore; S, somites.

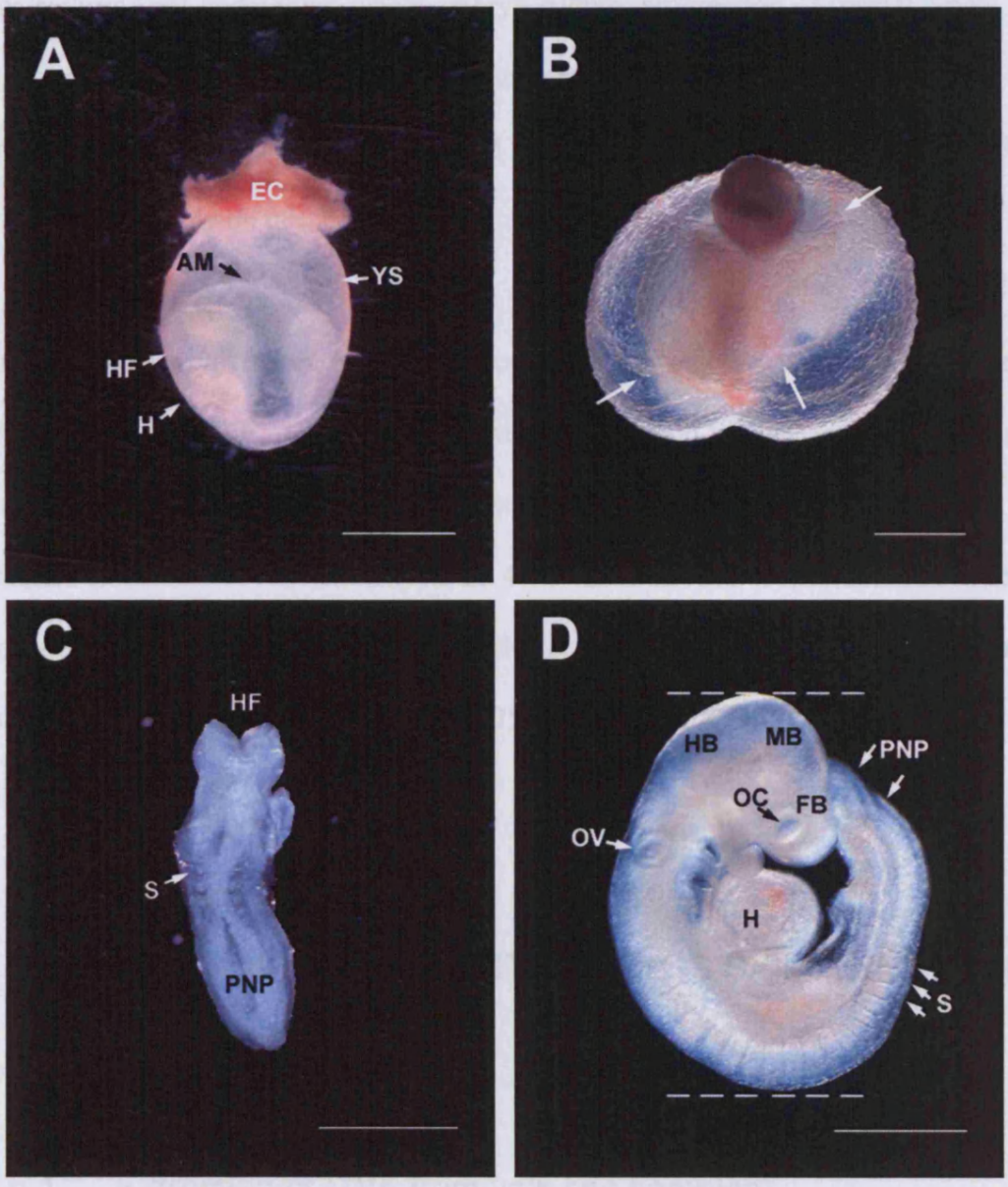
A
EC
AM
YS
HF
H
B
C
HF
S
PNP
D
HB
MB
PNP
OC
FB
OV
H
S

2.4 PROCESSING OF EMBRYOS

For embryos not undergoing whole embryo culture, progression of cranial neural tube closure, axial rotation, somite number and crown-rump length were noted for each embryo. Embryos were rinsed in PBS and fixed overnight in 4% PFA in DEPC-PBS or frozen immediately on dry ice.

Embryos that were frozen after dissection or whole embryo culture were stored at -80 °C until needed. Embryos that underwent fixation and were needed for histological analysis were dehydrated through a series of ethanols (30%, 50%, 60%) diluted with distilled water to 70 % and stored at 4 °C until needed. After fixation embryos undergoing whole mount *in situ* hybridisation or whole mount TUNEL were dehydrated through a methanol series (25%, 50%, 75% diluted with DEPC-PBS) to 100% and stored at -20 °C until needed.

2.5 GENOTYPING OF MUTANT EMBRYOS BY POLYMERASE CHAIN REACTION (PCR)

2.5.1 Extraction of DNA from yolk sac samples

Yolk sacs, previously dissected from the embryos, were digested with 10 μg/ml proteinase K (Invitrogen) in 50 μl PBS at 56 °C for 3 hours. Proteinase K was heat-inactivated at 105 °C for 10 minutes followed by centrifugation at 14,000 rpm for 5 minutes to pellet the cell debris. A 2 μl sample of the supernatant was used as the template for the PCR reaction.

2.5.2 PCR protocol

A reaction mixture was prepared that contained 1X NH_4-PCR buffer (Bioline), 1.5 mM $MgCl_2$, 0.25 mM of each deoxynucleoside triphosphate (dNTP), and 0.8 mM of both reverse and forward primers (Table 2.2). The reaction mixture was kept on ice and just before use 1 unit of Taq polymerase (Bioline) per reaction was added followed by distilled deionised water (ddH_2O) to give a final volume of 23 µl for each reaction. The

Forward Primer sequence	5' CCTCGGTAAGCTTCGCCCTCTG 3'
Reverse Primer sequence	5' CAGCGCAGGAGCAGAACCACCTTC 3'
PCR product size	Wild type allele 122bp Mutant allele 90bp

Table 2.2 The primer sequences and product sizes for genotyping *Sp^{2H}* mice.

resulting solution was mixed and 23 µl was added to 2 µl of yolk sac sample containing 20-100 ng of DNA. Controls were run with each PCR reaction; the negative control did not contain any DNA to ensure the reaction mixture was not contaminated and the positive control used previously genotyped heterozygous DNA to check the components of the reaction mixture. The amplification reaction was carried out on a PTC-200 DNA Engine (MJ Research) and involved an initial denaturation step at 94 °C for 4 minutes followed by amplification cycles of denaturation at 94 °C for 1 minute, annealing at 58 °C for 1 minute with an extension step at 72 °C for 1 minute. This amplification

cycle was repeated 30 times before a final extension step was carried out at 72 °C for 10 minutes.

The primers used to genotype Sp^{2H} mice were designed to span the 32 bp deletion in the paired box region of the *Pax3* gene, as described by Epstein and colleagues (1991), resulting in different sized bands for wild type and mutant alleles (Table 2.2, Figure 2.3). The PCR products were resolved by horizontal agarose gel electrophoresis (Section 2.5.3).

2.5.3 Agarose gel electrophoresis

A 2% agarose in 1X TAE (0.04 M Tris-acetate, 0.001 M EDTA) gel was made by melting the mixture in a microwave with occasional stirring. The gel was then left to cool, approximately 0.5 mg/ml ethidium bromide was added and the mixture was poured into a casting tray with combs and allowed to set at room temperature. Once the gel was solid and placed in a horizon gel tank (Gibco BRL) containing 1X TAE, 10 µl of the PCR products in 1X loading dye (0.25% bromophenol blue, 0.25% Xylene cyanol FF, 15% Ficoll in water) were loaded into the wells. A molecular weight marker (Hyperladder V, Bioline) was run in a lane alongside the samples on each gel to allow identification of the size of the products. After electrophoresis at 120 volts for 1 hour the PCR products were visualised under UV light and photographed using an alphaimager system (Alpha Innotech).

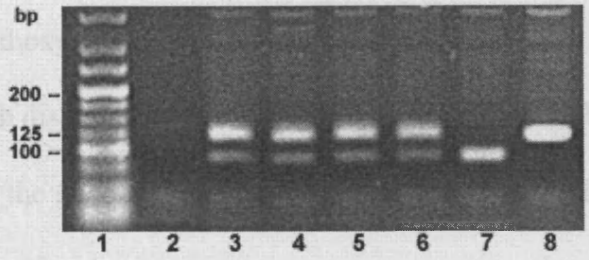

Figure 2.3 Visualisation of *Sp*^{2H} PCR products after agarose gel electrophoresis

Lane 1 contains 5 µl (960 ng DNA) of hyperladder V, and DNA bands of 100, 125 and 200 bp have been indicated. The negative and positive controls are shown in lanes 2 and 3 respectively. The positive control, using heterozygote DNA, illustrates both the wild type allele (the upper band at 122bp) and the mutant allele (the lower band at 90 bp). The remaining lanes show the genotyping of wild type (lane 8), heterozygous (lanes 4-6) and homozygous mutant (lane 7) embryos.

2.6 HISTOLOGICAL ANALYSIS

2.6.1 Embedding and sectioning

Embryos requiring wax embedding that had been stored in 70% ethanol were further dehydrated to 100% ethanol then washed twice for 20 minutes in HistoClear (National Diagnostics). Samples were successively incubated for 20-30 minutes at 60 °C in HistoClear, followed by a pre-warmed HistoClear: paraffin wax (56 °C melting point; Raymond Lamb) mixture (1:1), and three changes of fresh wax. Embryos were then transferred to a watchglass in fresh wax and orientated using heated needles. The wax was left to set at room temperature overnight. Sectioning was carried out by mounting wax blocks containing the embedded embryos onto wooden cubes and 7 µm sections

were cut with a rotary microtome (HM 325, Micron). The sections were floated onto 3-aminopropyltriethoxysilane (TESPA)-coated (Section 2.6.2) or Superfrost plus (BDH) slides covered with distilled water and warmed to 37 °C until fully expanded. The water was removed and the slides were dried overnight at 37 °C. Slides were stored at 4 °C until required for analysis.

After whole mount *in situ* hybridisation (Section 2.10), embryos requiring vibratome sectioning were equilibrated in a gelatin-albumin solution (27 g chicken albumin grade II, 18 g sucrose and 0.45 g of gelatin 300 Bloom) for a minimum of one hour. Embryos were orientated and embedded by addition of 2.5% (v/v) glutaraldehyde. Once orientated, the gelatin-albumin-glutaraldehyde mixture was left to set for one hour, after which the cubes were stored in PBS at 4 °C prior to sectioning. Thimerazol was added to prevent fungal growth (0.05% v/v). Embedded embryos were sectioned at 50 μm thickness with a Series 1000 vibratome (Agar Scientific). Sections were mounted on glass slides in a 50% glycerol-PBS solution and stored at 4 °C.

2.6.2 Preparation of TESPA-coated slides

Glass slides (Menzel-Glaser) were coated in TESPA in order to aid the binding of wax sections to the glass. This reagent acts to electrostatically charge the slide, making it 'sticky' to molecules within the tissue sections. Racks of slides were coated by briefly dipping them into baked glass troughs containing the necessary solutions. Initially the slides were cleaned by washes in 10% HCl in 70% ethanol, DEPC-H_2O and finally 95% ethanol. The slides were then wrapped in foil and dried at 80 °C for 5 minutes. The

slides were then coated by immersion in 2% TESPA in acetone for 10 seconds followed by two washes in acetone and two washes in distilled water (dH_2O). The slides were covered and left to dry overnight at 37 °C. When they were completely dry individual racks were wrapped in foil and stored at 4 °C until needed.

2.6.3 Haematoxylin and Eosin (H&E) staining

Wax was removed from the sections by two washes with HistoClear for 10 minutes each. The sections were then rehydrated through an ethanol series (100%, 95%, 70%, 50%) to distilled water. The slides were then immersed in haematoxylin (BDH), to stain the nuclei a dark blue/purple colour, for 1-2 minutes, rinsed in distilled water and briefly dipped in acid-alcohol (1% HCl in 70% ethanol). After a two minute wash in water the slides were stained with 1% aqueous eosin (Raymond Lamb), which stains the cytoplasm pink, for 2 minutes. The slides were then dehydrated through the ethanol series to 100% with two final 5 minute washes in HistoClear. Coverslips were mounted onto the slides with dextropropoxyphene (DPX) mounting medium (Fisher chemicals) and the slides were left to dry overnight.

2.7 IMMUNOHISTOCHEMISTRY WITH ANTI-PHOSPHORYLATED HISTONE H3 AND ANTI-ACTIVATED CASPASE 3 ANTIBODIES

2.7.1 Sample preparation

Embryos were embedded and sectioned following the protocols described in section 2.6.1. Embryos at the developmental stage of E8.5 were embedded in an orientation that gave transverse sections through the cranial region. E9.5 embryos were embedded to give sections of a coronal orientation. Embryos at E9.0 were embedded in either orientation. Pairs of sections were placed on alternate slides allowing both apoptosis (anti-activated caspase-3 staining) and proliferation (anti-phosphorylated histone H3 staining) to be investigated in each embryo.

2.7.2 Immunohistochemistry

Both antibodies used in this thesis, anti-activated caspase 3 (Cell Signalling Technology) and anti-phosphorylated histone H3 (Upstate) were raised in rabbit, allowing the same secondary antibody (biotinylated goat anti-rabbit, DAKO) and blocking serum (goat serum, DAKO) to be used. The initial steps of de-waxing, rehydration and antigen retrieval differed for the two antibodies.

Slides with sections undergoing immunohistochemistry for activated caspase 3 were placed in working concentration Declere (Cell Marque) (1:20 Declere:dH_2O) and heated in a microwave on the simmer setting for 20 minutes. After 10 minutes a fresh trough of

working strength Declere was placed into the microwave to warm up. The slides were transferred into the fresh pre-warmed Declere and left to cool to room temperature.

The anti-phosphorylated histone H3 antibody did not require an antigen retrieval step. Slides were de-waxed by two 5 minute washes in HistoClear and the HistoClear was removed by two 2 minute washes in 100% ethanol. The slides were then rehydrated through a series of ethanol (90%, 70%, 50%, 25%) diluted with distilled water.

For both antibodies subsequent steps of the protocol were the same. The slides were washed in PBS (all PBS washes in this protocol involve three 2 minutes washes) and then placed in 3% hydrogen peroxide in methanol for 10 minutes. This step inactivates endogenous peroxidases giving reduced background staining. Slides were washed in PBS and then laid flat in a humidified chamber, containing wet tissue. The slides were covered with 5% goat serum in PBS and incubated at room temperature for 30 minutes, to block any non-specific binding of the antibody to the tissue section. In the humidified chamber a strip of nescofilm, cut to size, was placed on top of the solution on each slide to ensure even coverage and to prevent evaporation during longer incubations. The slides were again washed with PBS and the primary antibody was diluted to the required concentration (1:1,000 for anti-activated caspase 3 and 1:500 for anti-phosphorylated histone H3) with 1% FCS in Tris buffered saline (TBS; 50 mM Tris-HCl pH 7.6, 150 mM NaCl). Slides were incubated with the primary antibody, in humidified chambers, overnight at room temperature.

Slides were washed with PBS while the biotinylated secondary antibody was diluted with 1% FCS in TBS to the required concentration (1:250). Slides were incubated in humidified chambers with diluted secondary antibody for 60 minutes. After washes with PBS the sections were overlaid with ABC reagent (Vectastain Elite ABC kit, Vector laboratories) made according to the manufacturer's instructions (2 drops reagent A [Avidin DH solution], 2 drops reagent B [Biotinylated peroxidase] in 5 ml PBS). Each avidin molecule within the ABC reagent has four binding sites for biotin. When reagent A and reagent B are mixed, a complex between avidin and the biotinylated enzyme is formed which still retains biotin-binding sites. The free biotin-binding sites attach to the secondary antibodies on the tissue sections, amplifying the signal.

After 30 minutes incubation in humidified chambers and subsequent washes with PBS, the slides were incubated with working strength 3,3-diaminobenzidine (DAB) solution (DAB substrate kit for peroxidase, Vector laboratories), according to manufacturer's instructions (2 drops buffer stock, 2 drops DAB stock, 2 drops hydrogen peroxide stock and 2 drops nickel solution in 5 ml dH_2O). The DAB solution acts as an electron donor for peroxidase activity. Upon oxidation, a coloured insoluble product is formed; in this case the presence of nickel chloride results in a grey/black product. Slides were incubated for 10 minutes and then washed in tap water for 5 minutes.

Sections were counterstained with nuclear fast red, which gave a pink nuclear stain that contrasts with the grey/black DAB staining. Slides were incubated for 1 minute in nuclear fast red solution (0.1% w/v nuclear fast red, 5% w/v aluminium sulfate, 1% v/v chloroform). The sections were washed twice in dH_2O for 2 minutes and dehydrated

through an ethanol series (25%, 50%, 70%, 90%) with two final washes in 100% ethanol. Slides were incubated for two 5 minute washes in HistoClear and mounted with DPX.

Five percent goat serum in PBS was used in place of the primary antibodies as negative controls and in no case was specific signal observed. The sections were photographed using a digital camera attached to a Zeiss Axiophot 2 microscope and images were imported into Adobe Photoshop v6.0 for further analysis.

2.8 WHOLE MOUNT TUNEL

TUNEL (TdT-mediated dUTP-biotin nick end labelling, (Gavrieli *et al.*, 1992)) was performed on whole embryos to detect apoptotic cells, according to the method of Martinez-Barbera and colleagues (2002). All PBT (PBS with 0.1% polyoxyethylenesorbitanmonolaurate [tween 20, Sigma]) washes were repeated three times at room temperature for 5 minutes unless otherwise stated.

2.8.1 Sample preparation

Embryos were rehydrated through a methanol series (75%, 50%, 25% diluted with PBT), followed by washes with PBT. They were then incubated in PBS with 10 μg/ml proteinase K at room temperature for different times depending on the size of the embryo (E8.5 for 1 minute, E9.5 for 3 minutes and E10.5 for 5 minutes). Digestion was stopped by a two minute wash in 2 mg/ml glycine in PBT, followed by two washes with PBT. The embryos were incubated at room temperature for 20 minutes in 4% PFA in

PBS and then washed in PBT. The embryos were re-fixed in pre-chilled ethanol: acetic acid (2:1) on ice for 10 mins, and then washed with PBT.

2.8.2 Terminal transferase reaction

The terminal transferase reaction used components from the ApopTag *In Situ* Apoptosis detection kit (Intergen). The embryos were incubated for 1 hour with equilibration buffer. After removal of the equilibration buffer, working strength terminal deoxynucleotidyl transferase (TdT) enzyme (reaction buffer: TdT enzyme, 2:1 with 0.3% (v/v) Triton X100) was added to cover the embryos and incubated overnight at 37 °C. The reaction was stopped by washing the embryos in working strength stop buffer (stop buffer diluted 1:17 in distilled water) for 3 hours at 37 °C with several changes, followed by three washes in PBT.

2.8.3 Detection

The embryos were blocked in a wash solution (2 mg/ml BSA [Sigma] in PBT) containing 5% (v/v) sheep serum (Sigma) for 1 hour then incubated with antibody solution (1/2,000 anti-digoxigenin-AP Fab [Roche], 1% sheep serum in wash solution) overnight at 4 °C. Excess antibody was removed by incubating the embryos throughout the day and overnight in a number of changes of wash solution at room temperature. The following day the embryos were equilibrated with NTMT (100 mM sodium chloride, 100 mM Tris.HCl pH 9.5, 50 mM magnesium chloride, 0.1% Tween-20) by three 10 minute washes and then incubated with 17 µl/ml nitroblue tetrazolium/5-bromo-4-chloro-indolyl-phosphatase (NBT/BCIP, Roche) in PBT in the dark for 15

minutes. The reaction was stopped by washes in PBT, the embryos were then fixed with 4% PFA in PBS for 30 minutes and washed in PBT. Embryos were stored at 4 °C, in the dark to prevent bleaching of the staining, in PBT with 0.05% thimerazol (Sigma) to prevent fungal growth. Embryos were analysed and the images captured using an imagemanager 1000 system (Leica).

2.9 PROBE GENERATION FOR WHOLE MOUNT *IN SITU* HYBRIDISATION

Digoxigenin-labelled RNA probes were generated from plasmids containing a cDNA insert of the gene of interest. All solutions used in the preparation of the riboprobes were treated with diethyl pyrocarbonate (DEPC), an inhibitor of ribonucleases, in order to avoid degradation of the newly synthesised RNA. DEPC was added to solutions at 0.05% v/v, mixed thoroughly and left overnight at room temperature before the solutions were autoclaved.

2.9.1 Transformation

To obtain large amounts of plasmid, DH5α competent cells (Promega) were transformed with the plasmid of interest and recombinants were selected on the basis of acquired antibiotic resistance to ampicillin.

A 50 µl aliquot of competent DH5α cells in a 1.5 ml eppendorf was thawed on ice for 10 minutes, 50 ng of plasmid DNA was added and mixed gently. A negative control, where no plasmid DNA was added, was carried out in parallel with each step. Cells

were incubated on ice for 30 minutes before heat-shocking at 42 °C for 45 seconds in a water bath. The cells were again placed on ice for 1-2 minutes and 1 ml of LB-broth (Invitrogen) containing 20 mM glucose, 2.5 mM KCl and 10 mM $MgCl_2$ was added. To allow expression of antibiotic resistance proteins, the bacteria were incubated at 37 °C with vigorous shaking for 1 hour before 100 µl was plated onto an LB-agar culture plate containing 50 µg/ml ampicillin. After incubation at room temperature for 15 minutes, the plates were inverted and incubated at 37 °C overnight.

The cDNAs of interest had been cloned into bluescript vectors (Stratagene) which contain the β-lactamase gene that confers resistance to ampicillin. Only bacteria containing a plasmid survive on the ampicillin-containing agar plates, as confirmed by the lack of colony growth on the negative control plates.

2.9.2 Isolation of plasmid DNA

Isolation of plasmid DNA was carried out using a HiSpeed Plasmid Midi kit (Qiagen) following the manufacturer's instructions. A single colony was grown for 8 hours at 37 °C with vigorous shaking in 5 ml LB-broth containing 50 µg/ml ampicillin. A 100 µl aliquot of this starter culture was then added to 50 ml fresh LB-broth (1:500 dilution) containing ampicillin (50 µg/ml) and incubated overnight at 37 °C with vigorous shaking. The cells were harvested by centrifugation at 6,000 g for 15 minutes at 4 °C. The bacterial pellet was resuspended in 6 ml buffer P1 (50 mM Tris.HCl, pH 8.0; 10 mM EDTA; 100 µg/ml RNase A). The cells were then lysed by addition of 6 ml buffer P2 (200 mM NaOH, 1% w/v SDS), followed by gentle mixing through the

inversion of the tube a number of times and incubation for 5 minutes at room temperature. The lysis reaction was stopped and the cell debris was precipitated by addition of 6 ml of chilled buffer P3 (3 M potassium acetate, pH 5.5) followed by gentle inversion to ensure complete precipitation. The lysate was then poured into the barrel of a filtration unit (QIAfilter Cartridge) to remove the unwanted cell debris. A HiSpeed-tip was equilibrated during the lysate-cartridge incubation by allowing 4 ml of buffer QBT (750 mM NaCl; 50 mM MOPS, pH 7.0; 15% v/v isopropanol; 0.15% v/v Triton X-100) to drain through the tip by gravity flow. After being left at room temperature for 10 minutes the lysate was pushed through the cartridge and collected in a previously equilibrated anion-exchange resin column (HiSpeed-tip). The cleared lysate was allowed to pass through the equilibrated HiSpeed-tip by gravity flow. The column was then washed twice with 20 ml buffer QC (1 M NaCl; 50 mM MOPS, pH 7.0; 15% v/v isopropanol) to remove any remaining contaminants; again gravity flow was used to pass the solution through the column. The DNA was eluted from the column with 5 ml buffer QF (1.25 M NaCl; 50 mM Tris.HCl, pH 8.5; 15% v/v isopropanol). The eluted DNA was precipitated by incubation with 3.5 ml of isopropanol for 5 minutes at room temperature. After the incubation period the solution was added to a syringe with a QIAprecipitator module attached to the end. The DNA was trapped in the QIAprecipitator when the solution was filtered through. To clean the DNA, 2 ml 70% ethanol was pushed through the syringe and then air was pushed through the filter to remove any remaining ethanol. Plasmid DNA was eluted from the QIAprecipitator with 1 ml buffer TE (10 mM Tris.HCl, pH8.0; 1 mM EDTA). The quantity of DNA recovered was determined by spectrophotometry (UVmini1240, Shimadzu). The

absorption of a DNA aliquot at 260 nm was measured and used to calculate the final concentration.

Concentration of plasmid DNA (μg/ml) = OD_{260nm} × dilution factor × 50

The purity of the DNA was also assessed by measuring the absorption at 280 nm; the ratio OD_{260nm}: OD_{280nm} for good quality DNA should be approximately 1.8.

2.9.3 Linearisation of plasmid DNA

Plasmids were linearised in preparation for the *in vitro* transcription reaction to generate riboprobes. A reaction mixture was prepared containing 5 μg plasmid DNA, 20 units of the appropriate enzyme (Table 2.3) and a final concentration of 1X of the corresponding reaction buffer, the volume was made up to 50 μl with DEPC-H_2O. The reaction mixture was incubated at 37 °C for 2-4 hours. The success of the linearisation was checked by comparison of a sample (5 μl) of each digestion to an uncut plasmid sample on a 1% agarose gel. After electrophoresis, linear DNA runs at an apparently different molecular weight than uncut circular DNA. The linearised plasmids were recovered from the reaction mixture by phenol-chloroform extraction (Section 2.9.4).

Plasmid	Insert size (bp)	Insert site	Linearised with	Transcribed with	Source
Dll 1	1117	EcoRI	HindIII	T3	(Bettenhausen *et al.*, 1995)
Dll 3	2100	EcoRI	NotI	T7	(Dunwoodie *et al.*, 1997)
Pax 3	519	PstI	HindIII	T7	(Goulding *et al.*, 1991)

Table 2.3 Antisense RNA probes used for whole mount *in situ* hybridisation

2.9.4 Phenol-chloroform DNA extraction

An equal volume of phenol-chloroform (International Biotechnologies Inc.) was added to the reaction mixture (Section 2.9.3), mixed thoroughly and then centrifuged at 12,000 g for 15 minutes. The aqueous layer was transferred to a clean tube and an equal volume of chloroform was added. After thorough mixing and centrifugation the aqueous phase was again transferred to a clean tube, three volumes of 1.3% potassium acetate in 95% ethanol was added and incubated at -20 °C overnight or -80 °C for 30 minutes to precipitate the DNA. After centrifugation for 10 minutes at 4 °C the supernatant was discarded and the pellet washed with two and a half volumes (of the original volume) of 70% ethanol. The pellet was collected by centrifugation for 2 minutes at 4 °C, followed by air drying for 10 minutes. The pellet was resuspended in 10 µl TE (10 mM Tris.HCl, pH 8.0; 1 mM EDTA) or distilled water and quantified by spectrophotometry.

2.9.5 Synthesis of digoxygenin (DIG)-labelled probes

Antisense and sense (control) riboprobes were synthesised and labelled using DIG RNA labelling mix (Roche). A transcription reaction was prepared containing 1X transcription buffer, 1X DIG RNA labelling mix, 1 µg linearised plasmid DNA, 40 units of the appropriate RNA polymerase (Table 2.3) and the volume was made up to 20 µl with DEPC-H_2O. The reaction mixture was briefly vortexed and incubated at 37 °C for 2 hours. Agarose gel electrophoresis was used to visualise the efficiency of the transcription reaction. Two bands were expected; a high molecular weight band corresponding to the plasmid DNA template and a low molecular weight band corresponding to the transcript, which after an efficient reaction should be approximately 10 times more intense than the template DNA band. The DIG labelled

RNA was precipitated by addition of 0.1 volumes DEPC-treated 3M sodium acetate, 3 volumes 100% ethanol and 1 µl tRNA and incubation at -20 °C overnight. The precipitate was pelleted by centrifugation at 13,000 rpm for 10 minutes at 4 °C, and then washed with 500 µl 70% ethanol to remove any remaining salts. After centrifugation at 13,000 rpm at 4 °C for 2 minutes the pellet was air dried and resuspended in DEPC-H_2O to give a final concentration of 0.1 µg/µl. One µl (36 u) RNAse guard (Amersham) was added and the riboprobes were stored at -20 °C.

2.10 WHOLE MOUNT *IN SITU* HYBRIDISATION

Whole mount *in situ* hybridisation was performed following the method described by Wilkinson (1992) with some adaptations (Ybot-Gonzalez *et al.*, 2005). Unless otherwise stated all washes were carried out at room temperature with rocking for 5-10 minutes, in 5-10 ml volumes.

2.10.1 Embryo pre-treatment

Embryos previously stored in 100% methanol at -20 °C were rehydrated through a methanol series (75%, 50%, 25%) diluted in PBT, followed by two washes for 10 minutes in PBT. In order to quench endogenous peroxidases, embryos were incubated in 6% hydrogen peroxide in PBT for 1 hour, followed by three washes in PBT. Embryos were treated with 10 µg/ml proteinase K in PBT for varying times depending on the size of the embryo (E8.5 for 1 minute, E9.5 for 4 minutes, E10.5 for 8 minutes) in order to permeabilise cell walls to allow penetration by the riboprobe. The reaction was stopped by washing in 2 mg/ml glycine in PBT followed by two washes in

PBT. Embryos were refixed in 4% PFA in PBS for 20 minutes, washed twice in PBT and then placed in 2 ml prehybridisation mixture (50% formamide, 5X SSC, 2.5 mg/ml yeast RNA, 1% SDS, 2.5 mg/ml heparin) at 65 °C. Once the embryos had sunk, the prehybridisation mix was replaced with 5 ml of fresh mix and incubated at 65 °C for 1 hour. Embryos were stored at -20 °C in the prehybridisation mixture.

2.10.2 Hybridisation and post-hybridisation washes

Embryos were placed in 1 ml of fresh prehybridisation mix, 0.1 μg/ml of digoxigenin-labelled probe was added and incubated at 70 °C overnight. The following day the hybridisation mix (prehybridisation mix with riboprobe) was removed and stored at -20 °C for use in one subsequent experiment. In order to remove excess probe, embryos were washed three times for 30 minutes at 70 °C in solution 1 (50% formamide, 5X SSC pH 4.5, 1% SDS) followed by two washes at 65 °C in solution 2 (50% formamide, 2X SSC pH 4.5, 1% SDS) for 30 minutes each. Embryos were then washed three times in TBST (0.14 M sodium chloride, 25 mM potassium chloride, 25 mM Tris.HCl pH 7.5, 1% Tween-20, 2 mM levamisole) for 10 minutes then blocked in 10% sheep serum in TBST for 90 minutes to avoid non-specific binding of the antibody. Embryos were incubated overnight in the preabsorbed antibody solution (Section 2.10.3) at 4 °C.

2.10.3 Preparation of preabsorbed antibody solution

A suitable volume of preabsorbed antibody solution was prepared to give a final volume of 2 ml for each tube of embryos. The volumes stated in this section are suitable for preparing enough antibody solution for one tube of embryos. Embryo powder was

prepared by homogenising E8.5-E14.5 embryos in a minimum volume of PBS. The homogenate was washed in four volumes of ice-cold acetone followed by centrifugation at 6,000 rpm for 10 minutes. The acetone wash was repeated and followed by centrifugation. The pellet was ground into a powder, spread on filter paper to air dry and stored at -20 °C. A 3 mg sample of embryo powder was incubated at 70 °C for 30 minutes with 0.5 ml TBST. After cooling on ice, 5 µl of sheep serum and 1 µl anti-digoxygenin antibody (alkaline phosphatase-conjugated Fab fragments, Boehringer Mannheim) were added. The mixture was incubated for 1 hour at 4 °C to preabsorb the antibody and then centrifuged at 6,000 rpm for 10 minutes at 4 °C. The antibody solution (supernatant) was removed and diluted to 2 ml with 1% sheep serum in TBST. The embryo powder was stored at -20 °C for re-use.

2.10.4 Post-antibody washes and development

The antibody solution was removed and the embryos were washed in TBST three times for 10 minutes followed by a minimum of five 1 hour washes and left overnight in TBST. Embryos were placed in glass pots and equilibrated with three 10 minute washes in NTMT before incubation with 17 µl/ml NBT/BCIP in 1 ml NTMT in the dark for 20 minutes with rocking. The incubation continued without rocking until the signal had developed. The reaction was stopped by two washes with PBT and embryos were stored at 4 °C in the dark in PBT with 0.05% thimerazol. Embryos were analysed and the images captured on an imagemanager 1000 system (Leica). No specific hybridisation signals were seen with the sense probes.

2.11 CELL CULTURE OF HUMAN EMBRYONIC FIBROBLASTS

2.11.1 Basic cell culture procedures

Sterile conditions were used throughout the cell culture procedures to minimize the possibility of contamination. Procedures were carried out in a class II microbiological safety cabinet (Envair) and, before use, all materials were sprayed with 70% industrial methylated spirit (IMS). Solutions were warmed to 37 °C before use. All the reagents used for cell culture were obtained from Sigma unless otherwise stated. DMEM containing 1.5 g/l sodium bicarbonate, 10% FCS, 2% chicken serum, 100 u penicillin and 100 μg/ml streptomycin was used as culture medium throughout this study and is referred to as "medium". Medium was made up in 500 ml bottles when needed, sterilized by vacuum driven filtration through a 0.22 μm filter stericup (Millipore) and used or discarded within a month. Cells were cultured in a Galaxy R CO_2 incubator (Scientific Laboratory Supplies Ltd), with 5% CO_2 at 37 °C.

2.11.2 Sample collection and processing

Samples of amniotic fluid, skin, cord or cartilage were collected with ethical permission by fetal pathologists at University College Hospital, from fetuses aged 12-21 weeks. Samples were allocated to one of three groups, NTD-affected, normal control or affected control (fetuses affected with malformations other than NTD). The samples were sent to Great Ormond Street Hospital (GOSH) Cytogenetics Laboratory where fibroblastic cell lines were established.

3T3 mouse fibroblast cells were obtained from the Dunn School Cell Bank (Department of Pathology, University of Oxford) by Dr. Andrew Stoker. A frozen aliquot was stored in liquid nitrogen until needed.

Human cell lines established by the GOSH Cytogenetics Laboratory were frozen down and stored in liquid nitrogen until required. Cells were removed from the culture flasks by trypsinisation. A stock solution of 10X trypsin–EDTA was diluted to 1X in PBS and 1 ml was added to the cells for 2-3 minutes until they had rounded up and begun to detach from the bottom of the flask. The digestion was stopped by adding 5 ml of medium and cells were pelleted by centrifugation for 5 minutes at 1,000 rpm and resuspended in 0.9 ml medium. The cell suspension was transferred to cryotubes and 0.1 ml dimethyl sulfoxide (DMSO) was added to give a final concentration of 10%. The tubes were immediately placed in an isopropanol tray (Nalgene) and transferred to -70 °C. When placed at -70 °C this tray allows cooling to occur at -1 °C/minute ensuring the cells were not damaged during the freezing process. Once frozen the tubes were transferred to liquid nitrogen until needed.

2.11.3 Maintenance of cells in culture

The 3T3 cells and human cell samples were treated in the same manner throughout these experiments, although 3T3 cells did grow at a much faster rate. Cells were defrosted and immediately placed in 5 ml medium to dilute the DMSO, which could cause cellular damage. The cells were pelleted by centrifugation at 1,000 rpm for 5 minutes. The supernatant was discarded and the cells were resuspended in 2 ml of medium then placed into a well of a 6-well plate (NUNC) and incubated at 37 °C in 5%

CO_2. Cells were grown to confluence with changes of medium when necessary; spent medium was removed by aspiration before fresh medium was added. The growth and health of cultures was checked daily using an inverted microscope (Zeiss). Once the cells were confluent they were passaged by trypsinisation (Section 2.11.2). After centrifugation the cells were resuspended in 4 ml medium and each sample was seeded in 2 wells (2 ml/well). Cells were again grown to confluence and subsequently passaged by trypsinisation. The cells were resuspended and seeded in 4 wells/sample. Once confluent, the cells from one of the wells were frozen down (passage 3) as described above (Section 2.11.2) while the other cells were seeded for the third time into two 25 cm^2 culture flasks. When the cells were confluent these flasks yielded enough cells to carry out the dU suppression test.

2.11.4 Solutions for the deoxyuridine (dU) suppression test

In initial experiments a series of deoxyuridine (dU) stocks (500 mM, 50 mM, 1 mM, 0.1 mM) were added to the culture medium as 1-3% (v/v) additions (10-30 µl/ml) to give final concentrations ranging from 1 µM to 500 µM. In later experiments, 1 mM dU was used as a 1-2% (v/v) addition giving final concentrations of 10 µM, 15 µM or 20 µM. In the inhibitor experiments the folate/methylation cycle inhibitors 5-fluorouracil, aminopterin and cycloleucine were added to the relevant flasks as 0.5-2% (v/v) additions to test the sensitivity of the experiment. Each test condition was carried out in duplicate within each experiment.

2.11.5 dU suppression test

Cells were seeded (passage 5) in 6-well plates at 0.5 $x10^6$ cells/well for 3T3 cells and 0.25 $x10^6$ cells/well for the human samples and incubated overnight to allow the cells to adhere. The dU and/or inhibitors were added to the appropriate wells and an equal volume of PBS was added to the untreated cells. After two hours of incubation the medium in all the wells was replaced with fresh medium containing 0.5 μCi/ml [^{3}H]-thymidine (Amersham Pharmacia). The dU, PBS and/or inhibitors were then added to the relevant wells as before. The cells were cultured for 24 hours after which the medium was removed and stored for disposal in a designated radioactive waste area. The cells were then detached by trypsinisation, pelleted by centrifugation and resuspended in 200 μl PBS containing 0.3 M sodium hydroxide. Cells were lysed by repeated freeze/thawing (three cycles) and stored at -20 °C. Samples were taken for determination of protein content (Section 2.11.6) and incorporation of [^{3}H]-thymidine into DNA (Section 2.11.7).

2.11.6 Determination of protein content

Duplicate 5 μl samples of homogenate were used for determination of protein content using the bicinchoninic acid (BCA) protein assay reagent (Pierce) following the manufacturer's instructions. A fresh series of standard protein solutions were made in duplicate from an initial 200 μg/ml standard protein solution (bovine serum albumin) for each protein assay. Water was added to standards and samples to a final volume of 50 μl. The BCA working reagent, a 50:1 mixture of reagents A and B (Pierce) was made fresh for each assay. BCA working reagent (1 ml) was added to each standard/sample tube and incubated for 30 minutes at 60 °C. The OD_{562nm} for each

sample and standard was read using a UVmini1240 spectrophotometer (Shimadzu), a standard curve was plotted and protein concentrations of the samples calculated, using pre-installed software.

2.11.7 Measurement of [^{3}H]-thymidine incorporation

The DNA was extracted from duplicate 40 µl samples of the homogenate by digestion with 10 µg/ml proteinase K at 56 °C for 3 hours followed by precipitation with three volumes of 1.3% potassium acetate in 95% ethanol (as described in Section 2.9.4). Following centrifugation, the pellet was resuspended in 60 µl ddH_2O and 0.8 ml scintillation cocktail (universol, ICN) was added, mixed thoroughly and the cpm was measured on a 1450 MicroBeta (Trilux) scintillation counter.

CHAPTER 3; INVESTIGATING THE EFFECT OF HOMOCYSTEINE ON CRANIAL NEURAL TUBE CLOSURE

3.1 INTRODUCTION

Metabolism of homocysteine provides the link between the methylation cycle and folate metabolism. Methionine is formed by the remethylation of homocysteine by methionine synthase in a vitamin-B_{12} and folate dependent reaction. The methyl donor in this reaction is 5-methyl tetrahydrofolate (5-methyl THF), generated in the folate cycle (Figure 1.6). As discussed earlier (Section 1.9), elevated levels of homocysteine have been implicated in the production of NTD (Steegers-Theunissen *et al.*, 1994;Mills *et al.*, 1995;Van der Put *et al.*, 1997a). Previous animal studies to investigate the possible deleterious effect of homocysteine on neural tube closure gave conflicting results. Treatment of chick embryos with homocysteine throughout neurulation induced NTD in 27% of the embryos and 23% exhibited heart defects (Rosenquist *et al.*, 1996). However, *in vitro* treatment of rat embryos with high doses of homocysteine did not cause NTD but was embryotoxic, causing growth retardation and somite defects (VanAerts *et al.*, 1994). In contrast to both of these studies, a recent investigation of the effect of homocysteine on neural tube closure in mouse embryos concluded that homocysteine is neither embryotoxic nor causes NTD (Hansen *et al.*, 2001). Therefore, I aimed to carry out a comprehensive study of the effect of homocysteine on cranial neural tube closure in mouse.

Cranial neural tube closure was investigated because in the initial study that identified homocysteine-induced neural tube defects in chick, the majority of NTD affected the cranial region (Rosenquist *et al.*, 1996). A large number of studies in several different animal models have shown that teratogens can affect cranial and spinal neural tube closure to varying degrees. For example, *in vitro* exposure of mouse embryos to sodium

arsenate throughout neurulation resulted in a 25% incidence of cranial NTD, with the caudal end of the embryo unaffected (Chaineau *et al.*, 1990). Maternal injection with 5-azacytidine produced exencephaly, but not spina bifida, in both mouse and rat embryos (Takeuchi and Murakami, 1978;Takeuchi and Takeuchi, 1985). In addition, rat embryos exposed throughout neurulation to high levels of oxygen fail to complete cranial neural tube closure (Morriss and New, 1979). Neural tube closure at this axial level may therefore be more sensitive to homocysteine treatment than more caudal regions.

Homocysteine thiolactone was used in the experiments in this chapter, because in the thiolactone form homocysteine is more stable within the whole embryo culture system (Hansen *et al.*, 2001). Homocysteine thiolactone has also been shown to simulate the physiological effects of homocysteine in experimental systems, as similar effects of homocysteine and the equivalent level of homocysteine thiolactone have been shown in chick (Rosenquist *et al.*, 1996) and rat embryos (VanAerts *et al.*, 1994).

Homocysteine thiolactone is synthesized naturally in the body and has been found in every cell type examined from bacteria to human (Carmel *et al.*, 2001). Some aminoacyl-tRNA synthetases (primarily methionyl-tRNA synthetase (Jakubowski and Goldman, 1993)) have an error-editing function to prevent the incorrect incorporation of homocysteine into protein. This error-editing function involves the misactivation of homocysteine and ATP, subsequently resulting in the production of the cyto-reactive thiolester, homocysteine thiolactone (Jakubowski and Fersht, 1981). Hydrolysis of homocysteine thiolactone results in its conversion back to homocysteine (Jakubowski, 1997).

In my study, homocysteine thiolactone exposure was observed to affect somite development (Table 3.2) and genetic markers of somite development (*Delta-like 1* and *Delta-like 3*) were used to investigate this phenomenon. *Delta-like* genes are mouse homologues of the *Drosophila* gene *Delta* which, along with its receptor *Notch*, is involved in cell fate determination during development. In vertebrates, *Notch* and *Delta* signalling is involved in neurogenesis and somitogenesis (Lewis, 1998). *Delta-like 1* (*Dll1*) and *Delta-like 3* (*Dll3*) have distinct expression patterns during somitogenesis and are believed to function together in the formation of somite borders and boundaries during segmentation (Dunwoodie *et al.*, 1997). *Dll1* is expressed in the paraxial mesoderm and in the caudal half of condensed somites (Bettenhausen *et al.*, 1995). In *Dll1*-deficient mouse embryos, somite boundaries are not maintained and there is no rostro-caudal polarity within the somites (De Angelis *et al.*, 1997). *Dll3* is expressed in the paraxial mesoderm and the rostral half of the most recently formed somite (Dunwoodie *et al.*, 1997). In the *Pudgy* mouse a mutation in the *Dll3* gene results in severe disruption of somite boundaries resulting in somites with irregular size and shape (Kusumi *et al.*, 1998).

3.2 RESULTS

Dose toxicity studies were carried out using non-mutant CD1 embryos cultured for 24 hours from E8.5 (4-6 somite stage) to E9.5 in the presence of homocysteine thiolactone. PBS was used as a vehicle control and embryos from within litters were randomly selected for different treatment groups to minimise any effect of litter to litter variation. At the end of the culture period embryos were assessed for developmental progression, growth and viability. Any morphological abnormalities were recorded for each embryo.

3.2.1 Dose-dependent embryotoxicity of homocysteine thiolactone in CD1 mice

Exposure of embryos to homocysteine thiolactone during the period of cranial neural tube closure resulted in a dose-dependent occurrence of developmental defects and toxicity. A homocysteine thiolactone concentration of 1.5 mM was embryotoxic, with none of the embryos surviving to the end of the culture period as illustrated by the absence of yolk sac circulation (Table 3.1). These embryos did survive for part of the culture period, however, as the embryo somite numbers increased from 4 to 6 to an average of 15 to 16 before the embryos died. Some of the embryos cultured in 1 mM homocysteine thiolactone survived throughout the culture period but they were growth-retarded, as indicated by significantly lower mean somite number and mean crown-rump length compared to embryos treated with PBS only (vehicle control) (Table 3.1). There were no indications of developmental or growth retardation in embryos treated with 500 μM and lower concentrations of homocysteine thiolactone.

Hcy conc. (mM)	No. embryos	No. viable embryos	Yolk Sac circulation	Somite number	Crown-rump length (mm)
0	59	58	2.61 ± 0.09	19.17 ± 0.38	2.43 ± 0.04
0.25	27	27	2.81 ± 0.09	18.85 ± 0.24	2.45 ± 0.05
0.5	72	71	2.44 ± 0.10	18.64 ± 0.27	2.40 ± 0.03
1.0	10	4	0.40 ± 0.16*	16.22 ± 0.81*	2.13 ± 0.10*
1.5	6	0	0.00 ± 0.00*	15.67 ± 0.67*	2.13 ± 0.04*

Table 3.1 Growth and development of CD1 mouse embryos cultured in the presence of homocysteine thiolactone

Embryos were assessed for viability, yolk sac circulation score (0-3) and growth parameters at the end of the culture period. Values are given as mean ± SEM. * indicates significant variation from control embryos cultured without Hcy. ($p<0.001$, tested by one-way ANOVA followed by pair-wise analysis by TUKEY test) Abbreviations: Hcy, homocysteine thiolactone.

3.2.2 Developmental defects in homocysteine thiolactone-treated embryos

Whole embryo culture with 500 μM and higher concentrations of homocysteine thiolactone induced a number of developmental abnormalities (Table 3.2). These abnormalities can be divided into two groups: (i) defects that reflect the growth retardation of the embryo and (ii) defects that are independent of growth retardation.

The failure to complete axial rotation and cranial neural tube closure observed in embryos treated with 1 mM and above concentrations of homocysteine thiolactone (Table 3.2) are associated with growth retardation. In CD1 mouse embryos, cranial

Hcy conc. (mM)	No. embryos	No. Abnormal embryos	Axial rotation failed	Cranial neural tube open	Cranial NTD	Blisters	Somite defects
0	59	6 (10.1)	4 (6.8)	4 (6.8)	1 (1.8)	0 (0.0)	0 (0.0)
0.25	27	4 (14.8)	1 (3.7)	1 (3.7)	0 (0.0)	0 (0.0)	0 (0.0)
0.5	72	37 (51.4)*	4 (5.5)	9 (12.3)	6 (9.0)	14 (19.4)*	21 (29.2)*
1.0	10	10 (100)*	2 (20.0)	3 (33.3)	1 (12.5)	2 (20.0)*	6 (60.0)*
1.5	6	6 (100)*	4 (66.7)*	3 (50.0)*	0 (0.0)	3 (50.0)*	2 (33.3)*

Table 3.2 Incidence of developmental defects in mouse embryos exposed to homocysteine thiolactone

The total incidence of abnormalities includes the absence of yolk sac circulation, failure of axial rotation and embryonic malformations. Cranial NTD are defined as failure to complete neural tube closure in embryos that have 16 or more somites. Data are presented as number of embryos with percentage in each treatment group in parentheses. * indicates significant variation from control embryos cultured without Hcy ($p<0.05$, tested by Z-test). Abbreviations: Hcy, homocysteine thiolactone.

neural tube closure is normally completed by the time embryos have developed to the 16 somite stage and axial rotation is completed at an earlier developmental stage (13-14 somites). At a concentration of 1.5 mM homocysteine thiolactone the cranial neural tube had not closed in half of the embryos treated. However, due to the toxic effect of homocysteine thiolactone none of these embryos developed to a stage at which closure would be expected to occur and cannot, therefore be described as exhibiting NTD. Only embryos which failed to complete cranial neural tube closure after they had reached the 16 somite stage of development were described as exhibiting an NTD. At 1 mM homocysteine thiolactone, a large proportion of treated embryos also exhibit open cranial neural tubes but are severely growth retarded. A few cases of NTD, in which the cranial neural tube remains open in embryos with at least 16 somites, do arise in embryos cultured in the presence of lower doses of homocysteine thiolactone (Table 3.2). However, there is no statistically significant difference in the incidence of NTD in treatment groups compared to the control group, tested by Z-test. These data suggest that homocysteine thiolactone treatment does not cause isolated cranial NTD in mouse embryos (Table 3.2).

Developmental defects observed in embryos treated with 500 μM homocysteine thiolactone are likely to be unrelated to growth retardation since, at this concentration, no significant reduction in somite number or crown-rump length after culture was observed. The most frequently observed abnormalities occurred in the caudal somites. In some cases, the most caudal two or three somites were difficult to identify individually, as the boundaries between somites were indistinct (Figure 3.1). In other cases the caudal-most somites were distinct but they were often irregular in size and

Figure 3.1. Developmental abnormalities induced by homocysteine thiolactone treatment

A-D show CD1 embryos after 24 hour culture with PBS (**A**, **C**) or 500 μM homocysteine thiolactone (**B**, **D**). **C** and **D** are magnified images of the embryos in **A** and **B** respectively. Significant developmental abnormalities induced by homocysteine thiolactone treatment included blisters on the surface epithelium of embryos (white arrow in **B**) and defects in the caudal-most somites. In some homocysteine thiolactone-exposed embryos a greater length of paraxial mesoderm remains unsegmented therefore the last few identifiable somites were in a more rostral position than those in the PBS treated control embryos (compare the three white arrowheads in **C** and **D**). Subsequent somites were often irregular in size and shape or indistinguishable (white arrow in **D**). Scale bars represent 200 μm. Abbreviations: Hcy, homocysteine thiolactone.

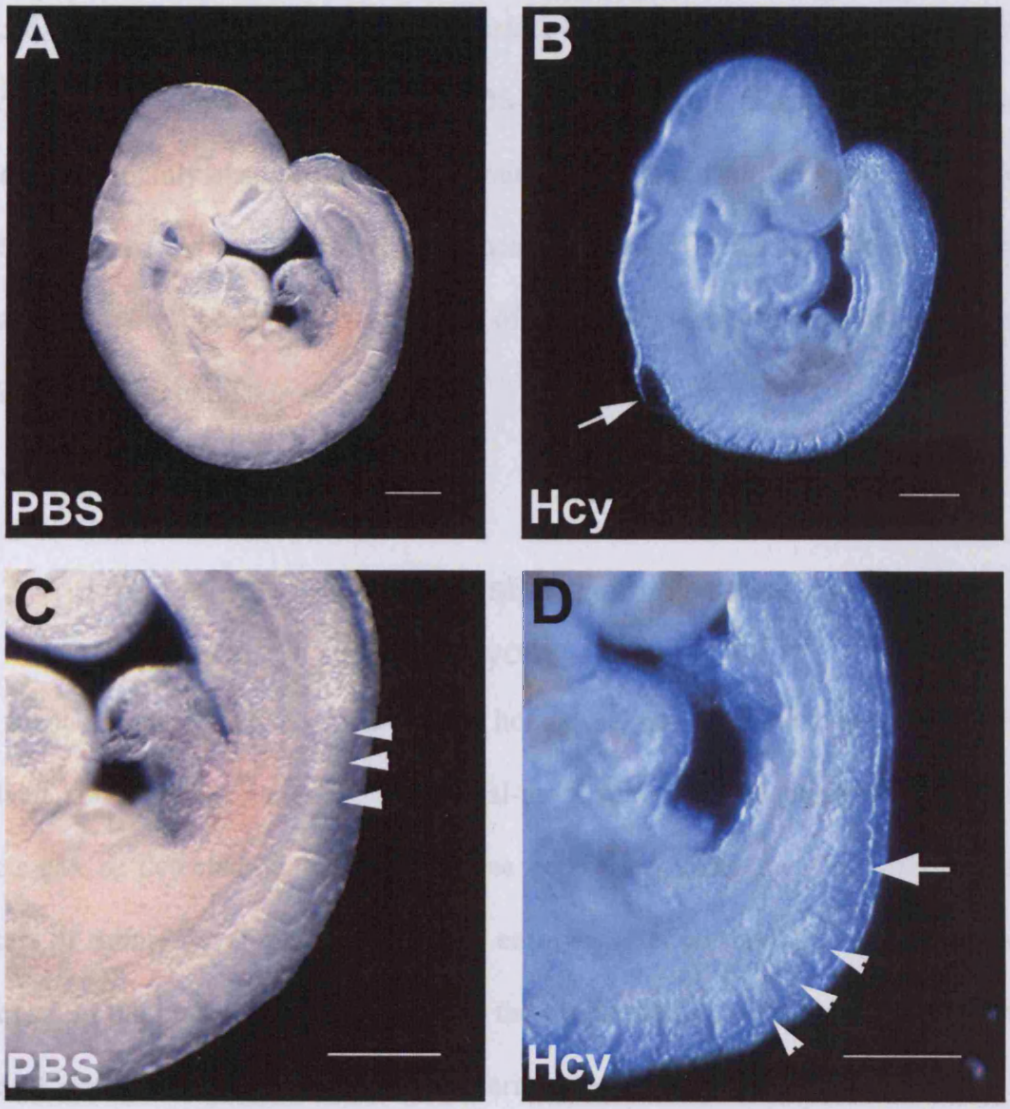
A
PBS
B
Hcy
C
PBS
D
Hcy

shape. Exposure to 500 μM or greater concentrations of homocysteine thiolactone also induced the formation of blisters on the surface epithelium of a significant number of embryos ($p<0.001$) when compared to PBS-treated controls (Figure 3.1, Table 3.2). Blisters were mainly observed on the forebrain and hindbrain surface but were also seen on other areas. Less common defects induced by homocysteine thiolactone treatment included an uneven or crinkled appearance of the surface epithelium and a reduction in the size of the forebrain.

3.2.3 The effect of homocysteine thiolactone treatment on somitogenesis in CD1 embryos

The most frequent defect observed in homocysteine thiolactone-treated embryos involved abnormal formation of the caudal-most somites. I examined whether these defects can be detected at the level of gene expression using the *Delta-like* genes as markers of somite development. In control embryos after culture, *Dll1* transcripts were expressed in the presomitic mesoderm and the caudal half of each somite. There was a stripe of strong *Dll1* expression in the anterior presomitic mesoderm that appeared to mark the nascent somites. In mature somites lower levels of transcript were restricted to the posterior halves of the somites (Figure 3.2 A,D). *Dll1* expression was also observed in the cranial neuroepithelium in the presumptive forebrain and midbrain (Figure 3.2 E) and in the spinal neural tube (Figure 3.2 D,E,F). *Dll3* was expressed in the presomitic mesoderm and the rostral half of the nascent somite. The highest level of transcript accumulation was in the presomitic mesoderm with lower levels expressed in the somite being formed (Figure 3.2 G). These expression patterns correspond to previous reports

of *Dll1* and *Dll3* expression in E9.5 embryos (Bettenhausen *et al.*, 1995;Dunwoodie *et al.*, 1997).

Expression of the *Delta-like* genes in the presomitic paraxial mesoderm of homocysteine thiolactone-treated embryos, with affected or unaffected somites, did not differ from control embryos (Figure 3.2 A-H). However, homocysteine thiolactone-treated embryos with abnormal somites showed more diffuse expression of *Dll1* in the somites compared to controls or unaffected homocysteine thiolactone-treated embryos (Figure 3.2 C,F compared to A,D and B,E respectively) illustrating a loss of somite boundaries in some homocysteine thiolactone-treated embryos.

Figure 3.2 Expression of *Dll1* and *Dll3* in homocysteine thiolactone-treated embryos

Expression of *Dll1* (**A-F**) and *Dll3* (**G, H**) in CD1 mouse embryos after 24 hours culture with PBS (**A, D, G**) or 500 μM homocysteine thiolactone (**B, C, E, F, H**). The embryos in **A-C** have been re-positioned in **D-F** respectively to provide a clearer view of the somites. Homocysteine thiolactone treatment caused irregular or indistinct somites in some embryos (black arrows in **C, F**), whereas the somites in other treated embryos were not affected (black arrows in **B, E**). The expression of *Dll1* in the presomitic mesoderm (PS) including the stripe of strong expression indicating the nascent somite (black arrowheads) were comparable between treated embryos (**B, C, E, F**) and controls (**A, D**). *Dll1* expression in the somites of affected homocysteine thiolactone treated embryos (black arrows in **C, F**) was more diffuse than that of unaffected homocysteine thiolactone treated (black arrows in **B, E**) and control (black arrows in **A, D**) embryos. *Dll1* transcripts were also detected in the forebrain and midbrain neuroepithelium (**A**) and the closed spinal neural tube (white arrowheads) in control (**D**) and treated (**E, F**) embryos. The expression of *Dll3* in the presomitic mesoderm (PS) and rostral half of the nascent somite (black arrowheads) were comparable between control (**G**) and treated (**H**) embryos. Scale bars represent 500 μm. Abbreviations: Hcy, homocysteine thiolactone; PS, presomitic mesoderm; FB, forebrain; MB, midbrain; S, somites

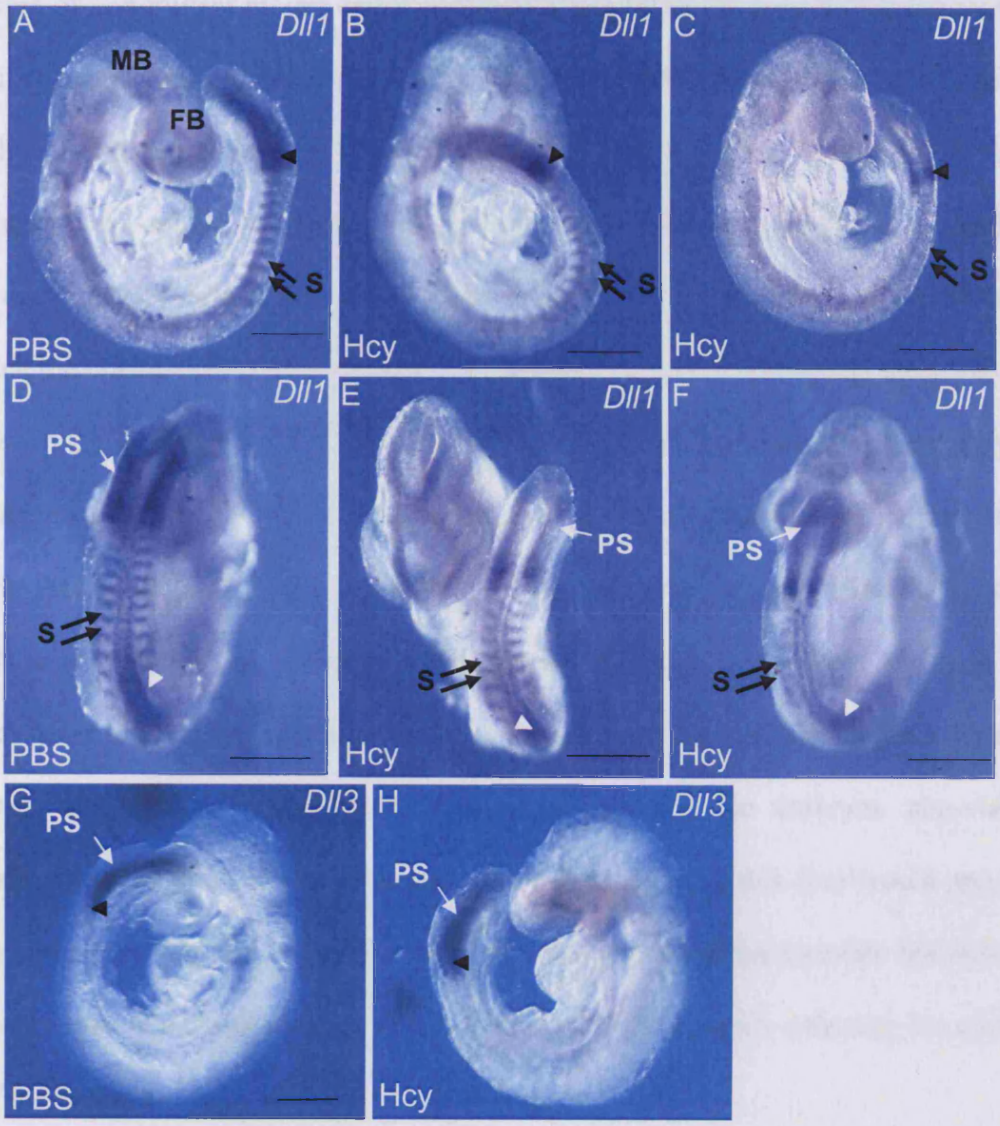
A
Dll1
MB
FB
S
PBS
B
Dll1
S
Hcy
C
Dll1
S
Hcy
D
Dll1
PS
S
PBS
E
Dll1
PS
S
Hcy
F
Dll1
PS
S
Hcy
G
Dll3
PS
PBS
H
Dll3
PS
Hcy

3.3 DISCUSSION

Exposure of non-mutant mouse embryos to homocysteine thiolactone during the period of cranial neural tube closure (24 hours from E8.5) resulted in dose-dependent toxicity, growth retardation and developmental abnormalities. Some of these abnormalities such as failure to turn appear secondary to the growth retardation. Many embryos exposed to high concentrations of homocysteine thiolactone failed to reach the developmental stage at which the cranial neural tube should have closed (16 somites). However, there was no increase in the incidence of NTD observed in homocysteine thiolactone-treated embryos that had reached the 16 somite stage compared to control embryos. Moreover, it is unlikely that a longer culture period with the highest doses of homocysteine thiolactone would have resulted in embryos with cranial NTD. All embryos exposed to homocysteine thiolactone concentrations of 1 mM and above developed abnormally and exposure to 1.5 mM homocysteine thiolactone left all the embryos non-viable suggesting that the toxic effects of homocysteine thiolactone at this dose would prevent the embryos reaching the 16 somite stage of development. Homocysteine thiolactone treatment induced a range of other abnormalities with the majority affecting the caudal end of the embryo.

Mice with null mutations in *Dll1* and *Dll3* exhibit defects in somite segmentation, suggesting that these genes may have a functional role in somite formation (De Angelis *et al.*, 1997;Kusumi *et al.*, 1998). The reduced definition of *Dll1* expression in the mature somites of affected homocysteine thiolactone-treated embryos illustrates the abnormal segmentation and compartmentalisation of the somites as observed morphologically. However, the apparently normal expression of *Dll1* and *Dll3* in the

presomitic mesoderm of homocysteine thiolactone-exposed embryos suggests that the segmentation defects observed in the newly formed somites are unlikely to result directly from loss of *Dll* gene expression during initial somite formation.

The defects observed in this study correlate with the reported effect of homocysteine on neurulation stage rat embryos (VanAerts *et al.*, 1994). In the rat, homocysteine treatment was embryotoxic, causing blisters and defects of the somites including irregular size and shape. However, there are discrepancies between my results and the previous study of homocysteine thiolactone treatment of mouse embryos (Hansen *et al.*, 2001). The authors did not find any toxic effects when mouse embryos were exposed to homocysteine thiolactone in whole embryo culture. Hansen *et al.* used the same mouse strain and homocysteine thiolactone was administered to the culture serum in a similar manner to this study. The differences in our findings are most likely due to the lower final concentration of homocysteine thiolactone tested in the previous study. An embryotoxic dose was probably not reached as the highest dose used was 0.65 mM (Hansen *et al.*, 2001) compared to 1.5 mM in this study.

The effects of homocysteine treatment on the development of mouse embryos shown in this chapter differ from those observed in the chick embryo where homocysteine treatment is reported to cause heart defects and NTD (Rosenquist *et al.*, 1996). The mode and dose of homocysteine application in the chick study differs greatly from the whole embryo culture system used in the rodent models. Rosenquist and colleagues, made a window in the eggshell and dropped 100 mM homocysteine thiolactone directly onto the inner embryonic membrane. This method involves much higher doses of

homocysteine and there could also be wide variation in the actual concentration each embryo was exposed to, depending on the position of the embryo. Differences in the yolk composition of each egg may affect the metabolism of compounds applied to chick embryos. In fact, previous work has shown that simply making a window in the eggshell can be enough to induce NTD in some chick embryos (Mann and Persaud, 1979). However, the study by Rosenquist and colleagues included numerous control groups suggesting this is not the cause of NTD in this study.

Not only are there differences between the outcome of homocysteine treatment of mammalian and chick embryos, but additional studies have led to conflicting results on the effect of homocysteine exposure in chick embryos. Afman and colleagues (2003a) found homocysteine thiolactone treatment *in ovo* did not cause NTD but did result in malformations similar to those found in rat (VanAerts *et al.*, 1994) and mouse embryos (Greene *et al.*, 2003). These abnormalities included blisters, somite deformation, caudal degeneration and disturbances in vein development. A later study by the Rosenquist group, Andaloro and colleagues (1998), repeated their original finding of a 28% NTD incidence after homocysteine thiolactone exposure. Further studies by Afman and colleagues (2003a) in which homocysteine thiolactone was applied to chick embryos in culture did show a transient widening of the anterior neuropore and delayed closure of the hindbrain neuropore. However, continued culture resulted in complete closure of the neural tube. Although this study did not reproduce the original *in ovo* results from Rosenquist and colleagues (1996) it does suggest that homocysteine treatment can affect the neurulation process. The possibility remains that if Afman and colleagues had given additional applications of homocysteine thiolactone throughout the culture period they

could have produced embryos with NTD. Another study investigated the effect of homocysteine thiolactone on caudal neural tube closure in chick embryos and demonstrated that exposure of embryos to 2.5 M homocysteine thiolactone gave an age-dependent incidence of NTD of up to 44% (Epeldegui *et al.*, 2002). Exposure to the very high concentrations of homocysteine thiolactone in this study also resulted in a significant number of embryos with gross abnormalities. A high incidence of spina bifida in the control group (10%) suggests that the white leghorn chicken strain used in this study was more susceptible to spinal NTD than strains used in previous studies.

One explanation for the possible differences in the effect of homocysteine on chick and mouse could be a species difference. Studies have shown species differences in response to other teratogenic agents. For example, TCDD (tetrachlorodibenzo-p-dioxin) has been shown to induce cleft palate when administered to mice (Neubert and Dillmann, 1972). In cell culture, similar effects of TCDD toxicity are seen in mouse and human cells although much higher doses are required in human cells to produce the same effects as lower doses in the mouse cells. Mechanistic studies have shown that the action of TCDD toxicity requires the aryl hydrocarbon receptor (Ahr) and Ahr nuclear translocator (ARNT) (Abbott *et al.*, 1998). Ahr expression in human tissue is 300 times lower than in mice, and this difference in gene expression may relate directly to the difference in tissue sensitivity to TCDD teratogenesis (Abbott *et al.*, 1999).

The toxic effect of homocysteine observed in mouse and rat embryos could be mediated through a direct teratogenic effect of homocysteine itself. Alternatively, an indirect

mechanism could be envisaged, in which homocysteine influences the levels of other metabolites within the cell, with a consequent toxic effect.

One of the possible mechanisms for direct toxicity by homocysteine could be through the homocysteinylation of proteins within the cell. Homocysteinylation of proteins occurs via the formation of homocysteine thiolactone. The reactive thiolactone group can readily acylate proteins, primarily at lysine residues, under physiological conditions (Jakubowski, 1999). The amount of homocysteine thiolactone produced in a cell is dependant on the level of homocysteine, and increases when the removal of homocysteine, via the transulphuration pathway or remethylation to methionine, is inhibited (Jakubowski, 1997). Homocysteinylation can cause protein damage. For example, homocysteinylation of 33% of the lysine residues in methionyl-tRNA synthetase and 88% of lysine residues in trypsin results in complete loss of enzyme activity (Jakubowski, 1999). Protein homocysteinylation could therefore affect cellular processes, which could subsequently result in the embryotoxicity caused by elevated levels of homocysteine.

The teratogenic effect of homocysteine in the chick embryo has been suggested to result from direct inhibition of the *N*-Methyl-D-aspartate (NMDA) receptor (Rosenquist *et al.*, 1996). NMDA receptor antagonists, including dextromethorphan, could induce NTD in chick embryos in a similar manner to homocysteine thiolactone, although not to the same degree (Andaloro *et al.*, 1998). However, administration of dextromethorphan to pregnant rats and rabbits did not result in any fetal malformations (Brent, 1998)

suggesting that this may be another example of a difference in gene-teratogen interaction between species.

The embryotoxicity observed in mouse embryos exposed to homocysteine could also be mediated via an indirect mechanism in which elevated homocysteine disrupts the levels of other metabolites in the cell, which subsequently have a toxic effect. Van Aerts and colleagues (1994) suggested that the embryotoxicity observed in rat embryos was due to an increase in cellular SAH levels. Elevated SAH levels would affect the SAM/SAH ratio in the cell, which has a regulatory role in both the methylation and folate cycles and so could act through disruption of one or both of these pathways (Finkelstein, 1998). At high concentrations, SAH acts as a product inhibitor of methyltransferase reactions, resulting in a suppression of critical methylation reactions. DNA methylation has an important role in the epigenetic control of the expression of some genes (Jones and Takai, 2001), changes which could potentially result in homocysteine-induced embryotoxicity. Inhibition of protein methylation has also been shown to affect the behaviour of proteins within the cell. In mouse cells lacking isoprenylcysteine carboxyl methyltransferase (ICMT), the methyltransferase responsible for the methylation of the Ras family of proteins, Ras proteins are mislocalised and unable to interact with microtubules (Chen *et al.*, 2000;Bergo *et al.*, 2000).

Several lines of evidence suggest that elevated homocysteine levels may influence methylation *in vivo*. DNA hypomethylation has been observed with elevated homocysteine levels in MTHFR-deficient mice (Chen *et al.*, 2001) and in human patients suffering from hyperhomocysteinaemia (Ingrosso *et al.*, 2003) or vascular

disease (Castro *et al.*, 2003). These studies indicate that abnormal cellular methylation is a possible mechanism of homocysteine-induced toxicity as changes in methylation have been associated with changes in homocysteine levels.

In addition to effects on the methylation cycle, the abundance of homocysteine or SAH can influence the folate cycle. An increase of SAH levels compared to SAM could increase the activity of MTHFR, driving the production of 5-methyl THF for the remethylation of homocysteine to methionine (Figure 1.6). This would deplete the availability of 5,10-methylene THF, the MTHFR substrate, for other reactions in the folate cycle including the *de novo* synthesis of dTMP and the production of THF and the purine ring (Figure 1.6).

In cell culture experiments, high concentrations of homocystine (the oxidation product of homocysteine) and methionine inhibited the *de novo* synthesis of dTMP (Fell and Selhub, 1990). This inhibition could be mediated by a reduced availability of 5,10-methylene THF. In addition to being the substrate for thymidylate synthase (TS) in the production of dTMP, 5,10-methylene THF is also required as a substrate for two other reactions in the cell; the production of 5-methyl THF by MTHFR and the conversion of 5,10-methylene THF back to THF via a number of enzymatic steps (Figure 1.6). The synthesis of 5,10-methylene THF from THF is mediated by serine hydroxymethyltransferase in a serine dependent manner. It was proposed that the mechanism responsible for the inhibition of dTMP synthesis was the depletion of 5,10-methylene THF production by serine hydroxymethyltransferase. This would result from an increased requirement for serine in the cell, for use in the removal of excess

homocysteine through the transulphuration pathway (Fell *et al.*, 1990) and limiting the production of 5,10 methylene THF. However, there is no evidence of an active transulphuration pathway in neurulation stage embryos, as activities of the enzymes involved in this pathway are not detected in E10 rat embryos (VanAerts *et al.*, 1995). Moreover, the only tissues in mammalian adults that have been reported to express the complete transulphuration pathway are the liver, pancreas and kidney (Finkelstein, 1990). If the transulphuration pathway is not active in mouse embryos undergoing neurulation, excessive flux through this pathway would be unlikely to result from exposure to homocysteine thiolactone, suggesting that this is not responsible for the observed toxic effects.

Further evidence that TS function is not significantly compromised in homocysteine-treated embryos comes from an additional study carried out in our laboratory. The incorporation of [^{3}H]-thymidine into DNA can be measured as one indicator of functional folate metabolism. An increase in the incorporation of exogenous tritium-labelled thymidine into DNA can indicate increased activity of the salvage pathway in the production of dTMP, which suggests that the thymidylate synthase-mediated *de novo* synthesis pathway is impaired. The incorporation of [^{3}H]-thymidine into DNA in homocysteine thiolactone-treated embryos did not differ from control embryos, suggesting that homocysteine thiolactone-induced embryotoxicity in the mouse is unlikely to result from the inhibition of thymidylate synthase (Greene *et al.*, 2003).

The experiments carried out in this chapter were not sufficient to establish whether the mechanism for homocysteine embryotoxicity is via a direct or indirect route. Further

experiments would be needed to distinguish the exact mechanism. One approach would be to separate the effect of elevated SAH on the development of the embryo as opposed to the effect of elevated homocysteine. This could potentially be achieved by inhibition of SAH hydrolase, the enzyme that converts SAH to homocysteine via a reversible reaction. The conversion of homocysteine to SAH is favoured by enzyme kinetics and uses adenosine as a co-substrate. However, the rapid removal of homocysteine drives the reaction in the opposite direction under normal conditions (Finkelstein, 1998).

How does the toxic effect of homocysteine thiolactone observed in animal studies relate to the doses that may be present during human pregnancy? Elevated homocysteine levels have been associated with human pregnancies affected by NTD (Steegers-Theunissen *et al.*, 1994;Mills *et al.*, 1995). Serum homocysteine values (8.6 μM) were significantly higher in mothers with NTD-affected pregnancies in the low but normal range of vitamin B_{12} serum concentration compared to vitamin B_{12} matched controls (7.9 μM) (Mills *et al.*, 1995). Elevated homocysteine plasma values were also found in mothers of spina bifida patients; 12.5 μM compared to 10.1 μM in controls (Van der Put *et al.*, 1997a). The lowest teratogenic dose used in the present study was 500 μM, about 50 times that found in humans. However, this dose of homocysteine thiolactone did not induce NTD in mouse. Although homocysteine treatment of chick embryos can induce NTD (Rosenquist *et al.*, 1996;Andaloro *et al.*, 1998;Epeldegui *et al.*, 2002) there are now three independent mammalian studies (VanAerts *et al.*, 1994;Hansen *et al.*, 2001;Greene *et al.*, 2003) and one study in chick (Afman *et al.*, 2003a) in which no increase in the incidence of NTD was observed following homocysteine treatment. Taken together, these studies suggest that it is unlikely that elevated homocysteine is

directly causal in the development of NTD. Instead it appears more likely that elevated homocysteine levels are an indicator of abnormalities in the folate and/or methylation cycles in association with NTD. The potential effect of methylation cycle disruption will be discussed in Chapter Four.

CHAPTER 4; THE EFFECT OF DISRUPTING THE METHYLATION CYCLE ON CRANIAL NEURAL TUBE CLOSURE

4.1 INTRODUCTION

In the studies described in Chapter 3 I concluded that elevated homocysteine levels per se are unlikely to cause NTD directly, but are more likely to be an indicator of abnormalities in the folate and/or methylation cycles. Elevated homocysteine and other risk factors for NTD such as sub-optimal folate or vitamin B_{12} status, and the polymorphic MTHFR variant with reduced enzyme activity (Section 1.9) could be associated with reduced methionine production. Methionine is the product of the remethylation of homocysteine via the methionine synthase mediated reaction (Figure 4.1). Therefore, elevated homocysteine levels may indicate an abnormal flux through the methylation cycle.

Methionine has been suggested to be essential for normal neural tube closure to occur. Rat embryos cultured in cow serum throughout neurulation develop NTD unless the serum is supplemented with methionine (Coelho *et al.*, 1989). In addition, canine serum requires supplementation with methionine and iron before it is capable of supporting the normal development and neural tube closure of neurulation-stage rat embryos in whole embryo culture (Flynn *et al.*, 1987). These studies suggest that an adequate supply of methionine is required for neurulation to be successfully completed. Further *in vitro* studies have suggested that serum methionine may be a limiting nutrient in organogenesis-stage embryos. For example, normal rat serum which contains around 70 μM methionine (Milakofsky *et al.*, 1984) and can support the growth and development of neurulation-stage rat and mouse embryos in whole embryo culture. However, the majority of methionine taken up by neurulation-stage embryos is in the form of serum proteins rather than free methionine (Lloyd *et al.*, 1996). Rat embryos

undergoing neurulation are more efficient at incorporating labelled methionine as opposed to labelled leucine from serum proteins into embryonic tissues (Lloyd *et al.*, 1996) possibly suggesting a greater requirement for methionine than leucine. In addition, increasing the levels of free methionine and leucine available to rat embryos undergoing neurulation, by 11-fold, resulted in a greater accumulation of methionine in both the embryo and the yolk sac than leucine. These experiments suggest that normal leucine levels are abundant relative to the embryonic requirement for leucine, whereas the methionine provided by rat serum proteins and free amino acid is barely sufficient for the embryos needs (Pugarelli *et al.*, 1999). These results may illustrate a high requirement for methionine in the developing embryo, as methionine is necessary for protein synthesis and a functioning methylation cycle.

Supplementation with methionine but not folic acid or vitamin B_{12}, has also been shown to reduce the incidence of NTD in the *Axial defects* (*Axd*) mouse model (Essien, 1992;Essien and Wannberg, 1993). A delay or failure in the closure of the PNP in homozygous *Axd* mice results in tail defects or spina bifida. The incidence of NTD is reduced by approximately 40% after methionine administration to pregnant females at E8 and E9, at the beginning and during neurulation. However, a low incidence of exencephaly is seen in the treated group that is not present in the control group. In contrast to the *Axd* model, *splotch* (Sp^{2H}) homozygotes are folate-responsive in respect to NTD (Fleming *et al.*, 1998). However, exposure of cultured Sp^{2H} mouse embryos to methionine throughout neurulation induced NTD in 47% of heterozygote embryos, which normally develop without a NTD phenotype. Therefore, although methionine is essential for neural tube closure in several models methionine supplementation in Sp^{2H}

mice appears to exacerbate the genetically determined susceptibility to NTD (Fleming *et al.*, 1998).

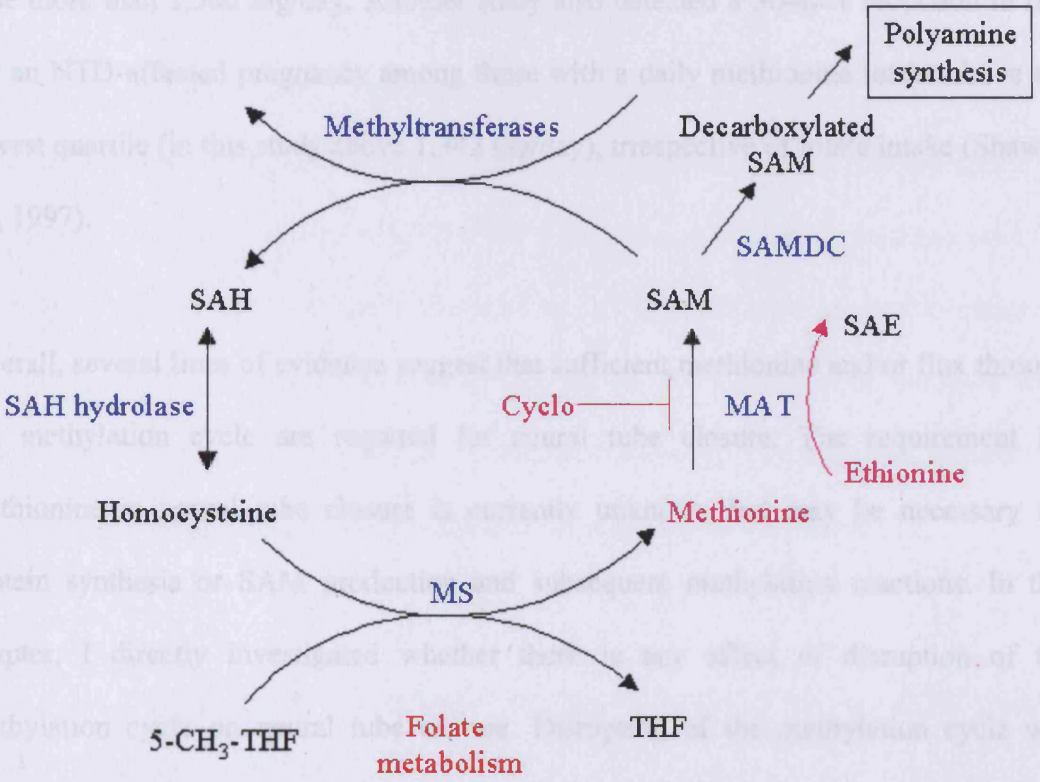

Figure 4.1 Simplified diagram of the methylation cycle

Key enzymes (blue text) and the sites of action of methylation cycle components and inhibitors utilised in this chapter (pink text) are highlighted.

Abbreviations: Cyclo, cycloleucine; MAT, methionine adenosyltransferase; MS, methionine synthase; SAH, S-adenosylhomocysteine; SAM, S-adenosylmethionine; SAMDC, S-adenosylmethionine decarboxylase; SAE, S-adenosylethionine; THF, tetrahydrofolate.

In humans, dietary studies have suggested that a high intake of methionine can reduce the risk of NTD. Shoob and colleagues (2001) found a 30-55% lower NTD risk among women whose daily dietary methionine intake was above the lowest quartile, in this case more than 1,580 mg/day. Another study also detected a 30-40% reduction in risk for an NTD-affected pregnancy among those with a daily methionine intake above the lowest quartile (in this study above 1,342 mg/day), irrespective of folate intake (Shaw *et al.*, 1997).

Overall, several lines of evidence suggest that sufficient methionine and/or flux through the methylation cycle are required for neural tube closure. The requirement for methionine in neural tube closure is currently unknown but may be necessary for protein synthesis or SAM production and subsequent methylation reactions. In this chapter, I directly investigated whether there is any effect of disruption of the methylation cycle on neural tube closure. Disruption of the methylation cycle was achieved using the whole embryo culture technique. CD1 mice embryos were cultured, throughout the period of cranial neural tube closure (E8.5-E9.5), in rat serum to which either methionine, ethionine or cycloleucine was added. Ethionine is a non-metabolic competitive inhibitor of methionine for MAT, it is converted to S-adenosylethionine (SAE) but cannot be metabolised any further (Figure 4.1) (Miller *et al.*, 1994). Cycloleucine inhibits the conversion of methionine to SAM (Figure 4.1) (Lombardini and Talalay, 1970).

4.2 RESULTS

4.2.1 Methionine, ethionine and cycloleucine specifically cause cranial NTD in CD1 mouse embryos

The effect of methionine, ethionine and cycloleucine on the development of neurulation-stage embryos was investigated in non-mutant CD1 embryos cultured for 24 hours from E8.5 (4-6 somites) to E9.5. PBS was used as a vehicle control and embryos from within litters were randomly allocated to different treatment groups to minimise any effect of litter to litter variation. At the end of the culture period embryos were assessed for developmental progress (as indicated by number of somites), growth and viability. Any morphological abnormalities were recorded for each embryo.

4.2.1.1 Methionine specifically causes cranial NTD in CD1 mouse embryos

Exposure to methionine concentrations of up to 10 mM did not adversely affect the viability of the embryos as indicated by similar mean yolk sac circulation scores at the end of the culture period in treated and control embryos (Table 4.1). The growth and developmental progression of embryos during the culture, as illustrated by the mean crown-rump length, somite number and incidence of failed axial rotation, was not affected by exposure to methionine (Table 4.1). Nevertheless, at methionine concentrations of 5 mM and above, a significant number of embryos exhibited open cranial neural tubes compared to PBS-treated control embryos (Table 4.1). As indicated

Table 4.1 Growth and development of mouse embryos cultured in the presence of methionine

Non-viable embryos were identified by an absence of yolk sac circulation. Cranial neural tube defects are defined as failure to complete cranial neural tube closure in embryos that have 16 or more somites. Values for yolk sac circulation, somite number and crown-rump length are given as mean ± SEM. There were no significant differences between the values (tested by one way-ANOVA). Data for failed axial rotation and open cranial neural tube are presented as number of embryos with percentage of total embryos in parentheses. Data for cranial neural tube defects are presented as number of embryos with percentage of embryos with 16 or more somites in parentheses. ϕ ($p<0.05$) and * ($p<0.001$) indicate significant variation from control embryos cultured without methionine (tested by z-test).

Methionine conc. (mM)	No. embryos	No. viable embryos	Yolk Sac circulation	No. failed axial rotation (%)	No. open cranial neural tube (%)	No. cranial neural tube defects (%)	Somite number	Crown-rump length (mm)
0	65	61	2.59 ± 0.11	11 (18.0)	10 (16.4)	4 (7.0)	19.3 ± 0.23	2.44 ± 0.04
0.25	3	3	3.00 ± 0.00	0 (0.0)	0 (0.0)	0 (0.0)	20.3 ± 0.33	2.44 ± 0.06
0.5	9	9	2.67 ± 0.24	2 (22.2)	2 (22.2)	1 (12.5)	18.0 ± 0.54	2.27 ± 0.04
1.0	8	8	3.00 ± 0.00	0 (0.0)	1 (12.5)	0 (0.00)	18.3 ± 0.42	2.20 ± 0.05
1.5	9	9	2.89 ± 0.11	0 (0.0)	3 (33.3)	1 (14.3)	18.7 ± 0.61	2.36 ± 0.08
2.0	17	16	2.62 ± 0.22	1 (5.8)	2 (11.8)	1 (6.25)	20.1 ± 0.28	2.58 ± 0.05
3.0	3	3	2.33 ± 0.67	0 (0.0)	0 (0.0)	0 (0.0)	19.7 ± 0.88	2.61 ± 0.07
4.0	4	4	2.50 ± 0.29	0 (0.0)	0 (0.0)	1 (25.0)	20.5 ± 0.50	2.67 ± 0.07
5.0	45	42	2.73 ± 0.11	4 (8.9)	20 (44.4)ϕ	16 (40.0)*	18.9 ± 0.30	2.23 ± 0.04
10.0	41	39	2.49 ± 0.14	5 (12.2)	23 (56.1)*	21 (56.8)*	19.5 ± 0.28	2.52 ± 0.04

by the mean number of somites (approximately 19 somites) a significant number of these embryos were exencephalic, as they had reached the developmental stage (16 somites or more) when cranial neural tube closure should have been completed (Table 4.1, Figure 4.2). This exencephaly occurred in the absence of any other apparent

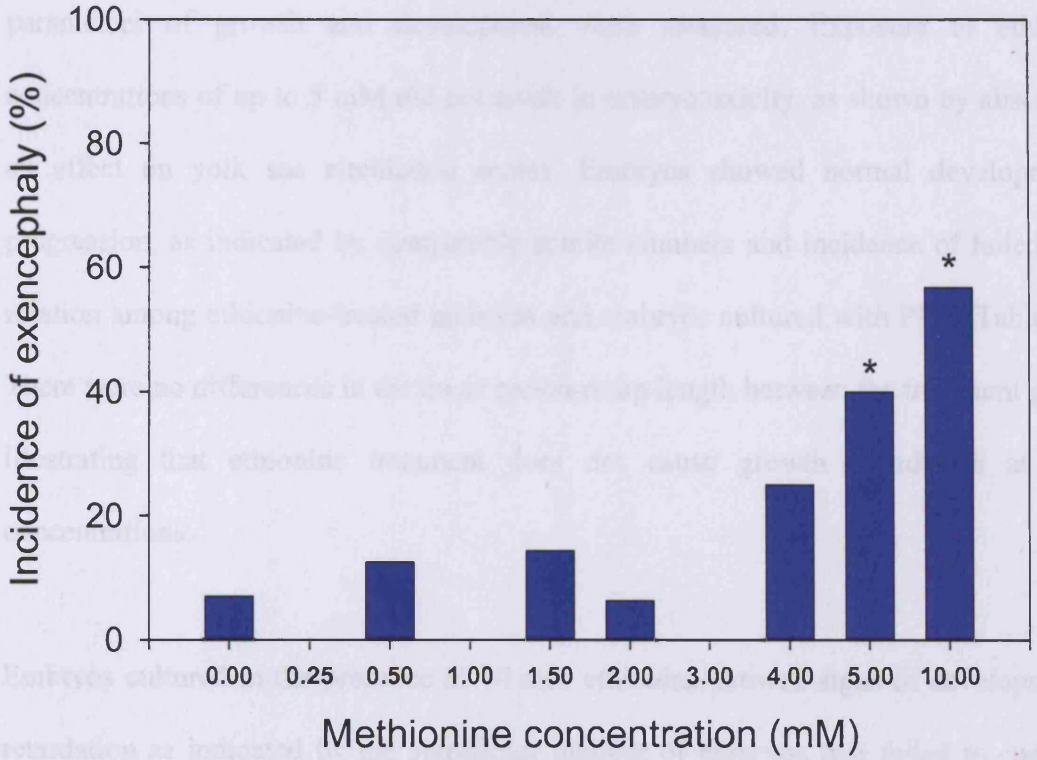

Figure 4.2 Methionine specifically causes cranial NTD in CD1 embryos

The percentage of embryos exhibiting cranial neural tube defects after exposure to increasing concentrations of methionine. * indicates a significant variation from control embryos cultured without methionine. ($p<0.001$, tested by Z-test).

abnormalities or defects in the embryos. Therefore, the results indicate that methionine, at concentrations of 5 mM or higher, causes exencephaly in mouse embryos through a

specific effect rather than as a secondary result of growth retardation or other morphological abnormalities.

4.2.1.2 Ethionine specifically causes NTD in CD1 mouse embryos

A series of embryos were cultured in the presence of a range of doses of ethionine and parameters of growth and development were measured. Exposure to ethionine concentrations of up to 5 mM did not result in embryotoxicity, as shown by absence of an effect on yolk sac circulation scores. Embryos showed normal developmental progression, as indicated by comparable somite numbers and incidence of failed axial rotation among ethionine-treated embryos and embryos cultured with PBS (Table 4.2). There were no differences in the mean crown-rump length between the treatment groups illustrating that ethionine treatment does not cause growth retardation at these concentrations.

Embryos cultured in the presence of 10 mM ethionine showed signs of developmental retardation as indicated by the significant number of embryos that failed to complete axial rotation. In addition, there was a noticeable, although not statistically significant, decrease in the mean somite number, crown-rump length and yolk sac circulation observed at the end of the culture period in the embryos treated with 10 mM ethionine compared to control embryos (Table 4.2). A large number of embryos in this treatment group failed to complete cranial neural tube closure by the end of the treatment period (Table 4.2). All of these embryos had reached at least the 16 somite stage of development indicating that exencephaly is induced at high incidence in embryos cultured in the presence of 10 mM ethionine (Table 4.2, Figure 4.3). However, a

Table 4.2 Growth and development of mouse embryos cultured in the presence of ethionine.

Non-viable embryos were identified by an absence of yolk sac circulation. Cranial neural tube defects are defined as failure to complete cranial neural tube closure in embryos that have 16 or more somites. Values for yolk sac circulation, somite number and crown-rump length are given as mean ± SEM. There were no significant differences between the values (tested by one way-ANOVA). Data for failed axial rotation and open cranial neural tube are presented as number of embryos with percentage of total embryos in parentheses. Data for cranial neural tube defects are presented as number of embryos with percentage of embryos with 16 or more somites in parentheses. ϕ ($p<0.05$) and * ($p<0.001$) indicate significant variation from control embryos cultured without ethionine (tested by z-test).

Ethionine conc. (mM)	No. embryos	No. viable embryos	Yolk sac circulation	No. failed axial rotation (%)	No. open cranial neural tube (%)	No. cranial neural tube defects (%)	Somite number	Crown-rump length
0.00	60	55	2.73 ± 0.11	3 (5.0)	3 (5.0)	1 (1.8)	18.9 ± 0.26	2.38 ± 0.03
0.10	6	6	3.00 ± 0.00	0 (0.0)	0 (0.0)	0 (0.0)	19.0 ± 0.52	2.50 ± 0.02
0.25	12	12	3.00 ± 0.19	0 (0.0)	2 (16.7)	2 (16.7)ϕ	18.0 ± 0.19	2.31 ± 0.07
0.50	15	15	2.60 ± 0.19	0 (0.0)	2 (13.3)	2 (14.3)	19.0 ± 0.50	2.37 ± 0.06
1.00	9	9	2.22 ± 0.28	2 (22.2)	2 (22.2)	1 (12.5)	18.9 ± 0.79	2.33 ± 0.07
1.50	6	6	3.00 ± 0.10	0 (0.0)	1 (16.7)	1 (16.7)	19.6 ± 0.56	2.44 ± 0.04
2.00	15	15	2.87 ± 0.09	0 (0.0)	4 (26.7)ϕ	3 (21.4)ϕ	19.4 ± 0.60	2.55 ± 0.08
3.00	6	6	3.00 ± 0.00	0 (0.0)	2 (33.3)	2 (33.3)ϕ	18.3 ± 0.42	2.24 ± 0.04
4.00	6	6	3.00 ± 0.00	0 (0.0)	1 (16.6)	1 (16.6)	20.0 ± 0.45	2.44 ± 0.06
5.00	46	45	2.80 ± 0.09	3 (6.5)	30 (65.2)*	26 (61.9)*	19.0 ± 0.38	2.30 ± 0.04
10.00	16	13	2.25 ± 0.31	5 (31.3)ϕ	14 (87.5)*	13 (100.0)*	16.5 ± 0.51	2.15 ± 0.09

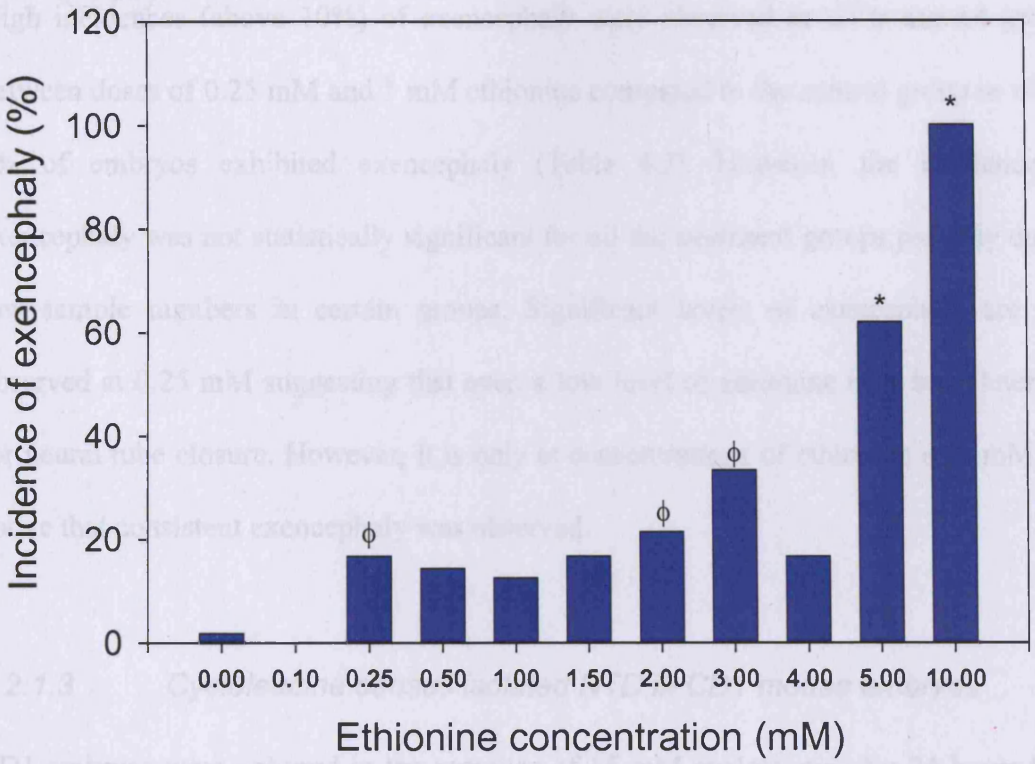

Figure 4.3 Ethionine specifically causes cranial NTD in CD1 embryos.

The percentage of embryos exhibiting cranial neural tube defects after exposure to increasing concentrations of ethionine. * and ϕ indicate significant variation from control embryos cultured without ethionine ($p<0.001$ and $p<0.05$ respectively, tested by Z-test).

number of exencephalic embryos failed to undergo axial rotation suggesting that failure of cranial neural tube closure was secondary to the abnormal development of the embryo at this concentration of ethionine. This is not the case at doses of 5 mM ethionine and below, where there was a significant increase in the number of embryos with cranial NTD compared to control embryos (Figure 4.3), without any other apparent detrimental effect on the developmental progression of the embryos.

High incidences (above 10%) of exencephaly were observed in all treatment groups between doses of 0.25 mM and 5 mM ethionine compared to the control group in which 2% of embryos exhibited exencephaly (Table 4.2). However, the incidence of exencephaly was not statistically significant for all the treatment groups possibly due to low sample numbers in certain groups. Significant levels of exencephaly are first observed at 0.25 mM suggesting that even a low level of ethionine may be deleterious for neural tube closure. However, it is only at concentrations of ethionine of 2 mM and above that consistent exencephaly was observed.

4.2.1.3 Cycloleucine causes isolated NTD in CD1 mouse embryos

CD1 embryos were cultured in the presence of 15 mM cycloleucine for 24 hours from E8.5, to observe the effect on cranial neural tube closure in non-mutant embryos. This concentration was used because previous studies showed that there was no non-specific toxicity whereas higher doses may be deleterious (A.J. Copp personal communication). The growth, development and viability of the cycloleucine treated embryos at the end of the culture period were comparable to control embryos (Table 4.3), suggesting that 15 mM cycloleucine does not have widespread embryotoxic effects. However, a significant proportion of cycloleucine-treated embryos ($p<0.05$, tested by Z-test) did exhibit cranial NTD; 58.3% compared to 14.3% in controls. NTD were observed in embryos with no other apparent defects, suggesting that cycloleucine treatment causes isolated cranial NTD in CD1 embryos.

Cycloleucine conc. (mM)	No. embryos	No. viable embryos	Yolk sac circulation	No. failed axial rotation (%)	No. open cranial neural tube (%)	No. cranial neural tube defects (%)	Somite number	Crown-rump length (mm)
0	25	24	2.28 ± 0.19	6 (24.0)	7 (28.0)	3 (14.3)	18.6 ± 0.58	2.53 ± 0.05
15	28	24	2.43 ± 0.20	5 (17.9)	18 (64.2)‡	14 (58.3)‡	19.3 ± 0.48	2.50 ± 0.05

Table 4.3 Growth and development of mouse embryos cultured in the presence of cycloleucine

Non-viable embryos were identified by an absence of yolk sac circulation. Cranial neural tube defects are defined as failure to complete cranial neural tube closure in embryos that have 16 or more somites. Values for yolk sac circulation, somite number and crown-rump length are given as mean ± SEM, and there were no significant differences between the values (tested by t-test). Data for failed axial rotation, open cranial neural tube and cranial neural tube defects are presented as number of embryos with percentage in parentheses. ‡ ($p<0.05$) indicates significant variation from control embryos cultured without cycloleucine (tested by z-test).

4.2.2 The morphological appearance of exencephaly differs between methionine, ethionine and cycloleucine-induced defects

Exposure of CD1 embryos to methionine, ethionine or cycloleucine can result in isolated cranial NTD. However, the varying ability of the compounds to cause exencephaly (ethionine appears to be more potent than methionine) suggests different mechanisms may be responsible for the failure of the cranial neural tube to close. As a preliminary step towards addressing this question, the region of cranial neural tube that remains open was noted for embryos from the different treatment groups (Figure 4.5). Embryos that developed exencephaly when cultured with PBS showed an approximately even distribution of phenotypes, in terms of the region of open neural folds (Figure 4.4). Methionine-treated embryos tended to exhibit areas of open neural

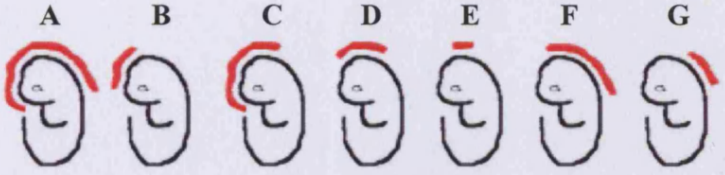

Treatment	% of embryos							n
PBS	11.1	0.0	33.3	11.1	22.2	11.1	11.1	8
Methionine	27.3	4.5	34.1	2.3	11.4	15.9	4.5	43
Ethionine	85.7	0.0	14.3	0.0	0.0	0.0	0.0	27
Cycloleucine	17.4	4.3	52.2	0.0	4.3	17.4	4.3	23

Figure 4.4 Regions of open neural tube in methionine, ethionine and cycloleucine-treated embryos.

The red line illustrates the position of open neural folds in the cranial region, examples of each position are shown in Figure 4.5. The data represents the proportion of embryos with corresponding regions of open neural tube in each treatment group (shown as percentage of total embryos exhibiting exencephaly, n).

Figure 4.5 Positions of open neural folds in the cranial region of embryos treated with methionine, ethionine or cycloleucine

Panels **A-G** show examples of embryos in groups A-G in Figure 4.4 respectively. White arrowheads (**A-G**) flank the areas of open neural tube. Examples of the different regions of cranial neural tube which failed to close after treatment with 5 mM methionine (**B, C, E**), 5 mM ethionine (**G**) and 15 mM cycloleucine (**A, D, F**) compared to PBS-treated embryos that completed cranial neural tube closure (**H**). Scale bars represent 200 μm.

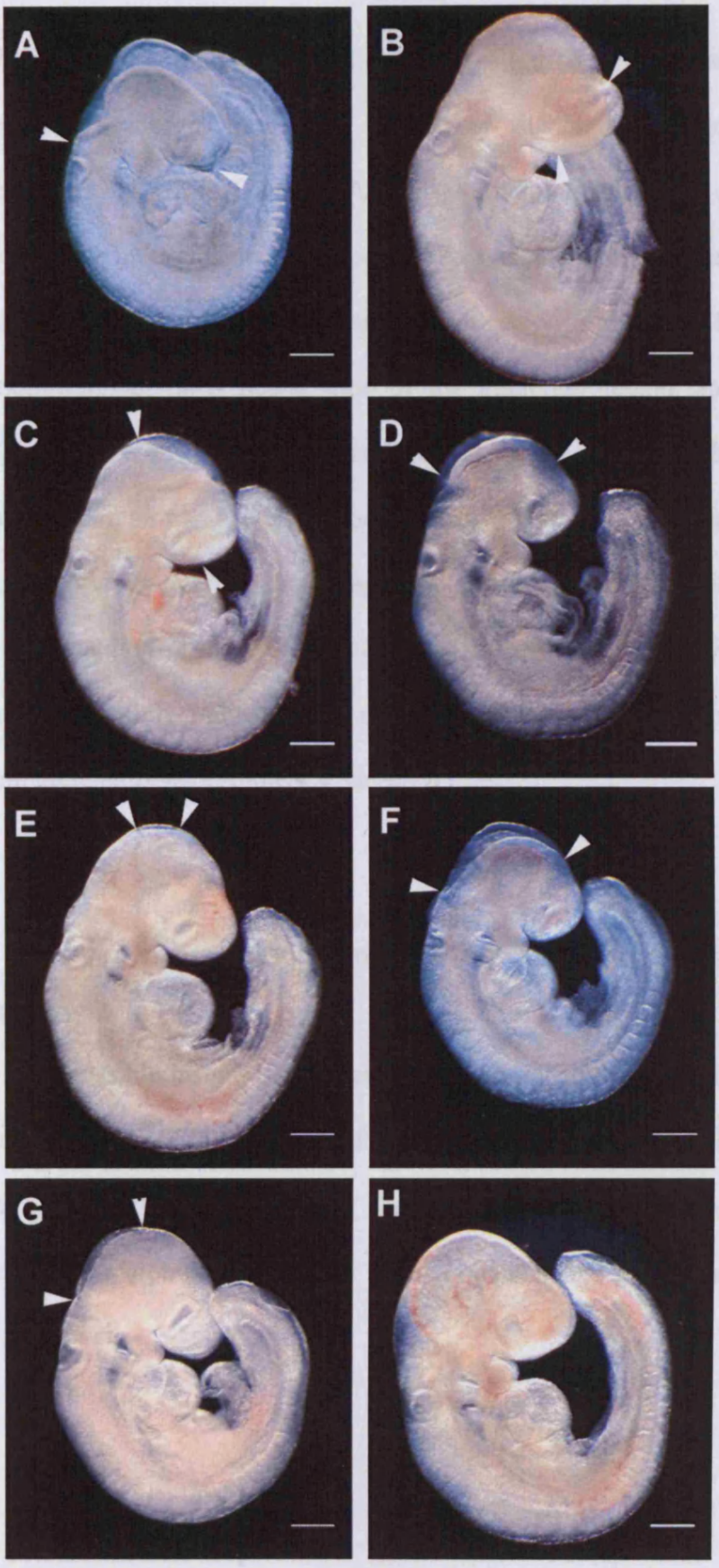
A
B
C
D
E
F
G
H

in the forebrain/midbrain region (Figure 4.4, Groups A-E). There were also a number of methionine-treated embryos in which closure of the hindbrain neuropore was incomplete (Figure 4.4, Group F and G). A similar variation in the region of open neural tube was observed in cycloleucine-treated embryos that developed exencephaly, the majority having a defect in the forebrain/midbrain region with a smaller number of embryos exhibiting an open neural tube in the hindbrain region. In contrast, all exencephalic embryos from the ethionine-exposed group exhibited open forebrain/midbrain regions. Therefore, the forebrain/midbrain region was commonly open in all categories, suggesting that initiation of closure at site 2 has failed. However, the extent of the region of open neural tube was greater in the majority of ethionine-treated embryos possibly indicating an additional problem with the progression of fusion within these embryos (Figure 4.4, Group A).

4.2.3 Different morphology through the cranial regions of treated embryos

In order to gain possible insight into underlying causative mechanisms for the induced NTD, embryos cultured in the presence of 5 mM methionine, 5 mM ethionine, 15 mM cycloleucine or PBS were examined at the histological level. Transverse sections through the cranial region of the embryos were cut and stained with haematoxylin and eosin prior to analysis.

4.2.3.1 Reduced cranial mesenchyme density in methionine-treated embryos

On transverse sections, the histological appearance of the cranial region of methionine-treated embryos in which cranial neural tube closure was complete, was indistinguishable from that of PBS-treated control embryos. In contrast, sections through the cranial region of methionine-treated embryos that developed exencephaly showed a number of differences to sections from control embryos (Figure 4.6 compare E-G to B-D). The neuroepithelium of some exencephalic methionine-exposed embryos was noticeably thinner than that of control embryos (Figure 4.6 compare F and C). Cell aggregates were also observed in two out of four (50%) exencephalic methionine-treated embryos (Figure 4.6 E) but not in embryos from any of the other treatment groups (six control embryos and six methionine-treated embryos in which neural tube closure was complete). In addition, all of the exencephalic methionine-treated embryos studied (four out of four) appeared to have a reduced cranial mesenchyme density, compared to embryos cultured with PBS (compare Figure 4.6 D and G). This phenotype was investigated further by quantitative analysis (Section 4.2.4).

Figure 4.6 Transverse sections stained with haematoxylin and eosin, through the cranial region of exencephalic methionine, ethionine and cycloleucine-treated embryos and control PBS-treated embryos

CD1 mouse embryos were cultured for 24 hours in the presence of PBS (**B-D**), 5 mM Methionine (**E-G**), 5mM Ethionine (**H-J**) or 15 mM Cycloleucine (**K-M**). Transverse sections were taken through the cranial region of the embryos at 25% (**B, E, H, K**), 50% (**C, F, I, L**) and 100% (**D, G, J, M**) of the distance between the cranial limit of the embryos and the first section showing the optic vesicles (dotted lines in **A**). Sections shown are from a normal control embryo (**B-D**) and treated embryos that failed to complete cranial neural tube closure (**E-M**). Regions of open cranial neural tube are indicated by Ex. The neural epithelium of methionine and ethionine exposed embryos appears thinner than that of control and cycloleucine-treated embryos (**C, F, I, L**, black arrowheads). The density of the cranial mesenchyme also seems to differ in methionine and cycloleucine-treated embryos compared to control or ethionine-treated embryos (**D, G, J, M** indicated by *). Methionine exposure appears to result in a reduced cranial mesenchyme density while cycloleucine exposure seems to increase the density of the cranial mesenchyme. Cell aggregates were observed in the mesenchyme of methionine-treated embryos (**E**, arrow). Scale bars represent 200 μm. Abbreviations; Ex; exencephaly, Meth; methionine, Eth; ethionine, Cyclo; cycloleucine.

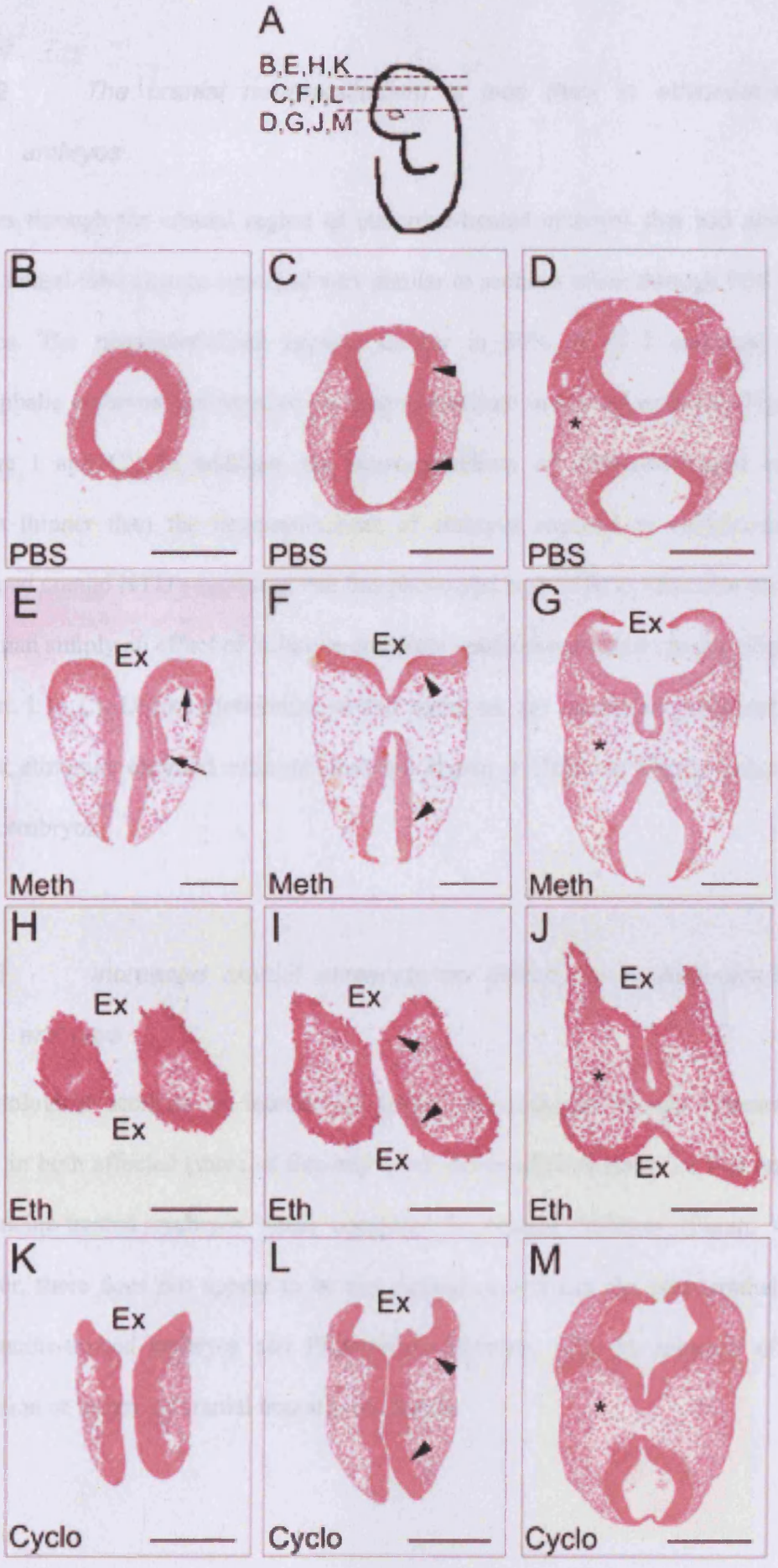
A
B,E,H,K
C,F,I,L
D,G,J,M
B
PBS
C
PBS
D
PBS
E
Ex
Meth
F
Ex
Meth
G
Ex
Meth
H
Ex
Ex
Eth
I
Ex
Ex
Eth
J
Ex
Ex
Eth
K
Ex
Cyclo
L
Ex
Cyclo
M
Cyclo

4.2.3.2 *The cranial neuroepithelium is less thick in ethionine-treated embryos*

Sections through the cranial region of ethionine-treated embryos that had completed cranial neural tube closure appeared very similar to sections taken through PBS-treated embryos. The neuroepithelium appears thinner in 80% (4 of 5 embryos) of the exencephalic embryos compared to the neuroepithelium in control embryos (Figure 4.6 compare I and C). In addition, the neuroepithelium of ethionine-treated embryos appears thinner than the neuroepithelium of embryos exposed to cycloleucine that developed cranial NTD suggesting that this phenotype is specific to ethionine treatment, rather than simply an effect of failure to complete cranial neural tube closure (Figure 4.6 compare I to L). Unlike methionine-treated embryos, the cranial mesenchyme of the affected ethionine exposed embryos does not appear to differ in density compared to control embryos.

4.2.3.3 *Increased cranial mesenchyme density in cycloleucine-treated embryos*

On histological sections an increase in cranial mesenchyme density appears to be present in both affected (three of five embryos) and unaffected (three of five embryos) cycloleucine-treated embryos when compared to control embryos (Figure 4.6 L). However, there does not appear to be any difference between the neuroepithelium of cycloleucine-treated embryos and PBS-treated embryos, with no apparent effect of completion or failure of cranial neural tube closure.

4.2.4 Quantitative analysis of neuroepithelial thickness and cranial mesenchyme density in methionine, ethionine, cycloleucine and PBS-treated embryos

Initial analysis of transverse sections through the cranial region suggested that there are differences in mesenchyme density and neuroepithelial thickness in treated embryos compared to control embryos. In order to make a quantitative comparison of neuroepithelial width and cranial mesenchyme density, measurements were taken as described in Section 4.2.4.1. Embryos exposed to 5 mM methionine, 5 mM ethionine and 15 mM cycloleucine were investigated, as these treatments resulted in isolated cranial neural tube defects, without affecting the viability, growth or development of the embryo. Embryos from each treatment were separated for analysis, according to whether cranial neural tube closure had been successful or not, and compared to PBS-treated embryos in which cranial neural tube closure was complete in all embryos.

4.2.4.1 Method for quantitative analysis of neuroepithelial thickness

In order to identify sections at comparable axial levels in different embryos, the optic vesicles were used as a morphological landmark. The most anterior section that showed the optic vesicle was labelled 'a'. All the remaining sections between section 'a' and the most anterior point of the embryo were counted, the section positioned a quarter of the distance between the last section and section 'a' was then labelled 'b' (Figure 4.7 A). These sections were photographed using a digital camera attached to a Zeiss Axiophot 2 microscope and the images were imported into Adobe Photoshop v6.0 where all further analysis was carried out.

Figure 4.7 Quantitative analysis of transverse sections, stained with haematoxylin and eosin, through the cranial region of methionine, ethionine, cycloleucine and PBS-treated embryos

The analysis of transverse sections through the cranial region of treated or control embryos was carried out at the level of the optic vesicles (**A**, dotted white line labelled a) and 25% of the distance between the most anterior point of the embryo and the optic vesicles (**A**, dotted white line labelled b). Neuroepithelial thickness measurements were made on sections a (**C**) and b (**B**). On section b, measurements were taken 25% and 75% along the length of both sides of the neuroepithelium, (**B**, black lines). In the sections labelled a (**C**), measurements were taken level with the front of the optic vesicles (OV) in the forebrain (FB) neuroepithelium (**C**, black lines) and half way along the neuroepithelium of the hindbrain (HB) (**C**, black lines). The cranial mesenchymal cell density was measured on sections a (**C**) and a+2 (**D**). Cells were counted in boxes of specific size and position on the section, in a central region (**D**, black arrow) and two lateral areas (**D**, black arrowheads). Scale bars represent 200 μm.

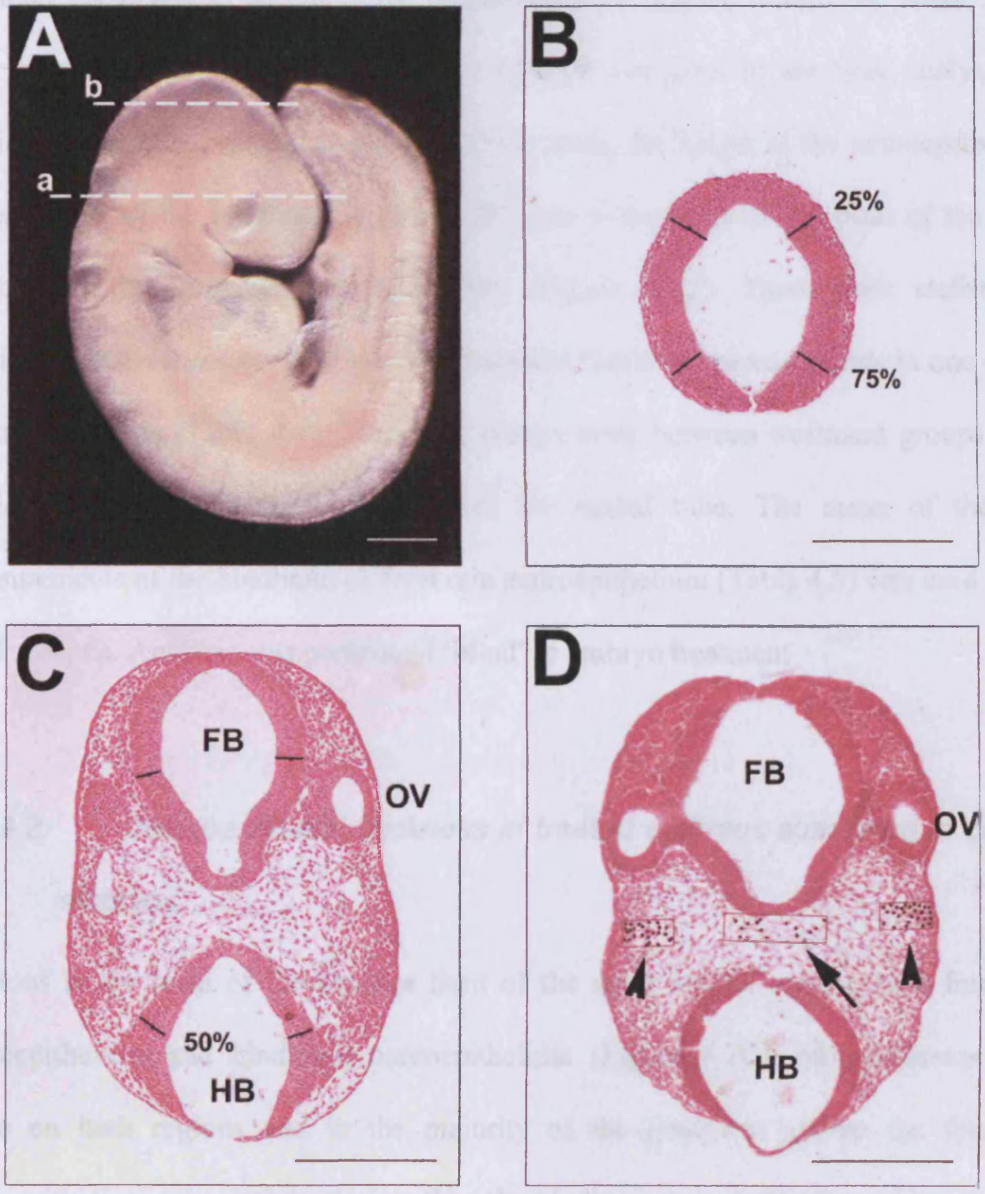
A
b
a
B
25%
75%
C
FB
OV
50%
HB
D
FB
OV
HB

The thickness of the neuroepithelium was measured in sections 'a' and 'b'. In section 'b' the apico-basal thickness of the neuroepithelium was measured at 25% and 75% of the total dorso-ventral length of the neuroepithelium (Figure 4.7B). The mean of the four measurements (Table 4.5) for each embryo was used in the final analysis. In section 'a' measurements were taken half way along the length of the neuroepithelium on each side of the hindbrain (Figure 4.7C) and at the level of the front of the optic vesicles in the forebrain neuroepithelium (Figure 4.7C). There were statistically significant differences between the hindbrain and forebrain measurements in one of the treatment groups (Table 4.4). Therefore, comparisons between treatment groups were carried out separately for both areas of the neural tube. The mean of the two measurements of the hindbrain or forebrain neuroepithelium (Table 4.5) was used in the final analysis. Analysis was performed 'blind' to embryo treatment

4.2.4.2 Neuroepithelial thickness in treated embryos compared to control embryos

Sections at the level of the anterior limit of the optic vesicle contain both forebrain neuroepithelium and hindbrain neuroepithelium (Figure 4.7C). Measurements were made on both regions and in the majority of the treatment groups the forebrain neuroepithelium was slightly thicker than the hindbrain neuroepithelium. This was not the case in cycloleucine treated embryos, in which the hindbrain neuroepithelium was thicker in both the exencephalic and normal embryos (Table 4.4). The differences between the forebrain and hindbrain measurements within each treatment group were not large enough to be statistically significant, with the exception of the ethionine-treated embryos that completed cranial neural tube closure (Table 4.4). In these

Treatment/ phenotype	No. of embryos	No. of measurements	HB mean (μm) ± SEM	FB mean (μm) ± SEM
PBS-C	6	10	34.9 ± 1.0	36.5 ± 1.0
M-C	6	10	37.2 ± 2.0	38.0 ± 3.0
M-O	4	8	40.4 ± 2.0	44.6 ± 2.0
E-C	3	6	27.0 ± 2.0*	38.6 ± 1.0*
E-O	5	8	35.2 ± 4.0	40.2 ± 4.0
C-C	3	6	42.7 ± 2.0	41.6 ± 3.0
C-O	5	10	41.0 ± 1.0	40.5 ± 5.0

Table 4.4 Comparison of the apical-basal thickness of the hindbrain and forebrain neuroepithelium in cultured embryos.

The number of embryos studied in each treatment group is stated with the number of actual measurements recorded. Some measurements could not be made, due to damaged sections. * indicates statistical differences between hindbrain (HB) and forebrain (FB) measurements identified by t-test ($p<0.05$).
Treatment abbreviations: PBS, PBS-treated embryos; M, methionine-treated embryos; E, ethionine-treated embryos; C, cycloleucine-treated embryos.
Phenotype abbreviations: C, embryos that completed cranial neural tube closure; O, embryos that failed to complete cranial neural tube closure.

embryos, the forebrain neuroepithelium was significantly thicker than the hindbrain neuroepithelium (Table 4.4). Comparisons between treatment groups were therefore carried out separately on both the forebrain neuroepithelium and the hindbrain neuroepithelium.

There are no differences in neuroepithelial thickness between methionine or cycloleucine-treated and control embryos. (Table 4.5, Figure 4.8). Ethionine-treatment results in reduced thickness of the cranial neuroepithelium in the midbrain compared to

Treatment/ phenotype	Number of embryos	section 'a' FB		section 'a' HB		section 'b' MB	
		n	mean neuroepithelial thickness (μm) ± SEM	n	mean neuroepithelial thickness (μm) ± SEM	n	mean neuroepithelial thickness (μm) ± SEM
PBS-C	6	10	36.5 ± 1.0	10	34.1 ± 1.0	24	49.6 ± 1.0
M-C	6	10	38.0 ± 3.0	10	37.2 ± 2.0	24	45.9 ± 2.0
M-O	4	8	44.6 ± 1.0	8	40.4 ± 1.0	16	51.1 ± 1.0
E-C	3	5	38.6 ± 2.0	6	27.0 ± 2.0	12	39.2 ± 1.0*
E-O	5	10	40.2 ± 4.0	8	35.2 ± 4.0	10	41.3 ± 1.0*
C-C	5	10	41.6 ± 3.0	9	42.7 ± 2.0	17	50.6 ± 2.0
C-O	5	10	40.5 ± 2.0	10	41.0 ± 1.0	10	43.6 ± 2.0

Table 4.5 Neuroepithelial thickness measurements in cranial sections after whole embryo culture with PBS, 5 mM methionine, 5 mM ethionine or 15 mM cycloleucine.

The number of embryos studied in each treatment group is stated with the number of actual measurements recorded (**n**). Some measurements could not be made, due to damaged sections. Section 'a' and 'b' and positions of measurements are as described in Section 4.2.4.1. * indicates neuroepithelial thickness that statistically differs ($p<0.001$) from that of PBS control embryos, tested by one-way ANOVA for each treatment group, followed by TUKEY test for pair-wise comparisons.

Abbreviations: FB, forebrain; HB, hindbrain; MB, midbrain. Treatment abbreviations: PBS, PBS-treated embryos; M, methionine-treated embryos; E, ethionine-treated embryos; C, cycloleucine-treated embryos. Phenotype abbreviations: C, embryos that completed cranial neural tube closure; O, embryos that failed to complete cranial neural tube closure.

Figure 4.8 Measurement of the width of the neuroepithelium in embryos after 24 hours culture in the presence of PBS, 5 mM methionine, 5 mM ethionine or 15 mM cycloleucine.

Data is presented as mean ± SEM. * indicates significant variation from PBS-treated control embryos that completed closure of the cranial neural tube ($p<0.001$ tested by one-way ANOVA for each treatment group, followed by TUKEY test for pair-wise comparisons). Sections 'a' and 'b' and measurement positions are as described in Section 4.2.4.1.

Abbreviations, FB, forebrain neuroepithelium; HB, hindbrain neuroepithelium; MB, midbrain neuroepithelium. Treatment abbreviations: PBS, PBS-treated embryos; M, methionine-treated embryos; E, ethionine-treated embryos; C, cycloleucine-treated embryos. Phenotype abbreviations: C, embryos that completed cranial neural tube closure; O, embryos that failed to complete cranial neural tube closure.

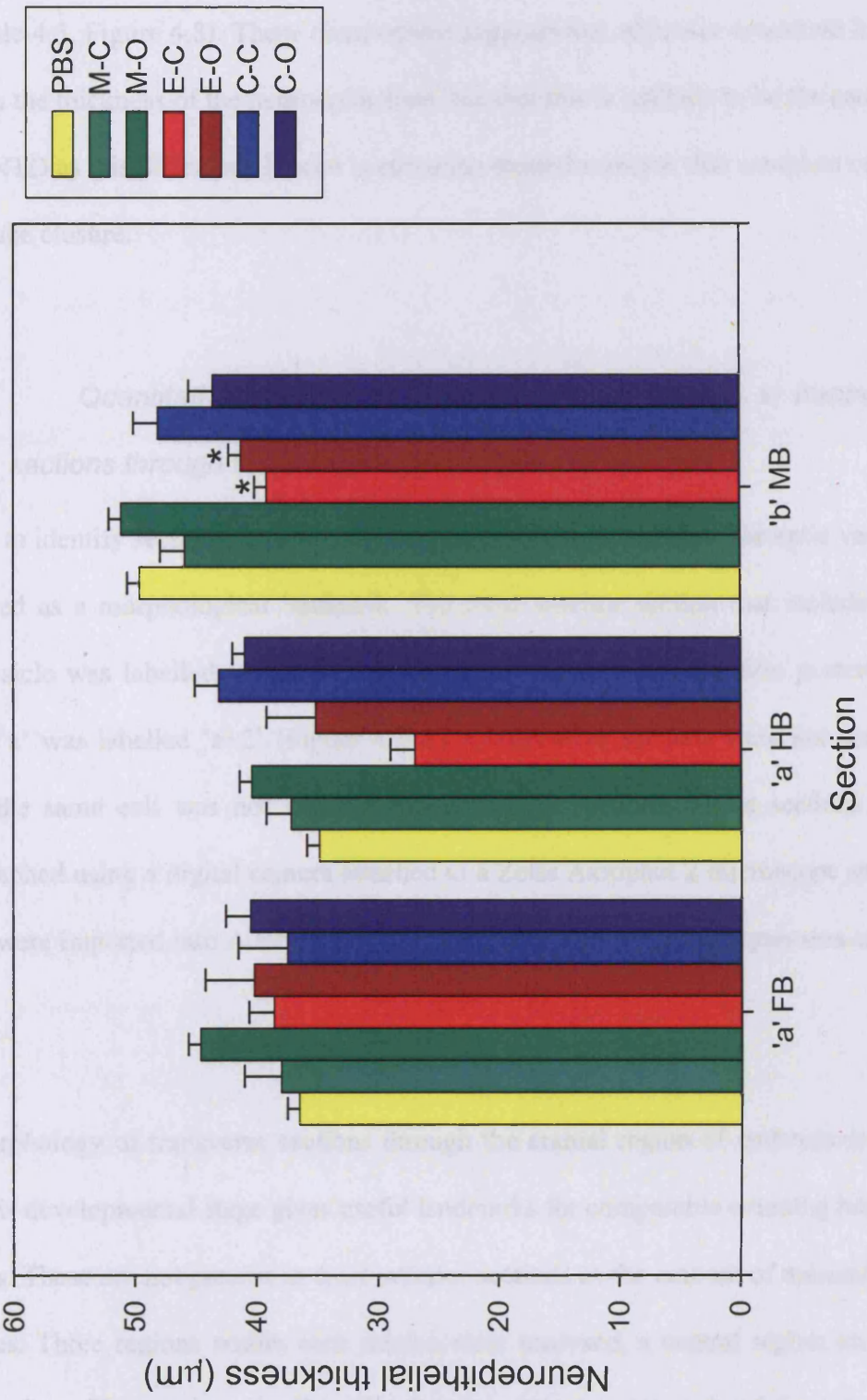
PBS
M-C
M-O
E-C
E-O
C-C
C-O
Neuroepithelial thickness (μm)
0
10
20
30
40
50
60
'a' FB
'a' HB
'b' MB
Section
*
*

PBS-treated embryos irrespective of whether the neural tube has completed closure or not (Table 4.5, Figure 4.8). These observations suggests that ethionine-treatment has an effect on the thickness of the neuroepithelium, but that this is unlikely to be the cause of cranial NTD as this difference is seen in ethionine-treated embryos that complete cranial neural tube closure.

4.2.4.3 Quantitative analysis of mesenchymal cell density in transverse sections through the cranial region of cultured embryos

In order to identify sections at comparable levels in different embryos, the optic vesicles were used as a morphological landmark. The most anterior section that included the optic vesicle was labelled 'a' (as in Section 4.2.4.1). The second section posterior to section 'a' was labelled 'a+2' (Figure 4.7 A). Consecutive sections were not used, to ensure the same cell was not counted twice, in both sections. These sections were photographed using a digital camera attached to a Zeiss Axiophot 2 microscope and the images were imported into Adobe Photoshop v6.0 where all further analysis was carried out.

The morphology of transverse sections through the cranial region of embryos at level 'a' at this developmental stage gives useful landmarks for comparable counting between embryos. These are not present in more anterior sections as the amount of mesenchyme decreases. Three regions within each section were analysed, a central region and two lateral regions. The number of cells within a certain area was counted and the value was normalised to the number of cells/mm^2. Cells overlapping the area boundaries were only counted on two sides (the top and right hand side of the box) to provide uniform

analysis and avoid over-estimation of cell numbers. The central area was defined by a box, 8.5% of the section width by 33.3% of the section width, placed immediately under the floorplate of the forebrain neural tube. The lateral areas were defined by boxes, 8.5% of the section width by 16.7% of the section width, placed laterally in line with the central area adjacent to the surface ectoderm (Figure 4.7D). Data from both sections ('a' and 'a+2') were combined to give one value (the mean of four measurements, Table 4.6) for the lateral mesenchyme density in each embryo and one value (the mean of two measurements, Table 4.6) for the central mesenchyme density in each embryo. Analysis was performed 'blind' to embryo treatment.

4.2.4.4 Cranial mesenchyme density in treated and control embryos

In all of the treatment groups, the mesenchyme density in lateral regions was much higher than the density in the central region and data for the two regions were therefore analysed separately. In the central and lateral regions, ethionine-treated embryos that failed to complete cranial neural tube closure had a significantly reduced mesenchyme density compared to PBS control embryos or ethionine-treated embryos that had completed cranial neural tube closure (Table 4.6, Figure 4.9). There was also a significant reduction in the lateral mesenchyme density of methionine-treated embryos that failed to complete cranial neural tube closure when compared to PBS-treated and methionine-treated embryos in which the cranial neural tube had closed (Table 4.6, Figure 4.9). The observed reduction in central mesenchyme density of methionine-treated embryos compared to control embryos does not reach a statistically significant level. The observed reduction in mesenchyme density does not appear to be an effect of failure to close the cranial neural folds, as exencephalic cycloleucine-treated embryos

did not exhibit reduced lateral or central mesenchyme density compared to control embryos (Table 4.6, Figure 4.9).

Treatment/ phenotype	No. of embryos	Lateral boxes		Central boxes	
		n	Mean cells/mm^2 (±SEM)	n	Mean cells/mm^2 (±SEM)
PBS-C	6	24	7621.3 ± 344.5	12	3055.9 ± 200.4
M-C	6	24	7143.9 ± 437.7	12	3120.3 ± 212.1
M-O	4	16	4492.4 ± 424.0*	8	2115.9 ± 364.5
E-C	3	12	7913.4 ± 415.7	6	3592.0 ± 260.9
E-O	5	20	3934.2 ± 639.7*	9	1499.1 ± 265.2*
C-C	5	20	6480.5 ± 488.8	6	3947.5 ± 128.7
C-O	5	18	6937.6 ± 365.5	8	3805.9 ± 157.0

Table 4.6 Cranial mesenchyme density measurements in sections after whole embryo culture with PBS, 5 mM methionine, 5 mM ethionine or 15 mM cycloleucine.

Measurement positions are as described in section 4.2.4.1., some measurements could not be made, due to damaged sections. The mean mesenchyme density for each treatment group is shown as mean cells/mm^2 ± SEM. * indicates density that statistically differs ($p<0.001$) from the PBS control embryos and morphologically different embryos exposed to the same treatment (M-O compared to M-C and E-O compared to E-C). Statistical differences were tested by one-way ANOVA for each treatment group, followed by TUKEY test for pair-wise comparisons.

Abbreviations: n, number of measurements; Treatment abbreviations: PBS, PBS-treated embryos; M, methionine-treated embryos; E, ethionine-treated embryos; C, cycloleucine-treated embryos. Phenotype abbreviations: C, embryos that completed cranial neural tube closure; O, embryos that failed to complete cranial neural tube closure.

Figure 4.9 Mesenchyme density in the cranial region of embryos after 24 hours in culture in the presence of PBS, 5 mM methionine, 5 mM ethionine or 15 mM cycloleucine.

Data are presented as mean ± SEM. * indicates a significant variation ($p<0.001$) from PBS control embryos and morphologically different embryos exposed to the same treatment (M-O compared to M-C and E-O compared to E-C). Statistical differences were tested by one-way ANOVA for each treatment group, followed by TUKEY test for pair-wise comparisons. Measurement positions are as described in section 4.2.4.1. Treatment abbreviations: PBS, PBS-treated embryos; M, methionine-treated embryos; E, ethionine-treated embryos; C, cycloleucine-treated embryos. Phenotype abbreviations: C, embryos that completed cranial neural tube closure; O, embryos that failed to complete cranial neural tube closure.

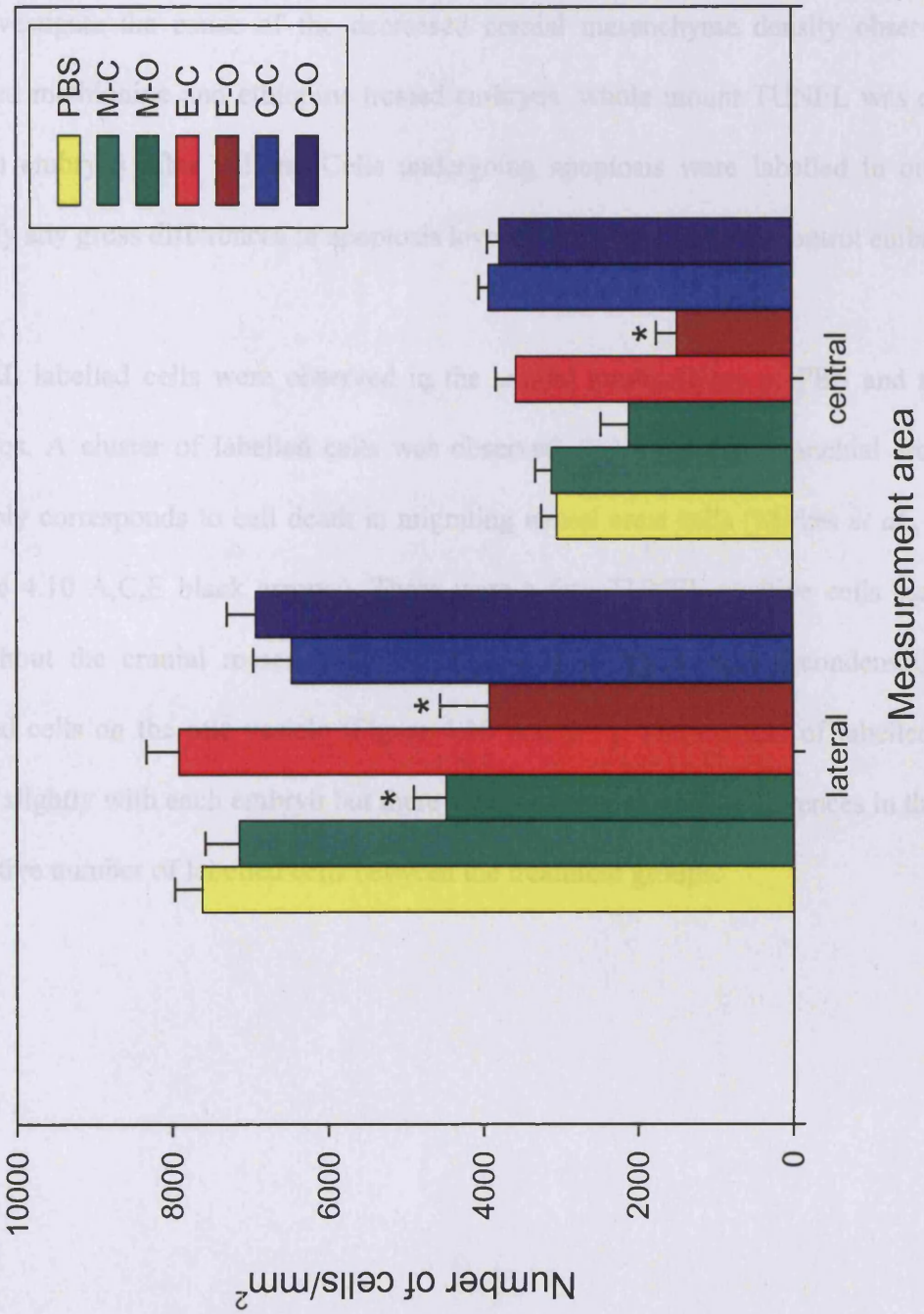
PBS
M-C
M-O
E-C
E-O
C-C
C-O
10000
8000
6000
4000
2000
0
Number of cells/mm2
lateral
central
Measurement area
*
*
*

4.2.5 Whole mount TUNEL analysis of methionine and ethionine-treated embryos

To investigate the cause of the decreased cranial mesenchyme density observed in affected methionine and ethionine-treated embryos, whole mount TUNEL was carried out on embryos after culture. Cells undergoing apoptosis were labelled in order to identify any gross differences in apoptosis levels between treated and control embryos.

TUNEL labelled cells were observed in the cranial mesenchyme of PBS and treated embryos. A cluster of labelled cells was observed above the first branchial arch and probably corresponds to cell death in migrating neural crest cells (Mirkes *et al.*, 2001) (Figure 4.10 A,C,E black arrows). There were a few TUNEL-positive cells scattered throughout the cranial mesenchyme of all treated embryos with a condensation of labelled cells on the otic vesicle (Figure 4.10 A,C,E *). The number of labelled cells varied slightly with each embryo but there were no obvious gross differences in the area or relative number of labelled cells between the treatment groups.

Figure 4.10 Whole mount TUNEL on methionine, ethionine and PBS-treated CD-1 embryos.

Whole mount TUNEL was carried out on CD1 embryos after 24 hours culture in the presence of PBS (**A,B**), 5 mM methionine (**C,D**) or 5 mM ethionine (**E,F**). Lateral (**A,C,E**) and corresponding dorsal (**B,D,F**) views are shown. Some methionine and ethionine-treated embryos developed exencephaly (regions of open neural tube are flanked by white arrowheads; **C,E**). Labelled cells appear purple/blue (black arrows **B,D,F**) and were observed throughout the cranial mesenchyme (**A,C,E**) and neuroepithelium (**B,D,F**) of all embryos studied. Heavy staining was observed above the proximal region of the first branchial arch (black arrows in **A,C,E**) and at the edge of the otic vesicle (* in **A,C,E**) of all embryos. No gross differences were detected between embryos from different treatment groups. Scale bars represent 200 μm.

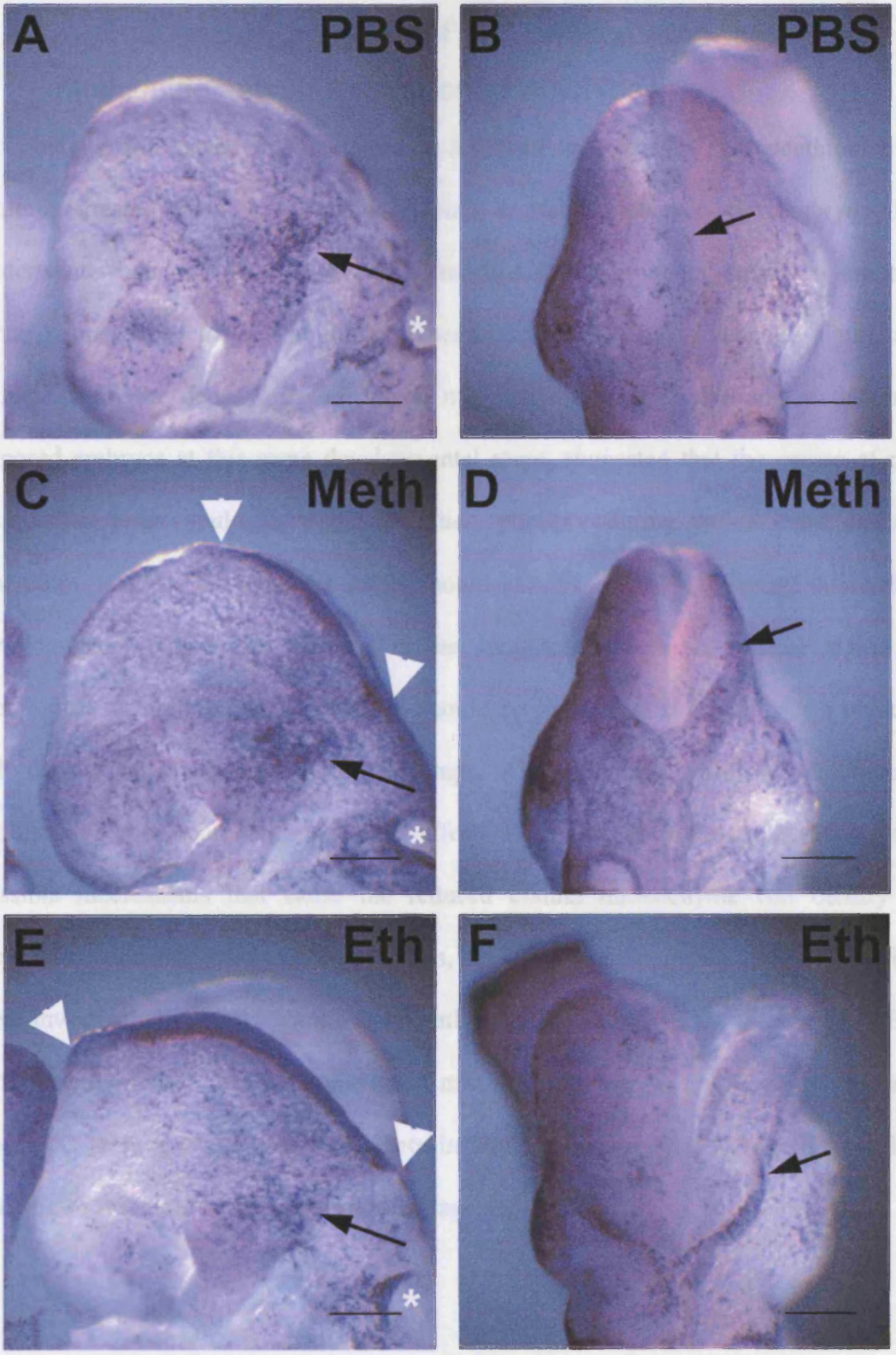
A
PBS
B
PBS
C
Meth
D
Meth
E
Eth
F
Eth

4.2.6 Quantitative analysis of proliferation and cell death in methionine and ethionine-treated embryos

No obvious differences were detected in levels of apoptosis in PBS, methionine or ethionine-treated embryos by whole mount TUNEL. However, the embryos that underwent whole mount TUNEL had all reached a developmental stage (16 somites) when neural tube closure should have been completed. The statistically significant reductions in the density of the cranial mesenchyme in ethionine and methionine-exposed embryos at this same developmental stage, suggested that the causes of cell number decrease could have acted earlier, possibly during neural tube closure. Therefore, analysis of apoptosis levels should also be carried out during this earlier developmental period. An increase in the apoptosis rate in the cranial region of methionine or ethionine-treated embryos could be postulated to account for a reduced cell density in this region at a later stage. Alternatively a reduction in the cell proliferation rate could also have this effect. Therefore, in order to investigate the possible mechanisms that cause the reduced cranial mesenchyme cell density in methionine and ethionine-treated embryos, the levels of apoptosis and proliferation were investigated in 12-15 somite stage embryos after culture in the presence of PBS, 5 mM methionine, 5 mM ethionine or 15 mM cycloleucine. At this stage, neural tube closure is in progress, and not complete in any of the embryos. Hence, factors that inhibit closure might be detectable at this stage.

4.2.6.1 Method for quantitative immunohistochemical analysis of proliferation and apoptosis in methionine, ethionine and cycloleucine-treated and control embryos

E8.5 embryos were cultured until just before completion of cranial neural tube closure (for 16 hours, from the 4-6 to 12-15 somite stages) in the presence of methionine, ethionine, cycloleucine or PBS as a vehicle control. Transverse sections were taken through the cranial region and alternate pairs were placed on separate slides for immunohistochemical analysis of proliferation (anti-phosphorylated histone H3) and apoptosis (anti-activated caspase 3) as described in Section 2.7. The latter approach was preferred to whole mount TUNEL to allow quantitative analysis.

As in previous analysis, the optic vesicles were used as a landmark to ensure comparable sections were used in each embryo. The most anterior section showing optic vesicles was labelled 'c'. One section from the next two pairs both rostrally ('b' and 'a') and caudally ('d' and 'e') were also used for further analysis (Figure 4.11). Labelled cells in the mesenchyme of each section were counted, and the total number of cells in the mesenchyme of each section was counted. Initial studies showed that the total cell number and labelling indices in section 'c' were very similar to the mean total number and indices for each section in an embryo (Table 4.7, Table 4.8). Therefore, for each embryo total cell counts were only carried out on section 'c' and this number was used to calculate the labelling indices. Within each treatment group there were no significant differences between developmental stages (12, 13, 14 or 15 somite stage embryos, tested by one-way ANOVA). Therefore, all the data for each treatment group were combined for the final analysis.

Figure 4.11 Sections used to calculate labelling indices for apoptosis and proliferation in the cranial mesenchyme of embryos after 16 hours culture in the presence of methionine, ethionine, cycloleucine or PBS.

After 16 hours in whole embryo culture alternate pairs of transverse sections were taken through the cranial region of CD1 embryos and underwent immunohistochemistry with an antibody against phosphorylated histone H3 (**A-E**). Sections used to quantify levels of proliferation are shown in panels **A-E**. Equivalent sections were used for quantification of apoptosis after immunohistochemistry with anti-activated caspase-3 antibodies. The anterior-most section showing the optic vesicles (**C** and dotted line in **F**) was used as a landmark to ensure comparisons between embryos were carried out at the same axial level. Additional sections used were the 4^{th} and 8^{th} sections anterior (**B** and **A** respectively) and posterior (**D** and **E** respectively) to section **C**. Labelled cells (arrowheads in **D**) were counted in all five sections and the total number of cells in section **C** was used to give an index of labelled cells for each embryo. **F,** shows a typical PBS-treated embryo at 12 somite stage. Scale bars represent 100 μm (**A-E**) or 200 μm (**F**). Abbreviations; CM, cranial mesenchyme; FB, presumptive forebrain; HB, presumptive hindbrain; OV, optic vesicles; N, rostral extremity of notochord

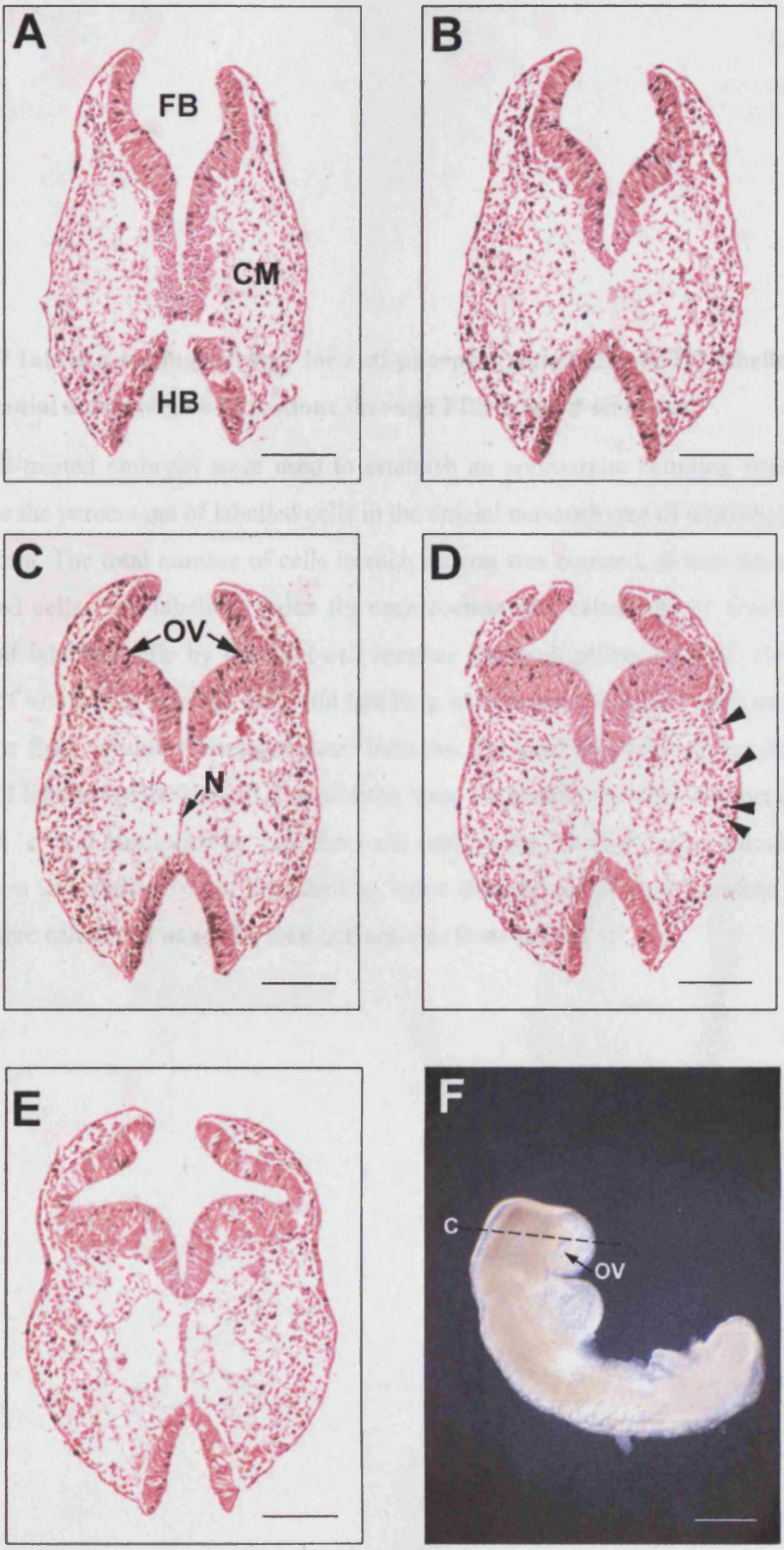
A
FB
CM
HB
B
C
OV
N
D
E
F
C
OV

Table 4.7 Initial counting strategy for anti-phosphorylated histone H3 labelled cells in the cranial mesenchyme in sections through PBS-treated embryos.

Four PBS-treated embryos were used to establish an appropriate counting strategy to determine the percentage of labelled cells in the cranial mesenchyme of treated embryos after culture. The total number of cells in each section was counted, as was the number of labelled cells. The labelling index for each section was calculated by dividing the number of labelled cells by the total cell number and multiplying by 100. The mean number of total cells, labelled cells and labelling indices are shown for each embryo ± SEM. The final column (Averaged data) indicates the labelling index when the mean number of labelled cells from all five sections were divided by the total number of cells in section 'c' and multiplied by 100. For each embryo the labelling index calculated in this fashion was within 5 % of the labelling index in each section, and therefore further indices were calculated using the total cell number from section 'c'.

Embryo L2305	Section position					mean ± SEM	Averaged data
	a	b	c	d	e		
Total cell number	544	671	782	924	965	777.2 ± 78.3	782
No. of labelled cells	21	18	33	24	38	26.8 ± 3.8	26.8
Labelling index	3.9	2.7	4.2	2.6	3.9	3.4 ± 0.3	3.4

Embryo L2301	Section position					mean ± SEM	Averaged data
	a	b	c	d	e		
Total cell number	467	625	565	629	709	599.0 ± 40.2	565
No. of labelled cells	16	26	35	11	25	22.6 ± 4.2	22.6
Labelling index	3.4	4.2	6.2	1.7	3.5	3.8 ± 0.7	4.0

Embryo L2194	Section position					mean ± SEM	Averaged data
	a	b	c	d	e		
Total cell number	305	343	439	535	603	445.0 ± 56.2	439
No. of labelled cells	45	37	44	35	51	42.4 ± 2.9	42.4
Labelling index	14.8	10.8	10.0	6.5	8.5	10.1 ± 1.4	9.6

Embryo L2196	Section position					mean ± SEM	Averaged data
	a	b	c	d	e		
Total cell number	82	199	216	289	231	198.4 ± 33.3	216
No. of labelled cells	10	20	20	32	39	24.2 ± 5.1	24.2
Labelling index	12.2	10.1	9.3	11.1	16.9	11.9 ± 1.3	11.2

Table 4.8 Initial counting strategy for anti-activated caspase 3 labelled cells in the cranial mesenchyme in sections through PBS-treated embryos.

Four PBS-treated embryos were used to establish an appropriate counting strategy to determine the percentage of labelled cells in the cranial mesenchyme of treated embryos after culture in a similar manner to that described previously (Table 4.7). The mean number of total cells, labelled cells and the labelling indices are shown for each embryo ± SEM. The final column shows the Average data (see Table 4.7) which for each embryo was within 5 % of the mean labelling index in each section, and therefore further indices were calculated using the total cell number from section 'c'.

Embryo L2705	Section position					mean ± SEM	Averaged data
	a	b	c	d	e		
Total cell number	231	303	284	353	362	306.6 ± 23.9	284
No. of labelled cells	2	10	2	6	18	7.6 ± 3.0	7.6
Labelling index	0.9	3.3	0.7	1.7	5.0	2.3 ± 0.8	2.7

Embryo L2706	Section position					mean ± SEM	Averaged data
	a	b	c	d	e		
Total cell number	395	424	432	405	364	404.0 ± 12.0	432
No. of labelled cells	7	3	6	5	4	5.0 ± 0.7	5.0
Labelling index	1.8	0.7	1.4	1.2	1.1	1.2 ± 0.2	1.2

Embryo L2194	Section position					mean ± SEM	Averaged data
	a	b	c	d	e		
Total cell number	212	355	443	437	443	378.0 ± 44.7	443
No. of labelled cells	2	9	3	2	2	3.6 ± 1.4	3.6
Labelling index	0.9	2.5	0.7	0.5	0.5	1.0 ± 0.4	0.8

Embryo L2196	Section position					mean ± SEM	Averaged data
	a	b	c	d	e		
Total cell number	128	202	296	295	286	241.4 ± 33.4	296
No. of labelled cells	1	1	3	4	3	2.4 ± 0.6	2.4
Labelling index	0.8	0.5	1.0	1.4	1.0	0.9 ± 0.2	0.8

4.2.6.2 *Analysis of proliferation in the cranial mesenchyme of methionine, ethionine and cycloleucine-treated embryos*

There were no statistically significant differences between the proliferation levels in any of the treatment groups. However, there was a non-significant decrease in the percentage of phosphorylated histone H3 positive cells in methionine-exposed embryos compared to PBS-exposed control embryos (Table 4.9, Figure 4.12). In these studies the embryos were analysed at a developmental stage before NTD are apparent, such that embryos could not be separated according to whether they would develop NTD or complete cranial neural tube closure. This might have lead to masking of an effect in the potentially exencephalic embryos by those developing normally. However, there were similar data ranges within treatment groups when compared to the control group, where all embryos are expected to complete cranial neural tube closure (Figure 4.12). These data suggest that the reduced cell density in methionine and ethionine-treated embryos is unlikely to arise from reduced cell proliferation and may be secondary to failure of the neural tube to close.

Treatment	No. of somites	No. of embryos	n	Index ± SEM
PBS	12	3	15	7.76 ± 1.35
	13	3	14	8.73 ± 1.73
	14	5	25	8.10 ± 0.73
	15	6	29	7.25 ± 1.35
5 mM Methionine	12	7	31	5.96 ± 0.43
	13	1	5	5.40 ± 0.00
	14	3	14	5.70 ± 1.72
	15	4	17	8.83 ± 0.74
5 mM Ethionine	12	1	5	6.20 ± 0.00
	13	2	10	6.60 ± 0.10
	14	3	15	8.63 ± 0.20
	15	3	15	7.63 ± 0.54
15 mM Cycloleucine	12	1	5	9.60 ± 0.00
	13	2	9	6.60 ± 1.20
	14	2	10	9.60 ± 0.80
	15	4	20	7.18 ± 0.45

Table 4.9 Cranial mesenchyme proliferation in embryos after culture with PBS, 5 mM methionine, 5 mM ethionine or 15 mM cycloleucine

Embryos at the 12-15 somite-stages of cranial neural tube closure were analysed for each treatment group. The number of embryos studied in each treatment group at each somite stage is stated with the number of actual measurements recorded (**n**). Some measurements could not be made, due to damaged sections. There were no statistically significant differences between the mean indices of each embryo group between or within the treatment groups, as tested by One-way ANOVA.

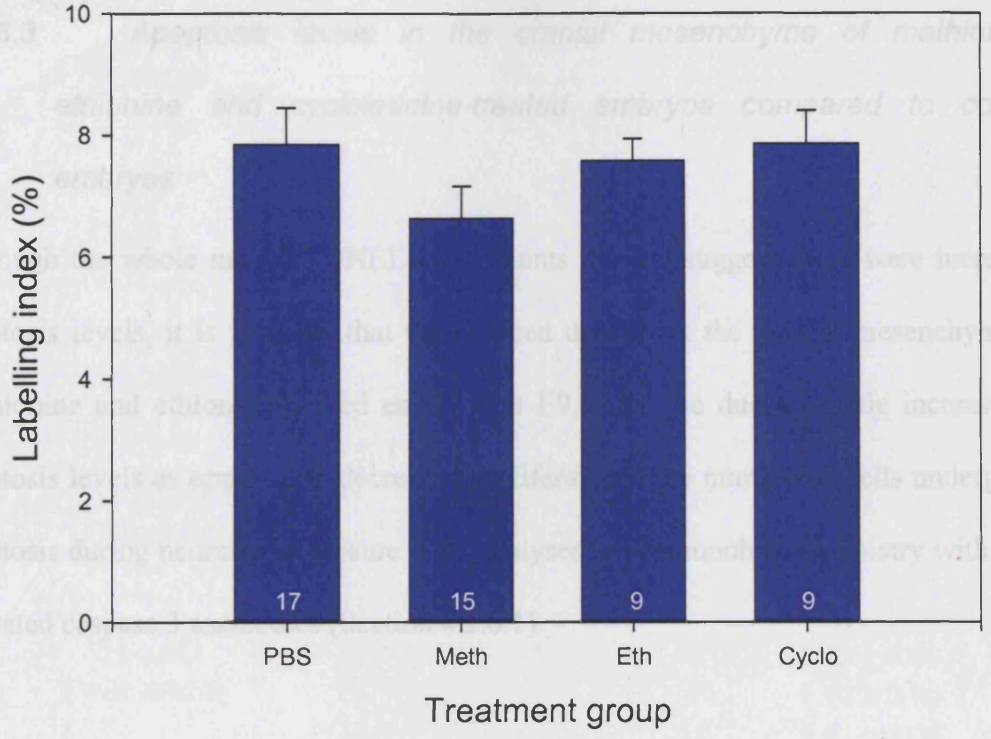

Figure 4.12 Cranial mesenchyme proliferation in embryos at the stage of cranial neural tube closure after culture with PBS, 5 mM methionine, 5 mM ethionine or 15 mM cycloleucine

Data is presented as mean ± SEM. Embryos at the 12-15 somite-stages of development were pooled together for each treatment group. The number of embryos analysed in each treatment group is shown within each bar. Abbreviations, Meth; 5 mM methionine, Eth; 5 mM ethionine, Cyclo; 15 mM cycloleucine

4.2.6.3 Apoptosis levels in the cranial mesenchyme of methionine, ethionine and cycloleucine-treated embryos compared to control embryos

Although the whole mount TUNEL experiments did not suggest there were increased apoptosis levels, it is possible that the reduced density in the cranial mesenchyme of methionine and ethionine-treated embryos at E9.5 may be due to subtle increases in apoptosis levels as opposed to decreased proliferation. The number of cells undergoing apoptosis during neural tube closure were analysed by immunohistochemistry with anti-activated caspase 3 antibodies (Section 4.2.6.1).

The level of apoptosis in the cranial mesenchyme of ethionine-exposed embryos is very similar to that of PBS-exposed embryos. The methionine and cycloleucine treatment groups have a higher index of cells labelled for activated caspase 3 than the control group, but these changes are not statistically significant (Table 4.10, Figure 4.13). These experiments cannot distinguish between affected and unaffected embryos in the treatment groups, leaving the possibility of 'normal' embryos masking an effect present in potential exencephalic embryos.

Treatment	No. of somites	No. of embryos	n	Index ± SEM
PBS	12	3	15	2.63 ± 1.09
	13	4	19	3.28 ± 2.48
	14	4	19	8.13 ± 3.31
	15	3	15	2.10 ± 0.47
5 mM Methionine	12	4	20	5.53 ± 2.38
	13	1	5	1.40 ± 0.00
	14	3	15	7.93 ± 2.07
	15	2	9	8.05 ± 0.85
5 mM Ethionine	12	0	0	0.00 ± 0.00
	13	2	9	5.75 ± 2.75
	14	1	5	1.60 ± 0.00
	15	5	25	4.18 ± 1.53
15 mM Cycloleucine	12	1	5	2.60 ± 0.00
	13	1	4	2.40 ± 0.00
	14	1	5	9.10 ± 0.00
	15	3	14	9.53 ± 2.16

Table 4.10 Cranial mesenchyme apoptosis in embryos after culture with PBS, 5 mM methionine, 5 mM ethionine or 15 mM cycloleucine

Embryos at the somite-stages of cranial neural tube closure were analysed for each treatment group. The number of embryos studied in each treatment group at each somite stage is stated with the number of actual measurements recorded (**n**). Some measurements could not be made, due to damaged sections. There were no statistically significant differences between the mean indices of each somite-stage embryo group between or within the treatment groups, as tested by One-way ANOVA.

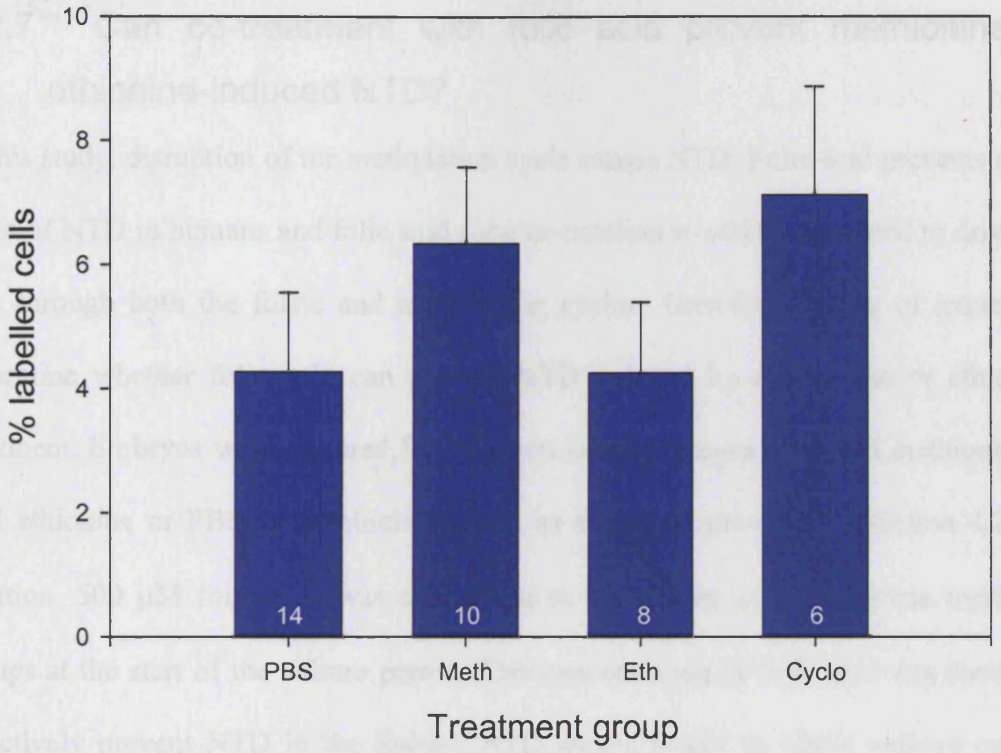

Figure 4.13 Cranial mesenchyme apoptosis levels in embryos at the time of cranial neural tube closure after culture with PBS, 5 mM methionine, 5 mM ethionine or 15 mM cycloleucine

Data is presented as mean ± SEM. Embryos at the 12-15 somite-stages of development were pooled together for each treatment group. The number of embryos measured in each treatment group is shown within each bar. Abbreviations, Meth, 5 mM methionine; Eth, 5 mM ethionine; Cyclo, 15 mM cycloleucine.

4.2.7 Can co-treatment with folic acid prevent methionine or ethionine-induced NTD?

In this study, disruption of the methylation cycle causes NTD. Folic acid prevents many cases of NTD in humans and folic acid supplementation would be predicted to drive the flux through both the folate and methylation cycles. Therefore, it was of interest to determine whether folic acid can prevent NTD induced by methionine or ethionine treatment. Embryos were cultured for 24 hours in the presence of 5 mM methionine, 5 mM ethionine or PBS as a vehicle control, as described previously (Section 4.2). In addition, 500 μM folic acid was also added to the culture serum of some treatment groups at the start of the culture period. This concentration of folic acid was shown to effectively prevent NTD in the *Splotch* NTD mouse model in whole embryo culture (Fleming *et al.*, 1998). Embryos were analysed as previously described (Section 4.2)

Culture of embryos in the presence of 5 mM methionine or 5 mM ethionine did not adversely affect the viability, growth or health of embryos (Table 4.11, Table 4.12) consistent with the findings described in Section 4.2.1. Embryos cultured with methionine alone developed cranial NTD in a significant proportion of embryos (37%), similar to my previous results (40%, Section 4.2.1.1). As before, NTD were also evident in the ethionine-exposed embryos with an incidence of 57%, compared to 61.9% previously (Section 4.2.1.2). Culture in the presence of methionine or ethionine and folic acid did not affect the development, health or viability of the embryos as measured by somite number, yolk sac circulation and heart beat respectively. There were no statistically significant differences between the treatment groups and control embryos in any of the parameters measured at the end of the culture period (Table 4.11, Table

4.12). Moreover, there was no reduction in the number of embryos developing cranial NTD in the presence of methionine or ethionine with folic acid compared to those without folic acid (Table 4.11, Table 4.12). In contrast, there were slight (but not significant) increases in the percentage of embryos developing NTD in the additional presence of folic acid, (methionine alone 37%, plus folic acid 48%) (ethionine alone 57.1%, plus folic acid 65.4%). These results suggest that folic acid does not have a preventative effect on the production of cranial NTD by excess methionine or ethionine.

Treatment	No. embryos	No. live embryos	Yolk Sac circulation	No. failed axial rotation (%)	No. cranial open neural tube (%)	No. cranial neural tube defects (%)	Somite number	Crown-rump length (mm)
PBS	13	13	2.92 ± 0.08	0 (0.0)	0 (0.0)	0 (0.0)	20.0 ± 0.52	2.41 ± 0.08
5 mM Methionine	27	27	2.89 ± 0.08	0 (0.0)	10 (37.0)‡	10 (37.0)‡	20.3 ± 0.32	2.43 ± 0.05
5 mM Methionine and 500 μM folic acid	25	23	2.60 ± 0.18‡	0 (0.0)	12 (48.0)‡	12 (48.0)‡	20.3 ± 0.45	2.40 ± 0.06

Table 4.11 Growth and development of mouse embryos cultured in the presence of methionine with or without folic acid

Dead embryos were identified by an absence of yolk sac circulation and were excluded from analysis. Cranial neural tube defects are defined as failure to complete cranial neural tube closure in live embryos that have 16 or more somites. Values for yolk sac circulation, somite number and crown-rump length are given as mean ± SEM. ‡ indicates significant variation from control embryos ($p<0.05$, tested by one-way ANOVA). Data for failed axial rotation and open cranial neural tube are presented as number of embryos, with percentage of total embryos in parentheses. Data for cranial neural tube defects are presented as number of embryos, with percentage of embryos with 16 or more somites in parentheses. ‡ indicates significant variation from control embryos ($p<0.05$, tested by z-test). There were no significant differences between values obtained for embryos cultured with methionine alone or with methionine and folic acid.

Treatment	No. embryos	No. live embryos	Yolk Sac circulation	No. failed axial rotation (%)	No. cranial open neural tube (%)	No. cranial neural tube defects (%)	Somite number	Crown-rump length (mm)
PBS	6	6	3.00 ± 0.00	0 (0.0)	0 (0.0)	0 (0.0)	20.2 ± 0.60	2.40 ± 0.05
5 mM Ethionine	23	23	2.96 ± 0.04	3 (13.4)	14 (60.9)‡	12 (57.1)	19.6 ± 0.48	2.47 ± 0.06
5 mM Ethionine and 500 μM folic acid	26	26	2.89 ± 0.08	2 (7.7)	17 (65.4)‡	17 (65.4)‡	20.8 ± 0.35	2.48 ± 0.06

Table 4.12 Growth and development of mouse embryos cultured in the presence of ethionine with or without folic acid

Cranial neural tube defects are defined as failure to complete cranial neural tube closure in embryos that have 16 or more somites. Values for yolk sac circulation, somite number and crown-rump length are given as mean ± SEM. There were no significant differences between the values (tested by one-way ANOVA). Data for failed axial rotation and open cranial neural tube are presented as number of embryos, with percentage of total embryos in parentheses. Data for cranial neural tube defects are presented as number of embryos, with percentage of embryos with 16 or more somites in parentheses ‡ indicates significant variation from control embryos ($p<0.05$, tested by z-test). There were no significant differences between values obtained for embryos cultured with ethionine alone or with ethionine and folic acid.

4.3 DISCUSSION

In this chapter, treatment of non-mutant embryos throughout cranial neural tube closure with methionine, ethionine or cycloleucine resulted in the development of isolated NTD. These compounds are predicted to disrupt of perturb the methylation cycle suggesting that this metabolic cycle is essential for closure of the cranial neural tube. Inhibition of the methylation cycle, by SAH-hydrolase or MAT inhibitors, has also been shown to cause a delay in closure of the anterior neuropore in cultured chick embryos, supporting a role for the methylation cycle in cranial neural tube closure (Afman *et al.*, 2005).

The process of cranial neural tube closure appears to be very sensitive to disruption in mouse, being susceptible to disruption by many teratogens (Copp *et al.*, 1990) and numerous single gene mutations. Thus the majority of mouse NTD models exhibit exencephaly (Juriloff *et al.*, 2000;Copp *et al.*, 2003b). In this study cranial neural tube defects were observed in the absence of growth retardation, delayed developmental progress or any other gross morphological defects suggesting that exposure to methionine, ethionine and cycloleucine has specific effects on processes required for cranial neural tube closure. Thus, the development of NTD in treated embryos does not appear to be secondary to other teratogenic effects of these treatments. The extent of the open region of the cranial neural folds differs between the treatment groups suggesting that different mechanisms may be involved in the production of exencephaly for each treatment. In addition, the morphology of the cranial region in exencephalic embryos differs between methionine, ethionine and cycloleucine-treated embryos.

Although initial observations suggested that both methionine and ethionine-treated embryos exhibit thinner neuroepithelium compared to control embryos, subsequent quantitative analysis showed that the decrease was statistically significant only in ethionine-treated embryos. In addition, this difference was present in the midbrain of all ethionine-treated embryos irrespective of whether or not the cranial neural tube completed closure, suggesting that the reduced thickness of neuroepithelium in ethionine-exposed embryos was not instrumental in failure of closure. Therefore, the differences in the thickness of neuroepithelium in cultured embryos was not investigated any further in this study.

Cell aggregates were observed in a subset of methionine-treated embryos. The type of cells that make up the aggregates was not investigated further in this study. Further work using cell-specific markers could determine the composition of the cell aggregates and may suggest possible roles in the production of NTD. For example, it is possible that the aggregates consist of neural crest cells that have delaminated from the neural folds but became arrested during their migration. The role of the aggregates in the production of methionine-induced NTD is unclear.

Exencephalic methionine and ethionine-exposed embryos exhibited reduced density of the cranial mesenchyme that was not observed in exencephalic, cycloleucine-exposed embryos or embryos that completed cranial neural tube closure in any treatment group. The observed decrease in cranial mesenchyme density in methionine and ethionine-treated embryos could potentially be secondary to the NTD as there were no differences in the cranial mesenchyme density of methionine or ethionine-treated embryos that

completed neural tube closure. However, embryos-exposed to cycloleucine that failed to complete cranial neural tube closure did not exhibit a reduced cranial mesenchyme density which argues against a secondary effect and suggests a possible role in the development of methionine and ethionine-induced cranial NTD.

Cranial mesenchyme is believed to play a role in cranial neurulation by providing mechanical support for the elevation and apposition of the cranial neural folds which enables neural tube closure to occur (Morriss *et al.*, 1978b) (Section 1.2.1). In support of this idea, disruption of the integrity of the cranial mesenchyme has been implicated in the development of exencephaly in some genetic mouse NTD models. For example, homozygous *Cart1* mutant embryos develop cranial neural tube defects in the midbrain region. Histological analysis of *Cart1* mutant embryos showed a reduction in cell number in the forebrain cranial mesenchyme during cranial neurulation, E9 (Zhao *et al.*, 1996). Increased levels of apoptosis in cells of the forebrain mesenchyme were detected in *Cart1* mutant embryos and are proposed to have resulted in the reduced cell density and subsequent cranial NTD (Zhao *et al.*, 1996). In addition, homozygous *twist* mutant embryos exhibit abnormal cranial mesenchyme prior to cranial neural tube closure and subsequently develop cranial NTD (Chen *et al.*, 1995). Therefore, methionine and ethionine-treatment may induce cranial NTD in embryos by disrupting the integrity of the cranial mesenchyme. There is no evidence suggesting that this mechanism may be involved in the production of cycloleucine-induced NTD.

Methionine and ethionine treatments were initially predicted to induce NTD through different mechanisms. One explanation for reduced cell density following methionine or

ethionine treatment could be a reduced rate of cellular proliferation. Both treatments have the potential to disrupt the SAM:SAH ratio which could affect the regulation of MTHFR and lead to the redistribution of folate cycle intermediates (Kutzbach and Stokstad, 1971). This could subsequently lead to the suppression of dTMP synthesis or purine production therefore inhibiting DNA synthesis and limiting proliferation. Alternatively methionine and/or ethionine treatment could affect the viability of cells within the cranial mesenchyme leading to premature cell death. In order to investigate these possible mechanisms the cranial mesenchyme proliferation and apoptosis levels of treated embryos were compared to those of control embryos.

Quantitative data of embryos during cranial neural tube closure showed that exposure to methionine or cycloleucine caused increased, but not statistically significant, levels of apoptosis compared to PBS or ethionine-treated embryos. In addition, analysis of the number of cells in M-phase of the cell cycle, as an indicator of proliferation rates in the cranial mesenchyme of cultured embryos showed reduced but not significant levels of proliferation in methionine-treated embryos compared to control embryos. The roles of proliferation and apoptosis rates in the cranial mesenchyme of methionine-treated embryos in the production of cranial NTD are not clear. A non-significant but apparent elevation in apoptosis level and slight reduction in proliferation levels in the cranial mesenchyme of methionine-treated embryos may together account for the subsequent reduced cell density. However, as the changes were not statistically significant no firm conclusions can be drawn.

No differences in proliferation levels in the cranial mesenchyme of ethionine or cycloleucine-treated embryos were detected when compared to PBS-treated embryos. As there is no evidence of reduced proliferation or increased apoptosis in the mesenchyme of exencephalic ethionine-treated embryos, I cannot rule out the possibility that the reduction in cell density is a secondary effect to failure of closure of the neural folds. Reduced mesenchyme density has been suggested to be a secondary effect to exencephaly in rat embryos cultured in diluted cow serum (Coelho and Klein, 1990). Cultured rat embryos exhibit reduced cranial mesenchyme density and cranial NTD, however, supplementation with methionine rescues the NTD phenotype but does not increase the cranial mesenchyme density suggesting that the cranial NTD are not caused by the reduced number of cranial mesenchyme cells (Coelho *et al.*, 1990).

In considering the mode of action at the biochemical level, the production of ethionine and cycloleucine-induced NTD are likely to involve similar mechanisms as both compounds inhibit SAM synthesis. Ethionine is an analogue of methionine that competes for MAT and is subsequently converted to SAE. SAE does not undergo any further metabolism, theoretically resulting in the decreased production of SAM and thereby limiting the supply of methyl groups for donation in the methyltransferase reactions. Cycloleucine is a chemical inhibitor of SAM-synthase that could also result in a reduction of available SAM. However, morphological analysis of ethionine and cycloleucine-treated embryos showed differences that may suggest different modes of action for the two treatments in the development of cranial NTD. SAE does not undergo further metabolism within the methylation cycle but has been shown to have a similar effect to SAM on the regulation of CBS (Miller *et al.*, 1994). Although CBS is not

believed to be active in neurulation-stage embryos (VanAerts *et al.*, 1995), these findings suggest SAE can be substituted for SAM in its regulatory roles and therefore, may affect the activity of MTHFR. Cycloleucine treatment would be unlikely to have this effect.

Methionine treatment was expected to act in an opposite manner to ethionine and cycloleucine treatment. Instead of limiting SAM production, increased methionine levels were expected to allow increased SAM production, possibly driving the flux through the methylation cycle.

Further experiments carried out in our laboratory have measured the levels of SAM and SAH in embryos that had been cultured for 17 hours (from E8.5 to E9) in the presence of 5mM methionine, 5 mM ethionine, 15 mM cycloleucine or PBS. All three treatments gave statistically significant reductions in the SAM:SAH ratio compared to PBS-treated embryos (Table 4.13). Thus, the mechanisms underlying the induction of NTD by ethionine, ethionine or cycloleucine treatment may all involve suppression of methylation reactions.

As expected, methionine-treatment results in an increase in SAM levels, whereas ethionine treatment results in reduced SAM levels, however, these changes are not statistically significant and are not primarily responsible for the changes in the SAM:SAH ratios. All three treatments result in elevated SAH levels compared to control embryos. The importance of SAM production in cell survival has led to the highly regulated control of SAM levels in the cell. Cells in the neurulation-stage

Treatment group	No. samples	SAM (nmole/mg protein)	SAH (nmole/mg protein)	Ratio SAM:SAH
PBS	5	3.79 ± 0.54	0.024 ± 0.004	167 ± 12.4
Methionine	5	4.40 ± 0.46	0.043 ± 0.006	104 ± 4.7*
Ethionine	5	2.67 ± 0.25	0.034 ± 0.004	79 ± 3.2*
Cycloleucine	5	3.68 ± 0.45	0.031 ± 0.004	120 ± 7.5*

Table 4.13 Quantification of SAM and SAH in cultured embryos

SAM and SAH were quantified by liquid chromatography coupled to tandem mass spectrometry. Samples consisted of 2-4 embryos pooled from a specific treatment group after whole embryo culture for 17 hours in the presence of 5 mM methionine, 5 mM ethionine, 15 mM cycloleucine or PBS. Values were normalised to protein content and are expressed as mean ± SEM. * indicates significant difference from the values of PBS-treated controls, $P<0.05$ tested by one-way ANOVA followed by the TUKEY test for pair-wise comparisons. (K. Burren, A.J. Copp, and N.D.E. Greene, personal communication)

mammalian embryo express the non-liver specific MAT isoform (MAT II) and therefore are relatively unaffected by fluctuations in methionine availability, because of a negative feedback inhibition mechanism. That is, SAM inhibits MAT II at concentrations only slightly higher than normal SAM intracellular levels ensuring cellular SAM levels are relatively constant (Finkelstein, 1990). The subsequent clearance of SAH is dependent on the rapid removal of homocysteine and adenosine. In the embryo, this may be a rate-limiting step as the methionine synthase-mediated reaction is the only pathway present that is capable of removing homocysteine from the cell. Delay in the removal of homocysteine may result in a build up of SAH levels in the cell as SAH-hydrolase favours the formation of SAH in the presence of homocysteine

(Finkelstein, 1998). SAH is a potent product inhibitor of methyltransferases (Zappia *et al.*, 1969). Therefore, SAH-mediated inhibition of methyltransferases by the treatments could potentially result in global hypomethylation, which may result in disrupted gene expression or protein function during neurulation. The fact that all three treatments change the methylation ratio within the embryo and cause cranial NTD may suggest a role for changes in cellular methylation processes in causing the observed NTD phenotypes.

During DNA methylation, methyl groups are transferred from SAM to cytosine residues primarily located in CpG islands that are generally clustered in the promoter regions of genes. DNA methylation has an important role in the epigenetic control of the expression of some genes. Although the mechanism is unclear, it has been suggested that methyl-cytosine binding proteins (MeCP) bind to methylated cytosine preventing the binding of transcription factors and so repressing gene expression (Hendrich and Bird, 1998;Jones *et al.*, 2001). Another theory suggests that MeCP-binding proteins recruit histone deacetylases that induce chromatin compaction and gene silencing (Malone *et al.*, 2001). Changes in DNA methylation of genes involved in neural tube closure could potentially lead to defects in the process of neurulation. For example, *in vivo* exposure to 5-azacytidine, a cytidine analogue that is incorporated into DNA but cannot be methylated, causes exencephaly in mice and rat embryos (Takeuchi *et al.*, 1978;Takeuchi *et al.*, 1985). Experiments carried out in our laboratory have shown that *in vitro* exposure of mice embryos to 5-azacytidine also induces cranial NTD (K. Burren, and N.D.E. Greene, Personal communication). In addition, mice lacking DNA

methyltransferase 3b (*Dnmt3b*) develop cranial NTD (Okano *et al.*, 1999), suggesting that inhibition of DNA methylation is sufficient to prevent neural tube closure.

DNA hypomethylation has been observed with elevated homocysteine levels in MTHFR-deficient mice (Chen *et al.*, 2001) and in human patients suffering from hyperhomocysteinaemia (Ingrosso *et al.*, 2003). Although elevated homocysteine is a risk factor for NTD, as described in Section 1.9, NTD have not been described in either of these studies. Moreover, in Chapter 3 I showed that homocysteine treatment does not result in cranial NTD in mouse embryos. If homocysteine teratogenesis acted through elevated SAH levels I would expect a similar phenotype as observed in treatments that do raise SAH levels within the embryo, that is methionine, ethionine and cycloleucine treatment. It is possible that changes in the methylation ratio and subsequent SAH-mediated hypomethylation is responsible for the methionine, ethionine and cycloleucine-induced NTD. These observations may suggest that homocysteine embryotoxicity is mediated through elevated levels of homocysteine per se, possibly by affecting yolk sac function and causing general toxicity at a dose that does not result in the elevation of SAH levels to a concentration that can disrupt cranial neural tube closure.

In addition to DNA, SAM is also the methyl donor for the methylation of proteins and phospholipids and it has been suggested that changes in protein methylation could affect cranial neural tube closure. Embryos cultured in cow serum exhibit NTD that are thought to be due to methionine deficiency (Coelho *et al.*, 1989). Coelho and colleagues (1990) detected differences in the levels of methylated amino acids in neural tube

proteins between methionine-supplemented cultures, in which embryos completed neural tube closure, and un-supplemented cultures, in which embryos developed cranial NTD. The reduction in methylation appears to be specific for proteins of the neural tube as the differences were not detected in heart proteins of the same embryos (Coelho *et al.*, 1990). In microfilament associated proteins from unsupplemented-embryo neural tube, the reduction of the proportion of methylated amino acids suggests that defective microfilament contraction could be involved in the production of cranial NTD caused by methionine-deficiency. In support of this idea, cytoskeletal proteins: β-actin, αβ-tubulin and neurofilament L have been identified as proteins that are methylated during neurulation (Moephuli *et al.*, 1997). The localisation of β-actin and αβ-tubulin to the basal and apical cytoplasm in neuroepithelial cells is disrupted in mouse embryos cultured in methionine-deficient serum (Moephuli *et al.*, 1997). Moreover, the integrity of the actin cytoskeleton has been shown to be essential for normal cranial neural tube closure to occur (Ybot-Gonzalez *et al.*, 1999) suggesting that this could be disrupted by aberrant methylation of cytoskeletal proteins.

In addition to methyltransferase-mediated reactions, SAM is required for polyamine synthesis. Therefore, treatments that affect the production of SAM may have an effect on polyamine biosynthesis. Polyamine synthesis is essential for embryo survival (Pendeville *et al.*, 2001;Nishimura *et al.*, 2002) but has not been investigated in relation to neural tube closure. Therefore the effects of changes in polyamine synthesis on cranial neural tube closure are currently unknown.

Interestingly, concomitant treatment with folic acid did not reduce the incidence of methionine or ethionine-induced NTD. It is possible that the concentration of folic acid (500 μM) used in these experiments was not sufficient to counteract the relatively high concentrations of 5 mM methionine and ethionine, and that higher doses of folic acid might have had a protective effect. However, this dose was sufficient to prevent NTD in mice caused by a mutation in the *Pax3* gene (Fleming *et al.*, 1998). The results in this chapter therefore suggest that folic acid does not prevent NTD through rectifying cellular processes affected by excess methionine or ethionine. This may be because folic acid treatment acts to prevent NTD by stimulating the folate cycle and allowing increased proliferation, whereas I did not find evidence that defective proliferation is solely responsible for the production of methionine or ethionine-induced cranial NTD.

In this chapter, I have shown that the integrity of the methylation cycle is required for normal cranial neural tube closure to occur. Further work investigating changes in DNA/protein methylation in methionine, ethionine and cycloleucine-treated embryos could address the possibility that changes in cellular methylation are responsible for the induction of NTD by defects in the methylation cycle.

CHAPTER 5; INVESTIGATION OF THE CAUSES OF CRANIAL NTD IN *SPLOTCH*^{2H} MICE

5.1 INTRODUCTION

Mutations in the *Pax3* locus in mice occur in the *Splotch* mutant mouse. There are six variants of the *Splotch* allele, and those that allow development to proceed beyond neurulation result in NTD among other defects (Section 1.10.1). The *Splotch*^{2H} mouse carries a 32 base pair deletion in the paired homeodomain of the *Pax3* gene, resulting in a truncated protein and a homozygous phenotype that includes exencephaly and/or spina bifida (Section 1.10.1) (Epstein *et al.*, 1991). The *Splotch* NTD phenotype has been shown to be rescued by p53 deficiency, following intercrosses of p53 knockout and *Splotch* mice (Pani *et al.*, 2002). None of the intercrossed embryos exhibited NTD (from a total of five) compared to 100 % of *Sp/Sp* embryos. The authors suggested that *Pax3* regulates neural tube closure by inhibiting p53-dependent apoptosis such that in the *Pax3* deficient *Sp/Sp* embryos there is an excess of p53-dependent apoptosis. In a previous study investigating apoptosis in E10.5 *Splotch* embryos, a high concentration of apoptotic cells was observed in the neural folds surrounding the open regions of the neural tube (Phelan *et al.*, 1997). In addition, down-regulation of *Pax* proteins induced apoptosis in cell culture experiments (Bernasconi *et al.*, 1996). The results of these studies have led to the suggestion that NTD in *Splotch* mutant embryos are caused by excessive apoptosis. This idea is supported by previous studies in which excess apoptosis has been suggested to be causal in other mouse mutants (Zhao *et al.*, 1996;Martinez-Barbera *et al.*, 2002). However, to date there has not been a detailed analysis of apoptosis rate in *Splotch* mutant embryos at the specific stages prior to and during neural tube closure.

This study was designed to determine if the levels of apoptosis during cranial neurulation in *Sp*^{2H}/*Sp*^{2H} embryos differ from those in wild type embryos. *Splotch*^{2H} embryos at three stages of development, E8.5, E9.5 and E10.5, underwent whole mount TUNEL to identify apoptosis patterns in embryos of each genotype. Further studies utilising immunohistochemistry allowed quantitative analysis of apoptosis and proliferation in the cranial neuroepithelium of *Splotch*^{2H} embryos immediately prior to and following cranial neural tube closure. Additional analysis was carried out to investigate apoptosis in relation to *Pax3* expression in the neuroepithelium of *Splotch*^{2H} embryos at the developmental stage immediately prior to cranial neural tube closure.

5.2 RESULTS

5.2.1 Whole mount TUNEL in *Splotch*^{2H} embryos during neural tube closure

To investigate the possibility that increased apoptosis is responsible for inducing NTD in homozygous *Splotch*^{2H} embryos, whole mount TUNEL was carried out on *Splotch*^{2H} embryos at stages throughout cranial neurulation (E8.5, E9.5 and E10.5). Cells undergoing apoptosis were labelled and cell death patterns were compared between homozygous and wild type *Splotch*^{2H} embryos.

At E8.5 whole mount TUNEL staining on wild type embryos showed few positive cells suggesting that only a few cells distributed throughout the embryo are undergoing apoptosis (Figure 5.1 A, C). No major differences were observed in the distribution or

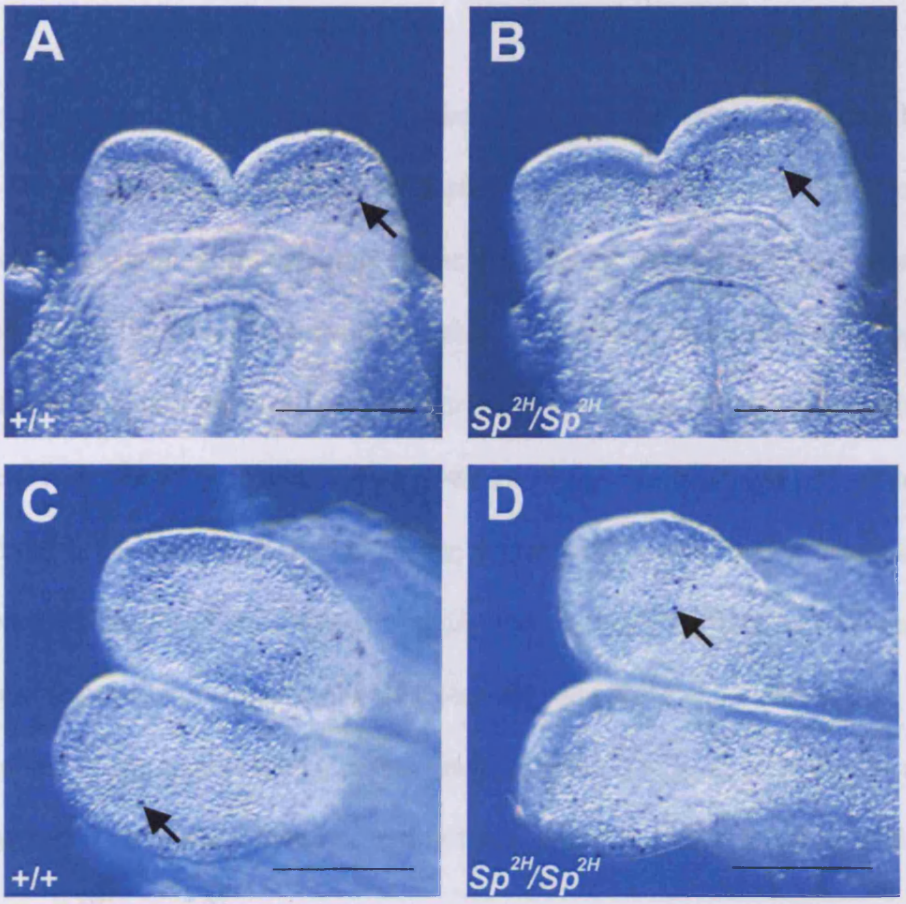

Figure 5.1 Whole mount TUNEL on E8.5 *Splotch*^{2H} embryos

Wild type (**A, C**) and homozygous (**B, D**) E8.5 *Splotch*^{2H} embryos after whole mount TUNEL. Ventral (**A, B**) and dorsal (**C, D**) views of the cranial region are shown. TUNEL positive cells are coloured purple (indicated by black arrows). There were no noticeable differences in distribution or quantity of TUNEL positive cells between the *splotch*^{2H} genotypes. This figure represents data from at least 6 embryos of each genotype. Scale bars represent 200 μm.

quantity of apoptotic cells in the cranial region of wild type and homozygous mutant embryos at this stage of development (Figure 5.1).

By E9.5 apoptotic cells are detected in specific areas in the embryo as shown by whole mount TUNEL staining (Figure 5.2). Clusters of apoptotic cells have previously been described in non-mutant mouse embryos at this stage of development. Cell death in the mesenchyme of the first and second branchial arches has previously been suggested to be occurring in neural crest cell derivatives (Mirkes *et al.*, 2001). TUNEL positive cells have also been detected in the neuroepithelium of the hindbrain (Mirkes *et al.*, 2001) and cell death has been described along the dorsal midline after neural tube closure has occurred (Schluter, 1973). Clusters of cells undergoing programmed cell death have also been observed surrounding the otic placode (Abbott *et al.*, 1995) and at the most rostral point of the neural tube (Geelen and Langman, 1977) in E9.5 mouse embryos. Wild type embryos were found to exhibit cell death in these areas at this stage of development (Figure 5.2).

Whole mount TUNEL staining of embryos at E9.5, just following the completion of cranial neural tube closure, differs in Sp^{2H}/Sp^{2H} embryos compared to wild type littermates. There appear to be a slight increase in the number of TUNEL positive cells in the region surrounding the otic vesicles and in the cranial mesenchyme in Sp^{2H}/Sp^{2H} embryos compared to wild type littermates (Figure 5.2 A,B). The distinct line of cell death along the midline of the fused neural tube in the forebrain and midbrain in wild type embryos is missing or incomplete in Sp^{2H}/Sp^{2H} embryos (Figure 5.2 C,D). All the homozygous mutant embryos studied at this developmental stage exhibited

Figure 5.2 Whole mount TUNEL on E9.5 *Splotch^{2H}* embryos

Wild type (**A**, **C**, **E**) and homozygous (**B**, **D**, **F**) E9.5 *Splotch^{2H}* embryos after whole mount TUNEL, labelled cells appear purple. Lateral (**A**, **B**), ventral (**C**, **D**) and corresponding dorsal (**E**, **F**) views are shown. All *Sp^{2H}/Sp^{2H}* embryos examined developed cranial NTD, and the regions of open neural tube are flanked by white arrowheads (**B**). There appears to be a greater number of TUNEL positive cells around the otic vesicle (black arrows in **A**, **B**, **E** and **F**) and in the cranial mesenchyme (asterix in **B**) in *Sp^{2H}/Sp^{2H}* embryos compared to wild type littermates. The distinct pattern of apoptotic neural epithelial cells along the fused neural tube in the forebrain is less distinct in homozygous embryos compared to wild type embryos (black arrowheads in **D** and **C**). However, the number and position of apoptotic cells in the fused or open midbrain/hindbrain neural tube appear similar in all *Splotch^{2H}* genotypes (black arrowheads in **E** and **F**). This figure represents data from at least 5 embryos of each genotype. Scale bars represent 200 μm.

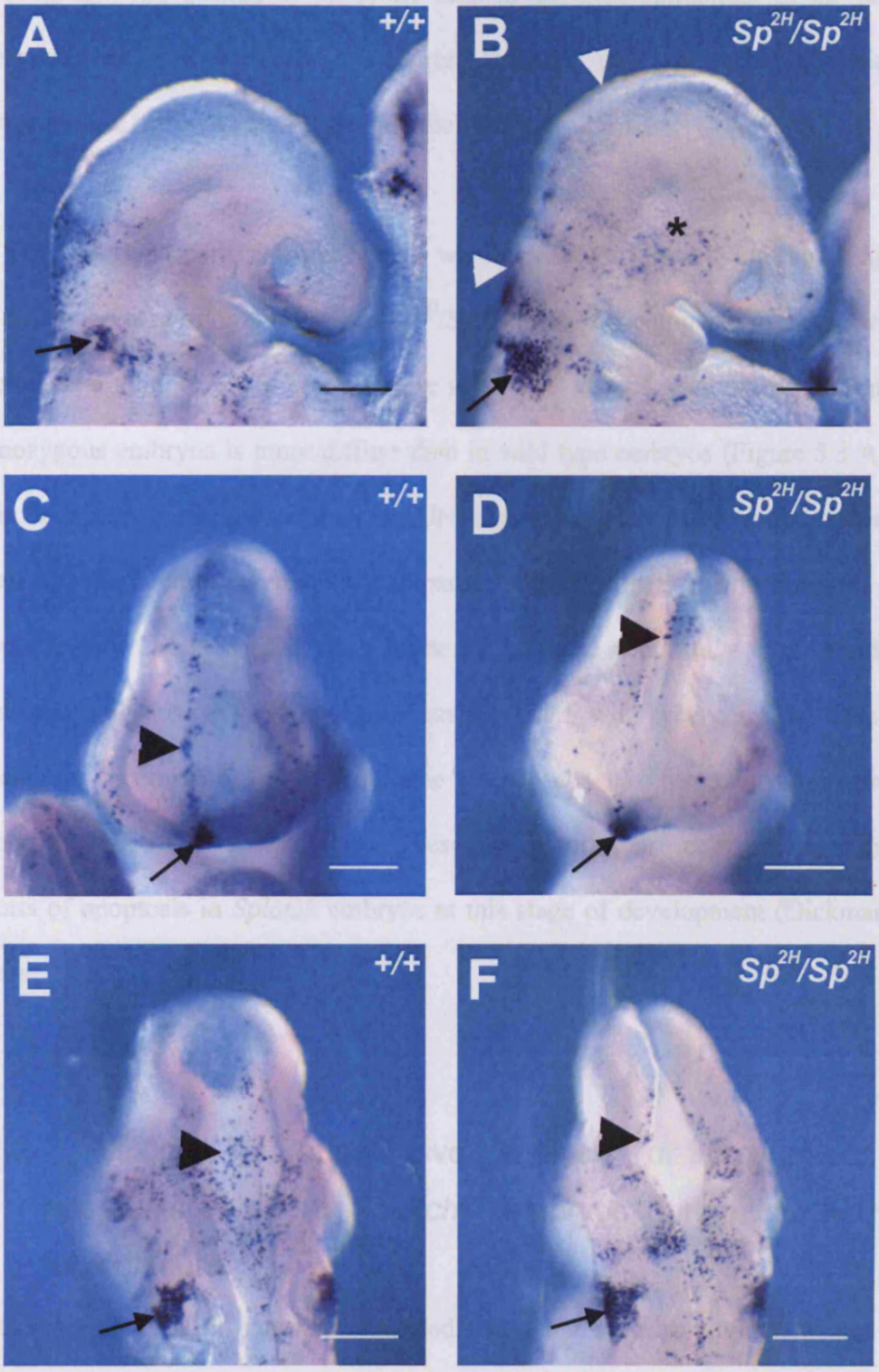
A
+/+
B
Sp2H/Sp2H
C
+/+
D
Sp2H/Sp2H
E
+/+
F
Sp2H/Sp2H

exencephaly. The pattern of apoptotic cells in the neuroepithelium of the hindbrain appeared unchanged between the different *Splotch*^{2H} genotypes (although this was a comparison of open and closed neural tube) (Figure 5.2 E,F).

At E10.5, defined patterns of apoptosis were observed in mouse embryos (Figure 5.3 A). When the pattern of apoptosis in *Sp*^{2H}/*Sp*^{2H} embryos is compared to that of wild type littermates a number of differences were seen. The TUNEL staining in the somites of homozygous embryos is more diffuse than in wild type embryos (Figure 5.3 A,B) and there is an increase in the number of TUNEL positive cells in the cranial mesenchyme in all *Sp*^{2H}/*Sp*^{2H} embryos studied, compared to their wild type littermates. A line of apoptotic cells can be seen at the midline of the fused neural tube in the forebrain of wild type embryos, as described previously in E9.5 wild type embryos. This line is missing or incomplete, even though the neural tube has fused, in all homozygous embryos studied (Figure 5.3 C,D). These observations are comparable to previous reports of apoptosis in *Splotch* embryos at this stage of development (Dickman *et al.*, 1999).

5.2.2 Method for quantitative analysis of proliferation and apoptosis levels in *Splotch*^{2H} embryos during cranial neural tube closure

Whole mount TUNEL staining suggested that there may be slight increases in the number of cells undergoing cell death in the cranial region of *Sp*^{2H}/*Sp*^{2H} embryos during neurulation, but this appears restricted to the mesenchyme not the neural tube. These findings are not in agreement with the suggestion of increased apoptosis as a causative

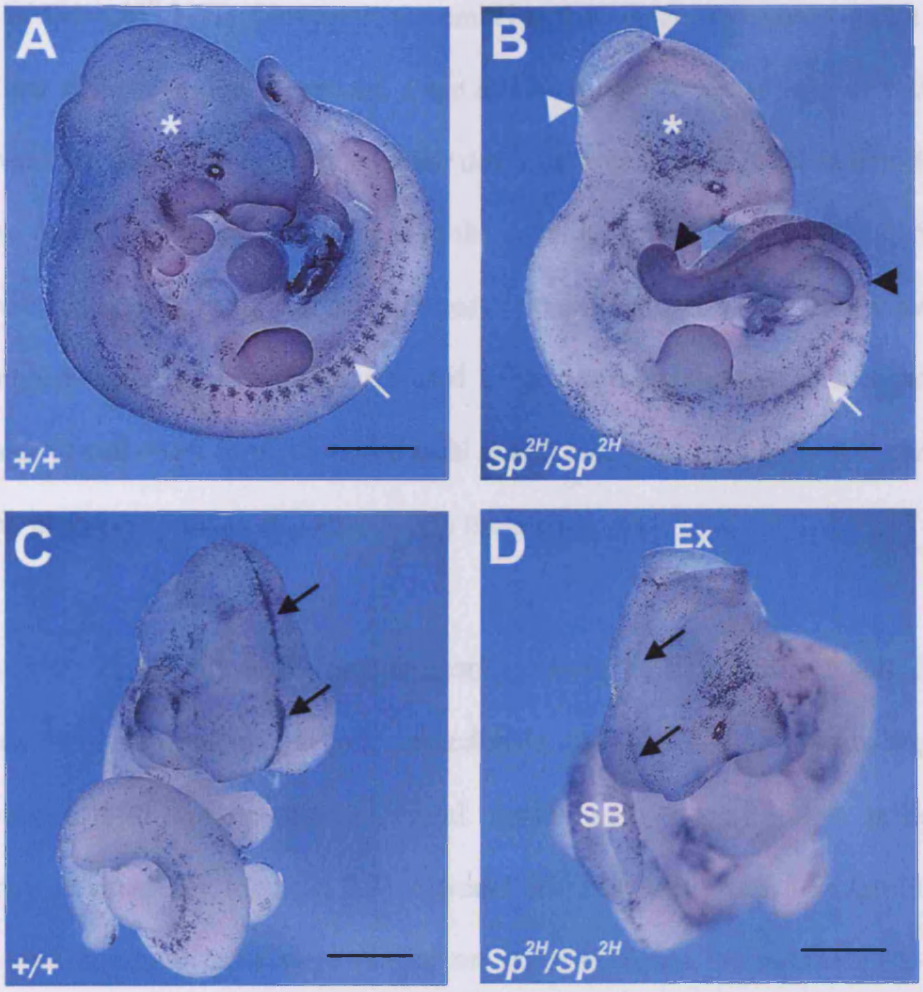

Figure 5.3 Whole mount TUNEL on E10.5 *Splotch*^{2H} embryos

Wild type (**A**, **C**) and homozygous mutant (**B**, **D**) embryos underwent whole mount TUNEL, with positive cells stained purple. *Sp*^{2H}/*Sp*^{2H} embryos exhibit exencephaly (Ex, in **D**; the region of open cranial neural tube is flanked by white arrowheads, **B**) and/or spina bifida (SB, in **D**; the region of open caudal neural tube is flanked by black arrowheads, **B**). There appears to be an increased level of apoptosis in the cranial mesenchyme of homozygous embryos compared to wild type littermates (asterix in **B** and **A**). The defined patterns of apoptotic cells observed in the somites (white arrow in **A**) and along the fused forebrain neural tube (black arrows in **C**) of wild type embryos are lost in homozygous embryos (white arrow in **B** and black arrows in **D**). This figure represents data from at least 5 embryos of each genotype. Scale bars represent 500 μm.

factor in *Splotch*^{2H} NTD. However, the embryos that underwent whole mount TUNEL had either reached a developmental stage at which cranial neural tube closure should have been completed or were at an earlier developmental age. In order to detect whether changes in cell death may play a role in the development of cranial NTD in *Splotch*^{2H} embryos it is necessary to analyse embryos temporally closer to the closure events. An immunohistochemical approach was used to generate quantitative data regarding the incidence of cell death in relation to cranial neural tube closure in *Splotch*^{2H} embryos. In parallel, proliferation was also analysed in these embryos.

Litters from *Splotch*^{2H} heterozygous matings were collected at E9 and E9.5 and embryos at developmental stages immediately prior to (13-15 somite-stages) and following (18-20 somite-stages) cranial neural tube closure were prepared for immunohistochemistry (Section 2.7). Coronal sections were taken through the cranial region and alternate pairs were placed on separate slides for immunohistochemical analysis of apoptosis (anti-activated caspase 3 antibody) and proliferation (anti-phosphorylated histone H3 antibody) as described in Section 2.7.

The first section in which distinct branchial arches were present was used as a landmark and labelled section 3. One section from the next two pairs dorsally (sections 2 and 1) were also photographed for further analysis (Figure 5.4). The number of labelled cells in the neuroepithelium of each of the three sections were counted and added to give the total number of labelled cells. The area of the neuroepithelium was measured on each section using Openlab 4.0.4 (Improvision) (Figure 5.4). The mean measurement for

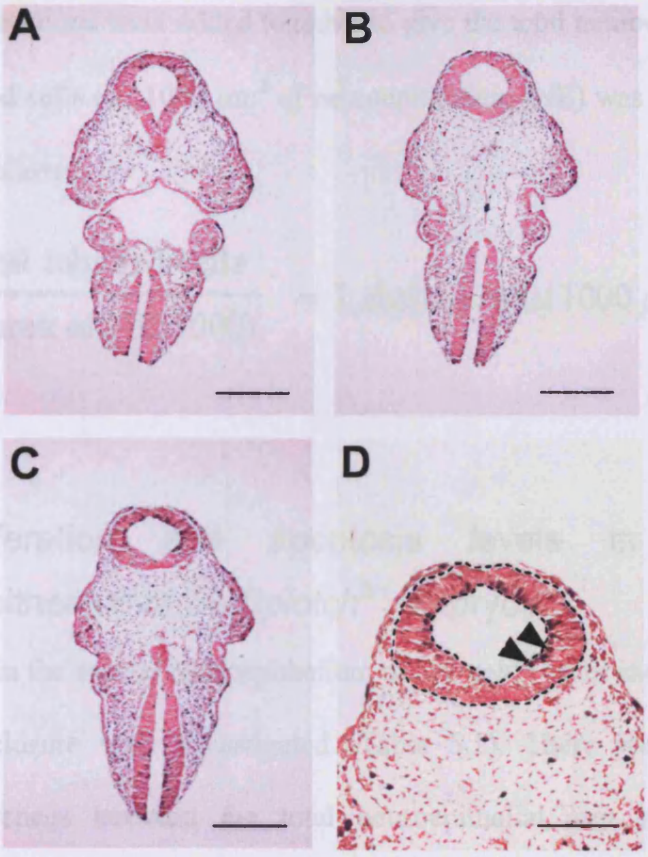

Figure 5.4 Analysis of apoptosis and proliferation in the cranial neuroepithelium of *Splotch*^{2H} embryos.

Alternate pairs of coronal sections were taken through the cranial region of *Splotch*^{2H} embryos and underwent immunohistochemistry with an antibody against phosphorylated histone H3 (**A-D**) or activated caspase 3. Sections used to quantify levels of proliferation are shown in panels **A-C**, with a higher magnification view of C in panel **D**. Equivalent sections were used for quantification of apoptosis. The first section showing distinct branchial arches (**A**) was labelled section 3 and used as a landmark to ensure comparisons between embryos were carried out at the same axial level. Additional sections used were the 4th and 8th sections dorsal to section 3 (**B** and **C** respectively). Labelled cells (arrowheads in **D**) were counted and the area of neuroepithelium was measured on each section (dotted line in **D**) in order to calculate the number of labelled cells/1000 μm^2 of neuroepithelium for each embryo. Scale bars represent 200 μm (**A-C**) or 100 μm (**D**).

each of the three sections were added together to give the total neuroepithelial area. The number of labelled cells per 1000 μm^2 of neuroepithelium (NE) was then calculated for each embryo as follows:

$$\frac{\text{No. total labelled cells}}{(\text{total area of NE}/1000)} = \text{Labelled cells}/1000\ \mu\text{m}^2\ \text{NE}$$

5.2.3 Proliferation and apoptosis levels in the cranial neuroepithelium of E9 *Splotch^{2H}* embryos

Apoptosis levels in the cranial neuroepithelium of *Splotch^{2H}* embryos immediately prior to neural tube closure were investigated (Table 5.1). There were no statistically significant differences between the total neuroepithelial area measured between embryos of the different *Splotch^{2H}* genotypes (tested by one-way ANOVA, Table 5.1). Although the *Sp^{2H}/Sp^{2H}* group did have non-significantly larger neuroepithelial areas than the other two genotypes this may be due to slight differences in the angle of the sections. When the number of labelled cells/1000 μm^2 neuroepithelium were compared between the *Splotch^{2H}* genotypes, a trend was immediately apparent (Table 5.1, Figure 5.5). The results suggest that there is an increase in apoptosis in *Sp^{2H}/Sp^{2H}* embryos compared to *Sp^{2H}*/+ which in turn exhibit higher levels of apoptosis compared to +/+ embryos. However, the differences between the genotype groups do not reach a statistically significant level (tested by one-way ANOVA).

Embryo No	mean NE area μm^2 ± SEM	Total NE area μm^2	Total no. labelled cells	labelled cells/1000 μm^2 NE
+/+				
1	14680.4 ± 2663.2	44041.1	1	**0.02**
2	13720.3 ± 364.9	14460.9	7	**0.17**
3	-	-	-	-
Sp^{2H}/+				
4	29653.7 ± 348.5	59307.5	0	**0.00**
5	12437.2 ± 336.5	37311.6	23	**0.62**
6	11241.8 ± 1081.6	33725.4	7	**0.21**
Sp^{2H}/*Sp*^{2H}				
7	15804.0 ± 2132.8	47412.0	1	**0.02**
8	19101.3 ± 525.7	57304.0	2	**0.03**
9	34480.0 ± 1452.8	68960.1	17	**0.25**
10	35317.2 ± 7723.7	105951.5	45	**0.42**
11	21071.9 ± 4868.6	63215.8	62	**0.98**

SUMMARY

Splotch^{2H} Genotype	No. of embryos	No. of sections	mean NE area (μm^2 ± SEM)	mean labelled cells /1000 μm^2 NE ± SEM
+/+	2	6	42601.0 ± 1440	0.095 ± 0.08
Sp^{2H}/+	3	8	43448.2 ± 7997	0.277 ± 0.18
Sp^{2H}/*Sp*^{2H}	5	14	68568.7 ± 10002	0.340 ± 0.18

Table 5.1 Anti-activated caspase 3 antibody labelling in the neuroepithelium of E9 *Splotch*^{2H} embryos

For each embryo, the mean neuroepithelial area (± SEM) of the sections analysed, and the total neuroepithelium area in μm^2 for each embryo (the sum of the mean neuroepithelial areas for each section) were measured. The total number of labelled cells in the sections investigated for each embryo were counted and used to calculate the number of labelled cells/1000 μm^2 of neuroepithelium. Some measurements/counts could not be made due to damaged sections. A summary of the data giving the mean values for embryos of each *Splotch*^{2H} genotype is given. There were no significant differences between the genotype groups for either the mean area of neuroepithelium measured or the number of labelled cells/1000 μm^2 NE (tested by one-way ANOVA). Abbreviation: NE, neuroepithelium.

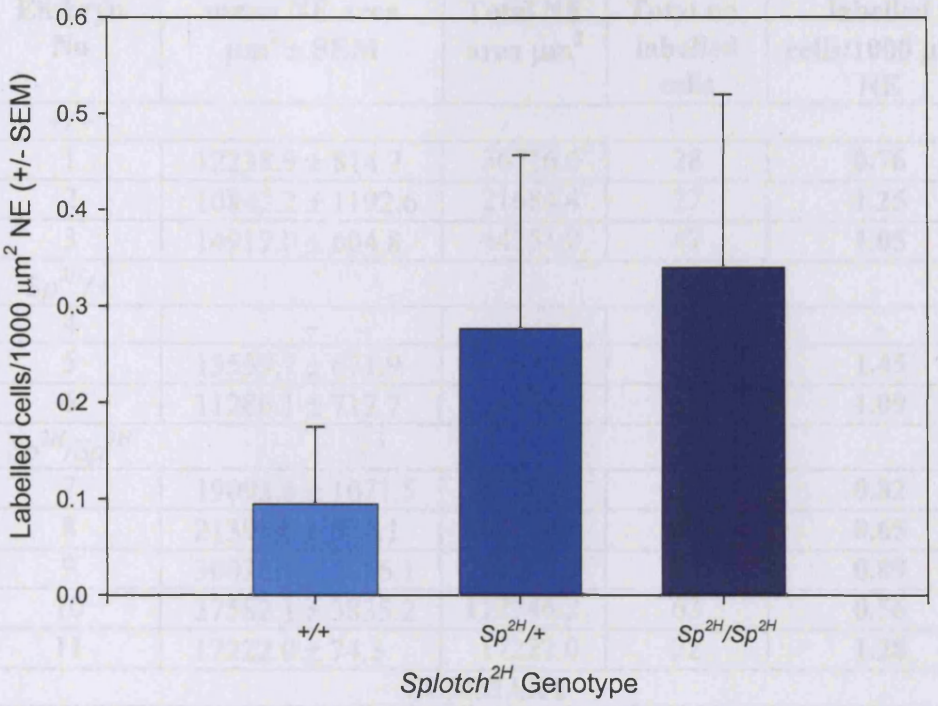

Figure 5.5 Apoptosis in the neuroepithelium of E9 *Splotch*^{2H} embryos.

The mean number of cells labelled with anti-activated caspase 3 antibody in the studied region of cranial neuroepithelium of *Splotch*^{2H} embryos was calculated and normalised to area of neuroepithelium. There are no statistically significant differences between the number of labelled cells/1000 μm^2 of neuroepithelium across the genotypes (tested by one-way ANOVA).

In sections that underwent immunohistochemistry with antibodies raised against phosphorylated histone H3 (Table 5.2) the neuroepithelial area for the *Sp*^{2H}/*Sp*^{2H} group was slightly larger than that of the other two genotype groups. However, there were no statistically significant differences between the different genotypes for the mean total neuroepithelial area (tested by one-way ANOVA, Table 5.2). This corresponds with the

Embryo No	mean NE area $\mu m^2 \pm$ SEM	Total NE area μm^2	Total no. labelled cells	labelled cells/1000 μm^2 NE
+/+				
1	12238.9 ± 814.7	36716.6	28	**0.76**
2	10842.2 ± 1192.6	21684.4	27	**1.25**
3	14917.0 ± 604.8	44751.0	47	**1.05**
Sp^{2H}/+				
4	-	-	-	-
5	13559.7 ± 671.9	40679.2	59	**1.45**
6	11286.1 ± 717.7	33858.2	37	**1.09**
Sp^{2H}/*Sp*^{2H}				
7	19093.6 ± 1071.5	57280.9	47	**0.82**
8	21391.6 ± 514.1	64174.7	42	**0.65**
9	30028.7 ± 1156.1	90086.1	80	**0.89**
10	37582.1 ± 3835.2	112746.2	63	**0.56**
11	17222.0 ± 74.3	17222.0	22	**1.28**

SUMMARY

Splotch^{2H} Genotype	No. of embryos	No. of sections	mean NE area ($\mu m^2 \pm$ SEM)	mean labelled cells /1000 μm^2 NE ± SEM
+/+	3	8	34384.0 ± 6760	1.02 ± 0.14
Sp^{2H}/+	2	6	37268.7 ± 3411	1.27 ± 0.18
Sp^{2H}/*Sp*^{2H}	5	13	68302.0 ± 16121	0.84 ± 0.13

Table 5.2 Anti-phosphorylated histone H3 antibody labelling in the neuroepithelium of E9 *Splotch*^{2H} embryos

For each embryo, the mean neuroepithelial area (± SEM) of the sections analysed, and the total neuroepithelium area in μm^2 for each embryo (the sum of the mean neuroepithelial areas for each section) were measured. The total number of labelled cells in the sections investigated for each embryo were counted and used to calculate the number of labelled cells/1000 μm^2 of neuroepithelium. Some measurements/counts could not be made due to damaged sections. A summary of the data giving the mean values for embryos of each *Splotch*^{2H} genotype is given. There were no significant differences between the genotype groups for either the mean area of neuroepithelium measured or the number of labelled cells/1000 μm^2 NE (tested by one-way ANOVA). Abbreviation: NE, neuroepithelium.

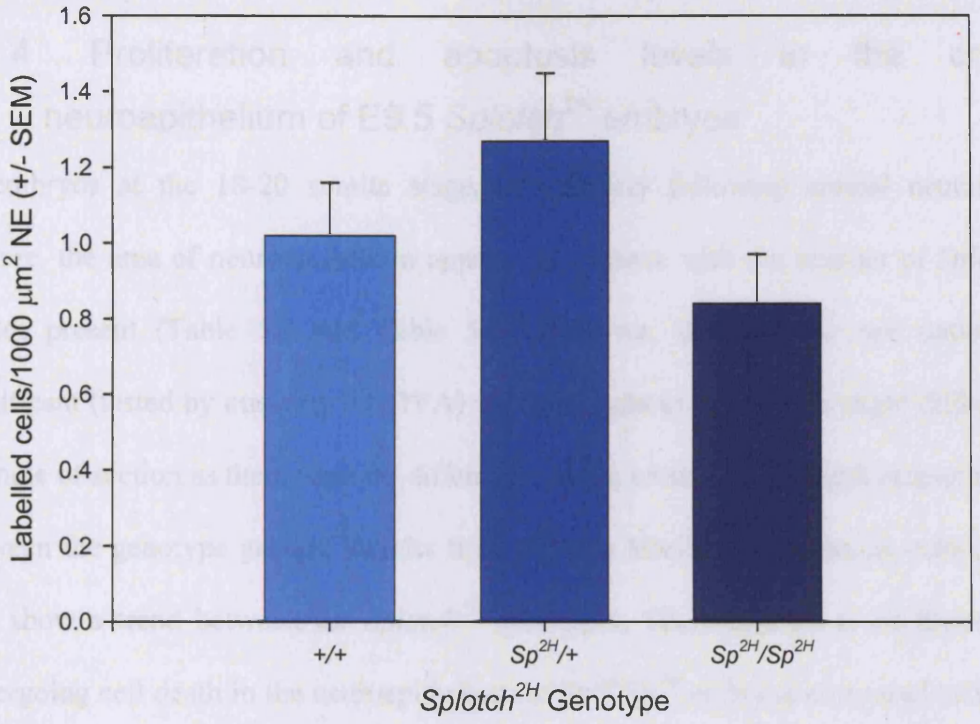

Figure 5.6 Proliferation in the neuroepithelium of E9 *Splotch*^{2H} embryos.

The mean number of cells labelled with anti-phosphorylated histone H3 antibody in the cranial neuroepithelium of *Splotch*^{2H} embryos was calculated and normalised to area of neuroepithelium. There were no statistically significant differences between the number of labelled cells/1000 μm^2 of neuroepithelium across the genotypes (tested by one-way ANOVA).

data collected for the sections used to investigate apoptosis in these embryos (Table 5.1). In addition, there were no differences in the number of labelled cells/1000 μm^2 of neuroepithelium between the *Splotch*^{2H} genotypes (Table 5.2, Figure 5.6).

5.2.4 Proliferation and apoptosis levels in the cranial neuroepithelium of E9.5 *Splotch^{2H}* embryos

In embryos at the 18-20 somite stage, immediately following cranial neural tube closure, the area of neuroepithelium appears to increase with the number of *Splotch^{2H}* alleles present (Table 5.3 and Table 5.4). However, this trend is not statistically significant (tested by one-way ANOVA) and is thought to result from slight differences in angle of section as there were no differences in the crown-rump length measurements between the genotype groups. Results from sections labelled for apoptotic cells (Table 5.3) show a trend between the *Splotch^{2H}* genotypes. There appears to be fewer cells undergoing cell death in the neuroepithelium of *Sp^{2H}/Sp^{2H}* embryos compared to *Sp^{2H}*/+ and +/+ embryos. However, the differences between the genotypes among E9.5 embryos are not statistically significant (tested by one-way ANOVA, Table). This trend is in contrast to the pattern observed in *Splotch^{2H}* embryos immediately prior to cranial neural tube closure (Table 5.1).

Analysis of phosphorylated-histone H3 positive cells in the neuroepithelium at this later stage of development showed that the number of labelled cells per area of neuroepithelium was comparable between the genotypes (Table 5.4). These findings suggest that there are no differences between the levels of proliferation in the cranial neuroepithelium in *Splotch^{2H}* embryos of different genotypes (Table 5.4, Figure 5.8).

Embryo No.	mean NE area μm^2 ± SEM	Total NE area μm^2	Total no. labelled cells	labelled cells/1000 μm^2 NE
+/+				
1	15746.8 ± 997.3	47240.3	16	**0.34**
2	21116.1 ± 800.7	63348.4	26	**0.41**
3	35360.3 ± 9174.6	106080.8	111	**1.05**
Sp^{2H}/+				
4	27249.2 ± 1224.1	81747.8	137	**1.68**
5	19432.5 ± 817.5	58297.5	8	**0.14**
6	20295.0 ± 1366.6	60884.9	17	**0.28**
7	37090.4 ± 5807.2	111271.1	12	**0.11**
8	35443.7 ± 1029.1	106331.1	91	**0.86**
9	19712.4 ± 2910.6	59137.0	5	**0.08**
10	45625.4 ± 509.9	136876.1	27	**0.20**
11	23960.7 ± 2222.1	71882.0	2	**0.03**
12	18887.0 ± 1490.2	56661.0	50	**0.88**
13	19498.8 ± 3173.8	58496.3	45	**0.77**
Sp^{2H}/*Sp*^{2H}				
14	28329.9 ± 5099.6	84989.6	5	**0.06**
15	61730.8 ± 5683.7	185192.4	56	**0.30**
16	-	-	-	-

SUMMARY

Splotch^{2H} Genotype	No. of embryos	No. of sections	mean NE area (μm^2 ± SEM)	mean labelled cells /1000 μm^2 NE ± SEM
+/+	3	9	72223.2 ± 17555	0.60 ± 0.23
Sp^{2H}/+	10	29	80158.5 ± 8977	0.50 ± 0.17
Sp^{2H}/*Sp*^{2H}	2	6	135091.0 ± 50101	0.18 ± 0.12

Table 5.3 Anti-activated caspase 3 antibody labelling in the neuroepithelium of E9.5 *Splotch*^{2H} embryos

For each embryo the mean neuroepithelial area (± SEM) of the sections analysed, and the total neuroepithelium area in μm^2 for each embryo (the sum of the mean neuroepithelial areas for each section) were measured. The total number of labelled cells in the sections investigated for each embryo were counted and used to calculate the number of labelled cells/1000 μm^2 of neuroepithelium. Some measurements/counts could not be made due to damaged sections. A summary of the data giving the mean values for embryos of each *Splotch*^{2H} genotype is given. There were no significant differences between the genotype groups for either the mean area of neuroepithelium measured or the number of labelled cells/1000 μm^2 NE (tested by one-way ANOVA). Abbreviation: NE, neuroepithelium.

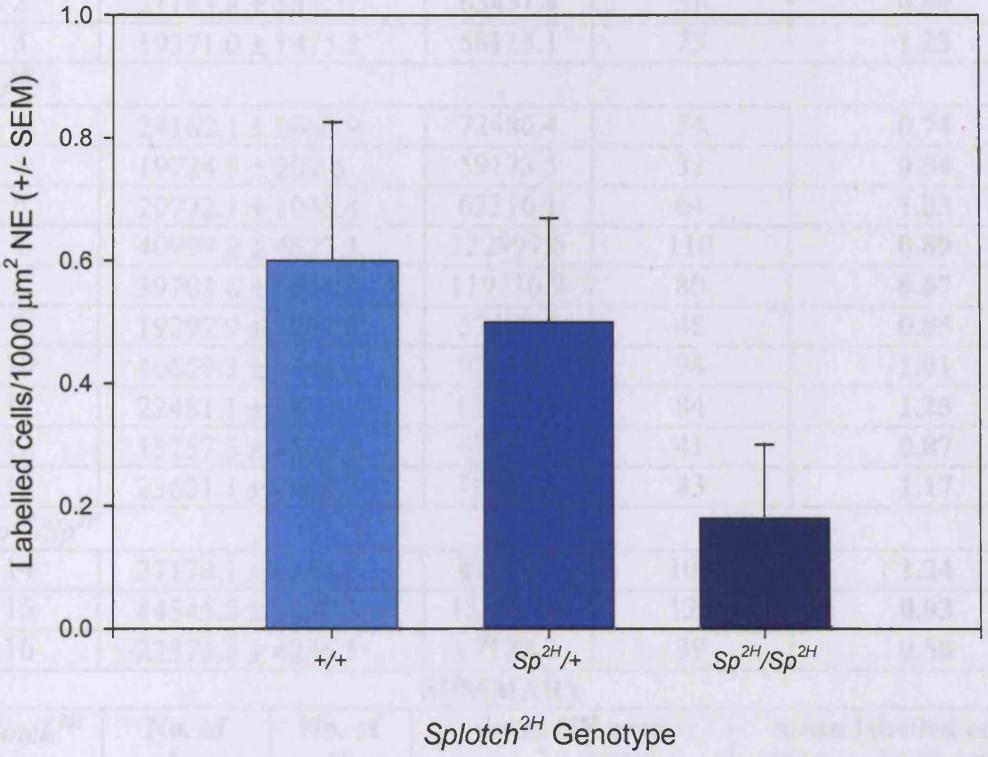

Figure 5.7 Apoptosis in the neuroepithelium of E9.5 *Splotch*^{2H} embryos.

The number of cells labelled with anti-activated caspase 3 antibody in the cranial neuroepithelium of *Splotch*^{2H} embryos was calculated and normalised to area of neuroepithelium. There were no statistically significant differences between the number of labelled cells/1000 μm^2 of neuroepithelium across the genotypes (tested by one-way ANOVA).

Embryo No.	mean NE area μm^2 ± SEM	Total NE area μm^2	Total no. labelled cells	labelled cells/1000 μm^2 NE
+/+				
1	18263.2 ± 1154.8	54789.6	38	**0.69**
2	21143.8 ± 588.7	63431.4	51	**0.80**
3	19371.0 ± 1975.2	58113.1	73	**1.23**
Sp^{2H}/+				
4	24162.1 ± 2669.9	72486.4	54	**0.74**
5	19724.5 ± 209.6	59173.5	32	**0.54**
6	20772.1 ± 1035.4	62316.1	64	**1.03**
7	40999.2 ± 4627.1	122997.6	110	**0.89**
8	39703.6 ± 1064.1	119110.9	80	**0.67**
9	19292.9 ± 3237.0	57878.7	48	**0.85**
10	46659.3 ± 1946.3	93318.6	94	**1.01**
11	22481.1 ± 281.9	67443.3	84	**1.25**
12	15757.3 ± 3392.2	47272.1	41	**0.87**
13	23621.1 ± 4413.1	70863.4	83	**1.17**
Sp^{2H}/*Sp*^{2H}				
14	27170.1 ± 1354.8	81510.3	101	**1.24**
15	44545.8 ± 7070.3	133637.4	124	**0.93**
16	22376.2 ± 4286.5	67128.8	39	**0.58**

SUMMARY

Splotch^{2H} Genotype	No. of embryos	No. of sections	mean NE area (μm^2 ± SEM)	mean labelled cells /1000 μm^2 NE ± SEM
+/+	3	9	58778.0 ± 2516	0.91 ± 0.17
Sp^{2H}/+	10	29	63031.6 ± 10569	0.90 ± 0.07
Sp^{2H}/*Sp*^{2H}	3	9	94092.2 ± 20204	0.92 ± 0.19

Table 5.4 Anti-phosphorylated histone H3 antibody labelling in the neuroepithelium of E9.5 *Splotch*^{2H} embryos

For each embryo the mean neuroepithelial area (± SEM) of the sections analysed, and the total neuroepithelium area in μm^2 for each embryo (the sum of the mean neuroepithelial areas for each section) were measured. The total number of labelled cells in the sections investigated for each embryo were counted and used to calculate the number of labelled cells/1000 μm^2 of neuroepithelium. Some measurements/counts could not be made due to damaged sections. A summary of the data giving the mean values for embryos of each *Splotch*^{2H} genotype is given. There were no significant differences between the genotype groups for either the mean area of neuroepithelium measured or the number of labelled cells/1000 μm^2 NE (tested by one-way ANOVA). Abbreviation: NE, neuroepithelium.

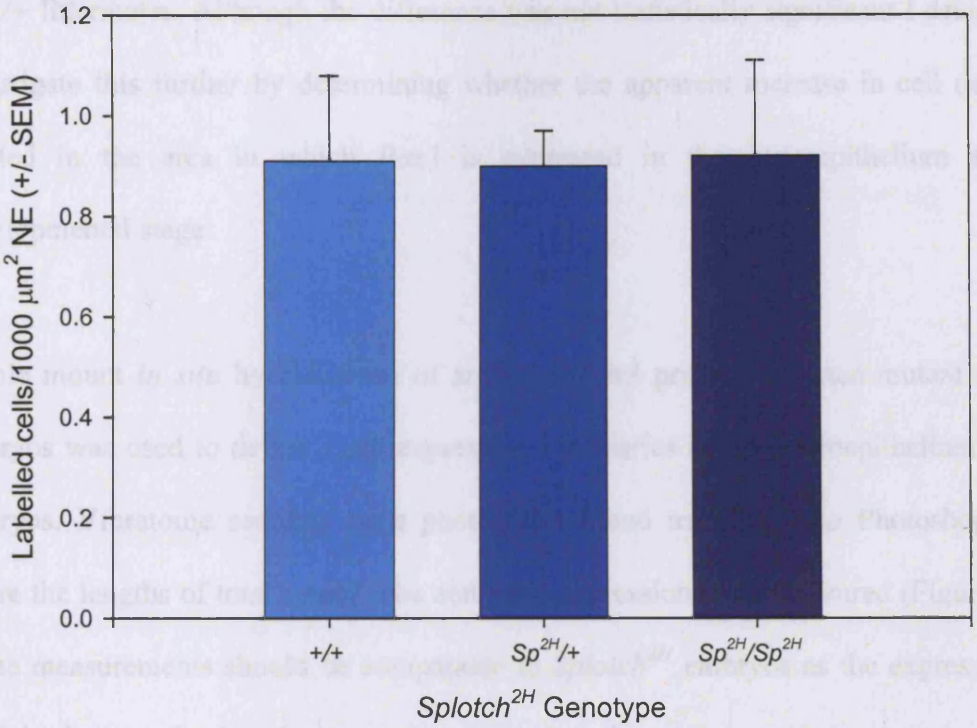

Figure 5.8 Proliferation in the neuroepithelium of E9.5 *Splotch*^{2H} embryos.

The mean number of cells labelled with anti-phosphorylated histone H3 antibody in the cranial neuroepithelium of *Splotch*^{2H} embryos was calculated and normalised to area of neuroepithelium. There were no statistically significant differences between the number of labelled cells/1000 µm^2 of neuroepithelium across the genotypes (tested by one-way ANOVA).

5.2.5 Method for quantitative analysis of apoptosis in the *Pax3* expression domain of the cranial neuroepithelium in E9 *Splotch*^{2H} embryos

Results in Section 5.2.3 suggested that there may be an increase in the number of cells undergoing apoptosis in the cranial neuroepithelium of E9 *Sp*^{2H}/*Sp*^{2H} embryos compared

to +/+ littermates. Although the difference was not statistically significant I decided to investigate this further by determining whether the apparent increase in cell death is located in the area in which *Pax3* is expressed in the neuroepithelium at this developmental stage.

Whole mount *in situ* hybridisation of antisense *Pax3* probes with non-mutant mouse embryos was used to define *Pax3* expression boundaries in the neuroepithelium in E9 embryos. Vibratome sections were photographed and transferred to Photoshop v6.0 where the lengths of total neural tube and Pax3 expression were measured (Figure 5.9). These measurements should be comparable to *Splotch^{2H}* embryos as the expression of *Pax3* in the neural tube of homozygous *Splotch* embryos is apparently normal and has been shown not to differ from that of wild type littermates (Dickman *et al.*, 1999).

The extent of *Pax3* expression in the neuroepithelium of four embryos was used as guidance for the analysis in *Splotch^{2H}* embryos (Table 5.5, Figure 5.9). There was some variation in the *Pax3* expression limit between the embryos investigated. Therefore, the boundaries were defined by the regions that were *Pax3* positive and negative in all the embryos (Table 5.5). The *Pax3* positive expression boundary in the neuroepithelium was defined in the dorsal region (0.38 of the total neuroepithelial length). The *Pax3* negative region was the ventral half of the neural tube (0.50 of the total neuroepithelial length). The region between these two domains was labelled the overlap zone and represented the region of the neural tube in which cells from different embryos were positive or negative for *Pax3*. Cells located in this area were excluded from this study.

	Proportion of NT length expressing *Pax3*		**Proportion of NT length not expressing *Pax3***	
Side of Neural tube	LHS	RHS	LHS	RHS
Embryo 1	0.48	0.47	0.52	0.53
Embryo 2	0.47	0.49	0.53	0.51
Embryo 3	0.40	0.39	0.60	0.61
Embryo 4	0.48	0.49	0.52	0.51
Estimated proportion limit	0.38		0.50	

Table 5.5 *Pax3* expression in coronal sections through the cranial region of E9 embryos

Measurements were made to establish the extent of *Pax3* expression in E9 mouse embryos. After whole mount *in situ* hybridisation the length of neural tube expressing *Pax3* was measured as a proportion of the total neural tube length (Figure 5.9). A value below the smallest proportion for each domain was used as the limit for which I was confident that *Pax3* is, or is not, expressed. Abbreviations: LHS, left hand side; RHS, right hand side; NT, neural tube.

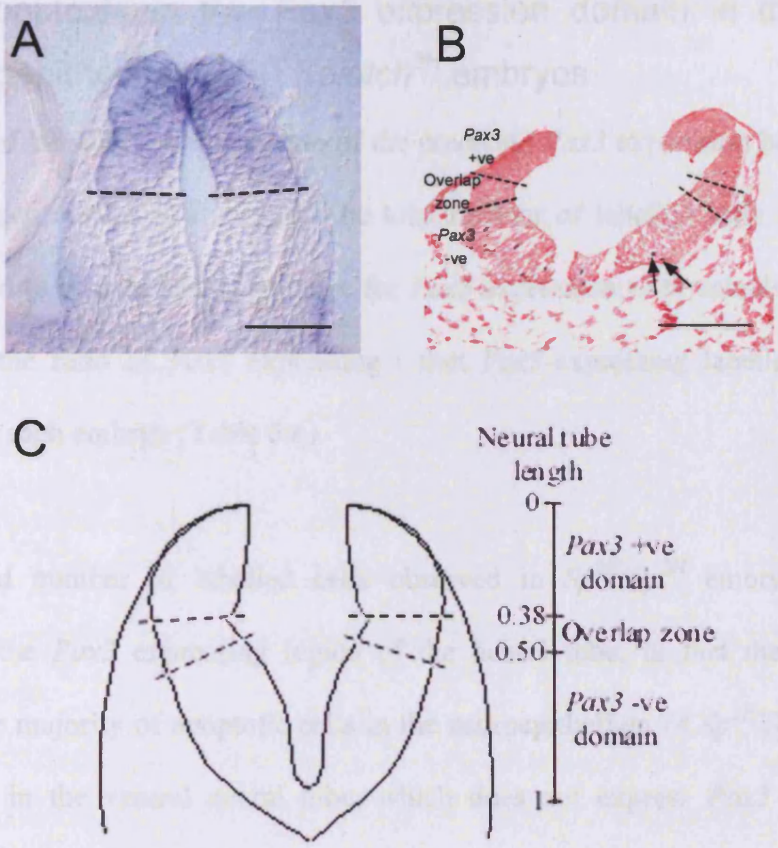

Figure 5.9 *Pax3* expression boundaries in the neural tube of E9 mouse embryos.

Measurements of coronal sections through the cranial region of E9 mouse embryos after whole mount *in situ* hybridisation with *Pax3* probe (Table 5.5) were used to define the *Pax3* expression boundary. The extent of *Pax3* expression (blue/purple staining and dotted lines in **A**) was measured as a proportion of the neural tube length. The smallest proportions of *Pax3*-expression and non-*Pax3* expression along the neural tube were used to define a *Pax3* positive domain and a *Pax3* negative domain, the area in between is described as the overlap zone (**C**). These boundaries were used to calculate probable *Pax3* expression domains for the E9 *Splotch*^{2H} sections that had undergone immunohistochemistry with anti-activated caspase 3 antibody (**B**). Labelled cells (arrows in **B**) were counted in the *Pax3* positive and negative domains. Scale bars represent 100 μm.

5.2.6 Apoptosis in the *Pax3* expression domain in the cranial neuroepithelium of E9 *Splotch^{2H}* embryos

The number of labelled cells each side of the predicted *Pax3* expression boundary was counted on each section (Table 5.6). The total number of labelled cells in areas that were predicted to be positive or negative for *Pax3* expression were calculated for each embryo and the ratio of *Pax3* expressing : non *Pax3*-expressing labelled cells was calculated for each embryo (Table 5.6).

The increased number of labelled cells observed in Sp^{2H}/Sp^{2H} embryos was not restricted to the *Pax3* expressing region of the neural tube; in fact the opposite is observed. The majority of apoptotic cells in the neuroepithelium of Sp^{2H}/Sp^{2H} embryos were located in the ventral neural tube, which does not express *Pax3* (Table 5.6). However, in $Sp^{2H}/+$ embryos the opposite effect is seen with the majority of cell death occurring in the *Pax3* expressing region of the neuroepithelium. The location of cells undergoing apoptosis in wild type embryos is similar to homozygous embryos, that is the majority of cell death occurs in the ventral neural tube.

Embryo No.	Total no. of labelled cells	Labelled cells in *Pax3* +ve domain	Labelled cells in *Pax3* -ve domain	Labelled cells in overlap zone	*Pax3* +ve / *Pax3* -ve
+/+					
1	1	0	1	0	0/1
2	7	1	6	0	1/6
Sp^{2H}/+					
3	0	0	0	0	0/0
4	23	19	3	1	19/3
5	7	5	1	1	5/1
Sp^{2H}/Sp^{2H}					
6	1	0	1	0	0/1
7	2	2	0	0	2/0
8	17	2	13	2	2/13
9	45	3	39	3	3/39
10	62	5	54	3	5/54

Table 5.6 Apoptosis in the neuroepithelium of E9 *Splotch*^{2H} embryos with regard to *Pax3* expression

The number of labelled cells in the *Pax3* positive (+ve) domain and *Pax3* negative (–ve) domains (as defined in Section 5.2.6) of cranial neuroepithelium in embryos prior to neural tube closure.

5.3 DISCUSSION

At E8.5, the developmental stage preceding cranial neural tube closure, there were no changes in the number or distribution of TUNEL-positive cells observed in Sp^{2H}/Sp^{2H} embryos compared to wild type littermates. However by E9.5, when cranial neural tube closure should have been completed, differences in the pattern of apoptotic cells were observed. Interestingly, an increase in the number of TUNEL-positive cells was observed in the cranial mesenchyme of E9.5 and E10.5 *Splotch*^{2H} homozygous embryos compared to wild type embryos. Increased apoptosis in the cranial mesenchyme has been suggested to be responsible for the incidence of exencephaly exhibited by *Cart-1*

mice (Zhao *et al.*, 1996). However, the increase in cell death in the cranial mesenchyme of *Splotch^{2H}* homozygous embryos was not detected prior to neural tube closure (E8.5) and so could be unrelated or secondary to failure of the neural tube to close. Therefore, it would be interesting to see if this increase in apoptosis is present in *Sp^{2H}/Sp^{2H}* embryos that do not develop exencephaly (all *Sp^{2H}/Sp^{2H}* embryos studied in this chapter exhibited exencephaly). However, as *Pax3* is not expressed in the cranial mesenchyme and is believed to act in a cell autonomous manner in the neuroepithelium (Mansouri *et al.*, 2001) this was not investigated further in this study.

The pattern of TUNEL-positive cells at E10.5 also shows differences between the *Splotch^{2H}* genotypes. The lack of labelled cells that I observed at the midline of the fused neural tube in the forebrain/midbrain has been described previously in E10.5 *Splotch^{2H}* embryos in which no apoptotic cells were observed in fused regions of the entire neural tube (Phelan *et al.*, 1997). The normal cell death in this area is believed to facilitate cell reorganisation after fusion has occurred. In contrast, it does not appear to be necessary for fusion to occur, as shown by the fact that the area of neural tube in which this line of apoptotic cells is missing has already completed closure. As discussed in Section 1.6.2.3, apoptosis is believed to be necessary for cranial neurulation to occur. There appears to be two roles for apoptosis in the process of cranial neurulation, firstly the correct regulation of apoptosis in the neuroepithelium and cranial mesenchyme may be essential for the apposition and fusion of the neural folds, as indicated by mouse NTD models in which apoptosis is misregulated resulting in either increased or decreased levels of apoptosis in the neuroepithelium or the cranial mesenchyme (Section 1.6.2.3, Table 1.1). The second role of apoptosis is the reorganisation along the

midline following fusion. The results in this thesis suggest this process is not essential for the closure of the forebrain region during cranial neurulation.

The somites of E10.5 *Sp^{2H}/Sp^{2H}* embryos also exhibited differences in the pattern of TUNEL-positive cells compared to wild type littermates. *Pax3* is expressed in the dermomyotome (Goulding *et al.*, 1991), and is believed to regulate the structural organisation of the somites (Mansouri *et al.*, 2001). *Splotch^{2H}* homozygous mutant embryos exhibit disturbed somite boundaries (Henderson *et al.*, 1999;Schubert *et al.*, 2001) and, it is therefore perhaps not surprising that the pattern of cell death in the somites of *Sp^{2H}/Sp^{2H}* embryos differs from that of wild type littermates .

If excess apoptosis is responsible for the development of NTD in *Sp^{2H}/Sp^{2H}* embryos we would expect to see changes in the number of TUNEL-positive cells before or during neural tube closure. However, changes in TUNEL-positive cell distribution in the cranial region of homozygous *Splotch^{2H}* embryos were only observed after closure should have been completed (E9.5). Therefore, analysis of embryos at developmental stages closer to the time of cranial neural tube closure was used in the subsequent experiments.

Immediately prior to cranial neural tube closure (13-15 somite-stage) embryos showed a trend towards increased apoptosis in the cranial neuroepithelium with the number of mutant *Pax3* alleles present, whereas the opposite trend was observed in slightly older embryos at the 18-20 somite stage. However, in neither case did the differences between the genotypes reach statistical significance suggesting that the observed variation may

not be biologically relevant. The finding of opposite effects at two temporally close stages also supports this idea.

Pax3 acts in a cell autonomous manner in the neural tube (Mansouri *et al.*, 2001). Therefore, if the loss of *Pax3* function resulted in the induction of apoptosis we would expect to observe increased cell death in the *Pax3*-expressing area of the neuroepithelium of homozygous mutant embryos compared to wild type littermates. Further experiments investigating the location of cells undergoing cell death in relation to *Pax3* expression were thus used as a more sensitive measurement of the effect of loss of *Pax3* function on apoptosis levels. There was no increase in the number of activated caspase-3 positive cells in the *Pax3*-expressing area of the cranial neuroepithelium in E9 homozygous Sp^{2H}/Sp^{2H} embryos compared to wild type and heterozygous littermates in which the neural tube closes. These findings suggest that cranial NTD in *Splotch*^{2H} mutants is not induced by excess apoptosis in response to reduced *Pax3* function.

Additional experiments carried out in our laboratory support these results. If excess apoptosis was responsible for the production of exencephaly in *Splotch*^{2H} embryos, direct inhibition of this process should potentially rescue the NTD. *Splotch*^{2H} embryos were cultured throughout the period of neural tube closure, E8.5-E10, in the presence of the caspase inhibitor Z-VAD-FMK (Van Noorden, 2001). In contrast to the expected rescue effect of this treatment, an increased incidence of exencephaly was observed in Sp^{2H}/Sp^{2H} embryos exposed to Z-VAD-FMK compared to PBS treated controls. Moreover, a low incidence of exencephaly was observed in heterozygous embryos which would normally complete cranial neural tube closure (N.D.E. Greene, Personal

communication). These results further suggest that excess apoptosis is not the cause of exencephaly in *Sp*^{2H}/*Sp*^{2H} embryos.

Previous studies in which it was suggested that NTD in *Splotch* embryos are a result of excess apoptosis have all used the *Splotch* mouse model, a different *Splotch* variant to the one used in this chapter. The different *Splotch* alleles can result in production of different proteins with variation in the functional domains that are present, leading to the possibility that *Pax3* in different *Splotch* variants act in different ways (Section 1.10.1). Therefore, the functional capability of alleles in certain pathways may differ and should not be assumed to be the same for *Splotch* and *Splotch*^{2H}. The effects of the *Splotch* and *Splotch*^{2H} mutations on the functional capability of the resultant Pax3 protein is unclear, both are thought to result in null proteins. It is possible that there could be some residual function, particularly in *Splotch*^{2H} mice as the paired box domain of the Pax3 protein is not affected by the 32 base pair deletion and has been shown to have independent binding ability in *in vitro* studies (Chalepakis *et al.*, 1994). Alternatively, if both mutations do result in null proteins, differences in the genetic background of the mice strains may account for differences between the *Splotch* alleles. Changing the genetic background has been shown to affect the phenotype penetrance in different mouse mutants, including *curly-tail* (Neumann *et al.*, 1994) and *Splotch*^{2H} (Fleming *et al.*, 2000).

Despite the differences in the *Splotch* alleles used in previous studies and the current study, our results, which suggest that excess apoptosis is not the cause of NTD in *Splotch*^{2H} embryos, is likely to hold true for all *Splotch* variants. For example, the

analysis of apoptosis in *Splotch* embryos in the previous studies have all been carried out at E10.5, a developmental stage after cranial neural tube closure should have been completed (Phelan *et al.*, 1997;Pani *et al.*, 2002). Therefore, the increased levels of apoptosis observed in these studies could be secondary to the failure of the neural tube to complete closure rather than directly causative. Moreover, previous studies have not indicated an excess of apoptosis in the neural tube in the absence of *Pax3* expression. For example, some Pax3-mediated responses have been shown to be cell type specific. In a study using chimeric embryos, *Pax3*-deficiency in cells of the lateral dermomyotome induced excess apoptosis, whereas, this effect was not detected in *Pax3*-deficient cells of the neural tube (Mansouri *et al.*, 2001). In addition, excess apoptosis was observed in newly formed somites of *Splotch* mutant embryos but not in the neural tube or mature somites (Borycki *et al.*, 1999).

The structure of the Pax3 protein allows specific binding to a large array of DNA sequences, permitting Pax3 to function in the activation or repression of a broad spectrum of genes involved in a variety of pathways (Machado *et al.*, 2001). Pax3 can act as a transcriptional repressor as well as an activator (Machado *et al.*, 2001). Inactivation of *p53* by transcriptional repression has been shown to be mediated by Pax2, Pax5 and Pax8 but not Pax3 (Stuart *et al.*, 1995) suggesting that Pax3 is unlikely to suppress apoptosis via the repression of *p53*. Therefore the rescue effect observed on the *Splotch* NTD phenotype by intercrosses with *p53* knockout mutants (Pani *et al.*, 2002) could be acting through a different pathway than apoptosis.

In addition to an anti-apoptotic role, Pax3 has also been suggested to play a role in regulating cell cycle progression and cell differentiation. The NTD phenotype of *Splotch* mutants could be postulated to arise from a disruption in these pathways. Therefore, in parallel with analysis of cell death, proliferation levels in *Splotch*^{2H} embryos were investigated in order to assess cell cycle progression in the neuroepithelium of mutant embryos. The proliferation levels did not differ between genotypes at either E9 or E9.5 stages, immediately prior to and following cranial neural tube closure. These results suggest that lack of *Pax3* function does not affect proliferation and therefore, cell cycle progression, in the neuroepithelium of *Splotch*^{2H} embryos during cranial neural tube closure.

Pax3 has been shown to play a role in maintaining an undifferentiated cell phenotype. For example, transfection of antisense *Pax3* RNA into an undifferentiated neuronal cell line led to cellular differentiation, suggesting that *Pax3* expression is necessary to maintain the undifferentiated phenotype (Reeves *et al.*, 1999). In addition, *Pax3* expression in Schwann cell precursors is downregulated immediately prior to terminal differentiation (Kioussi *et al.*, 1995) and the DNA-binding activity of Pax3 has also been shown to be rapidly downregulated during neuronal cell differentiation (Reeves *et al.*, 1998). Pax3 can also inhibit the differentiation of cultured myoblast cells (Epstein *et al.*, 1995) and adult melanocyte stem cell differentiation (Lang *et al.*, 2005). Therefore, it is possible that premature differentiation of cells in the neuroepithelium of *Splotch*^{2H} mutant embryos may be involved in the failure of the neural folds to complete closure.

A possible alternation in differentiation would also be consistent with the reported rescue of *Splotch* NTD in *p53/Splotch* double mutants (Pani *et al.*, 2002). The p53 protein is activated in response to stress signals and can result in cellular apoptosis, cell cycle arrest, senescence or cell differentiation (Vousden and Lu, 2002). It is possible that the rescue effect of *p53*-deficiency on the NTD phenotype of *Splotch* mutant embryos (Pani *et al.*, 2002) was mediated through an alternative function such as suppression of differentiation rather than through changes in apoptosis. Experiments carried out in this chapter did not detect any differences in the number of cells undergoing proliferation in the neuroepithelium of Sp^{2H}/Sp^{2H} embryos compared to wild type littermates which may suggest that misregulation of cell cycle checkpoint control is an unlikely candidate for the mode of NTD rescue by *p53*-deficiency. However, it is possible that loss of p53 function may rescue *Sp/Sp* NTD by causing a delay in cellular differentiation. A number of *in vitro* and *in vivo* assays have demonstrated that adding exogenous wild-type p53 to undifferentiated cells can result in progression from an undifferentiated to a more differentiated state (Almog and Rotter, 1997;Hall and Lane, 1997) and, as discussed earlier, *Pax3* has been shown to inhibit cell differentiation in some systems. Therefore, it could be hypothesised that *Sp/Sp* NTD are induced by premature cellular differentiation which could then be rescued by a delay in differentiation caused by p53-deficiency. Further work investigating cellular differentiation in both mouse models would be needed to test this possibility.

CHAPTER 6; DETECTION OF FOLATE CYCLE ABNORMALITIES IN CELL CULTURE BY THE DEOXYURIDINE MONOPHOSPHATE SUPPRESSION TEST

6.1 INTRODUCTION

The ability of peri-conceptional folic acid supplementation to prevent up to 70% of human NTD is generally accepted, although it is unclear how folates act to prevent the development of NTD. It is possible that folic acid supplementation may rescue some NTD by overcoming a defect in folate metabolism. In several cases it has been suggested that folate-responsive NTD mouse models have defects in folate metabolism (Section 1.10.2.2). For example, folate-binding protein 1 (*Folbp1)* null homozygous embryos, in which folate transport is limited, develop NTD if rescued from embryonic lethality by folic acid treatment (Piedrahita *et al.*, 1999). In addition, it has been suggested that *Pax3*-deficient Sp^{2H} homozygous embryos have impaired folate metabolism (Fleming *et al.*, 1998) (Section 1.10.1). Moreover, exposure of mouse embryos to valproic acid (VPA) induces NTD (Padmanabhan *et al.*, 2003) and the mode of teratogenic action for VPA has been proposed to include an effect on folate metabolism and homocysteine remethylation (Hishida and Nau, 1998).

In humans, folate deficiency is unlikely to be sufficient to cause NTD alone, but it is possible that a slight deficiency may be pathogenic when in association with a maternal or fetal metabolic abnormality in folate metabolism. Several folate-related risk factors for NTD have been identified (Section 1. 9) and there is additional evidence that impaired maternal folate metabolism may play a role in some NTD cases. For example, women who have had two previous pregnancies affected by NTD required a higher dietary folate intake to achieve the same 5-methyl tetrahydrofolate levels as control women (Lucock *et al.*, 1994), suggesting a defect in folate metabolism. There are obvious difficulties in studying folate metabolism in human embryos during

neurulation. So far only one study has used tissue arising from the early embryo itself to examine folate metabolism in relation to NTD. Habibzadeh and colleagues (1993) used trophoblast cells isolated from NTD-affected and unaffected (control) fetuses at 16-20 weeks of gestation. Cell culture experiments showed a delay in the incorporation of labelled 5-methyl tetrahydrofolate in NTD-affected samples compared to control samples. This lag in incorporation suggests a disturbance in uptake or utilisation of 5-methyl tetrahydrofolate and therefore a defect of folate metabolism in some of the NTD-derived samples (Habibzadeh *et al.*, 1993). However, although trophoblast cells are derived from the same embryonic tissue as the fetus they are specialised in that they undergo non-random X chromosome inactivation unlike other embryonic tissues (Hemberger, 2002). Therefore, there is still a need for direct analysis of folate metabolism in non-specialised embryonic tissues from NTD-affected pregnancies.

The aim of this study was to test the hypothesis that a defect in the metabolism of folate derivatives in the embryo is associated with the development of NTD. In order to detect a wide range of folate-related defects the deoxyuridine monophosphate (dUMP) suppression test was used (Figure 6.1). The dUMP suppression test analyses the ability of cells to provide the folate intermediate 5,10-methylene tetrahydrofolate (5,10-methylene THF) and, was established as an indicator of defective DNA metabolism in patients with megaloblastic anemia (Killmann, 1964). Impaired DNA metabolism in these patients is caused by an inadequate supply of 5,10-methylene THF, a substrate for the *de novo* pathway of pyrimidine biosynthesis. In these patients, a limited supply of 5,10-methylene THF indicates defective folate and/or vitamin B_{12} supply. The dUMP suppression test can also indicate efficacy of the folate cycle (Section 1.10.1), for

example dUMP suppression test scores of colonocytes from folate-deficient rats showed reduced suppression compared to folate-replete rats. Moreover, the reduction was rectified by the addition of folinic acid to the culture medium demonstrating the validity of dUMP suppression test as a measure of folate status (Cravo *et al.*, 1991). Traditionally the dUMP suppression test was applied to bone marrow suspension cultures, however, it has also been adapted for use in whole embryo culture (Fleming *et al.*, 1998).

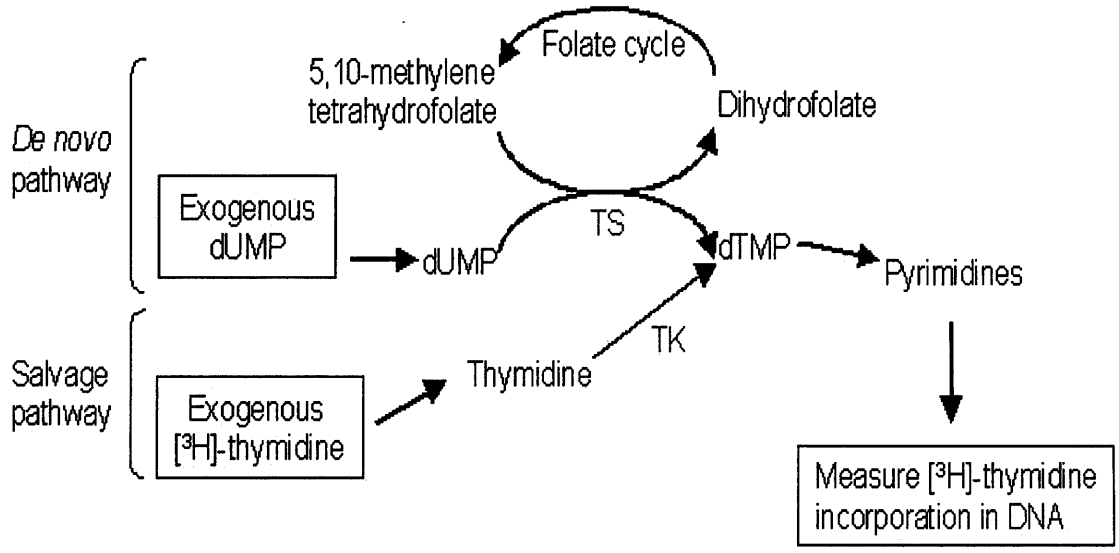

Figure 6.1 The deoxyuridine suppression test

Manipulation of the *de novo* and salvage pathways in pyrimidine biosynthesis are used to detect abnormalities in folate metabolism. The incorporation of exogenous [^{3}H]-thymidine into DNA via the salvage pathway is measured. Exogenous dUMP drives the folate cycle, producing pyrimidines via the *de novo* pathway and thereby suppressing the incorporation of [^{3}H]-thymidine into DNA. The ability of dUMP to suppress [^{3}H]-thymidine incorporation is reduced when the folate cycle is impaired. Abbreviations; TS, thymidylate synthase; TK, thymidine kinase; dUMP, deoxyuridine monophosphate; dTMP, deoxythymidine monophosphate.

In this chapter, the dUMP suppression test has been adapted for use with embryonic fibroblast cells derived from human fetuses. Three groups of samples have been collected; cells from fetuses with NTD (NTD samples), normal fetuses (normal controls) and fetuses with malformations other than NTD (affected controls). Fibroblastic cell lines were established from foetal skin, cartilage, umbilical cord or amniotic fluid samples by the Cytogenetics Department at Great Ormond Street Hospital. Parameters for cell number, test duration and reagent concentrations were initially established. Inhibitors of the folate and methylation cycle were then used in order to test whether the dUMP suppression test can detect abnormalities in folate metabolism in cell culture using these parameters. Aminopterin, 5-fluorouracil and cycloleucine inhibit folate and methionine metabolism at different points of the cycle (Figure 6.2) and so allow analysis of the sensitivity of the dUMP suppression test.

The uracil analogue, 5-fluorouracil, produces an active metabolite, 5-fluorodeoxyuridine monophosphate, that is a tight-binding inhibitor of thymidylate synthase (TS) and therefore can inhibit the conversion of dUMP to deoxythymidine monophosphate (dTMP) (Figure 6.2) (Myers *et al.*, 1975). Aminopterin is a folate-analogue that once transported into the cell is polyglutamated and subsequently binds to dihydrofolate reductase (DHFR), inhibiting its activity and thus the conversion of dihydrofolate to tetrahydrofolate (Figure 6.2) (McGuire, 2003). Cycloleucine is an inhibitor of methionine adenosyltransferase (MAT), the methylation cycle enzyme that mediates the conversion of methionine to S-adenosylmethionine (Figure 6.2) (Lombardini *et al.*, 1970).

Figure 6.2 A simplified diagram of the folate and methylation cycles

Inhibitors and their site of action are shown in pink. Key enzymes are in blue and the exogenous agents utilised in the dUMP suppression test are shown in green.

Abbreviations: AP, aminopterin; Cyclo, cycloleucine; DHF, dihydrofolate; DHFR, dihydrofolate reductase; dUMP, deoxyuridine monophosphate; dTMP, deoxythymidine monophosphate; FU, 5-fluorouracil; MAT, methionine adenosyltransferase; SAH, S-adenosylhomocysteine; SAM, S-adenosylmethionine; THF, tetrahydrofolate; TS, thymidylate synthase.

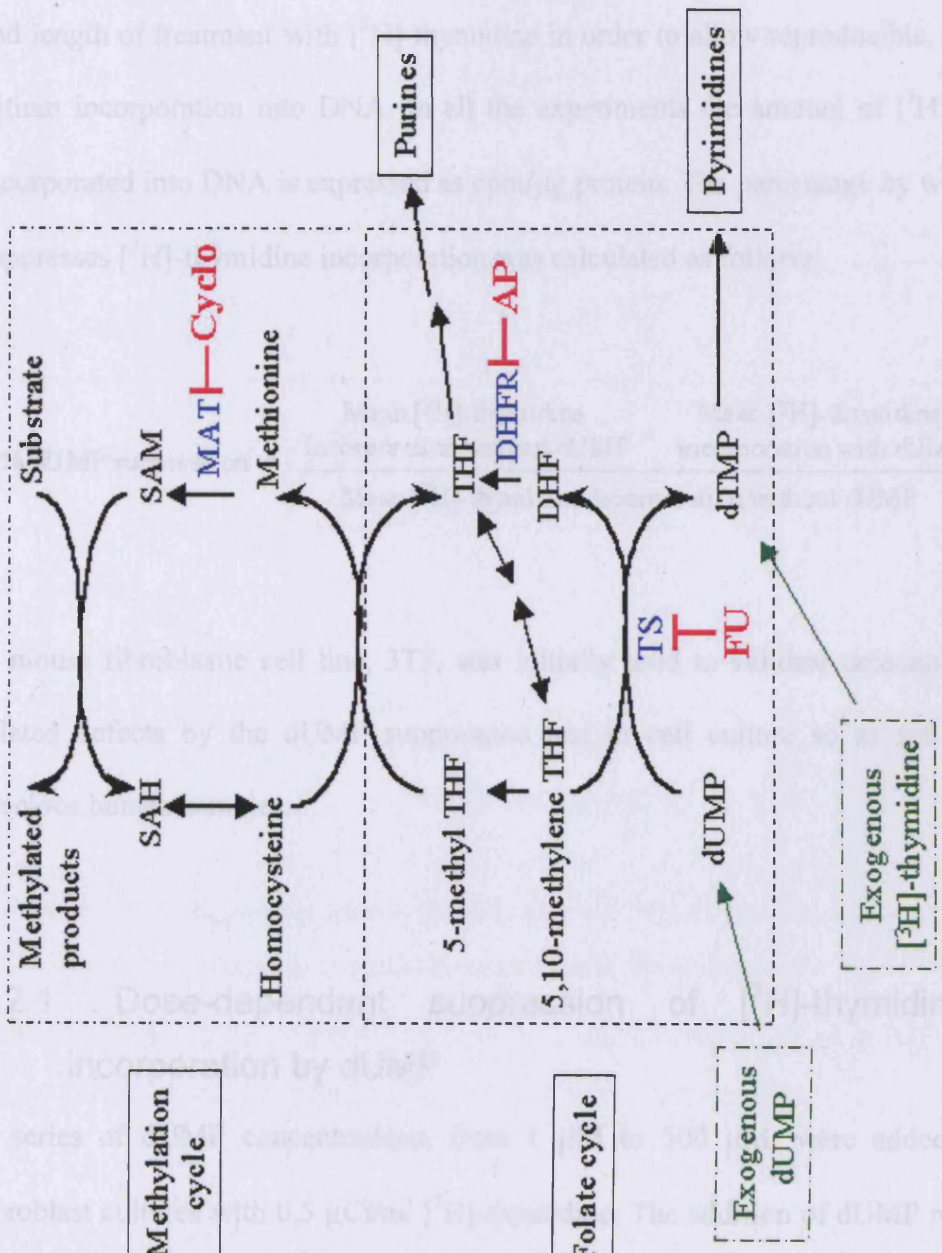
Purines
Pyrimidines
Substrate
SAM
MAT
Cyclo
Methionine
THF
DHFR
AP
DHF
dTMP
TS
FU
Methylated products
SAH
Homocysteine
5-methyl THF
5,10-methylene THF
dUMP
Exogenous [3H]-thymidine
Exogenous dUMP
Methylation cycle
Folate cycle

6.2 RESULTS

Initial tests were designed to establish parameters for cell number, and concentration and length of treatment with [^{3}H]-thymidine in order to allow reproducible, measurable tritium incorporation into DNA. In all the experiments the amount of [^{3}H]-thymidine incorporated into DNA is expressed as cpm/μg protein. The percentage by which dUMP suppresses [^{3}H]-thymidine incorporation was calculated as follows:

$$\% \text{ dUMP suppression} = \frac{\text{Mean [}^3\text{H]-thymidine incorporation without dUMP} - \text{Mean [}^3\text{H]-thymidine incorporation with dUMP}}{\text{Mean [}^3\text{H]-thymidine incorporation without dUMP}} \times 100$$

A mouse fibroblastic cell line, 3T3, was initially used to validate detection of folate-related defects by the dUMP suppression test in cell culture so as not to exhaust precious human samples.

6.2.1 Dose-dependant suppression of [^{3}H]-thymidine DNA incorporation by dUMP

A series of dUMP concentrations, from 1 μM to 500 μM, were added to mouse fibroblast cultures with 0.5 μCi/ml [^{3}H]-thymidine. The addition of dUMP resulted in a dose-dependent suppression of [^{3}H]-thymidine incorporation in mouse fibroblasts (Figure 6.3). The degree of suppression increases with dUMP concentration up to 50 μM when it reached a plateau of approximately 70% (data points at 500 μM are not

shown). These results show that exogenous dUMP can suppress the incorporation of exogenous [^{3}H]-thymidine into DNA in cultured mouse cells.

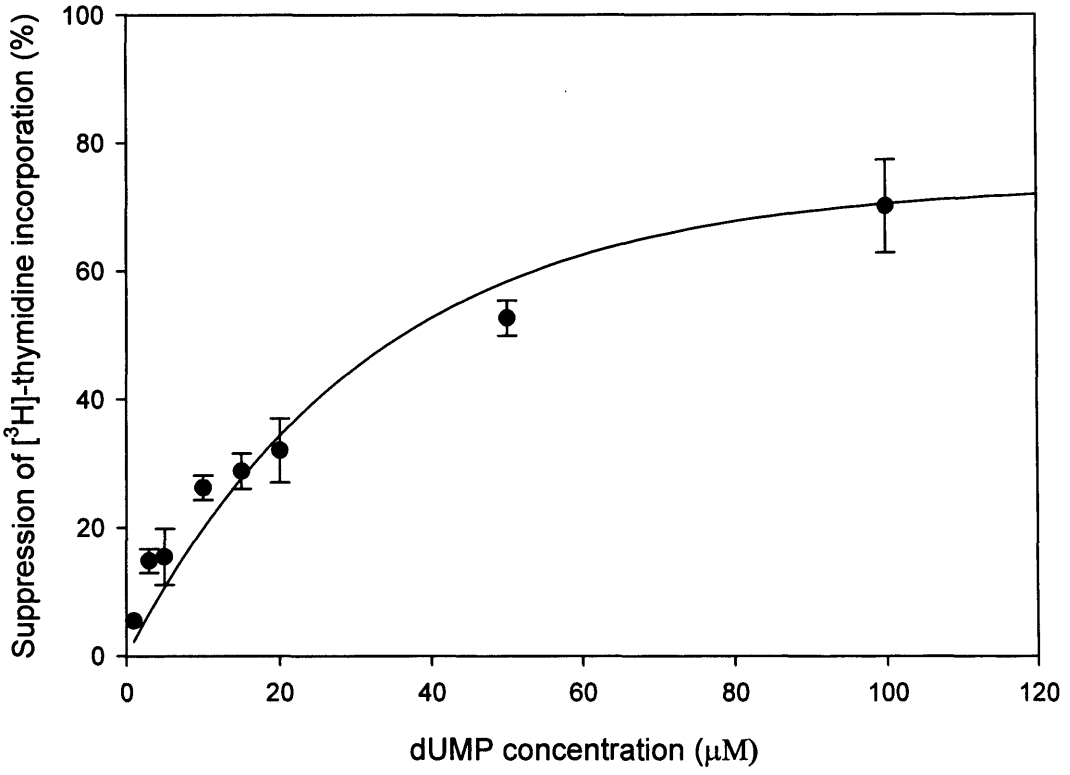

Figure 6.3 The dose-dependent suppression of [^{3}H]-thymidine incorporation into DNA by deoxyuridine monophosphate in mouse fibroblast cells

The magnitude of suppression increases with the concentration of dUMP used. Each data point represents the mean ± SEM from at least 3 experiments.

Concentrations of dUMP ranging from 1 μM to 500 μM are able to suppress the incorporation of [^{3}H]-thymidine into DNA in mouse embryonic fibroblast cells and this concentration range was therefore used with human normal control cells. As for mouse cells, a series of dUMP concentrations were added to human fibroblast cultures together

with [^{3}H]-thymidine. The addition of dUMP resulted in a dose-dependent suppression of [^{3}H]-thymidine incorporation into DNA in human fibroblasts (Figure 6.4). The degree of suppression increases with the dUMP concentration up to 50 μM when it reached a plateau of approximately 80% (data points at 500 μM are not shown).

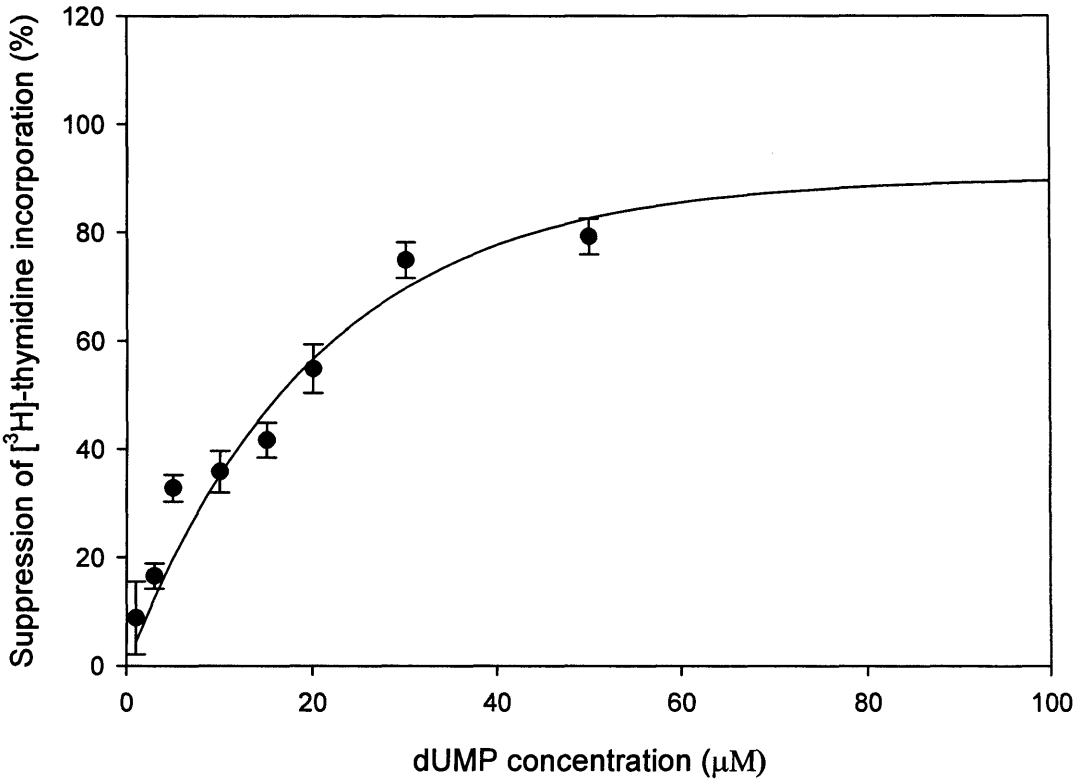

Figure 6.4 Dose-dependent suppression of [^{3}H]-thymidine incorporation into DNA by deoxyuridine monophosphate in human fibroblast cells

[^{3}H] thymidine incorporation into the DNA of human embryonic fibroblasts is suppressed by the presence of dUMP. The degree of suppression increases with the concentration of dUMP. Data points represent the mean ± SEM of at least three experiments.

Human embryonic fibroblast cells appear to be more sensitive to the dUMP suppression of [^{3}H]-thymidine incorporation than mouse embryonic fibroblasts. Lower doses of dUMP have a greater effect on [^{3}H]-thymidine incorporation in human cells than equivalent dUMP doses in mouse cells (compare Figure 6.3 to Figure 6.4).

6.2.2 Detection of impaired folate metabolism by the dUMP suppression test in mouse fibroblasts

Before the dUMP suppression test could be carried out on human samples an appropriate dose of dUMP for the test needed to be established. An appropriate dose would need to induce a large percentage suppression of [^{3}H]-thymidine incorporation but still allow detection of possible abnormalities in folate metabolism. Therefore initial inhibition studies with mouse fibroblasts were carried out using a series of dUMP concentrations (10 μM, 15 μM and 50 μM) and inhibitors of the folate or methylation cycles (Section 6.1). These studies showed that 10 μM dUMP was capable of inducing a relatively large suppression of [^{3}H]-thymidine incorporation but appeared to not be high enough to mask deficiencies in folate metabolism. In the subsequent inhibitor experiments with human normal control cells, this concentration of dUMP was therefore used.

6.2.2.1 Inhibition of [^{3}H]-thymidine incorporation into DNA by 5-fluorouracil

Previously 50 μM FU has been used to demonstrate that the dUMP suppression test can be used to assess folate status in rat colonic epithelium (Cravo *et al.*, 1991). Therefore, this concentration of FU was initially used to test the sensitivity of the dUMP

suppression test in mouse embryonic fibroblast cells. The total protein measured in samples cultured with 50 μM FU was noticeably lower than that of cultures with [^{3}H]-thymidine, with or without dUMP, suggesting that FU is toxic at this concentration. Lower concentrations of FU, 25 μM and 35 μM, did not affect the viability of cultures as indicated by total protein content and therefore these concentrations were used in this study.

The incorporation of [^{3}H]-thymidine into the DNA of mouse fibroblast cells was suppressed by dUMP in a dose-dependent manner as described previously (Section 6.2.1). Although 10 μM dUMP does not significantly suppress incorporation compared to cells treated with [^{3}H]-thymidine alone, 15 μM and 50 μM dUMP do cause significant suppression (Figure 6.5). Addition of 25 μM FU results in a statistically significant increase in the incorporation of tritium-labelled thymidine into DNA at all the dUMP concentrations tested, compared to cells treated with the equivalent dUMP dose alone (Figure 6.5). At the higher concentration (35 μM), FU significantly inhibited the dUMP mediated suppression of [^{3}H]-thymidine incorporation at 10 μM and 15 μM dUMP. Similar levels of [^{3}H]-thymidine incorporation were detected in all experiments that included the inhibitor, suggesting that 25 μM FU is sufficient to inhibit thymidylate synthase (Figure 6.5), resulting in increased incorporation of thymidine generated through the *de novo* pathway.

In human cells, 10 μM dUMP significantly suppressed the incorporation of [^{3}H]-thymidine compared to cells exposed to [^{3}H]-thymidine alone (Figure 6.6). The addition of FU at a concentration of 25 μM eliminated the suppression of [^{3}H]-thymidine by

Figure 6.5 Inhibition of the dUMP mediated suppression of [^{3}H]-thymidine incorporation into DNA by 5-fluorouracil in mouse fibroblast cells.

Data is described as the percentage of [^{3}H]-thymidine incorporated into DNA with respect to the [^{3}H]-thymidine alone treatment, which is normalised to 100%. For each treatment, data is presented as mean ± SEM of three separate experiments. * indicates statistically significant variation from the thymidine alone treatment. ϕ indicates statistically significant variation from the equivalent thymidine plus dUMP treatment group ($p<0.05$ tested by one-way ANOVA followed by TUKEY test for pairwise comparisons).

Abbreviations: Thy, [^{3}H]-thymidine; dUMP, deoxyuridine monophosphate; FU, 5-fluorouracil.

Figure 6.6 Inhibition of the dUMP mediated suppression of [^{3}H]-thymidine incorporation into DNA by 5-fluorouracil in human fibroblast cells.

Data is described as the percentage of [^{3}H]-thymidine incorporated into DNA with respect to the [^{3}H]-thymidine alone treatment, which is normalised to 100%. For each treatment, data is presented as mean ± SEM of three separate experiments. * indicates statistically significant variation from the thymidine alone treatment. ϕ indicates statistically significant variation from the thymidine plus dUMP treatment group ($p<0.05$ tested by t-test).

.Abbreviations: Thy, [^{3}H]-thymidine; dUMP, deoxyuridine monophosphate; FU, 5-fluorouracil.

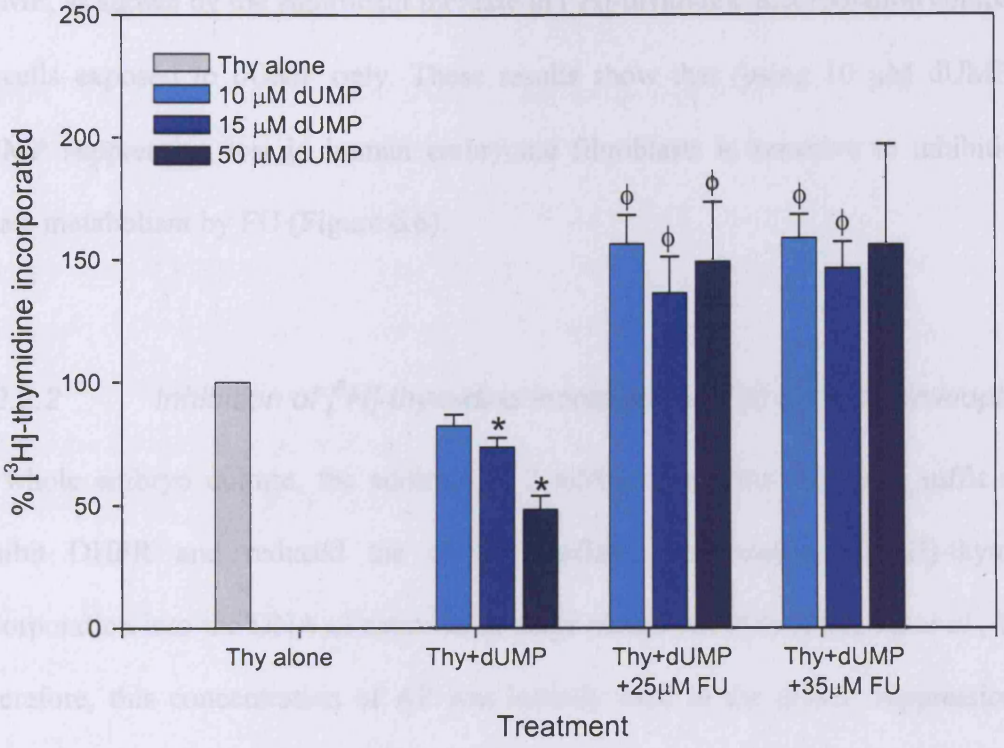
Thy alone
10 μM dUMP
15 μM dUMP
50 μM dUMP
% [3H]-thymidine incorporated
250
200
150
100
50
0
*
*
ϕ
ϕ
ϕ
ϕ
ϕ
Thy alone
Thy+dUMP
Thy+dUMP +25μM FU
Thy+dUMP +35μM FU
Treatment

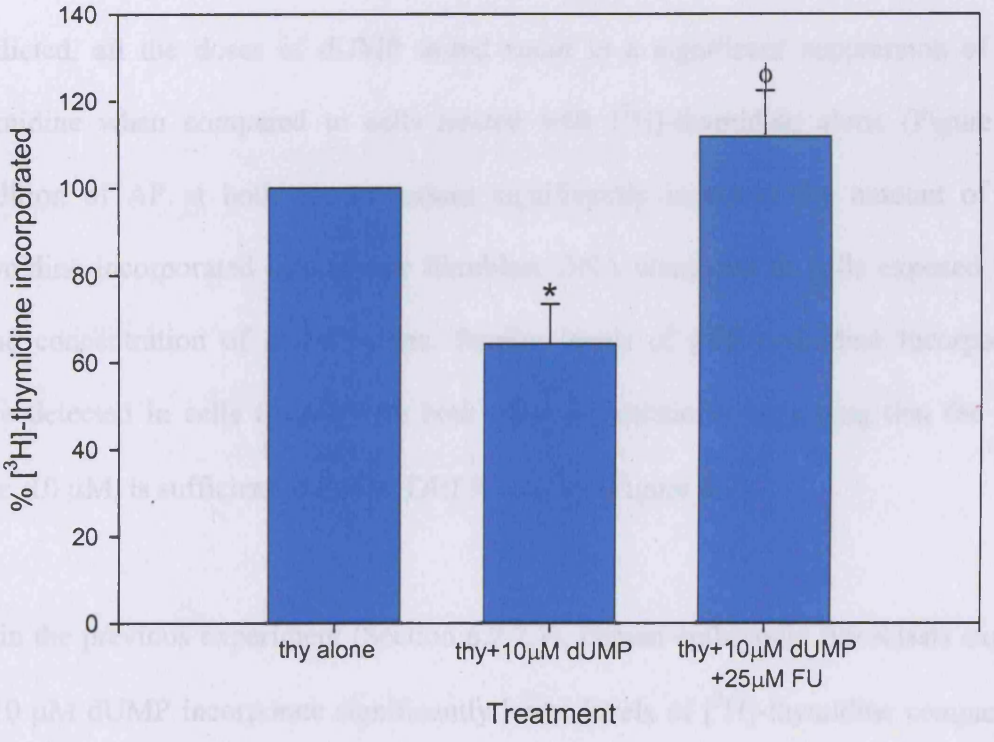
% [3H]-thymidine incorporated
140
120
100
80
60
40
20
0
*
ϕ
thy alone
thy+10μM dUMP
thy+10μM dUMP +25μM FU
Treatment

dUMP, as shown by the significant increase in [^{3}H]-thymidine incorporation compared to cells exposed to dUMP only. These results show that (using 10 μM dUMP) the dUMP suppression test in human embryonic fibroblasts is sensitive to inhibition of folate metabolism by FU (Figure 6.6).

6.2.2.2 Inhibition of [^{3}H]-thymidine incorporation into DNA by aminopterin

In whole embryo culture, the addition of 2 mM aminopterin (AP) was sufficient to inhibit DHFR and reduced the dUMP mediated suppression of [^{3}H]-thymidine incorporation into the DNA of neurulation-stage mouse embryos (Fleming *et al.*, 1998). Therefore, this concentration of AP was initially used in the dUMP suppression test with mouse embryonic fibroblast cells. However, this concentration was cytotoxic and so lower doses of 10 μM and 100 μM AP were used in further experiments. As predicted, all the doses of dUMP tested result in a significant suppression of [^{3}H]-thymidine when compared to cells treated with [^{3}H]-thymidine alone (Figure 6.7). Addition of AP at both concentrations significantly increases the amount of [^{3}H]-thymidine incorporated into mouse fibroblast DNA compared to cells exposed to the same concentration of dUMP alone. Similar levels of [^{3}H]-thymidine incorporation were detected in cells treated with both AP concentrations suggesting that the lower dose, 10 μM, is sufficient to inhibit DHFR activity (Figure 6.7).

As in the previous experiment (Section 6.2.2.1), human embryonic fibroblasts exposed to 10 μM dUMP incorporate significantly lower levels of [^{3}H]-thymidine compared to those exposed to [^{3}H]-thymidine alone (Figure 6.8). Addition of 10 μM AP appears to

Figure 6.7 Inhibition of the dUMP mediated suppression of [^{3}H]-thymidine incorporation into DNA by aminopterin in mouse fibroblast cells.

Data is described as the percentage of [^{3}H]-thymidine incorporated into DNA with respect to the [^{3}H]-thymidine alone treatment, which is normalised to 100%. For each treatment, data is presented as mean ± SEM of at least three separate experiments. * indicates statistically significant variation from the thymidine alone treatment. ϕ indicates statistically significant variation from the equivalent thymidine plus dUMP treatment group ($p<0.05$ tested by one-way ANOVA followed by TUKEY test for pairwise comparisons).

Abbreviations: Thy, [^{3}H]-thymidine; dUMP, deoxyuridine monophosphate; AP, aminopterin.

Figure 6.8 Inhibition of the dUMP mediated suppression of [^{3}H]-thymidine incorporation into DNA by aminopterin in human fibroblast cells.

Data is described as the percentage of [^{3}H]-thymidine incorporated into DNA with respect to the [^{3}H]-thymidine alone treatment, which is normalised to 100%. For each treatment, data is presented as mean ± SEM of three separate experiments. * indicates statistically significant variation from the thymidine alone treatment. ϕ indicates statistically significant variation from the thymidine plus dUMP treatment group ($p<0.05$ tested by t-test).

Abbreviations: Thy, [^{3}H]-thymidine; dUMP, deoxyuridine monophosphate; AP, aminopterin.

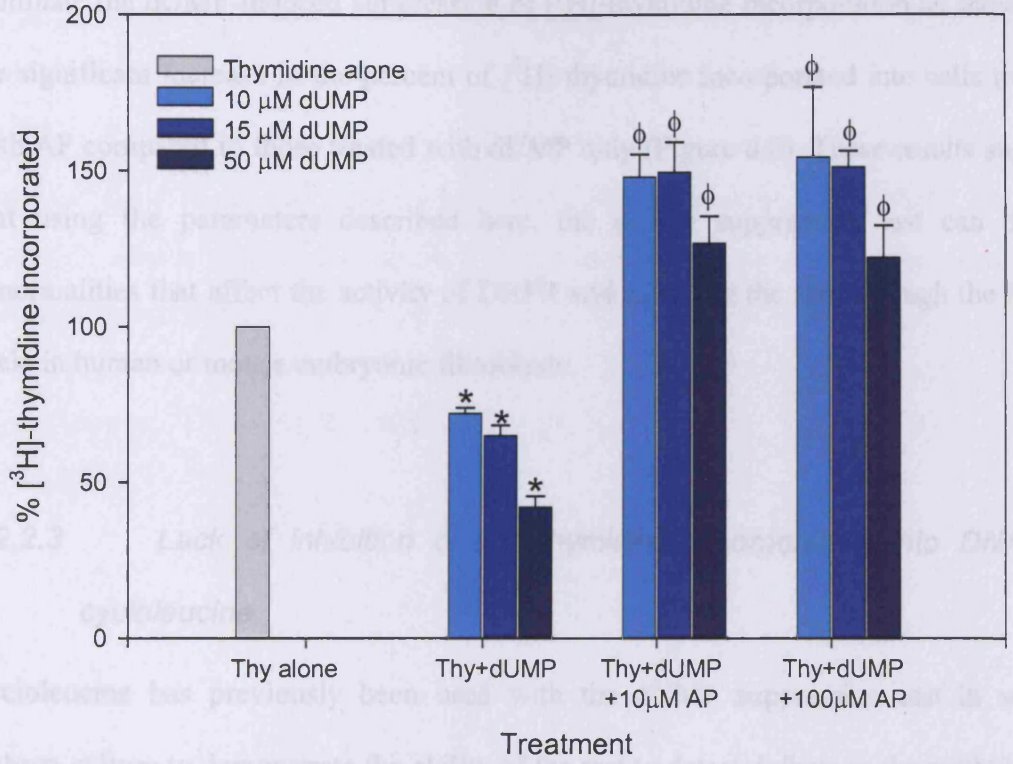
200
150
100
50
0
% [3H]-thymidine incorporated
Thymidine alone
10 μM dUMP
15 μM dUMP
50 μM dUMP
Thy alone
Thy+dUMP
Thy+dUMP +10μM AP
Thy+dUMP +100μM AP
Treatment

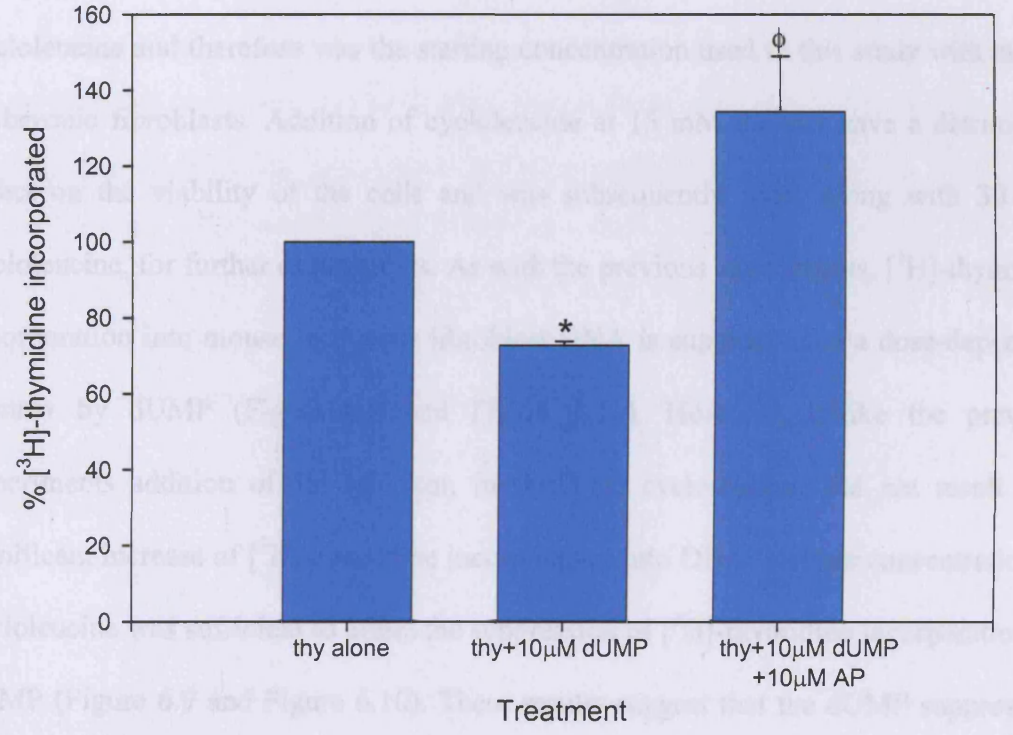
160
140
120
100
80
60
40
20
0
% [3H]-thymidine incorporated
thy alone
thy+10μM dUMP
thy+10μM dUMP +10μM AP
Treatment

eliminate the dUMP-induced suppression of [^{3}H]-thymidine incorporation as shown by the significant increase in the percent of [^{3}H]-thymidine incorporated into cells treated with AP compared to those treated with dUMP only (Figure 6.8). These results suggest that using the parameters described here, the dUMP suppression test can detect abnormalities that affect the activity of DHFR and therefore the flux through the folate cycle in human or mouse embryonic fibroblasts.

6.2.2.3 Lack of inhibition of [^{3}H]-thymidine incorporation into DNA by cycloleucine

Cycloleucine has previously been used with the dUMP suppression test in whole embryo culture to demonstrate the ability of the test to detect defects in the methylation cycle (Fleming *et al.*, 1998). The concentration used in that study was 15 mM cycloleucine and therefore was the starting concentration used in this study with mouse embryonic fibroblasts. Addition of cycloleucine at 15 mM did not have a detrimental effect on the viability of the cells and was subsequently used, along with 30 mM cycloleucine, for further experiments. As with the previous experiments, [^{3}H]-thymidine incorporation into mouse or human fibroblast DNA is suppressed in a dose-dependent manner by dUMP (Figure 6.9 and Figure 6.10). However, unlike the previous experiments addition of the inhibitor, in this case cycloleucine, did not result in a significant increase of [^{3}H]-thymidine incorporation into DNA. Neither concentration of cycloleucine was sufficient to affect the suppression of [^{3}H]-thymidine incorporation by dUMP (Figure 6.9 and Figure 6.10). These results suggest that the dUMP suppression test, with the parameters described, is unable to detect abnormalities in the methylation cycle in human or mouse embryonic fibroblasts.

Figure 6.9 Lack of inhibition of the dUMP mediated suppression of [^{3}H]-thymidine incorporation into DNA by cycloleucine in mouse fibroblast cells.

Data is described as the percentage of [^{3}H]-thymidine incorporated into DNA with respect to the [^{3}H]-thymidine alone treatment, which is normalised to 100%. For each treatment, data is presented as mean ± SEM of at least three separate experiments. * indicates statistically significant variation from the thymidine alone treatment. ($p<0.05$ tested by one-way ANOVA followed by TUKEY test for pairwise comparisons).
Abbreviations: Thy, [^{3}H]-thymidine; dUMP, deoxyuridine monophosphate; cyclo, cycloleucine.

Figure 6.10 Lack of inhibition of the dUMP mediated suppression of [^{3}H]-thymidine incorporation into DNA by cycloleucine in human fibroblast cells.

Data is described as the percentage of [^{3}H]-thymidine incorporated into DNA with respect to the [^{3}H]-thymidine alone treatment, which is normalised to 100%. For each treatment, data is presented as mean ± SEM of three separate experiments. * indicates statistically significant variation from the thymidine alone treatment ($p<0.05$ tested by one-way ANOVA followed by TUKEY test for pairwise comparisons).
Abbreviations: Thy, [^{3}H]-thymidine; dUMP, deoxyuridine monophosphate; cyclo, cycloleucine.

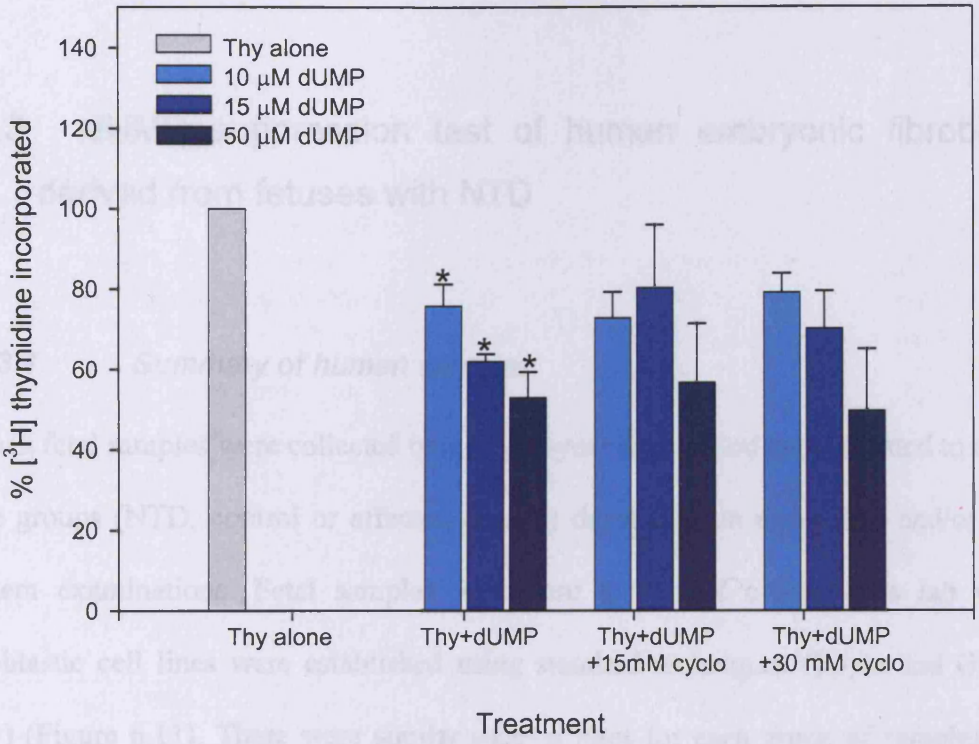
Thy alone
10 μM dUMP
15 μM dUMP
50 μM dUMP
% [3H] thymidine incorporated
140
120
100
80
60
40
20
0
*
*
*
Thy alone
Thy+dUMP
Thy+dUMP +15mM cyclo
Thy+dUMP +30 mM cyclo
Treatment

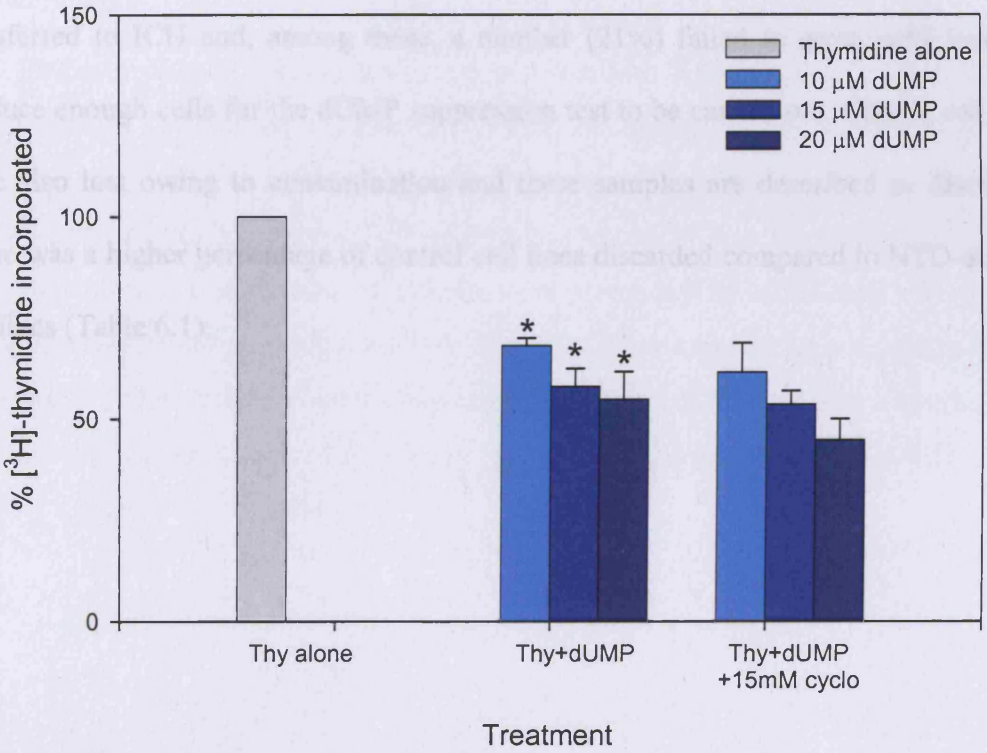
Thymidine alone
10 μM dUMP
15 μM dUMP
20 μM dUMP
% [3H]-thymidine incorporated
150
100
50
0
*
*
*
Thy alone
Thy+dUMP
Thy+dUMP +15mM cyclo
Treatment

6.2.3 dUMP suppression test of human embryonic fibroblasts derived from fetuses with NTD

6.2.3.1 Summary of human samples

Human fetal samples were collected over a four-year time period and allocated to one of three groups (NTD, control or affected control) depending on ultrasound and/or post-mortem examinations. Fetal samples were sent to GOSH cytogenetics lab where fibroblastic cell lines were established using standard techniques (Boyle and Griffin, 2001) (Figure 6.11). There were similar success rates for each group of samples with 93% of all samples producing cell lines (Table 6.1). Established cell lines were transferred to ICH and, among these, a number (21%) failed to grow sufficiently to produce enough cells for the dUMP suppression test to be carried out. Certain cell lines were also lost owing to contamination and these samples are described as discarded. There was a higher percentage of control cell lines discarded compared to NTD-derived cell lines (Table 6.1).

Group	No. samples collected (%)	No. cell lines established (%)	No. established cell lines discarded (%)	No. established cell lines failed dUST (%)	No. established cell lines analysed (%)
NTD	34 (40.0)	32 (94.1)	7 (21.9)	3 (9.4)	22 (68.8)
NC	27 (31.8)	25 (92.6)	11 (44.0)	7 (28.0)	7 (28.0)
AC	21 (24.7)	19 (90.5)	13 (68.4)	2 (10.5)	4 (21.1)
UK	3 (3.5)	3 (100)	3 (100)	0 (0.0)	0 (0.0)
Total	85 (100)	79 (92.9)	34 (43.0)	12 (15.2)	33 (41.8)

Table 6.1 Summary of human samples collected for dUMP suppression test investigation.

Data for the number of samples collected are given with the percentage of total samples in parentheses. Data for the number of cell lines established are given with the number as a percentage of collected samples for that group in parentheses. Data for cell lines that were discarded, failed the dUMP suppression test (dUST) or for which analysis was completed are given as number of samples with percentage of established cell lines for that group in parentheses. Cell lines were discarded when samples became contaminated or failed to grow. Samples were considered to fail the dUST test when results were inconsistent. Abbreviations: AC, affected controls; NC, normal controls; NTD, NTD affected foetuses; UK, unknown.

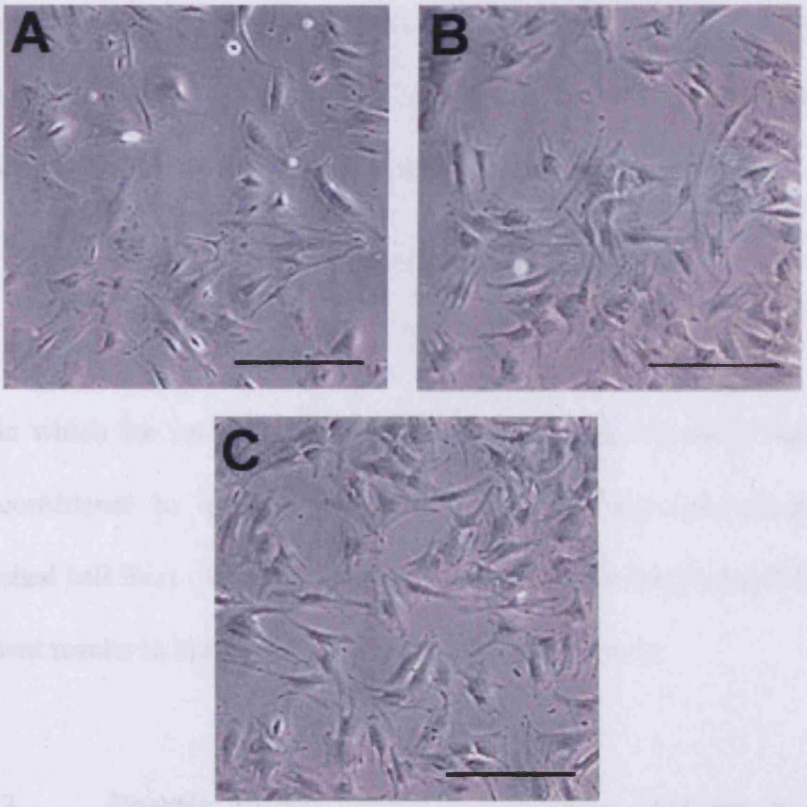

Figure 6.11 Human embryonic fibroblast cell lines

Cell lines were established from samples from human fetuses. The examples shown include cell lines from each group; normal control (**A**), affected control (**B**) and NTD-affected (**C**) which were derived from amniotic fluid (**A** and **B**) and skin (**C**) samples. The morphology of the cell lines was identical despite the different fetal phenotypes or the different sources of the fibroblasts. Scale bars represent 200 μm.

For cell lines that did produce enough cells for the dUMP suppression test to be carried out, at least two wells were used for each treatment in every experiment. Thus, a minimum of four cultures were tested – two with [^{3}H]-thymidine alone and two with [^{3}H]-thymidine and dUMP. To ensure accurate, consistent results, the wells with cells exposed to the same treatments were required to have [^{3}H]-thymidine incorporation within a coefficient of variation (CV) of 15%. The CV provides a relative measure of data dispersion compared to the mean and was calculated as follows:

$$CV = \frac{\text{Standard deviation}}{\text{Mean}} \times 100$$

Tests in which the variation between cells of the same treatment was larger than 15% were considered to have failed the test. A relatively low proportion (15.2% of established cell lines (26.7% of samples that underwent test)) of cell lines failed to give consistent results in the dUMP suppression test (Table 6.1).

6.2.3.2 Results of the dUMP suppression test on human embryonic fibroblast cells

Control samples (normal and affected) were grouped together for comparison with NTD-affected samples. Comparison of the mean gestational age at which samples were collected showed no statistical differences between the control group and samples derived from NTD-affected pregnancies (Table 6.2). However, there was a statistically significant difference in the mean dUMP suppression score between NTD-derived and control cell lines (Table 6.2, Figure 6.12, t-test $p<0.05$), indicating that some NTD-derived samples have a lower dUMP suppression test score than control cell lines. This

is also suggested by the fact that the seven lowest dUMP suppression scores in this study occurred in NTD-affected samples (Figure 6.12). In addition, when the distribution of dUMP suppression scores for each group are analysed, the skewed NTD data compared to the control distribution is evident (Figure 6.13). These results suggest that some NTD-affected embryos may have impaired folate metabolism as indicated by a reduced dUMP suppression test score. There are a number of variables that may affect the results of the dUMP suppression test, however, low sample numbers have made it difficult for statistical assessment. I am therefore unable to assess the effect of gestational age, tissue source or subtype of NTD on the dUMP suppression test scores in this study. However, no obvious correlations were observed (Table 6.3).

Group	No. samples analysed	NTD subtype (%)			Average gestational age sample collected (weeks ± SEM)	Tissue type (%)			Mean dUST score (% ± SEM)
		An	SB	UK		Amnio	Skin/ cartilage/ placenta	UK	
NTD	22	6 (27.3)	14 (63.6)	2 (9.1)	18.2 ± 0.93	4 (18.2)	13 (59.1)	5 (22.7)	36.7 ± 1.78*
Control	11	NA			18.2 ± 0.59	9 (81.8)	2 (18.2)	0 (0.00)	42.7 ± 1.81

Table 6.2 Summary of human samples used in the dUMP suppression test investigation.

Values are given as sample number with percentage of total samples in parentheses. Gestational age of samples in weeks is given as mean ± SEM, there were no statistical differences between the treatment groups as tested by t-test. * indicates significant variation from the control score as tested by t-test $p<0.05$. Abbreviations: Amnio, amniotic fluid; AC, affected controls; An, anencephaly; dUST, dUMP suppression test; SB, spina bifida; NA, not applicable; NC, normal controls; NTD, NTD affected fetuses; UK, unknown.

Figure 6.12 dUMP suppression test results for human embryonic fibroblast cell lines

The percentage suppression of [^{3}H]-thymidine incorporation (cpm/μg protein) by addition of 10 μM dUMP to human embryonic fibroblasts. Coloured data points represent individual samples that have been separated into sample type groups; affected control (AC, yellow circles), normal control (NC, green squares) and NTD-affected samples (NTD, red triangles). Black data points represent the mean ± SEM for control (circle) and NTD-affected (triangle) samples.

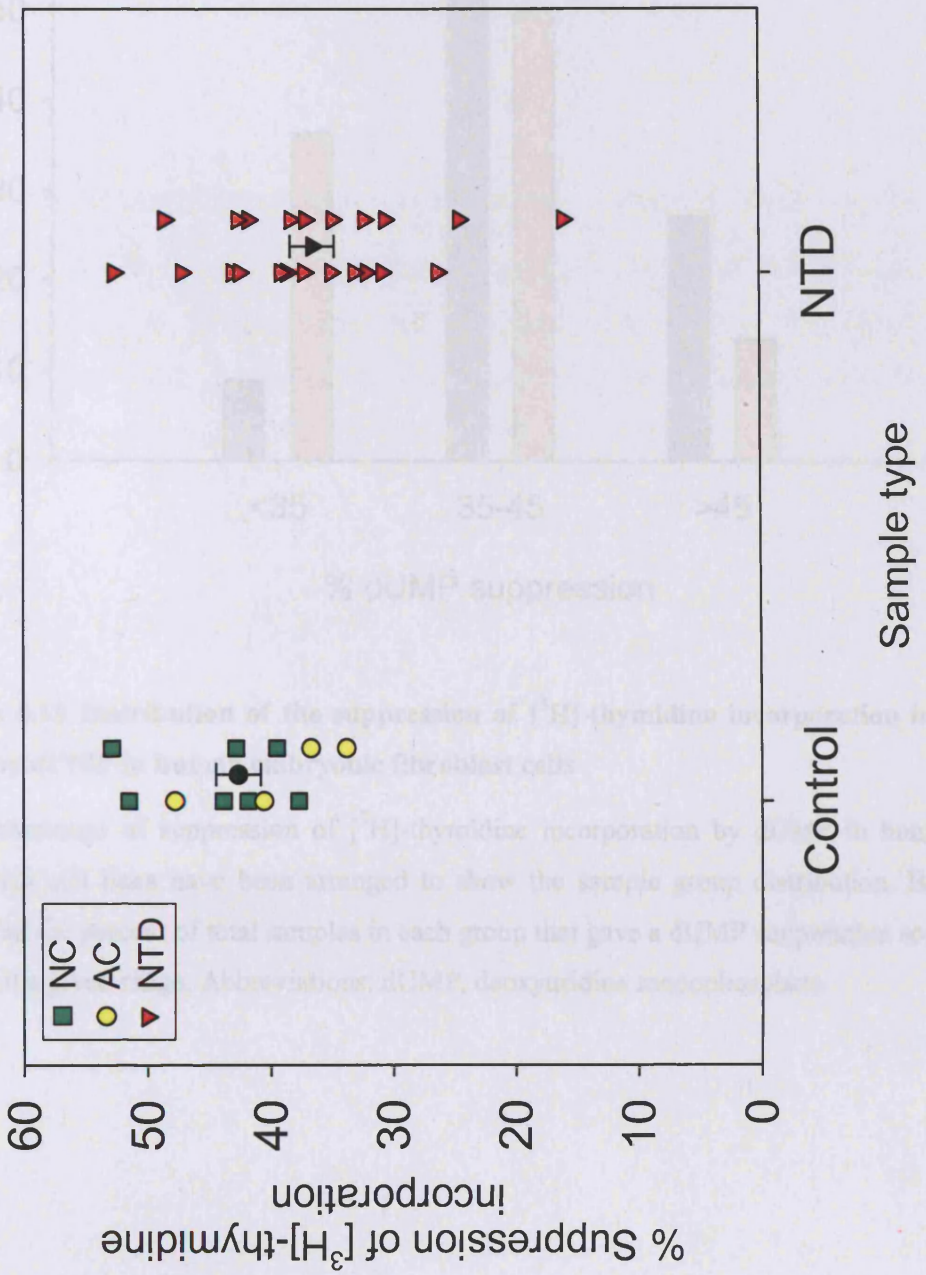
% Suppression of [3H]-thymidine incorporation
0
10
20
30
40
50
60
NC
AC
NTD
Control
NTD
Sample type

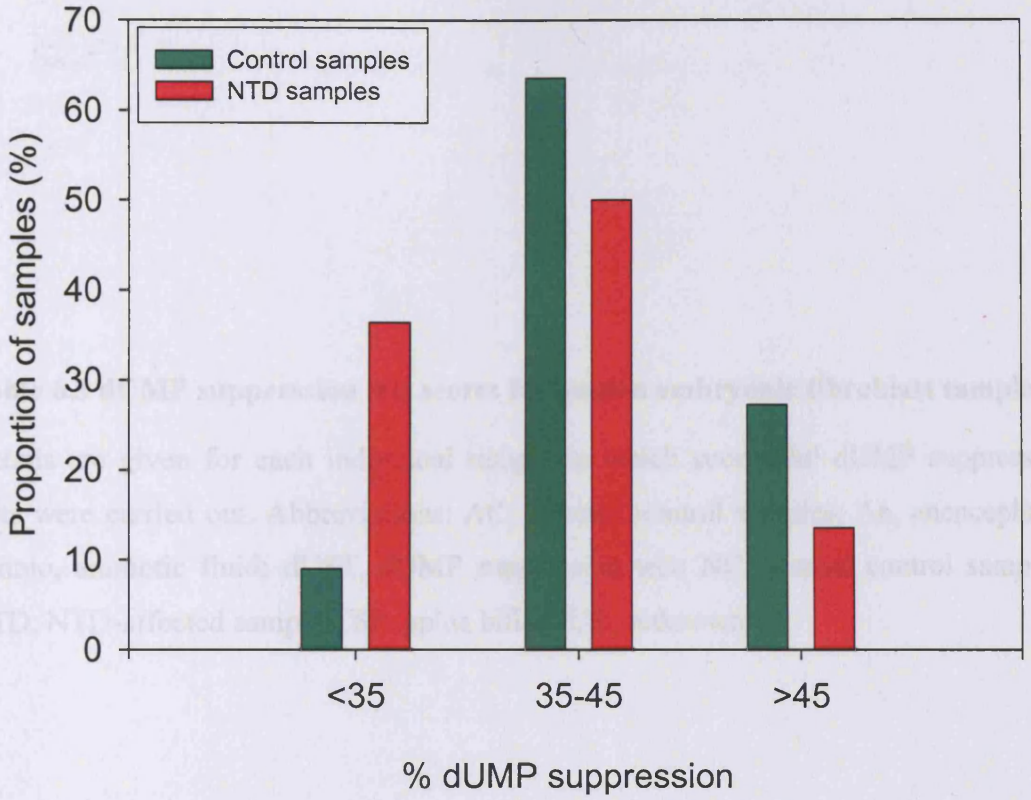

Figure 6.13 Distribution of the suppression of [^{3}H]-thymidine incorporation into DNA by dUMP in human embryonic fibroblast cells

The percentage of suppression of [^{3}H]-thymidine incorporation by dUMP in human fibroblast cell lines have been arranged to show the sample group distribution. Bars represent the percent of total samples in each group that gave a dUMP suppression score within the given range. Abbreviations: dUMP, deoxyuridine monophosphate.

Table 6.3 dUMP suppression test scores for human embryonic fibroblast samples

Details are given for each individual sample in which successful dUMP suppression tests were carried out. Abbreviations: AC, affected control samples; An, anencephaly; Amnio, amniotic fluid; dUST, dUMP suppression test; NC, normal control samples; NTD, NTD-affected samples; SB, spina bifida; UK, unknown.

Group/ Sample number	NTD subtype	Tissue source	Gestational age (weeks)	dUST score (%)
NTD				
1	An	Placenta	UK	35.2
2	An	Cartilage/skin	UK	43.2
3	SB	Cartilage/skin	13.0	16.1
5	SB	Amniotic fluid	21.7	47.3
6	SB	Skin	17.7	38.8
7	An	Skin	UK	35.1
8	An	Skin/placenta	17.0	24.7
9	SB	Amniotic fluid	25.0	31.0
10	SB	Skin	22.1	32.5
34	SB	Skin	18.7	26.5
37	An	UK	11.3	39.9
39	An	UK	12.3	33.3
40	SB	Skin	19.0	41.9
45	SB	Skin/placenta	21.1	38.5
47	UK	UK	UK	37.3
48	SB	Amniotic fluid	UK	48.7
49	UK	Skin	UK	42.6
53	SB	Cartilage/skin	18.0	30.8
65	SB	UK	20.3	37.4
71	SB	UK	16.9	32.3
81	SB	Amniotic fluid	15.4	42.8
82	SB	Cartilage/ placenta	19.0	52.8
NC				
12		Amniotic fluid	16.7	37.8
13		Amniotic fluid	17.0	39.6
14		Amniotic fluid	17.0	51.5
19		Amniotic fluid	20.3	42.9
23		Amniotic fluid	16.7	52.9
24		Amniotic fluid	15.9	41.9
88		Amniotic fluid	16.7	43.9
AC				
4		Amniotic fluid	21.0	36.8
35		Amniotic fluid	19.9	47.8
66		Cartilage	18.1	33.9
68		Skin/cartilage/ placenta	21.1	40.6

6.3 DISCUSSION

In this chapter, the dUMP suppression test was adapted for use with mammalian fibroblastic cell lines. Exogenous dUMP suppressed the incorporation of exogenous [^{3}H]-thymidine into DNA in a dose-dependent manner in both mouse 3T3 and human fibroblastic cell lines. These results are in accordance with the original observations using the dUMP suppression test in bone marrow suspension cultures (Killmann, 1964) and demonstrate that these fibroblast cells possess both the *de novo* and salvage pathway of dTMP synthesis. Moreover, experiments using the folate cycle inhibitor 5-fluorouracil are consistent with the known action of FdUMP, a derivative of FU, as a potent inhibitor of thymidylate synthase and therefore the *de novo* synthesis pathway in which dUMP is converted to dTMP. The presence of 5-fluorouracil or aminopterin (a DHFR inhibitor) completely counteracted the suppression of [^{3}H]-thymidine incorporation into DNA by dUMP. In fact, the presence of the inhibitors resulted in an increase in [^{3}H]-thymidine incorporation compared to cells exposed to [^{3}H]-thymidine alone, suggesting that both inhibitors were successful in inhibiting the *de novo* pathway. These results indicate that the dUMP suppression test, as adapted in this study, is capable of detecting inhibition of the folate cycle and therefore may be capable of detecting genetically determined defects in folate metabolism.

Inhibition of the methylation cycle by cycloleucine did not result in changes in the dUMP suppression test score suggesting that the dUMP suppression test, when using the conditions described in this chapter, cannot detect defects in the methylation cycle. Cycloleucine inhibits the conversion of methionine to S-adenosylmethionine (SAM) by methionine adenosyltransferase (MAT), and is capable of inducing cranial NTD in non-

mutant mouse embryos as described in chapter 4 (L.P.E. Dunlevy, K.A. Burren, K. Mills, L.S.Chitty, A.J. Copp and N.D.E. Greene. Submitted). There are several possible explanations for why the inhibition of MAT by cycloleucine was not detected by the dUMP suppression test in this study. It is possible the cycloleucine concentrations used were not high enough to cause an effect. However, cycloleucine has previously been shown to reduce MAT activity by 50% at concentrations as low as 2.4 mM (Lombardini *et al.*, 1970) or 4 mM in cell culture (Gomes *et al.*, 1998). Moreover, at the lowest concentration used in this study (15 mM) cycloleucine has been shown to affect the SAM/SAH ratio in cultured mouse embryos (Chapter 4). Therefore, it is unlikely that the cycloleucine concentrations used in this study were inadequate to inhibit MAT and more likely that the sensitivity of the test is currently unable to detect inhibition of the methylation cycle. This is perhaps due to a feedback response of folate metabolism allowing adaptation to reduced MAT activity (Finkelstein, 1990).

When human fibroblastic cell lines were used, a number of the samples did not give a final dUMP suppression test score for a variety of reasons including, poor cell proliferation, contamination or inconsistent results. Cells were likely to be less robust as they are primary cell lines. The success rate differed greatly between the cell line groups (NTD compared to control cell lines. $p=0.001$, tested by Chi-squared) even though events such as contamination were random. One possible reason for the differences in success rate for each group may be due to the type of tissue source for each cell line. For ethical reasons all normal control cell lines were derived from amniotic fluid samples whereas the majority of cell lines from NTD-affected embryos were derived from skin, cartilage or placenta samples. The majority of cell lines derived from

affected controls were also sourced from amniotic fluid samples (Table 6.4). Established cell lines derived from tissues other than amniotic fluid had a greater success rate than those from amniotic fluid samples (Table 6.4), resulting in a larger number of NTD-derived cell lines completing the dUMP suppression test than control cell lines.

Although the source of the cell lines may have affected the success rate for dUMP suppression test completion it does not appear to have affected the dUMP suppression test score as there are no obvious correlations between tissue source and dUMP suppression test score in the NTD and AC groups (Section 6.2.3.2).

Group	No. of established cell lines derived from each source (%)			No. of established cell lines discarded/failed dUST (%)		
	Amnio	Tissue	Unknown	Amnio	Tissue	Unknown
NTD	11 (34.4)	16 (50.0)	5 (15.6)	7 (63.6)	3 (18.8)	0 (0.0)
NC	25 (100.0)	0 (0.0)	0 (0.0)	18 (72.0)	0 (0.0)	0 (0.0)
AC	15 (78.9)	4 (21.1)	0 (0.0)	13 (86.7)	2 (50.0)	0 (0.0)

Table 6.4 Source of established cell lines

The majority of control cell lines (NC, normal controls and AC, affected controls) were derived from amniotic fluid samples whereas the majority of NTD samples were derived from other tissue sources. A larger proportion of established cell lines derived from amniotic fluid samples were discarded or failed the dUMP suppression test than those from other sources in all three groups. Tissue sources include skin, cartilage and placenta. Abbreviations: Amnio, amniotic fluid sample; dUST, deoxyuridine monophosphate suppression test.

There is a statistically significant difference in the mean dUMP suppression test score between the control group and NTD-affected cell lines suggesting that some NTD-derived samples may have impaired folate metabolism. The inhibitor studies carried out in this chapter suggest that defects in the methylation cycle will not be detected by the dUMP suppression test, using the current conditions. Therefore, the low dUMP suppression test scores appear to indicate defects within the folate cycle itself. It is possible that defects in folate transport may be present although the ability of the dUMP suppression test to detect these types of defects has not been analysed in this study. Therefore, this study supports the findings of Habibzadeh and colleagues (1993) in suggesting that some NTD-affected fetuses may have intrinsic defects in folate metabolism.

Several folate-related environmental risk factors for NTD in human embryos are known, such as maternal folate, vitamin B_{12} and homocysteine levels (Section 1.9). However, these can be discounted as the cause of abnormal dUMP suppression scores in this study as the cell lines underwent several passages in uniform conditions, suggesting that intrinsic, genetically-determined defects may be involved. In the embryo such defects could interact with environmental risks and summate to cause NTD, as discussed previously (Section 1.9). Many genetic risk factors have been investigated in individuals with NTD, patient groups usually consisting of children or young adults with spina bifida as anencephaly is not compatible with life. There is some evidence for intrinsic, folate-related genetic risk factors although it is currently limited. Associations of NTD risk with polymorphisms in folate-related genes (such as MTHFR C667T (Shields *et al.*, 1999)) in some populations suggest that the genotype of the embryo could affect folate

metabolism. Some polymorphisms have been shown to affect protein function, for example, individuals homozygous for the MTHFR 677 T allele produce a thermolabile variant of the enzyme with reduced activity (Frosst *et al.*, 1995). These findings suggest that some embryos may have an impaired ability to metabolise folates during neural tube closure.

CHAPTER 7; GENERAL DISCUSSION

7.1 GENERAL DISCUSSION

The overall aim of this thesis was to investigate the role of the folate and methylation cycles in the cause and prevention of NTD. To achieve this goal the initial approach taken was to investigate the effect of methylation cycle intermediates and inhibitors on cranial neural tube closure (Chapter 3 and 4). Exposure of non-mutant mouse embryos to homocysteine, methionine or the MAT inhibitors, cycloleucine and ethionine, was investigated. The results in chapter 3 show that homocysteine is embryotoxic but does not induce NTD. This suggests that elevated levels of homocysteine are not directly causal in the production of cranial NTD. However, it appears that the integrity of methylation cycle is essential for cranial neural tube closure to occur, as both excess methionine and inhibition of MAT resulted in cranial neural tube defects (Chapter 4). Further investigations (courtesy of K. Burren) have showed that inhibition of MAT and treatment with excess methionine result in increased SAH levels (Chapter 4) and suggest that the toxicity caused by homocysteine treatment shown in Chapter 3 was a result of the increased homocysteine levels per se not subsequent increases in SAH levels.

Further experiments could determine the mode of action of homocysteine toxicity. The general embryotoxicity observed after homocysteine treatment could have been caused by a toxic effect of homocysteine per se on the yolk sac, reducing the amount of nutrients that could reach the embryo. Elevated homocysteine levels have previously been reported in association with vascular disease (Hankey and Eikelboom, 1999;Ueland and Vollset, 2004). Alternatively, protein homocysteinylation may be responsible as discussed in Section 3.3.

Whole embryo culture is a useful tool in investigating the direct effect of a treatment on embryonic development, however, the true physiological processes are more complicated. Mammalian development occurs within the maternal environment, and effects of the maternal metabolism on the treatment compound before it reaches the embryo are therefore integral in understanding the complete effect of the treatment. To that end, *in vivo* experiments would allow the investigation of the effect of elevated maternal homocysteine levels on the development of non-mutant embryos. Differences in the one-carbon metabolism pathways in adult and embryonic tissues may result in alternative results for the effect of elevated maternal homocysteine levels on embryonic neural tube closure.

Experiments are being carried out to further investigate the mechanisms underlying the ability of methionine, ethionine and cycloleucine to induce cranial NTD. These experiments may shed light on particular events that are crucial for cranial NTD. The measurement of SAH and SAM levels in embryos cultured in this thesis has shown that methionine, ethionine and cycloleucine treatment can change the ratio of these compounds (SAH and SAM) in the cell (Chapter 4). This could affect methylation of a wide range of biomolecules including DNA, proteins and lipids. Further studies could investigate the effect of changes in the methylation ratio on particular methylation events. For example, in order to investigate whether the changes in SAH:SAM ratio are sufficient to induce changes in DNA methylation and subsequently whether these changes are able to alter gene expression could be tested by measuring global and specific DNA methylation in cultured embryos. In addition, possible changes in protein methylation could be investigated. There are many possible methylation targets and it

would be difficult to investigate each one individually. However, candidates could be suggested by previous evidence of a role in the process of neurulation, for example cytoskeletal proteins. Apart from changes in cellular methylation processes, treatment with methionine, ethionine or cycloleucine may also affect polyamine synthesis, as SAM is a precurser of this process. The effect of misregulation of polyamine synthesis on neural tube closure is currently unknown and is therefore an area of interest for further studies.

The data presented in this thesis has added weight to the argument that elevated levels of homocysteine are not directly causal in the production of NTD (VanAerts *et al.*, 1994;Hansen *et al.*, 2001;Greene *et al.*, 2003). These results suggest that elevated homocysteine levels in maternal plasma are probably an indicator of other defects in one-carbon metabolism that may increase risk of NTD as opposed to being the direct causative agent.

An important area of research is the investigation of whether other agents besides folic acid, can help prevent neural tube defects in humans. A few studies have highlighted an increased risk for developing NTD associated with low maternal dietary methionine intake (Shaw *et al.*, 1997;Shoob *et al.*, 2001) and supplementary methionine has been suggested as a candidate to be used in combination with folic acid in the prevention of NTD . However, the experiments carried out in this thesis show that great care needs to be taken as supplementation with methionine may have an unanticipated effect, such that use as a preventative method against the development of NTD may be contra-

indicated. Methionine supplementation could potentially increase rather than decrease the risk of a NTD-affected pregnancy.

The action of folic acid in the prevention of NTD is unknown and experiments in this thesis have attempted to elucidate possible answers. Folic acid treatment did not rescue the NTD induced by methionine or ethionine treatment in whole embryo culture. These results suggest that folic acid cannot prevent the occurrence of NTD caused by defects in the methylation cycle. Higher doses could be tested, and recent reports suggest that folic acid supplements can affect DNA methylation in the offspring (Waterland and Jirtle, 2003).

In order to understand the role of folic acid in preventing NTD in a particular model it is useful to initially understand the cause of the defects. Experiments utilising the folic acid-responsive mouse model *Splotch*^{2H} were carried out in order to investigate the mechanisms involved in the production of cranial NTD by *Pax3*-deficiency (Chapter 5). Analysis of apoptosis and proliferation in the neuroepithelium of mutant embryos suggest that the *Splotch*^{2H} NTD phenotype is not induced by excess apoptosis in the neural tube. This in turn suggests that folic acid rescue of *Splotch*^{2H} NTD is not facilitated by reduction or compensation for excess cell death in the neuroepithelium. Previous suggestions that NTD in the *Splotch*^{2H} mutant embryos is caused by excess apoptosis and prevented by folic acid through stimulation of proliferation are unlikely to be correct. Therefore, the future direction of this investigation should address the other known functions of *Pax3*. Investigation into the role of *Pax3* in cellular differentiation in the neural tube may suggest possible mechanisms of NTD production in *Splotch*^{2H}

embryos. In order to approach this, the question whether *Pax3*-deficency in the neural tube of homozygous *Splotch*^{2H} embryos results in premature cellular differentiation should be tested. The analysis of cell-type specific gene expression and protein levels in the neuroepithelium of *Splotch*^{2H} mutant embryos compared to wild type littermates could be carried out in order to identify those genes that are misregulated when *Pax3* function is lost. In addition, in order to assess the mode of action of folate-prevention of NTD in this mouse model, folic acid treated embryos could be examined for correction of key gene/protein expression changes.

Many potential risk factors have been described for the production of NTD in humans and, in order to establish whether intrinsic defects in folate metabolism in the embryo could be involved in determining susceptibility to NTD, folate metabolism in human embryonic fibroblastic cell lines was investigated (Chapter 6). The dUMP suppression test was adapted for use with these cell lines and was shown to be able to detect inhibition of folate metabolism by specific inhibitors. However, inhibition of the methylation cycle enzyme, MAT, was not detectable. The dUMP suppression test was used with human embryonic fibroblast cells and showed that NTD-derived cell lines gave a significantly lower mean dUMP suppression test score than cell lines derived from control embryos. These results suggest that embryos may have intrinsic defects in folate metabolism. This is the first time cells from the embryo proper have been shown to exhibit defects in the folate cycle in association with NTD.

The use of the dUMP suppression test for analysis of human embryonic cell lines could potentially provide a useful tool in investigating folate metabolism abnormalities in

association with human NTD. In the course of this present study, cell line aliquots were stored for possible future analysis, including screening for possible genetic determinants of the abnormal dUMP suppression test results. Subsequently these samples have been screened for known polymorphisms in folate-related genes that have been identified as possible risk factors for developing NTD (Table 7.1, Section 1.9). Although some polymorphisms are present in NTD-affected samples there are currently insufficient numbers to establish possible links between genotype, phenotype and dUMP suppression test scores. However, it is clear that the abnormal results in the dUMP suppression test do not result from the TT C677T MTHFR genotype, the genotype for which there is so far the strongest evidence for a link to NTD (Van der Put *et al.*, 2001). Further work is continuing on the stored samples, including investigations of levels of folate metabolites in order to define possible specific defects in the folate cycle in those samples with low dUMP suppression test scores.

Overall, it appears that the flux through the methylation and folate cycles during the period of neurulation is of critical importance for the successful closure of the neural tube. Understanding the manner in which variations in the environment and embryonic/maternal genotype interact and influence neural tube closure will contribute greatly to understanding the causes of NTD.

Table 7.1 The genotype of the successful dUST cell lines for several known polymorphisms in folate-related genes

Cell pellets from each cell line were stored for genotype analysis of potential genetic risk factors for NTD. The polymorphisms investigated were MTHFR C677T (Frosst *et al.*, 1995), MTHFR A1298C (Van der Put *et al.*, 1998), MTHFRD1 G1958A (Brody *et al.*, 2002), DHFR 19 bp deletion (Johnson *et al.*, 2004), GCPII C1565T (Vieira *et al.*, 2005), MTR A2756G (Leclerc *et al.*, 1996) and MTRR A66G (Leclerc *et al.*, 1998). Wild type alleles are depicted as 1 and the alternative as 2. Results courtesy of Dr. K. Doudney. Abbreviations: DHFR, dihydrofolate reductase; dUST, deoxyuridine monophosphate suppression test; GCPII, glutamate carboxypeptidase II; MTHFR, methylene-tetrahydrofolate reductase; MTHFRD1, methylenetetrahydrofolate dehydrogenase /methenyltetrahydrofolate cyclohydrolase /formyltetrahydrofolate synthetase; MTR, methionine synthase; MTRR methionine synthase reductase.

Cell line No.	MTHFR 677	MTHFR 1298	MTHFR D1	DHFR del	GCPII	MTR	MTRR	dUST score
NTD								
1	12	11	12	12	11	11	12	35.2
2	12	12	11	22	11	11	22	43.2
3	12	-	-	11	11	11	22	16.1
5	12	11	12	11	11	11	12	47.3
6	12	11	11	12	11	11	11	38.8
7	11	11	12	11	11	11	12	35.1
8	11	12	12	12	11	11	12	24.7
9	11	22	12	11	11	11	12	31.0
10	12	12	11	11	11	11	12	32.5
34	12	12	11	12	11	22	12	26.5
37	12	11	12	11	11	22	12	39.9
39	12	11	12	22	11	11	12	33.3
40	12	11	12	12	11	11	11	41.9
45	12	11	12	12	11	11	12	38.5
47	12	12	11	12	11	11	22	37.3
48	11	12	11	11	11	11	11	48.7
49	11	11	12	22	11	11	22	42.6
53	12	11	11	12	11	11	12	30.8
65	12	12	12	12	11	11	12	37.4
71	-	-	-	-	-	-	-	32.3
81	12	11	11	11	11	11	11	42.8
82	12	11	22	12	11	22	12	52.8
Control								
4	11	12	22	12	11	11	12	36.8
12	11	12	12	22	11	11	12	37.8
13	12	11	11	12	11	11	12	39.6
14	-	-	-	-	-	-	-	51.5
19	-	-	-	-	-	-	-	42.9
23	-	-	-	-	-	-	-	52.9
24	11	12	12	11	11	11	12	40.7
35	11	11	11	11	11	11	12	47.8
66	-	-	-	-	-	-	-	33.9
68	11	12	11	12	11	22	11	40.6
88	-	-	-	-	-	-	-	43.9

References

Abbott,B.D., Ebron-McCoy,M., and Andrews,J.E. (1995). Cell death in rat and mouse embryos exposed to methanol in whole embryo culture. *Toxicology,* **97,** 159-171.

Abbott,B.D., Held,G.A., Wood,C.R., Buckalew,A.R., Brown,J.G., and Schmid,J. (1999). AhR, ARNT, and CYP1A1 mRNA quantitation in cultured human embryonic palates exposed to TCDD and comparison with mouse palate in vivo and in culture. *Toxicol. Sci.,* **47,** 62-75.

Abbott,B.D., Probst,M.R., Perdew,G.H., and Buckalew,A.R. (1998). AH receptor, ARNT, glucocorticoid receptor, EGF receptor, EGF, TGF alpha, TGF beta 1, TGF beta 2, and TGF beta 3 expression in human embryonic palate, and effects of 2,3,7,8-tetrachlorodibenzo-p-dioxin (TCDD). *Teratology.,* **58,** 30-43.

Afman,L.A., Blom,H.J., Drittij,M.J., Brouns,M.R., and van Straaten,H.W. (2005). Inhibition of transmethylation disturbs neurulation in chick embryos. *Brain Res. Dev. Brain Res.,* **158,** 59-65.

Afman,L.A., Blom,H.J., van der Put,N.M., and van Straaten,H.W. (2003a). Homocysteine interference in neurulation: a chick embryo model. *Birth Defects Res. Part A Clin. Mol. Teratol.,* **67,** 421-428.

Afman,L.A., Lievers,K.J., Kluijtmans,L.A., Trijbels,F.J., and Blom,H.J. (2003b). Gene-gene interaction between the cystathionine beta-synthase 31 base pair variable number of tandem repeats and the methylenetetrahydrofolate reductase 677C > T polymorphism on homocysteine levels and risk for neural tube defects. *Mol. Genet. Metab,* **78,** 211-215.

Almog,N. and Rotter,V. (1997). Involvement of p53 in cell differentiation and development. *Biochim. Biophys. Acta Rev. Cancer,* **1333,** F1-F27.

Andaloro,V.J., Monaghan,D.T., and Rosenquist,T.H. (1998). Dextromethorphan and other N-methyl-D-aspartate receptor antagonists are teratogenic in the avian embryo model. *Pediatr. Res.*, **43,** 1-7.

Auerbach,R. (1954). Analysis of the developmental effects of a lethal mutation in the house mouse. *J. Exp. Zool.*, **127,** 305-329.

Bailey,L.B., Rampersaud,G.C., and Kauwell,G.P. (2003). Folic acid supplements and fortification affect the risk for neural tube defects, vascular disease and cancer: evolving science. *J. Nutr.*, **133,** 1961S-1968S.

Baird,P.A. (1983). Neural tube defects in the Sikhs. *Am. J. Med. Genet.*, **16,** 49-56.

Bamforth,S.D., Braganτa,J., Eloranta,J.J., Murdoch,J.N., Marques,F.I.R., Kranc,K.R., Farza,H., Henderson,D.J., Hurst,H.C., and Bhattacharya,S. (2001). Cardiac malformations, adrenal agenesis, neural crest defects and exencephaly in mice lacking Cited2, a new Tfap2 co-activator. *Nature Genet.*, **29,** 469-474.

Barber,R.C., Shaw,G.M., Lammer,E.J., Greer,K.A., Biela,T.A., Lacey,S.W., Wasserman,C.R., and Finnell,R.H. (1998). Lack of association between mutations in the folate receptor- α gene and spina bifida. *Am. J. Med. Genet.*, **76,** 310-317.

Beechey,C.V. and Searle,A.G. (1986). Mutations at the *Sp* locus. *MNL,* **75,** 28.

Bergo,M.O., Leung,G.K., Ambroziak,P., Otto,J.C., Casey,P.J., and Young,S.G. (2000). Targeted inactivation of the isoprenylcysteine carboxyl methyltransferase gene causes mislocalization of K-Ras in mammalian cells. *J. Biol. Chem.*, **275,** 17605-17610.

Berk,M., Desai,S.Y., Heyman,H.C., and Colmenares,C. (1997). Mice lacking the ski proto-oncogene have defects in neurulation, craniofacial, patterning, and skeletal muscle development. *Genes Dev.*, **11,** 2029-2039.

Bernasconi,M., Remppis,A., Fredericks,W.J., Rauscher,F.J., III, and Schäfer,B.W. (1996). Induction of apoptosis in rhabdomyosarcoma cells through down-regulation of PAX proteins. *Proc. Natl. Acad. Sci. USA,* **93,** 13164-13169.

Berry,R.J., Li,Z., Erickson,J.D., Li,S., Moore,C.A., Wang,H., Mulinare,J., Zhao,P., Wong,L.Y.C., Gindler,J., Hong,S.X., Correa,A., and China-US Collaborative Project Neu (1999). Prevention of neural-tube defects with folic acid in China. *N. Engl. J. Med.,* **341,** 1485-1490.

Bettenhausen,B., De Angelis,M.H., Simon,D., Guénet,J.-L., and Gossler,A. (1995). Transient and restricted expression during mouse embryogenesis of *Dll1*, a murine gene closely related to *Drosophila Delta. Development.,* **121,** 2407-2418.

Borycki,A.G., Li,J., Jin,F., Emerson,C.P., and Epstein,J.A. (1999). Pax3 functions in cell survival and in pax7 regulation. *Development.,* **126,** 1665-1674.

Boyle,T. and Griffin,D. (2001). The cytogenetics of pregnancy. In Rooney,D.E. (Ed.), *Human cytogenetics: constitutional analysis*, . Oxford University Press.

Brent,R.L. (1998). Teratogenesis of dextromethorphan in the avian embryo. *Pediatr. Res.,* **44(3),** 415-416.

Brody,L.C., Conley,M., Cox,C., Kirke,P.N., McKeever,M.P., Mills,J.L., Molloy,A.M., O'Leary,V.B., Parle-McDermott,A., Scott,J.M., and Swanson,D.A. (2002). A polymorphism, R653Q, in the trifunctional enzyme methylenetetrahydrofolate dehydrogenase/methenyltetrahydrofolate cyclohydrolase/formyltetrahydrofolate synthetase is a maternal genetic risk factor for neural tube defects: report of the Birth Defects Research Group. *Am. J. Hum. Genet.,* **71,** 1207-1215.

Brook,F.A., Estibeiro,J.P., and Copp,A.J. (1994). Female predisposition to cranial neural tube defects is not because of a difference between the sexes in rate of embryonic growth or development during neurulation. *J. Med. Genet.*, **31,** 383-387.

Brook,F.A., Shum,A.S.W., Van Straaten,H.W.M., and Copp,A.J. (1991). Curvature of the caudal region is responsible for failure of neural tube closure in the curly tail (ct) mouse embryo. *Development.*, **113,** 671-678.

Brouns,M.R., Matheson,S.F., Hu,K.Q., Delalle,I., Caviness,V.S., Jr., Silver,J., Bronson,R.T., and Settleman,J. (2000). The adhesion signaling molecule p190 RhoGAP is required for morphogenetic processes in neural development. *Development.*, **127,** 4891-4903.

Burgoon,J.M., Selhub,J., Nadeau,M., and Sadler,T.W. (2002). Investigation of the effects of folate deficiency on embryonic development through the establishment of a folate deficient mouse model. *Teratology.*, **65,** 219-227.

Campbell,N.R.C. (1996). How safe are folic acid supplements. *Arch. Intern. Med.*, **156,** 1638-1644.

Carmel,R. and Jacobsen,W. (2001). *Homocysteine in health and disease.* Cambridge University Press, Cambridge.

Carter,C.O., David,P.A., and Laurence,K.M. (1968). A family study of major central nervous system malformations in South Wales. *J. Med. Genet.*, **5,** 81-106.

Carter,C.O. and Evans,K.A. (1973). Spina bifida and anencephalus in Greater London. *J. Med. Genet.*, **10,** 209-234.

Carter,M., Ulrich,S., Oofuji,Y., Williams,D.A., and Ross,M.E. (1999). *Crooked tail* (*Cd*) models human folate-responsive neural tube defects. *Hum. Mol. Genet.*, **8,** 2199-2204.

Castro,R., Rivera,I., Ravasco,P., Camilo,M.E., Jakobs,C., Blom,H.J., and De Almeida,I.T. (2004). 5,10-methylenetetrahydrofolate reductase (MTHFR) 677C-->T and 1298A-->C mutations are associated with DNA hypomethylation. *J Med. Genet.*, **41,** 454-458.

Castro,R., Rivera,I., Struys,E.A., Jansen,E.E., Ravasco,P., Camilo,M.E., Blom,H.J., Jakobs,C., and Tavares,d.A., I (2003). Increased homocysteine and S-adenosylhomocysteine concentrations and DNA hypomethylation in vascular disease. *Clin Chem.*, **49,** 1292-1296.

Chaineau,E., Binet,S., Pol,D., Chatellier,G., and Meininger,V. (1990). Embryotoxic effects of sodium arsenite and sodium arsenate on mouse embryos in culture. *Teratology.*, **41,** 105-112.

Chalepakis,G., Jones,F.S., Edelman,G.M., and Gruss,P. (1994). Pax-3 contains domains for transcription activation and transcription inhibition. *Proc. Natl. Acad. Sci. USA,* **91,** 12745-12749.

Chen,W.-H., Morriss-Kay,G.M., and Copp,A.J. (1994). Prevention of spinal neural tube defects in the curly tail mouse mutant by a specific effect of retinoic acid. *Dev. Dyn.*, **199,** 93-102.

Chen,Z., Otto,J.C., Bergo,M.O., Young,S.G., and Casey,P.J. (2000). The C-terminal polylysine region and methylation of K-Ras are critical for the interaction between K-Ras and microtubules. *J. Biol. Chem.*, **275,** 41251-41257.

Chen,Z.T., Karaplis,A.C., Ackerman,S.L., Pogribny,I.P., Melnyk,S., Lussier-Cacan,S., Chen,M.F., Pai,A., John,S.W.M., Smith,R.S., Bottiglieri,T., Bagley,P., Selhub,J., Rudnicki,M.A., James,S.J., and Rozen,R. (2001). Mice deficient in methylenetetrahydrofolate reductase exhibit hyperhomocysteinemia and decreased methylation capacity, with neuropathology and aortic lipid deposition. *Hum. Mol. Genet.,* **10,** 433-443.

Chen,Z.-F. and Behringer,R.R. (1995). *twist* is required in head mesenchyme for cranial neural tube morphogenesis. *Genes Dev.,* **9,** 686-699.

Chi,H., Sarkisian,M.R., Rakic,P., and Flavell,R.A. (2005). Loss of mitogen-activated protein kinase kinase kinase 4 (MEKK4) results in enhanced apoptosis and defective neural tube development. *Proc. Natl. Acad. Sci. U. S. A,* **102,** 3846-3851.

Chiang,P.K., Gordon,R.K., Tal,J., Zeng,G.C., Doctor,B.P., Pardhasaradhi,K., and McCann,P.P. (1996). S-Adenosylmethionine and methylation. *FASEB J.,* **10,** 471-480.

Christensen,B., Arbour,L., Tran,P., Leclerc,D., Sabbaghian,N., Platt,R., Gilfix,B.M., Rosenblatt,D.S., Gravel,R.A., Forbes,P., and Rozen,R. (1999). Genetic polymorphisms in methylenetetrahydrofolate reductase and methionine synthase, folate levels in red blood cells, and risk of neural tube defects. *Am. J. Med. Genet.,* **84,** 151-157.

Cockroft,D.L. (1990). Dissection and culture of postimplantation embryos. In Copp,A.J. and Cockroft,D.L. (Eds.), *Postimplantation Mammalian Embryos: A Practical Approach*, . IRL Press, Oxford, pp. 15-40.

Coelho,C.N.D. and Klein,N.W. (1990). Methionine and neural tube closure in cultured rat embryos: Morphological and biochemical analyses. *Teratology.,* **42,** 437-451.

Coelho,C.N.D., Weber,J.A., Klein,N.W., Daniels,W.G., and Hoagland,T.A. (1989). Whole rat embryos require methionine for neural tube closure when cultured on cow serum. *J. Nutr.,* **119,** 1716-1725.

Cogram,P., Hynes,A., Dunlevy,L.P.E., Greene,N.D.E., and Copp,A.J. (2004). Specific isoforms of protein kinase C are essential for prevention of folate-resistant neural tube defects by inositol. *Hum. Mol. Genet.,* **13,** 7-14.

Copp,A.J. and Bernfield,M. (1994). Etiology and pathogenesis of human neural tube defects: Insights from mouse models. *Curr. Opin. Pediatr.,* **6,** 624-631.

Copp,A.J. and Brook,F.A. (1989). Does lumbosacral spina bifida arise by failure of neural folding or by defective canalisation? *J. Med. Genet.,* **26,** 160-166.

Copp,A.J., Brook,F.A., Estibeiro,J.P., Shum,A.S.W., and Cockroft,D.L. (1990). The embryonic development of mammalian neural tube defects. *Prog. Neurobiol.,* **35,** 363-403.

Copp,A.J., Brook,F.A., and Roberts,H.J. (1988a). A cell-type-specific abnormality of cell proliferation in mutant (curly tail) mouse embryos developing spinal neural tube defects. *Development.,* **104,** 285-295.

Copp,A.J., Crolla,J.A., and Brook,F.A. (1988b). Prevention of spinal neural tube defects in the mouse embryo by growth retardation during neurulation. *Development.,* **104,** 297-303.

Copp,A.J. and Greene,N.D.E. (2000). Neural tube defects: prevention by folic acid and other vitamins. *Indian J. Pediatr.,* **67,** 915-921.

Copp,A.J., Greene,N.D.E., and Murdoch,J.N. (2003a). Dishevelled: linking convergent extension with neural tube closure. *Trends Neurosci.,* **26,** 453-455.

Copp,A.J., Greene,N.D.E., and Murdoch,J.N. (2003b). The genetic basis of mammalian neurulation. *Nat. Rev. Genet.,* **4,** 784-793.

Cravo,M.L., Mason,J.B., Selhub,J., and Rosenberg,I.H. (1991). Use of the deoxyuridine suppression test to evaluate localized folate deficiency in rat colonic epithelium. *Am. J Clin Nutr.,* **53,** 1450-1454.

Curtin,J.A., Quint,E., Tsipouri,V., Arkell,R.M., Cattanach,B., Copp,A.J., Fisher,E.M., Nolan,P.M., Steel,K.P., Brown,S.D.M., Gray,I.C., and Murdoch,J.N. (2003). Mutation of *Celsr1* disrupts planar polarity of inner ear hair cells and causes severe neural tube defects in the mouse. *Curr. Biol.,* **13,** 1-20.

Czeizel,A.E. and Dudás,I. (1992). Prevention of the first occurrence of neural-tube defects by periconceptional vitamin supplementation. *N. Engl. J. Med.,* **327,** 1832-1835.

De Angelis,M.H., McIntyre,J., II, and Gossler,A. (1997). Maintenance of somite borders in mice requires the *Delta* homologue *Dll1*. *Nature,* **386,** 717-721.

De Marco,P., Calevo,M.G., Moroni,A., Arata,L., Merello,E., Finnell,R.H., Zhu,H., Andreussi,L., Cama,A., and Capra,V. (2002). Study of MTHFR and MS polymorphisms as risk factors for NTD in the Italian population. *J. Hum. Genet.,* **47,** 319-324.

De Marco,P., Moroni,A., Merello,E., De Franchis,R., Andreussi,L., Finnell,R.H., Barber,R.C., Cama,A., and Capra,V. (2000). Folate pathway gene alterations in patients with neural tube defects. *Am. J. Med. Genet.,* **95,** 216-223.

Detrait,E.R., George,T.M., Etchevers,H.C., Gilbert,J.R., Vekemans,M., and Speer,M.C. (2005). Human neural tube defects: developmental biology, epidemiology, and genetics. *Neurotoxicol. Teratol.,* **27,** 515-524.

Dickie,M.M. (1964). New splotch alleles in the mouse. *J. Hered.,* **55,** 97-101.

Dickman,E.D., Rogers,R., and Conway,S.J. (1999). Abnormal skeletogenesis occurs coincident with increased apoptosis in the *Splotch* (Sp^{2H}) mutant: Putative roles for *Pax3* and *PDGFRα* in rib patterning. *Anat. Rec.*, **255,** 353-361.

Dixon,J., Brakebusch,C., Fässler,R., and Dixon,M.J. (2000). Increased levels of apoptosis in the prefusion neural folds underlie the craniofacial disorder, Treacher Collins syndrome. *Hum. Mol. Genet.*, **9,** 1473-1480.

Doolin,M.T., Barbaux,S., McDonnell,M., Hoess,K., Whitehead,A.S., and Mitchell,L.E. (2002). Maternal genetic effects, exerted by genes involved in homocysteine remethylation, influence the risk of spina bifida. *Am. J. Hum. Genet.*, **71,** 1222-1226.

Dunwoodie,S.L., Henrique,D., Harrison,S.M., and Beddington,R.S.P. (1997). Mouse *Dll3*: A novel divergent *Delta* gene which may complement the function of other *Delta* homologues during early pattern formation in the mouse embryo. *Development.*, **124,** 3065-3076.

Economides,D.l., Ferguson,J., MacKenzie,I.Z., Darley,J., Ware,H., and Holmes-Siedle,M. (1992). Folate and vitamin B_{12} concentrations in maternal and fetal blood, and amniotic fluid in second trimester pregnancies complicated by neural tube defects. *Br. J. Obstet. Gynaecol.*, **99,** 23-25.

Elwood,J.M. and Elwood,J.H. (1980). *Epidemiology of anencephalus and spina bifida.* Oxford University Press, Oxford.

Epeldegui,M., Pe±a-Melian,A., Varela-Moreiras,G., and Pθrez-Miguelsanz,J. (2002). Homocysteine modifies development of neurulation and dorsal root ganglia in chick embryos. *Teratology.*, **65,** 171-179.

Epstein,D.J., Vekemans,M., and Gros,P. (1991). splotch (Sp^{2H}), a mutation affecting development of the mouse neural tube, shows a deletion within the paired homeodomain of Pax-3. *Cell,* **67,** 767-774.

Epstein,D.J., Vogan,K.J., Trasler,D.G., and Gros,P. (1993). A mutation within intron 3 of the *Pax-3* gene produces aberrantly spliced mRNA transcripts in the splotch (*Sp*) mouse mutant. *Proc. Natl. Acad. Sci. USA,* **90,** 532-536.

Epstein,J.A., Lam,P., Jepeal,L., Maas,R.L., and Shapiro,D.N. (1995). Pax3 inhibits myogenic differentiation of cultured myoblast cells. *J Biol Chem.,* **270,** 11719-11722.

Essien,F.B. (1992). Maternal methionine supplementation promotes the remediation of axial defects in *Axd* mouse neural tube mutants. *Teratology.,* **45,** 205-212.

Essien,F.B. and Wannberg,S.L. (1993). Methionine but not folinic acid or vitamin B-12 alters the frequency of neural tube defects in *Axd* mutant mice. *J. Nutr.,* **123,** 27-34.

EUROCAT Working Group (1991). Prevalence of neural tube defects in 20 regions of Europe and the impact of prenatal diagnosis, 1980-1986. *J. Epidemiol. Community Health,* **45,** 52-58.

Felix,T.M., Leistner,S., and Giugliani,R. (2004). Metabolic effects and the methylenetetrahydrofolate reductase (MTHFR) polymorphism associated with neural tube defects in southern Brazil. *Birth Defects Res. Part A Clin. Mol. Teratol.,* **70,** 459-463.

Fell,D. and Selhub,J. (1990). Disruption of thymidylate synthesis and glycine-serine interconversion by L-methionine and L-homocystine in Raji cells. *Biochim. Biophys. Acta,* **1033,** 80-84.

Finkelstein,J.D. (1990). Methionine metabolism in mammals. *J. Nutr. Biochem.,* **1,** 228-237.

Finkelstein,J.D. (1998). The metabolism of homocysteine: pathways and regulation. *Eur. J Pediatr.,* **157 Suppl 2,** S40-S44.

Finnell,R.H., Moon,S.P., Abbott,L.C., Golden,J.A., and Chernoff,G.F. (1986). Strain differences in heat-induced neural tube defects in mice. *Teratology.,* **33,** 247-252.

Fleming,A. and Copp,A.J. (1998). Embryonic folate metabolism and mouse neural tube defects. *Science,* **280,** 2107-2109.

Fleming,A. and Copp,A.J. (2000). A genetic risk factor for mouse neural tube defects: defining the embryonic basis. *Hum. Mol. Genet.,* **9,** 575-581.

Fleming,J., Pearce,A., Brown,S.D.M., and Steel,K.P. (1996). The Sp^{4H} deletion may contain a new locus essential for postimplantation development. *Genomics,* **34,** 205-212.

Flynn,T.J., Friedman,L., Black,T.N., and Klein,N.W. (1987). Methionine and iron as growth factors for rat embryos cultured in canine serum. *J. Exp. Zool.,* **244,** 319-324.

Franz,T. (1989). Persistent truncus arteriosus in the Splotch mutant mouse. *Anat. Embryol.,* **180,** 457-464.

Friso,S., Choi,S.W., Girelli,D., Mason,J.B., Dolnikowski,G.G., Bagley,P.J., Olivieri,O., Jacques,P.F., Rosenberg,I.H., Corrocher,R., and Selhub,J. (2002). A common mutation in the 5,10-methylenetetrahydrofolate reductase gene affects genomic DNA methylation through an interaction with folate status. *Proc. Natl. Acad. Sci. USA,* **99,** 5606-5611.

Frosst,P., Blom,H.J., Milos,R., Goyette,P., Sheppard,C.A., Matthews,R.G., Boers,G.J.H., Den Heijer,M., Kluijtmans,L.A.J., Van den Heuvel,L.P., and Rozen,R. (1995). A candidate genetic risk factor for vascular disease: A common mutation in methylenetetrahydrofolate reductase. *Nature Genet.,* **10,** 111-113.

Gavrieli,Y., Sherman,Y., and Ben-Sasson,S.A. (1992). Identification of programmed cell death in situ via specific labeling of nuclear DNA fragmentation. *J. Cell Biol.,* **119,** 493-501.

Geelen,J.A.G. and Langman,J. (1977). Closure of the neural tube in the cephalic region of the mouse embryo. *Anat. Rec.,* **189,** 625-640.

Giles,J.J. and Bannigan,J.G. (1997). The effects of lithium on neurulation stage mouse embryos. *Arch. Toxicol.,* **71,** 519-528.

Golden,J.A. and Chernoff,G.F. (1993). Intermittent pattern of neural tube closure in two strains of mice. *Teratology.,* **47,** 73-80.

Golden,J.A. and Chernoff,G.F. (1995). Multiple sites of anterior neural tube closure in humans: Evidence from anterior neural tube defects (anencephaly). *Pediatrics,* **95,** 506-510.

Gomes,T.C., Ekblom,J., and Oreland,L. (1998). Regulation of methionine adenosyltransferase catalytic activity and messenger RNA in SH-SY5Y human neuroblastoma cells. *Biochem. Pharmacol.,* **55,** 567-571.

Goulding,M., Sterrer,S., Fleming,J., Balling,R., Nadeau,J., Moore,K.J., Brown,S.D.M., Steel,K.P., and Gruss,P. (1993). Analysis of the *Pax-3* gene in the mouse mutant *splotch. Genomics,* **17,** 355-363.

Goulding,M.D., Chalepakis,G., Deutsch,U., Erselius,J.R., and Gruss,P. (1991). Pax-3, a novel murine DNA binding protein expressed during early neurogenesis. *EMBO J.,* **10,** 1135-1147.

Gowen,L.C., Johnson,B.L., Latour,A.M., Sulik,K.K., and Koller,B.H. (1996). *Brca1* deficiency results in early embryonic lethality characterized by neuroepithelial abnormalities. *Nature Genet.,* **12,** 191-194.

Greene,N.D. and Copp,A.J. (2005). Mouse models of neural tube defects: investigating preventive mechanisms. *Am. J. Med. Genet. C. Semin. Med. Genet.,* **135,** 31-41.

Greene,N.D.E. and Copp,A.J. (1997). Inositol prevents folate-resistant neural tube defects in the mouse . *Nature Med.,* **3,** 60-66.

Greene,N.D.E., Dunlevy,L.E., and Copp,A.J. (2003). Homocysteine is embryotoxic but does not cause neural tube defects in mouse embryos. *Anat. Embryol.,* **206,** 185-191.

Gruneberg,H. (1954). Genetical studies on the skeleton of the mouse. VIII. Curly tail. *J. Genet.,* **52,** 52-67.

Gueant-Rodriguez,R.M., Rendeli,C., Namour,B., Venuti,L., Romano,A., Anello,G., Bosco,P., Debard,R., Gerard,P., Viola,M., Salvaggio,E., and Gueant,J.L. (2003). Transcobalamin and methionine synthase reductase mutated polymorphisms aggravate the risk of neural tube defects in humans. *Neurosci. Lett.,* **344,** 189-192.

Gunn,T.M., Juriloff,D.M., and Harris,M.J. (1995). Genetically determined absence of an initiation site of cranial neural tube closure is causally related to exencephaly in SELH/Bc mouse embryos. *Teratology.,* **52,** 101-108.

Gurniak,C.B., Perlas,E., and Witke,W. (2005). The actin depolymerizing factor n-cofilin is essential for neural tube morphogenesis and neural crest cell migration. *Dev. Biol.,* **278,** 231-241.

Habibzadeh,N., Schorah,C.J., Seller,M.J., Smithells,R.W., and Levene,M.I. (1993). Uptake and utilization of DL-5-[methyl-14C] tetrahydropteroylmonoglutamate by cultured cytotrophoblasts associated with neural tube defects. *Proc. Soc. Exp. Biol. Med.,* **203,** 45-54.

Hall,J.G., Friedman,J.M., Kenna,B.A., Popkin,J., Jawanda,M., and Arnold,W. (1988). Clinical, genetic, and epidemiological factors in neural tube defects. *Am. J. Hum. Genet.,* **43,** 827-837.

Hall,P.A. and Lane,D.P. (1997). Tumor suppressors: a developing role for p53? *Curr. Biol,* **7,** R144-R147.

Hamblet,N.S., Lijam,N., Ruiz-Lozano,P., Wang,J., Yang,Y., Luo,Z., Mei,L., Chien,K.R., Sussman,D.J., and Wynshaw-Boris,A. (2002). Dishevelled 2 is essential for cardiac outflow tract development, somite segmentation and neural tube closure. *Development.,* **129,** 5827-5838.

Hankey,G.J. and Eikelboom,J.W. (1999). Homocysteine and vascular disease. *Lancet,* **354,** 407-413.

Hansen,D.K., Grafton,T.F., Melnyk,S., and James,S.J. (2001). Lack of embryotoxicity of homocysteine thiolactone in mouse embryos in vitro. *Reprod. Toxicol.,* **15,** 239-244.

Harding,B.N. and Copp,A.J. (2002). Congenital malformations. In Graham,D.I. and Lantos,P.L. (Eds.), *Greenfield's Neuropathology,* . Arnold, London, pp. 357-483.

Harris,B.S., Franz,T., Ullrich,S., Cook,S., Bronson,R.T., and Davisson,M.T. (1997). Forebrain overgrowth (*fog*): A new mutation in the mouse affecting neural tube development. *Teratology.,* **55,** 231-240.

Heid,M.K., Bills,N.D., Hinrichs,S.H., and Clifford,A.J. (1992). Folate deficiency alone does not produce neural tube defects in mice. *J. Nutr.,* **122,** 888-894.

Heil,S.G., van der Put,N.M., Waas,E.T., Den Heijer,M., Trijbels,F.J., and Blom,H.J. (2001). Is mutated serine hydroxymethyltransferase (SHMT) involved in the etiology of neural tube defects? *Mol. Genet. Metab,* **73,** 164-172.

Hemberger,M. (2002). The role of the X chromosome in mammalian extra embryonic development. *Cytogenet. Genome Res.,* **99,** 210-217.

Henderson,D.J., Conway,S.J., and Copp,A.J. (1999). Rib truncations and fusions in the Sp^{2H} mouse reveal a role for Pax3 in specification of the ventro-lateral and posterior parts of the somite. *Dev. Biol.,* **209,** 143-158.

Hendrich,B. and Bird,A. (1998). Identification and characterization of a family of mammalian methyl-CpG binding proteins. *Mol. Cell Biol.,* **18,** 6538-6547.

Herrera,E., Samper,E., and Blasco,M.A. (1999). Telomere shortening in mTR-/- embryos is associated with failure to close the neural tube. *EMBO J,* **18,** 1172-1181.

Hertrampf,E., Cortes,F., Erickson,J.D., Cayazzo,M., Freire,W., Bailey,L.B., Howson,C., Kauwell,G.P., and Pfeiffer,C. (2003). Consumption of folic acid-fortified bread improves folate status in women of reproductive age in Chile. *J. Nutr.,* **133,** 3166-3169.

Hildebrand,J.D. and Soriano,P. (1999). Shroom, a PDZ domain-containing actin-binding protein, is required for neural tube morphogenesis in mice. *Cell,* **99,** 485-497.

Hishida,R. and Nau,H. (1998). VPA-induced neural tube defects in mice. I. Altered metabolism of sulfur amino acids and glutathione. *Teratogenesis Carcinog. Mutagen.*, **18,** 49-61.

Holmberg,J., Clarke,D.L., and Frisén,J. (2000). Regulation of repulsion versus adhesion by different splice forms of an Eph receptor. *Nature,* **408,** 203-206.

Holmes,L.B., Driscoll,S.G., and Atkins,L. (1976). Etiologic heterogeneity of neural-tube defects. *N. Engl. J. Med.,* **294,** 365-369.

Homanics,G.E., Maeda,N., Traber,M.G., Kayden,H.J., Dehart,D.B., and Sulik,K.K. (1995). Exencephaly and hydrocephaly in mice with targeted modification of the apolipoprotein B (*Apob*) gene. *Teratology.,* **51,** 1-10.

Honarpour,N., Gilbert,S.L., Lahn,B.T., Wang,X.D., and Herz,J. (2001). *Apaf-1* deficiency and neural tube closure defects are found in fog mice. *Proc. Natl. Acad. Sci. USA,* **98,** 9683-9687.

Ikeda,A., Ikeda,S., Gridley,T., Nishina,P.M., and Naggert,J.K. (2001). Neural tube defects and neuroepithelial cell death in *Tulp3* knockout mice. *Hum. Mol. Genet.,* **10,** 1325-1334.

Ingrosso,D., Cimmino,A., Perna,A.F., Masella,L., De Santo,N.G., De Bonis,M.L., Vacca,M., D'Esposito,M., D'Urso,M., Galletti,P., and Zappia,V. (2003). Folate treatment and unbalanced methylation and changes of allelic expression induced by hyperhomocysteinaemia in patients with uraemia. *Lancet,* **361,** 1693-1699.

Ishibashi,M., Ang,S.-L., Shiota,K., Nakanishi,S., Kageyama,R., and Guillemot,F. (1995). Targeted disruption of mammalian *hairy* and *Enhancer of split* homolog-1 (*HES-1*) leads to up-regulation of neural helix-loop-helix factors, premature neurogenesis, and severe neural tube defects. *Genes Dev.,* **9,** 3136-3148.

Jakubowski,H. (1999). Protein homocysteinylation: possible mechanism underlying pathological consequences of elevated homocysteine levels. *FASEB J.,* **13,** 2277-2283.

Jakubowski,H. (1997). Metabolism of homocysteine thiolactone in human cell cultures. Possible mechanism for pathological consequences of elevated homocysteine levels. *J. Biol. Chem.,* **272,** 1935-1942.

Jakubowski,H. and Fersht,A.R. (1981). Alternative pathways for editing non-cognate amino acids by aminoacyl-tRNA synthetases. *Nucleic Acids Res.,* **9,** 3105-3117.

Jakubowski,H. and Goldman,E. (1993). Synthesis of homocysteine thiolactone by methionyl-tRNA synthetase in cultured mammalian cells. *FEBS Lett.,* **317,** 237-240.

Janerich,D.T. (1973). Epidemic waves in the prevalence of anencephaly and spina bifida in New York State. *Teratology.,* **8,** 253-256.

Janerich,D.T. and Piper,J. (1978). Shifting genetic patterns in anencephaly and spina bifida. *J. Med. Genet.,* **15,** 101-105.

Johnson,W.G., Stenroos,E.S., Spychala,J.R., Chatkupt,S., Ming,S.X., and Buyske,S. (2004). New 19 bp deletion polymorphism in intron-1 of dihydrofolate reductase (DHFR): a risk factor for spina bifida acting in mothers during pregnancy? *Am. J. Med. Genet.,* **124A,** 339-345.

Jones,P.A. and Takai,D. (2001). The role of DNA methylation in mammalian epigenetics. *Science,* **293,** 1068-1070.

Juriloff,D.M. and Harris,M.J. (2000). Mouse models for neural tube closure defects. *Hum. Mol. Genet.,* **9,** 993-1000.

Juriloff,D.M., Harris,M.J., Tom,C., and MacDonald,K.B. (1991). Normal mouse strains differ in the site of initiation of closure of the cranial neural tube. *Teratology.*, **44,** 225-233.

Kao,J., Brown,N.A., Schmid,B.P., Goulding,W.H., and Fabro,S. (1981). Teratogenicity of valproic acid: in vivo and in vitro investigations. *Teratogenesis Carcinog. Mutagen.*, **1,** 367-376.

Kaufman,M.H. (1979). Cephalic neurulation and optic vesicle formation in the early mouse embryo. *Am. J. Anat.*, **155,** 425-444.

Kibar,Z., Vogan,K.J., Groulx,N., Justice,M.J., Underhill,D.A., and Gros,P. (2001). *Ltap*, a mammalian homolog of *Drosophila Strabismus/Van Gogh*, is altered in the mouse neural tube mutant Loop-tail. *Nature Genet.*, **28,** 251-255.

Killmann,S.A. (1964). Effect of deoxyuridine on incorporatin of tritiated thymidine: Difference between normoblasts and megaloblasts. *Acta Med. Scand.*, **175,** 483-488.

Kim,Y.I. (2004). Will mandatory folic acid fortification prevent or promote cancer? *Am. J. Clin. Nutr.*, **80,** 1123-1128.

Kioussi,C., Gross,M.K., and Gruss,P. (1995). Pax3: a paired domain gene as a regulator in PNS myelination. *Neuron,* **15,** 553-562.

Kirke,P.N. and Elwood,J.H. (1984). Anencephaly in the United Kingdom and Republic of Ireland. *Br. Med. J. (Clin. Res. Ed),* **289,** 1621.

Kirke,P.N., Molloy,A.M., Daly,L.E., Burke,H., Weir,D.G., and Scott,J.M. (1993). Maternal plasma folate and vitamin B_{12} are independent risk factors for neural tube defects. *Q. J. Med.*, **86,** 703-708.

Koch,M.C., Stegmann,K., Ziegler,A., Schröter,B., and Ermert,A. (1998). Evaluation of the MTHFR C677T allele and the MTHFR gene locus in a German spina bifida population. *Eur. J. Pediatr.*, **157,** 487-492.

Koleske,A.J., Gifford,A.M., Scott,M.L., Nee,M., Bronson,R.T., Miczek,K.A., and Baltimore,D. (1998). Essential roles for the Abl and Arg tyrosine kinases in neurulation. *Neuron,* **21,** 1259-1272.

Kuan,C.Y., Yang,D.D., Roy,D.R.S., Davis,R.J., Rakic,P., and Flavell,R.A. (1999). The Jnk1 and Jnk2 protein kinases are required for regional specific apoptosis during early brain development. *Neuron,* **22,** 667-676.

Kuida,K., Haydar,T.F., Kuan,C.Y., Gu,Y., Taya,C., Karasuyama,H., Su,M.S., Rakic,P., and Flavell,R.A. (1998). Reduced apoptosis and cytochrome c-mediated caspase activation in mice lacking caspase 9. *Cell,* **94,** 325-337.

Kusumi,K., Sun,E.S., Kerrebrock,A.W., Bronson,R.T., Chi,D.-C., Bulotsky,M.S., Spencer,J.B., Birren,B.W., Frankel,W.N., and Lander,E.S. (1998). The mouse pudgy mutation disrupts *Delta* homologue *Dll3* and initiation of early somite boundaries. *Nature Genet.*, **19,** 274-278.

Kutzbach,C. and Stokstad,E.L. (1971). Mammalian methylenetetrahydrofolate reductase. Partial purification, properties, and inhibition by S-adenosylmethionine. *Biochim. Biophys. Acta,* **250,** 459-477.

Lang,D., Lu,M.M., Huang,L., Engleka,K.A., Zhang,M., Chu,E.Y., Lipner,S., Skoultchi,A., Millar,S.E., and Epstein,J.A. (2005). Pax3 functions at a nodal point in melanocyte stem cell differentiation. *Nature,* **433,** 884-887.

Lanier,L.M., Gates,M.A., Witke,W., Menzies,A.S., Wehman,A.M., Macklis,J.D., Kwiatkowski,D., Soriano,P., and Gertler,F.B. (1999). Mena is required for neurulation and commissure formation. *Neuron,* **22,** 313-325.

Leck,I. (1966). Changes in the incidence of neural-tube defects. *Lancet,* **2,** 791-793.

Leclerc,D., Campeau,E., Goyette,P., Adjalla,C.E., Christensen,B., Ross,M., Eydoux,P., Rosenblatt,D.S., Rozen,R., and Gravel,R.A. (1996). Human methionine synthase: CDNA cloning and identification of mutations in patients of the *cblG* complementation group of folate/cobalamin disorders. *Hum. Mol. Genet.,* **5,** 1867-1874.

Leclerc,D., Wilson,A., Dumas,R., Gafuik,C., Song,D., Watkins,D., Heng,H.H.Q., Rommens,J.M., Scherer,S.W., Rosenblatt,D.S., and Gravel,R.A. (1998). Cloning and mapping of a cDNA for methionine synthase reductase, a flavoprotein defective in patients with homocystinuria. *Proc. Natl. Acad. Sci. USA,* **95,** 3059-3064.

Lewis,J. (1998). Notch signalling and the control of cell fate choices in vertebrates. *Semin. Cell Dev. Biol.,* **9,** 583-589.

Li,Q.T., Estepa,G., Memet,S., Israel,A., and Verma,I.M. (2000). Complete lack of NF-kappaB activity in IKK1 and IKK2 double-deficient mice: additional defect in neurulation. *Genes Dev.,* **14,** 1729-1733.

Liu,S., West,R., Randell,E., Longerich,L., O'connor,K.S., Scott,H., Crowley,M., Lam,A., Prabhakaran,V., and McCourt,C. (2004). A comprehensive evaluation of food fortification with folic acid for the primary prevention of neural tube defects. *BMC. Pregnancy. Childbirth.,* **4,** 20.

Lloyd,J.B., Brent,R.L., and Beckman,D.A. (1996). Sources of amino acids for protein synthesis during early organogenesis in the rat. 3. Methionine incorporation. *Placenta,* **17,** 629-634.

Loeken,M.R. (2005). Current perspectives on the causes of neural tube defects resulting from diabetic pregnancy. *Am. J. Med. Genet. C. Semin. Med. Genet.*, **135,** 77-87.

Lombardini,J.B. and Talalay,P. (1970). Formation, functions and regulatory importance of S-adenosyl-L-methionine. *Adv. Enzyme Regul.*, **9,** 349-384.

Lucock,M. (2000). Folic acid: nutritional biochemistry, molecular biology, and role in disease processes. *Mol. Genet. Metab,* **71,** 121-138.

Lucock,M.D., Wild,J., Schorah,C.J., Levene,M.I., and Hartley,R. (1994). The methylfolate axis in neural tube defects: in vitro characterisation and clinical investigation. *Biochem. Med. Metab Biol,* **52,** 101-114.

Lynch,S.A. (2005). Non-multifactorial neural tube defects. *Am. J. Med. Genet. C. Semin. Med. Genet.*, **135,** 69-76.

MacDonald,K.B., Juriloff,D.M., and Harris,M.J. (1989). Developmental study of neural tube closure in a mouse stock with a high incidence of exencephaly. *Teratology.*, **39,** 195-213.

Machado,A.F., Martin,L.J., and Collins,M.D. (2001). Pax3 and the splotch mutations: structure, function, and relationship to teratogenesis, including gene-chemical interactions. *Curr. Pharm. Des,* **7,** 751-785.

Maclean,M.H. and MacLeod,A. (1984). Seasonal variation in the frequency of anencephalus and spina bifida births in the United Kingdom. *J. Epidemiol. Community Health,* **38,** 99-102.

MacMahon,B. and Yen,S. (1971). Unrecognised epidemic of anencephaly and spina bifida. *Lancet,* **1,** 31-33.

Malone,C.S., Miner,M.D., Doerr,J.R., Jackson,J.P., Jacobsen,S.E., Wall,R., and Teitell,M. (2001). CmC(A/T)GG DNA methylation in mature B cell lymphoma gene silencing. *Proc. Natl. Acad. Sci. USA,* **98,** 10404-10409.

Mann,R.A. and Persaud,T.V. (1979). Morphology of experimental spina bifida in the chick embryo. *Anat. Anz.,* **145,** 182-191.

Mansouri,A., Pla,P., Larue,L., and Gruss,P. (2001). *Pax3* acts cell autonomously in the neural tube and somites by controlling cell surface properties. *Development.,* **128,** 1995-2005.

Marasas,W.F.O., Riley,R.T., Hendricks,K.A., Stevens,V.L., Sadler,T.W., Gelineau-van Waes,J., Missmer,S.A., Cabrera,J., Torres,O., Gelderblom,W.C.A., Allegood,J., Martinez,C., Maddox,J., Miller,J.D., Starr,L., Sullards,M.C., Roman,A.V., Voss,K.A., Wang,E., and Merrill,A.H. (2004). Fumonisins disrupt sphingolipid metabolism, folate transport, and neural tube development in embryo culture and in vivo: a potential risk factor for human neural tube defects among populations consuming fumonisin-contaminated maize. *J. Nutr.,* **134,** 711-716.

Martinez-Barbera,J.P., Rodriguez,T.A., Greene,N.D.E., Weninger,W.J., Simeone,A., Copp,A.J., Beddington,R., and Dunwoodie,S. (2002). Folic acid prevents exencephaly in *Cited2* deficient mice. *Hum. Mol. Genet.,* **11,** 283-293.

Martinez-Frias,M.L., Urioste,M., Bermejo,E., Sanchis,A., and Rodriquez-Pinilla,E. (1996). Epidemiological analysis of multi-site closure failure of neural tube in humans. *Am. J. Med. Genet.,* **66,** 64-68.

Matthews,R.G., Sheppard,C., and Goulding,C. (1998). Methylenetetrahydrofolate reductase and methionine synthase: biochemistry and molecular biology. *Eur. J. Pediatr.,* **157 Suppl. 2,** S54-S59.

McGuire,J.J. (2003). Anticancer antifolates: current status and future directions. *Curr. Pharm. Des,* **9,** 2593-2613.

McKeever,M.P., Weir,D.G., Molloy,A., and Scott,J.M. (1991). Betaine-homocysteine methyltransferase: organ distribution in man, pig and rat and subcellular distribution in the rat. *Clin. Sci. (Lond),* **81,** 551-556.

Migliorini,D., Denchi,E.L., Danovi,D., Jochemsen,A., Capillo,M., Gobbi,A., Helin,K., Pelicci,P.G., and Marine,J.C. (2002). Mdm4 (Mdmx) regulates p53-induced growth arrest and neuronal cell death during early embryonic mouse development. *Mol. Cell Biol.,* **22,** 5527-5538.

Milakofsky,L., Hare,T.A., Miller,J.M., and Vogel,W.H. (1984). Comparison of amino acid levels in rat blood obtained by catheterization and decapitation. *Life Sci.,* **34,** 1333-1340.

Miller,J.W., Nadeau,M.R., Smith,J., Smith,D., and Selhub,J. (1994). Folate-deficiency-induced homocysteinaemia in rats: disruption of S-adenosylmethionine's co-ordinate regulation of homocysteine metabolism. *Biochem. J,* **298 (Pt 2),** 415-419.

Mills,J.L., McPartlin,J.M., Kirke,P.N., Lee,Y.J., Conley,M.R., Weir,D.G., and Scott,J.M. (1995). Homocysteine metabolism in pregnancies complicated by neural-tube defects. *Lancet,* **345,** 149-151.

Mills,J.L. and Signore,C. (2004). Neural tube defect rates before and after food fortification with folic acid. *Birth Defects Res. Part A Clin. Mol. Teratol.,* **70,** 844-845.

Mills,J.L., Tuomilehto,J., Yu,K.F., Colman,N., Blaner,W.S., Koskela,P., Rundle,W.E., Forman,M., Toivanen,L., and Rhoads,G.G. (1992). Maternal vitamin levels during pregnancies producing infants with neural tube defects. *J. Pediatr.,* **120,** 863-871.

Milunsky,A., Jick,H., Jick,S.S., Bruell,C.L., MacLaughlin,D.S., Rothman,K.J., and Willett,W. (1989). Multivitamin/folic acid supplementation in early pregnancy reduces the prevalence of neural tube defects. *JAMA,* **262,** 2847-2852.

Mirkes,P.E., Little,S.A., and Umpierre,C.C. (2001). Co-localization of active caspase-3 and DNA fragmentation (TUNEL) in normal and hyperthermia-induced abnormal mouse development. *Teratology.,* **63,** 134-143.

Moase,C.E. and Trasler,D.G. (1989). Spinal ganglia reduction in the splotch-delayed mouse neural tube defect mutant. *Teratology.,* **40,** 67-75.

Moephuli,S.R., Klein,N.W., Baldwin,M.T., and Krider,H.M. (1997). Effects of methionine on the cytoplasmic distribution of actin and tubulin during neural tube closure in rat embryos. *Proc. Natl. Acad. Sci. USA,* **94,** 543-548.

Morris-Wiman,J. and Brinkley,L.L. (1990). Changes in mesenchymal cell and hyaluronate distribution correlate with in vivo elevation of the mouse mesencephalic neural folds. *Anat. Rec.,* **226,** 383-395.

Morrison,K., Edwards,Y.H., Lynch,S.A., Burn,J., Hol,F., and Mariman,E. (1997). Methionine synthase and neural tube defects. *J. Med. Genet.,* **34,** 958.

Morriss,G.M. and New,D.A.T. (1979). Effect of oxygen concentration on morphogenesis of cranial neural folds and neural crest in cultured rat embryos. *J. Embryol. Exp. Morphol.,* **54,** 17-35.

Morriss,G.M. and Solursh,M. (1978a). Regional differences in mesenchymal cell morphology and glycosaminoglycans in early neural-fold stage rat embryos. *J. Embryol. Exp. Morphol.,* **46,** 37-52.

Morriss,G.M. and Solursh,M. (1978b). The role of primary mesenchyme in normal and abnormal morphogenesis of mammalian neural folds. *Zoon,* **6,** 33-38.

Morriss,G.M. and Steele,C.E. (1974). The effect of excess vitamin A on the development of rat embryos in culture. *J. Embryol. Exp. Morphol.,* **32,** 505-514.

Morriss-Kay,G., Wood,H., and Chen,W.-H. (1994). Normal neurulation in mammals. *Ciba. Found. Symp.,* **181,** 51-63.

Morriss-Kay,G.M. (1981). Growth and development of pattern in the cranial neural epithelium of rat embryos during neurulation. *J. Embryol. Exp. Morphol.,* **65 (Suppl.),** 225-241.

Morriss-Kay,G.M. and Crutch,B. (1982). Culture of rat embryos with beta-D-xyloside: evidence of a role for proteoglycans in neurulation. *J Anat,* **134 (Pt 3),** 491-506.

Morriss-Kay,G.M. and Tuckett,F. (1985). The role of microfilaments in cranial neurulation in rat embryos: effects of short-term exposure to cytochalasin D. *J. Embryol. Exp. Morphol.,* **88,** 333-348.

Mulinare,J., Cordero,J.F., Erickson,J.D., and Berry,R.J. (1988). Periconceptional use of multivitamins and the occurrence of neural tube defects. *JAMA,* **260,** 3141-3145.

Müller,F. and O'Rahilly,R. (1987). The development of the human brain, the closure of the caudal neuropore, and the beginning of secondary neurulation at stage 12. *Anat. Embryol.,* **176,** 413-430.

Murdoch,J.N., Doudney,K., Paternotte,C., Copp,A.J., and Stanier,P. (2001). Severe neural tube defects in the *loop-tail* mouse result from mutation of *Lpp1*, a novel gene involved in floor plate specification. *Hum. Mol. Genet.,* **10,** 2593-2601.

Murdoch,J.N., Henderson,D.J., Doudney,K., Gaston-Massuet,C., Phillips,H.M., Paternotte,C., Arkell,R., Stanier,P., and Copp,A.J. (2003). Disruption of *scribble* (*Scrb1*) causes severe neural tube defects in the *circletail* mouse. *Hum. Mol. Genet.,* **12,** 87-98.

Myers,C.E., Young,R.C., and Chabner,B.A. (1975). Biochemical determinants of 5-fluorouracil response in vivo. The role of deoxyuridylate pool expansion. *J Clin. Invest,* **56,** 1231-1238.

Naggan,L. and MacMahon,B. (1967). Ethnic differences in the prevalence of anencephaly and sina bifida in Boston, Massachusetts. *N. Engl. J. Med.,* **277,** 1119-1123.

Nakatsu,T., Uwabe,C., and Shiota,K. (2000). Neural tube closure in humans initiates at multiple sites: evidence from human embryos and implications for the pathogenesis of neural tube defects. *Anat. Embryol.,* **201,** 455-466.

Neubert,D. and Dillmann,I. (1972). Embryotoxic effects in mice treated wtih 2,4,5-trichlorophenoxyacetic acid and 2,3,7,8-tetrachlorodibenzo-p-dioxin. *Naunyn Schmiedebergs Arch. Pharmacol.,* **272,** 243-264.

Neumann,P.E., Frankel,W.N., Letts,V.A., Coffin,J.M., Copp,A.J., and Bernfield,M. (1994). Multifactorial inheritance of neural tube defects: Localization of the major gene and recognition of modifiers in *ct* mutant mice. *Nature Genet.,* **6,** 357-362.

Nishimura,K., Nakatsu,F., Kashiwagi,K., Ohno,H., Saito,T., and Igarashi,K. (2002). Essential role of S-adenosylmethionine decarboxylase in mouse embryonic development. *Genes Cells,* **7,** 41-47.

O'Leary,V.B., Mills,J.L., Kirke,P.N., Parle-McDermott,A., Swanson,D.A., Weiler,A., Pangilinan,F., Conley,M., Molloy,A.M., Lynch,M., Cox,C., Scott,J.M., and Brody,L.C. (2003). Analysis of the human folate receptor beta gene for an association with neural tube defects. *Mol. Genet. Metab,* **79,** 129-133.

O'Leary,V.B., Mills,J.L., Pangilinan,F., Kirke,P.N., Cox,C., Conley,M., Weiler,A., Peng,K., Shane,B., Scott,J.M., Parle-McDermott,A., Molloy,A.M., and Brody,L.C. (2005). Analysis of methionine synthase reductase polymorphisms for neural tube defects risk association. *Mol. Genet. Metab,* **85,** 220-227.

O'Rahilly,R. and Müller,F. (2002). The two sites of fusion of the neural folds and the two neuropores in the human embryo. *Teratology.,* **65,** 162-170.

Okano,M., Bell,D.W., Haber,D.A., and Li,E. (1999). DNA methyltransferases Dnmt3a and Dnmt3b are essential for de novo methylation and mammalian development. *Cell,* **99,** 247-257.

Olteanu,H., Wolthers,K.R., Munro,A.W., Scrutton,N.S., and Banerjee,R. (2004). Kinetic and thermodynamic characterization of the common polymorphic variants of human methionine synthase reductase. *Biochemistry,* **43,** 1988-1997.

Padmanabhan,R. and Shafiullah,M.M. (2003). Amelioration of sodium valproate-induced neural tube defects in mouse fetuses by maternal folic acid supplementation during gestation. *Congenit. Anom. (Kyoto),* **43,** 29-40.

Pani,L., Horal,M., and Loeken,M.R. (2002). Rescue of neural tube defects in Pax-3-deficient embryos by p53 loss of function: implications for Pax-3-dependent development and tumorigenesis. *Genes Dev.,* **16,** 676-680.

Papapetrou,C., Lynch,S.A., Burn,J., and Edwards,Y.H. (1996). Methylenetetrahydrofolate reductase and neural tube defects. *Lancet,* **348,** 58.

Parle-McDermott,A., Mills,J.L., Kirke,P.N., O'Leary,V.B., Swanson,D.A., Pangilinan,F., Conley,M., Molloy,A.M., Cox,C., Scott,J.M., and Brody,L.C. (2003). Analysis of the MTHFR 1298A-->C and 677C-->T polymorphisms as risk factors for neural tube defects. *J. Hum. Genet.,* **48,** 190-193.

Peeters,M.C.E., Hekking,J.W.M., Shiota,K., Drukker,J., and Van Straaten,H.W.M. (1998a). Differences in axial curvature correlate with species-specific rate of neural tube closure in embryos of chick, rabbit, mouse, rat and human. *Anat. Embryol.,* **198,** 185-194.

Peeters,M.C.E., Viebahn,C., Hekking,J.W.M., and Van Straaten,H.W.M. (1998b). Neurulation in the rabbit embryo. *Anat. Embryol.,* **197,** 167-175.

Pei,L., Zhu,H., Ren,A., Li,Z., Hao,L., Finnell,R.H., and Li,Z. (2005). Reduced folate carrier gene is a risk factor for neural tube defects in a Chinese population. *Birth Defects Res. A Clin. Mol. Teratol.,* **73,** 430-433.

Pendeville,H., Carpino,N., Marine,J.C., Takahashi,Y., Muller,M., Martial,J.A., and Cleveland,J.L. (2001). The ornithine decarboxylase gene is essential for cell survival during early murine development. *Mol. Cell Biol,* **21,** 6549-6558.

Perez,A.B., D'Almeida,V., Vergani,N., de Oliveira,A.C., de Lima,F.T., and Brunoni,D. (2003). Methylenetetrahydrofolate reductase (MTHFR): incidence of mutations C677T and A1298C in Brazilian population and its correlation with plasma homocysteine levels in spina bifida. *Am. J. Med. Genet.,* **119A,** 20-25.

Phelan,S.A., Ito,M., and Loeken,M.R. (1997). Neural tube defects in embryos of diabetic mice - Role of the Pax-3 gene and apoptosis. *Diabetes,* **46,** 1189-1197.

Piedrahita,J.A., Oetama,B., Bennett,G.D., Van Waes,J., Kamen,B.A., Richardson,J., Lacey,S.W., Anderson,R.G.W., and Finnell,R.H. (1999). Mice lacking the folic acid-binding protein Folbp1 are defective in early embryonic development. *Nature Genet.*, **23,** 228-232.

Pietrzyk,J.J. and Bik-Multanowski,M. (2003). 776C>G polymorphism of the transcobalamin II gene as a risk factor for spina bifida. *Mol. Genet. Metab,* **80,** 364.

Pugarelli,J.E., Brent,R.L., and Lloyd,J.B. (1999). Effects of methionine supplement on methionine incorporation in rat embryos cultured in vitro. *Teratology.,* **60,** 6-9.

Rader,J.I. (2002). Folic acid fortification, folate status and plasma homocysteine. *J. Nutr.,* **132,** 2466S-2470S.

Rader,J.I. and Yetley,E.A. (2002). Nationwide folate fortification has complex ramifications and requires careful monitoring over time. *Arch. Intern. Med.,* **162,** 608-609.

Rampersaud,E., Melvin,E.C., Siegel,D., Mehltretter,L., Dickerson,M.E., George,T.M., Enterline,D., Nye,J.S., and Speer,M.C. (2003). Updated investigations of the role of methylenetetrahydrofolate reductase in human neural tube defects. *Clin. Genet.,* **63,** 210-214.

Rankin,J., Glinianaia,S., Brown,R., and Renwick,M. (2000). The changing prevalence of neural tube defects: a population-based study in the north of England, 1984-96. Northern Congenital Abnormality Survey Steering Group. *Paediatr. Perinat. Epidemiol.,* **14,** 104-110.

Ray,J.G. and Blom,H.J. (2003). Vitamin B12 insufficiency and the risk of fetal neural tube defects. *Q. J. Med.,* **96,** 289-295.

Reeves,F.C., Burdge,G.C., Fredericks,W.J., Rauscher,F.J., and Lillycrop,K.A. (1999). Induction of antisense Pax-3 expression leads to the rapid morphological differentiation of neuronal cells and an altered response to the mitogenic growth factor bFGF. *J Cell Sci.,* **112 (Pt 2),** 253-261.

Reeves,F.C., Fredericks,W.J., Rauscher,F.J., III, and Lillycrop,K.A. (1998). The DNA binding activity of the paired box transcription factor Pax-3 is rapidly downregulated during neuronal cell differentiation. *FEBS Lett.,* **422,** 118-122.

Relton,C.L., Wilding,C.S., Pearce,M.S., Laffling,A.J., Jonas,P.A., Lynch,S.A., Tawn,E.J., and Burn,J. (2004). Gene-gene interaction in folate-related genes and risk of neural tube defects in a UK population. *J Med. Genet.,* **41,** 256-260.

Renwick,J.H. (1972). Hypothesis: Anencephaly and spina bifida are usually preventable by avoidance of a specific but unidentified substance present in certain potato tubers. *Br. J. prev. soc. Med.,* **26,** 67-88.

Reynolds,E.H. (2002). Benefits and risks of folic acid to the nervous system. *J. Neurol. Neurosurg. Psychiatry,* **72,** 567-571.

Robert,E. and Guidbaud,P. (1982). Maternal valproic acid and congenital neural tube defects. *Lancet,* **2,** 937.

Rosenquist,T.H., Ratashak,S.A., and Selhub,J. (1996). Homocysteine induces congenital defects of the heart and neural tube: Effect of folic acid. *Proc. Natl. Acad. Sci. USA,* **93,** 15227-15232.

Ruland,J., Duncan,G.S., Elia,A., Barrantes,I.D., Nguyen,L., Plyte,S., Millar,D.G., Bouchard,D., Wakeham,A., Ohashi,P.S., and Mak,T.W. (2001). Bcl10 is a positive regulator of antigen receptor-induced activation of NF-kappaB and neural tube closure. *Cell,* **104,** 33-42.

Russell,W.L. (1947). Splotch: a new mutation in the house mouse. *Genetics,* **32,** 350-358.

Sadler,T.W., Merrill,A.H., Stevens,V.L., Sullards,M.C., Wang,E., and Wang,P. (2002). Prevention of fumonisin B1-induced neural tube defects by folic acid. *Teratology.,* **66,** 169-176.

Sakai,Y. (1989). Neurulation in the mouse: manner and timing of neural tube closure. *Anat. Rec.,* **223,** 194-203.

Schluter,G. (1973). Ultrastructural observations on cell necrosis during formation of the neural tube in mouse embryos. *Z. Anat. Entwickl. -Gesch.,* **141,** 251-264.

Schoenwolf,G.C. (1984). Histological and ultrastructural studies of secondary neurulation of mouse embryos. *Am. J. Anat.,* **169,** 361-374.

Schoenwolf,G.C., Folsom,D., and Moe,A. (1988). A reexamination of the role of microfilaments in neurulation in the chick embryo. *Anat. Rec.,* **220,** 87-102.

Schoenwolf,G.C. and Smith,J.L. (1990). Mechanisms of neurulation: Traditional viewpoint and recent advances. *Development.,* **109,** 243-270.

Schorle,H., Meier,P., Buchert,M., Jaenisch,R., and Mitchell,P.J. (1996). Transcription factor AP-2 essential for cranial closure and craniofacial development. *Nature,* **381,** 235-238.

Schubert,F.R., Tremblay,P., Mansouri,A., Faisst,A.M., Kammandel,B., Lumsden,A., Gruss,P., and Dietrich,S. (2001). Early mesodermal phenotypes in Splotch suggest a role for Pax3 in the formation of epithelial somites. *Dev. Dyn.,* **222,** 506-521.

Scott,J.M., Weir,D.G., Molloy,A., McPartlin,J., Daly,L., and Kirke,P. (1994). Folic acid metabolism and mechanisms of neural tube defects. In Bock,G. and Marsh,J. (Eds.), *Neural Tube Defects (Ciba Foundation Symposium 181)*, . John Wiley & Sons, Chichester, pp. 180-187.

Seller,M.J. (1987). Neural tube defects and sex ratios. *Am. J. Med. Genet.*, **26,** 699-707.

Seller,M.J. (1994). Vitamins, folic acid and the cause and prevention of neural tube defects. In Bock,G. and Marsh,J. (Eds.), *Neural Tube Defects (Ciba Foundation Symposium 181)*, . John Wiley & Sons, Chichester, pp. 161-173.

Seller,M.J. (1995). Multi-site neural tube closure in humans and maternal folate supplementation. *Am. J. Med. Genet.*, **58,** 222-224.

Seller,M.J. and Adinolfi,M. (1981). The curly-tail mouse: an experimental model for human neural tube defects. *Life Sci.*, **29,** 1607-1615.

Sever,L.E. (1982). An epidemiologic study of neural tube defects in Los Angeles County II. Etiologic factors in an area with low prevalence at birth. *Teratology.*, **25,** 323-334.

Shaw,G.M., Velie,E.M., and Schaffer,D.M. (1997). Is dietary intake of methionine associated with a reduction in risk for neural tube defect-affected pregnancies. *Teratology.*, **56,** 295-299.

Shields,D.C., Kirke,P.N., Mills,J.L., Ramsbottom,D., Molloy,A.M., Burke,H., Weir,D.G., Scott,J.M., and Whitehead,A.S. (1999). The "thermolabile" variant of methylenetetrahydrofolate reductase and neural tube defects: An evaluation of genetic risk and the relative importance of the genotypes of the embryo and the mother. *Am. J. Hum. Genet.*, **64,** 1045-1055.

Shin,J.H. and Shiota,K. (1999). Folic acid supplementation of pregnant mice suppresses heat- induced neural tube defects in the offspring. *J. Nutr.,* **129,** 2070-2073.

Shiota,K. (1988). Induction of neural tube defects and skeletal malformations in mice following brief hyperthermia in utero. *Biol. Neonate,* **53,** 86-97.

Shoob,H.D., Sargent,R.G., Thompson,S.J., Best,R.G., Drane,J.W., and Tocharoen,A. (2001). Dietary methionine is involved in the etiology of neural tube defect-affected pregnancies in humans. *J. Nutr.,* **131,** 2653-2658.

Shum,A.S.W. and Copp,A.J. (1996). Regional differences in morphogenesis of the neuroepithelium suggest multiple mechanisms of spinal neurulation in the mouse. *Anat. Embryol.,* **194,** 65-73.

Smithells,R.W., Ankers,C., Carver,M.E., Lennon,D., Schorah,C.J., and Sheppard,S. (1977). Maternal nutrition in early pregnancy. *Br. J Nutr.,* **38,** 497-506.

Smithells,R.W., Sheppard,S., and Schorah,C.J. (1976). Vitamin deficiencies and neural tube defects. *Arch. Dis. Child.,* **51,** 944-950.

Smithells,R.W., Sheppard,S., Schorah,C.J., Seller,M.J., Nevin,N.C., Harris,R., Read,A.P., and Fielding,D.W. (1981). Apparent prevention of neural tube defects by periconceptional vitamin supplementation. *Arch. Dis. Child.,* **56,** 911-918.

Snyder,R.D., Fakadej,A.F., and Riggs,J.E. (1991). Anencephaly in the United States, 1968-1987: the declining incidence among white infants. *J. Child Neurol.,* **6,** 304-305.

Solloway,M.J. and Robertson,E.J. (1999). Early embryonic lethality in *Bmp5;Bmp7* double mutant mice suggests functional redundancy within the 60A subgroup. *Development.,* **126,** 1753-1768.

Steegers-Theunissen,R.P.M., Boers,G.H.J., Trijbels,F.J.M., Finkelstein,J.D., Blom,H.J., Thomas,C.M.G., Borm,G.F., Wouters,M.G.A.J., and Eskes,T.K.A.B. (1994). Maternal hyperhomocysteinemia: A risk factor for neural tube defects. *Metabolism,* **43,** 1475-1480.

Steen,M.T., Boddie,A.M., Fisher,A.J., Macmahon,W., Saxe,D., Sullivan,K.M., Dembure,P.P., and Elsas,L.J. (1998). Neural-tube defects are associated with low concentrations of cobalamin (vitamin B_{12}) in amniotic fluid. *Prenatal Diag.,* **18,** 545-555.

Stone,D.H. (1987). The declining prevalence of anencephalus and spina bifida: its nature, causes and implications. *Dev. Med. Child Neurol.,* **29,** 541-546.

Stuart,E.T., Haffner,R., Oren,M., and Gruss,P. (1995). Loss of p53 function through PAX-mediated transcriptional repression. *EMBO J.,* **14,** 5638-5645.

Stumpo,D.J., Bock,C.B., Tuttle,J.S., and Blackshear,P.J. (1995). MARCKS deficiency in mice leads to abnormal brain development and perinatal death. *Proc. Natl. Acad. Sci. USA,* **92,** 944-948.

Suarez,L., Felkner,M., and Hendricks,K. (2004). The effect of fever, febrile illnesses, and heat exposures on the risk of neural tube defects in a Texas-Mexico border population. *Birth Defects Res. A Clin. Mol. Teratol.,* **70,** 815-819.

Swanson,D.A., Pangilinan,F., Mills,J.L., Kirke,P.N., Conley,M., Weiler,A., Frey,T., Parle-McDermott,A., O'Leary,V.B., Seltzer,R.R., Moynihan,K.A., Molloy,A.M., Burke,H., Scott,J.M., and Brody,L.C. (2005). Evaluation of transcobalamin II polymorphisms as neural tube defect risk factors in an Irish population. *Birth Defects Res. A Clin. Mol. Teratol.,* **73,** 239-244.

Takeuchi,I.K. and Murakami,U. (1978). The preventive influence of cysteamine on the teratogenic action of 5-azacytidine. *Life Sci.*, **23,** 897-900.

Takeuchi,I.K. and Takeuchi,Y.K. (1985). 5-Azacytidine-induced exencephaly in mice. *J. Anat.*, **140,** 403-412.

Ting,S.B., Wilanowski,T., Auden,A., Hall,M., Voss,A.K., Thomas,T., Parekh,V., Cunningham,J.M., and Jane,S.M. (2003). Inositol- and folate-resistant neural tube defects in mice lacking the epithelial-specific factor Grhl-3. *Nature Med.*, **9,** 1513-1519.

Toriello,H.V. and Higgins,J.V. (1983). Occurrence of neural tube defects among first-, second-, and third-degree relatives of probands: results of a United States study. *Am. J. Med. Genet.*, **15,** 601-606.

Trotz,M., Wegner,C., and Nau,H. (1987). Valproic acid-induced neural tube defects: reduction by folinic acid in the mouse. *Life Sci.*, **41,** 103-110.

Tuckett,F. and Morriss-Kay,G.M. (1985). The kinetic behaviour of the cranial neural epithelium during neurulation in the rat. *J. Embryol. Exp. Morphol.*, **85,** 111-119.

Ueland,P.M. and Vollset,S.E. (2004). Homocysteine and folate in pregnancy. *Clin. Chem.*, **50,** 1293-1295.

Ueno,N. and Greene,N.D.E. (2003). Planar cell polarity genes and neural tube closure. *Birth Defects Research (Part C),* **69,** 318-324.

Van Allen,M.I., Kalousek,D.K., Chernoff,G.F., Juriloff,D., Harris,M., McGillivray,B.C., Yong,S.-L., Langlois,S., MacLeod,P.M., Chitayat,D., Friedman,J.M., Wilson,R.D., McFadden,D., Pantzar,J., Ritchie,S., and Hall,J.G. (1993). Evidence for multi-site closure of the neural tube in humans. *Am. J. Med. Genet.*, **47,** 723-743.

Van der Put,N.M.J., Gabreëls,F., Stevens,E.M.B., Smeitink,J.A.M., Trijbels,F.J.M., Eskes,T.K.A.B., Van den Heuvel,L.P., and Blom,H.J. (1998). A second common mutation in the methylenetetrahydrofolate reductase gene: An additional risk factor for neural-tube defects. *Am. J. Hum. Genet.,* **62,** 1044-1051.

Van der Put,N.M.J., Steegers-Theunissen,R.P.M., Frosst,P., Trijbels,F.J.M., Eskes,T.K.A.B., Van den Heuvel,L.P., Mariman,E.C.M., Den Heyer,M., Rozen,R., and Blom,H.J. (1995). Mutated methylenetetrahydrofolate reductase as a risk factor for spina bifida. *Lancet,* **346,** 1070-1071.

Van der Put,N.M.J., Thomas,C.M.G., Eskes,T.K.A.B., Trijbels,F.J.M., Steegers-Theunissen,R.P.M., Mariman,E.C.M., De Graaf-Hess,A., Smeitink,J.A.M., and Blom,H.J. (1997a). Altered folate and vitamin B_{12} metabolism in families with spina bifida offspring. *Q. J. Med.,* **90,** 505-510.

Van der Put,N.M.J., Van den Heuvel,L.P., Steegers-Theunissen,R.P.M., Trijbels,F.J.M., Eskes,T.K.A.B., Mariman,E.C.M., Den Heyer,M., and Blom,H.J. (1996). Decreased methylene tetrahydrofolate reductase activity due to the 677C-->T mutation in families with spina bifida offspring. *J. Mol. Med.,* **74,** 691-694.

Van der Put,N.M.J., Van der Molen,E.F., Kluijtmans,L.A.J., Heil,S.G., Trijbels,J.M.F., Eskes,T.K.A.B., Van Oppenraaij-Emmerzaal,D., Banerjee,R., and Blom,H.J. (1997b). Sequence analysis of the coding region of human methionine synthase: Relevance to hyperhomocysteinaemia in neural- tube defects and vascular disease. *Q. J. Med.,* **90,** 511-517.

Van der Put,N.M.J., Van Straaten,H.W.M., Trijbels,F.J.M., and Blom,H.J. (2001). Folate, homocysteine and neural tube defects: An overview. *Proceedings of the Society for Experimental Biology and Medicine,* **226,** 243-270.

Van Noorden,C.J. (2001). The history of Z-VAD-FMK, a tool for understanding the significance of caspase inhibition. *Acta Histochem.,* **103,** 241-251.

Van Straaten,H.W.M., Blom,H., Peeters,M.C.E., Rousseau,A.M.J., Cole,K.J., and Seller,M.J. (1995). Dietary methionine does not reduce penetrance in *curly tail* mice but causes a phenotype-specific decrease in embryonic growth. *J. Nutr.,* **125,** 2733-2740.

Van Straaten,H.W.M. and Copp,A.J. (2001). Curly tail: a 50-year history of the mouse spina bifida model. *Anat. Embryol.,* **203,** 225-237.

Van Straaten,H.W.M., Jansen,H.C.J.P., Peeters,M.C.E., Copp,A.J., and Hekking,J.W.M. (1996). Neural tube closure in the chick embryo is multiphasic. *Dev. Dyn.,* **207,** 309-318.

Van Straaten,H.W.M., Peeters,M.C.E., Hekking,J.W.M., and Van der Lende,T. (2000). Neurulation in the pig embryo. *Anat. Embryol.,* **202,** 75-84.

VanAerts,L.A.G.J.M., Blom,H.J., Deabreu,R.A., Trijbels,F.J.M., Eskes,T.K.A.B., Peereboom-Stegeman,J.H.J.C., and Noordhoek,J. (1994). Prevention of neural tube defects by and toxicity of L-homocysteine in cultured postimplantation rat embryos. *Teratology.,* **50,** 348-360.

VanAerts,L.A.G.J.M., Poirot,C.M., Herberts,C.A., Blom,H.J., De Abreu,R.A., Trijbels,J.M.F., Eskes,T.K.A.B., Peereboom-Stegeman,J.H.J.C., and Noordhoek,J. (1995). Development of methionine synthase, cystathionine-β-synthase and S-adenosyl-homocysteine hydrolase during gestation in rats. *J. Reprod. Fertil.,* **103,** 227-232.

Verma,I.C. (1978). High frequency of neural-tube defects in North India. *Lancet,* **1,** 879-880.

Vieira,A.R., Murray,J.C., Trembath,D., Orioli,I.M., Castilla,E.E., Cooper,M.E., Marazita,M.L., Lennon-Graham,F., and Speer,M. (2005). Studies of reduced folate carrier 1 (RFC1) A80G and 5,10-methylenetetrahydrofolate reductase (MTHFR) C677T polymorphisms with neural tube and orofacial cleft defects. *Am. J. Med. Genet. A,* **135,** 220-223.

Vogan,K.J., Epstein,D.J., Trasler,D.G., and Gros,P. (1993). The *splotch-delayed (Sp^d)* mouse mutant carries a point mutation within the paired box of the *Pax-3* gene. *Genomics,* **17,** 364-369.

Volcik,K.A., Shaw,G.M., Zhu,H.P., Lammer,E.J., Laurent,C., and Finnell,R.H. (2003). Associations between polymorphisms within the thymidylate synthase gene and spina bifida. *Birth Defects Res. Part A Clin Mol. Teratol.,* **67,** 924-928.

Volpe,J.J. (1995). *Neurology of the newborn.* W.B. Saunders Company, Philadelphia.

Vousden,K.H. and Lu,X. (2002). Live or let die: the cell's response to p53. *Nat. Rev. Cancer,* **2,** 594-604.

Wald,N., Sneddon,J., Densem,J., Frost,C., Stone,R., and MRC Vitamin Study Res Group (1991). Prevention of neural tube defects: Results of the Medical Research Council Vitamin Study. *Lancet,* **338,** 131-137.

Wald,N.J., Law,M.R., Morris,J.K., and Wald,D.S. (2001). Quantifying the effect of folic acid. *Lancet,* **358,** 2069-2073.

Wallingford,J.B., Fraser,S.E., and Harland,R.M. (2002). Convergent extension: the molecular control of polarized cell movement during embryonic development. *Dev. Cell,* **2,** 695-706.

Waterland,R.A. and Jirtle,R.L. (2003). Transposable elements: targets for early nutritional effects on epigenetic gene regulation. *Mol. Cell Biol.*, **23,** 5293-5300.

Wenstrom,K.D., Johanning,G.L., Owen,J., Johnston,K.E., Acton,S., and Tamura,T. (2000). Role of amniotic fluid homocysteine level and of fetal 5,10-methylenetetrahydrafolate reductase genotype in the etiology of neural tube defects. *Am. J. Med. Genet.*, **90,** 12-16.

Whitehead,A.S., Gallagher,P., Mills,J.L., Kirke,P.N., Burke,H., Molloy,A.M., Weir,D.G., Shields,D.C., and Scott,J.M. (1995). A genetic defect in 5,10 methylenetetrahydrofolate reductase in neural tube defects. *Q. J. Med.*, **88,** 763-766.

Wilding,C.S., Relton,C.L., Sutton,M.J., Jonas,P.A., Lynch,S.A., Tawn,E.J., and Burn,J. (2004). Thymidylate synthase repeat polymorphisms and risk of neural tube defects in a population from the northern United Kingdom. *Birth Defects Res. Part A Clin. Mol. Teratol.*, **70,** 483-485.

Wilkinson,D.G. (1992). *In Situ Hybridisation: A Practical Approach.* IRL Press, Oxford.

Williams,L.J., Mai,C.T., Edmonds,L.D., Shaw,G.M., Kirby,R.S., Hobbs,C.A., Sever,L.E., Miller,L.A., Meaney,F.J., and Levitt,M. (2002). Prevalence of spina bifida and anencephaly during the transition to mandatory folic acid fortification in the United States. *Teratology.*, **66,** 33-39.

Wilson,A., Platt,R., Wu,Q., Leclerc,D., Christensen,B., Yang,H., Gravel,R.A., and Rozen,R. (1999). A common variant in methionine synthase reductase combined with low cobalamin (vitamin B12) increases risk for spina bifida. *Mol. Genet. Metab.*, **67,** 317-323.

Wilson,D.B. and Wyatt,D.P. (1988). Closure of the posterior neuropore in the vl mutant mouse. *Anat. Embryol.,* **178,** 559-563.

Wu,M., Chen,D.F., Sasaoka,T., and Tonegawa,S. (1996). Neural tube defects and abnormal brain development in F52-deficient mice. *Proc. Natl. Acad. Sci. U. S. A,* **93,** 2110-2115.

Xiao,K.Z., Zhang,Z.Y., Su,Y.M., Liu,F.Q., Yan,Z.Z., Jiang,Z.Q., Zhou,S.F., He,W.G., Wang,B.Y., Jiang,H.P., Yang,H.G., Li,M.M., Ju,Z.H., Hong,S.Q., Yao,J.S., Xing,G.K., Li,H., Den,H.Y., Yu,W.Z., Chen,H.X., Liu,L.W., Bao,G.Z., Shang,H.Q., and Zhou,M.M. (1990). Central nervous system congenital malformations, especially neural tube defects in 29 provinces, metropolitan cities and autonomous regions of China: Chinese Birth Defects Monitoring Program. *Int. J. Epidemiol.,* **19,** 978-982.

Xu,W.M., Baribault,H., and Adamson,E.D. (1998). Vinculin knockout results in heart and brain defects during embryonic development. *Development.,* **125,** 327-337.

Ybot-Gonzalez,P., Cogram,P., Gerrelli,D., and Copp,A.J. (2002). Sonic hedgehog and the molecular regulation of neural tube closure. *Development.,* **129,** 2507-2517.

Ybot-Gonzalez,P. and Copp,A.J. (1999). Bending of the neural plate during mouse spinal neurulation is independent of actin microfilaments. *Dev. Dyn.,* **215,** 273-283.

Ybot-Gonzalez,P., Copp,A.J., and Greene,N.D.E. (2005). Expression pattern of glypican-4 suggests multiple roles during mouse development. *Dev. Dyn.,* **233,** 1013-1017.

Yen,I.H., Khoury,M.J., Erickson,J.D., James,L.M., Waters,G.D., and Berry,R.J. (1992). The changing epidemiology of neural tube defects: United States, 1968-1989. *Am. J. Dis. Child.,* **146,** 857-861.

Yoshida,H., Kong,Y.Y., Yoshida,R., Elia,A.J., Hakem,A., Hakem,R., Penninger,J.M., and Mak,T.W. (1998). Apaf1 is required for mitochondrial pathways of apoptosis and brain development. *Cell,* **94,** 739-750.

Zacharias,J.F., Jenkins,J.H., and Marion,J.P. (1984). The incidence of neural tube defects in the fetus and neonate of the insulin-dependent diabetic woman. *Am. J. Obstet. Gynecol.,* **150,** 797-798.

Zappia,V., Zydek-Cwick,R., and Schlenk,F. (1969). The specificity of S-adenosylmethionine derivatives in methyl transfer reactions. *J. Biol. Chem.,* **244,** 4499-4509.

Zhao,Q., Behringer,R.R., and De Crombrugghe,B. (1996). Prenatal folic acid treatment suppresses acrania and meroanencephaly in mice mutant for the *Cart1* homeobox gene. *Nature Genet.,* **13,** 275-283.

Zhong,W.M., Jiang,M.M., Schonemann,M.D., Meneses,J.J., Pedersen,R.A., Jan,L.Y., and Jan,Y.N. (2000). Mouse *numb* is an essential gene involved in cortical neurogenesis. *Proc. Natl. Acad. Sci. USA,* **97,** 6844-6849.

Zhu,H., Curry,S., Wen,S., Wicker,N.J., Shaw,G.M., Lammer,E.J., Yang,W., Jafarov,T., and Finnell,R.H. (2005). Are the betaine-homocysteine methyltransferase (BHMT and BHMT2) genes risk factors for spina bifida and orofacial clefts? *Am. J. Med. Genet. A,* **135,** 274-277.

Zhu,H., Wicker,N.J., Shaw,G.M., Lammer,E.J., Hendricks,K., Suarez,L., Canfield,M., and Finnell,R.H. (2003). Homocysteine remethylation enzyme polymorphisms and increased risks for neural tube defects. *Mol. Genet. Metab,* **78,** 216-221.

Appendix - Publications

Anat Embryol (2003) 206:185–191
DOI 10.1007/s00429-002-0284-3

ORIGINAL ARTICLE

Nicholas D.E. Greene · Louisa P.E. Dunlevy
Andrew J. Copp

Homocysteine is embryotoxic but does not cause neural tube defects in mouse embryos

Accepted: 26 September 2002 / Published online: 24 January 2003

FEBS Letters 580 (2006) 2803–2807

Excess methionine suppresses the methylation cycle and inhibits neural tube closure in mouse embryos

Louisa P.E. Dunlevy[a], Katie A. Burren[a], Lyn S. Chitty[b], Andrew J. Copp[a], Nicholas D.E. Greene[a,*]

Edited by Jesus Avila

Amendments

8.1 WHOLE EMBRYO CULTURE

In the whole embryo culture experiments throughout the thesis, there was a variation in the number of control embryos exhibiting NTD. This variation is probably due to an improvement in my culturing technique as the project progressed. It is also possible there were differences in the quality of rat serum. However, in each experiment, embryos in control and treatment groups were cultured simultaneously such that the effect of batch to batch variation in rat serum on data would be minimised.

The rat serum used for culture would have contained endogenous levels of methionine high enough to ensure neural tube closure could occur. These levels of methionine were not measured in this thesis and are an additional source of variability in these experiments. Steps were taken to reduce the effect of the variability. Before exsanguination all rats were keep in our animal facility and fed the same chow for 6 days, then the serum taken from 30 rats were pooled together before aliquots were made and stored. Experiments were then carried out using serum from the same batch for both control and treated groups. In addition, methionine levels in rat serum have been measured in other studies (pg 136) (Milakofsky *et al,* 1984) and were found to be a fraction of the concentrations that we found were capable of inducing NTD (70 μM in serum compared to 5 mM added).

After embryo culture, individual embryos were given a number code which was recorded with the treatment and post-culture measurements for the embryo. The embryo was identified by the number alone throughout all subsequent processes. Hence all

immunohistochemistry and histological analyses were carried out blind to the embryo treatment until after all the sectioning, labelling and counting had been carried out.

Measurements taken after whole embryo culture included somite number, crown-rump length, yolk sac circulation score and whether cranial neural tube closure had been completed. As the project developed I noticed the area of neural tube that remained open differed between exencephalic embryos. Subsequently I recorded which area of the cranial neural tube remained open after culture. This delay in recording the detail of closure failure is responsible for the discrepancies in the number of embryos in each group in Figure 4.4 compared to the total number of embryos cultured. Unfortunately this delay in recording information leads to low numbers of embryos for the analyses, particularly in the control group.

8.2 WHOLE MOUNT TUNEL

Figure 4.10. There appear to be slight differences in the whole mount TUNEL staining of PBS-treated control embryos to non-cultured wild type *Splotch*^{2H} embryos stained at a later date (Figure 5.2). There are slightly more labelled cells in the mesenchyme and slightly less in the hindbrain of cultured embryos. This could be due to differences in the developmental stage of the embryos, although both groups of embryos were at E9.5 they varied in somite stages between 16 and 20. The differences could alternatively be due to effects of whole embryo culture. Direct comparison at the time between whole mount TUNEL staining of uncultured CD1 embryos at E9.5 with the PBS-treated cultured embryos could have demonstrated whether whole embryo culture was responsible for the observed differences, however, these experiments were not carried out.

8.3 CHAPTER SIX

The differences observed in the survival and completion of the dUMP suppression test in cells from amniotic fluid samples compared to those derived from other tissues suggests that there are intrinsic differences in the cultures established from different tissue sources. Therefore, a comparison of dUMP suppression test scores of samples taken from the same tissue source should be considered.

	NTD	Control
dU suppression test scores	47.3	37.8
	31.0	39.6
	48.7	51.5
	42.8	42.9
		52.9
		41.9
		43.9
		36.8
		47.8
Mean ± SEM	42.5 ± 4.02	43.9 ± 1.92

Table 8.1 Comparison of dUMP suppression test scores of human samples derived from amniotic fluid samples

dUMP suppression test scores of cells derived from amniotic fluid samples were compared for NTD-affected and control fetuses. There was no statistically significant difference between the mean scores (tested by t-test).

There were no statistically significant differences between the mean dUMP suppression test scores between NTD-affected or control cells derived from amniotic fluid samples (Table 8.1). There were not enough numbers of cells derived from skin, cartilage or placental samples to carry out separate analysis of these groups. In order to make a comprehensive conclusion with regards to this study more samples are needed.

However, the results shown here suggest there is no difference in the mean dUMP suppression test score between amniocytes derived from control and NTD-affected fetuses.

8.4 CHAPTER SEVEN

Possible folate-related mechanisms in the causation of NTDs

Work carried out by Rothenberg and collegues (2004) showed the presence of autoantibodies against folate receptors in serum of mothers with NTD-affected pregnancies. This suggests that impaired maternal cellular folate absorption may be associated with NTD-affected pregnancies. This is an interesting discovery but so far is an isolated result. Further studies with increased sample numbers are needed to validate the hypothesis that maternal autoantibodies to folate receptors may be involved in the production of NTDs by limiting folate availability to the embryo.

Mechanisms by which suppression of methylation may be associated with NTDs

Results shown in Chapter 4 suggest that changes in cellular methylation processes may be responsible for the induced NTD following methionine, ethionine or cycloleucine treatment. DNA and protein methylation could potentially be affected. Changes in methylation may affect neural tube closure via changes in histone methylation. Histones are methylated at arginine and lysine residues and this post-translational modification has a regulatory role in gene expression (Martin and Zhang, 2005). Therefore, a possible target of disruption of the methylation cycle could be histone methylation, subsequently affecting gene expression. Future experiments could investigate this possibility by utilising methylation specific histone antibodies (Perez-Burgos *et al.*, 2004).

Folate-related gene polymorphisms

Further work carried out on the cell lines samples from Chapter 6 by Dr. Kit Doudney investigated folate gene polymorphisms in cell lines derived from NTD-affected fetuses. The genotype analysis for the known polymorphisms in folate-related genes were carried out as previously described in the literature and detailed in Table 8.2.

Folate-related gene	Polymorphism	Detection Method	Reference
MTHFR	C667T	PCR-RFLP with *Hinfl*. The polymorphism creates a *Hinfl* site	(Frosst *et al.*, 1995)
MTHFR	A1298C	PCR-RFLP with *Mbo*II. The polymorphism abolishes an *Mbo*II site.	(Van der Put *et al.*, 1998)
MTHFRD1	G1958A	PCR-RFLP with *Hpa*II. The polymorphism abolishes an *Hpa*II site.	(Brody *et al.*, 2002)
DHFR	19 bp deletion	PCR	(Johnson *et al.*, 2004)
GCPII	C1565T	PCR-RFLP with *Acc*I. The polymorphism creates an *Acc*I site.	(Devlin *et al.*, 2000)
MTR	A2756G	PCR-RFLP with *Hae*III. The polymorphism creates a *Hae*III site.	(Leclerc *et al.*, 1996)
MTRR	A66G	PCR-RFLP with *Ndel*. The polymorphism abolishes an *Ndel* site.	(Wilson *et al.*, 1999)

Table 8.2 Method of genotype analysis used to generate data in Table 7.1

The methods used to genotype cell samples for known folate-relate gene polymorphisms. Abbreviations: DHFR, dihydrofolate reductase; GCPII, glutamate carboxypeptidase II; MTHFR, methylene-tetrahydrofolate reductase; MTHFRD1, methylenetetrahydrofolate dehydrogenase /methenyltetrahydrofolate cyclohydrolase /formyltetrahydrofolate synthetase; MTR, methionine synthase; MTRR methionine synthase reductase; PCR-RFLP, polymerase chain reaction-restriction fragment length polymorphism.

Additional References

Devlin,A.M., Ling,E.H., Peerson,J.M., Fernando,S., Clarke,R., Smith,A.D., Halsted,C.H. (2000). Glutamate carboxypeptidase II: a polymorphism associated with lower levels of serum folate and hyperhomocysteinemia. *Hum Mol Genet.*, **9,** 2837-44.

Martin,C., Zhang,Y. (2005). The diverse functions of histone lysine methylation. *Nat Rev Mol Cell Biol.* **6,** 838-49.

Perez-Burgos,L., Peters,A.H., Opravil,S., Kauer,M., Mechtler,K., Jenuwein,T. (2004). Generation and characterization of methyl-lysine histone antibodies. *Methods Enzymol.* **376,** 234-54.

Rothenberg,S.P., da Costa,M.P., Sequeira,J.M., Cracco,J., Roberts,J.L., Weedon,J., Quadros,E.V. (2004). Autoantibodies against folate receptors in women with a pregnancy complicated by a neural-tube defect. *N Engl J Med.* **350,** 134-42.